INTRAVASCULAR ULTRASOUND

A TECHNIQUE IN EVOLUTION

METHODOLOGICAL CONSIDERATIONS

PETER PATRICK KEARNEY

DOCTOR OF MEDICINE

UNIVERSITY COLLEGE CORK

NOVEMBER 1995

Supervisor Dr G R SUTHERLAND

Head of Department Dr T R D SHAW

Department CARDIOLOGY DEPARTMENT
WESTERN GENERAL HOSPITAL
EDINBURGH
SCOTLAND

ACKNOWLEDGEMENTS

I start by thanking William Fennell for his encouragement and support of my initial interest in intravascular ultrasound. Although the all the work described in the thesis apart from chapter 4 was conducted in Edinburgh, my grounding in the field of intravascular ultrasound was obtained in Mainz. Great gratitude is due to Professor Raimund Erbel for the enthusiastic and energetic guidance he gave me during my stay in Germany. Thanks also go to Professor Jürgen Meyer, and my colleagues in the catheterisation laboratory, Junbo Ge and Thomas Voigtländer and particularly to my colleagues in Biophysics, Lothar Koch, and Thomas Roth, from whom I learned so much. I must express especial gratitude to George Sutherland who was instrumental in my move to Edinburgh, and in providing the means for me to continue in this field of research; thanks also to Stuart Shaw and Ian Starkey who have enthusiastically supported and facilitated the work, and to my colleagues in the intravascular ultrasound group Pauliina Ramo and Timothy Spencer. My greatest thanks go to Olive Murphy for her remarkable patience and support throughout.

Contents *page*

CHAPTER 1

Intravascular Ultrasound: An overview

CHAPTER 2

A comprehensive analysis of the short term reproducibility of intravascular ultrasound quantitation

CHAPTER 3

A study of the quantitative and qualitative impact of catheter shaft angulation in a mechanical intravascular ultrasound transducer

CHAPTER 4

Differences in the morphology of unstable and stable coronary lesions and their impact on the mechanisms of angioplasty

CHAPTER 5

The application of intravascular ultrasound in coronary stenting Observations in a consecutive series of ultrasound guided stent implantations in a single centre over an 18 month period

LIST OF TABLES AND FIGURES

PREFACE

As the title of the thesis suggests, intravascular ultrasound has been, and continues to be, an imaging technique that is in active evolution. Image quality has improved dramatically from the crude, low resolution 'black and white' images of the first generation of intravascular ultrasound scanners and transducers are now small enough to image most arteries before intervention. Although intravascular ultrasound is increasingly seen as the most informative method of assessing the coronary arteries, there are outstanding problems that must be addressed and overcome before its full potential can be achieved.

The aim of this thesis is to examine a number of these methodological shortcomings of intravascular ultrasound so that appropriate solutions can be found.

After a general overview, provided in Chapter 1, the reproducibility of intravascular ultrasound quantitation is assessed in Chapter 2. For reasons elaborated above, ultrasound is seen as the best technique to study the acute and long term outcome of coronary interventions and the effect of plaque modifying agents. Without detailed data concerning its reproducibility, such studies are uninterpretable.

Chapter 3 deals with the impact of catheter malfunction on the geometric integrity of intravascular ultrasound images. At present, the mechanical ultrasound devices are the most widely used systems. All mechanical systems are potentially subject to the problem of non-uniform rotation of the transducer, and to date its impact has been poorly characterised.

The difficulty encountered in discriminating unstable coronary lesions is examined in Chapter 4. There is a widely held view that acute coronary lesions

cannot be discriminated using intravascular ultrasound. Specific echographic markers are described that are found in the majority of unstable lesions. Close scrutiny of grey scale images allows identification of acute lesions and may allow discrimination of thrombus from underlying atheromatous plaque.

In the last two chapters, methodological issues relating to the clinical application of intravascular ultrasound in guiding coronary stenting are explored. In chapter 5, the findings of an observational study confirm the potential of intravascular ultrasound to provide additional information in cases in which favourable angiographic appearances have been achieved. However, the choice of one particular 'expansion index' over another is seen to impact significantly on the proportion of lesions that are judged to be successful. Before ultrasound guidance based on the attainment of specific quantitative expansion criteria be advocated as a widely applied technique, the reproducibility of reference segment measurements must be known. This issue is studied in chapter 6.

Separate studies are described in each of the data chapters. A similar layout is employed in each, consisting of the study aims, methods, findings, discussion and conclusion. At the risk of introducing a degree of repetition in the methods sections of each chapter, the ultrasound examination and image interpretation protocol are elaborated in each case, as important differences exist between the studies.

Chapter 1

Intracoronary Ultrasound

An overview

Contents *page*

1.1. Introduction

For the last thirty years, coronary angiography has been the definitive method of evaluating coronary artery anatomy. Recently, the limitations of angiography in defining the distribution and extent of coronary wall disease and in accurately representing the shape and size of disrupted coronary lumens have become apparent. The introduction of percutaneous coronary revascularisation, and in particular the development of ablative and cutting devices, has stimulated interest in acquiring precise information concerning the anatomy and consitution of treated vessels. A growing appreciation of the pathophysiological and prognostic significance of different plaque types, and the potential for modifying both constitution and risk with therapeutic agents such as lipid lowering drugs has further highlighted the need to study the coronary wall in vivo.

An intravascular imaging device was first developed by Cyzienski in the late 1950s in an effort to overcome the problem of poor transcutaneous penetration of ultrasound [Cyzienski, 1959]. Using a transvenous approach, he succeeded in acquiring A-mode signals of the canine heart and liver. Interest in pursuing the further development of the technique waned as matching materials for transducers were developed that permitted effective transcutaneous imaging. Now, over 30 years later, a new generation of intravascular ultrasound imaging devices has been developed as a means of providing high resolution images of the coronary and other arteries in vivo. After an initial period of technical evolution, intravascular ultrasound offers a highly informative complimentary method of imaging the coronary arteries.

1.2. Technical considerations

Intravascular imaging creates complex new demands in transducer design and manufacture. Despite this, a range of effective miniaturised transducers have been

developed which can be used to image vessels of ≤1.0 mm internal lumen diameter. The necessary reduction in transducer size decreases both power output and sensitivity, and in addition reduces the length of the 'near field' where beam width and hence lateral resolution is stable. Fortunately, lateral resolution is proportional to transducer diameter and improves within the near field as transducer size decreases. Near field depth is increased by raising transmitter carrier frequency. The negative impact of the limited power and sensitivity of the miniaturised transducer and the greater attenuation of high frequency signals is mitigated by the low attenuation and effective acoustic coupling offered by the surrounding blood and the short distances interrogated.

To date, both mechanical and solid state transducers have been developed with each transducer type having specific strengths and weaknesses. Mechanical transducers operate at higher frequencies, provide better resolution and have been miniaturised to a greater extent than their solid state counterparts. On the other hand, electronic systems do not suffer from the rotation angle artefact that arises from non-uniform transducer rotation. Imaging with solid state transducers is devoid of guidewire and strut artefacts as the transducers are arranged circumferentially on the catheter surface. In addition, catheters that combine imaging and therapeutic functions may theoretically more easily be configured without moving parts or a drive shaft.

1.2.1. Mechanical transducers

A mechanical intravascular imaging system has a single element piezoelectric crystal transducer (operating at 20-30 MHz) which is rotated by a motor driven flexible drive shaft. In the simplest configuration, the transducer is positioned at the end of the drive shaft and emits ultrasound at or near 90° to the long axis of the catheter. The 2D image is then reconstructed from multiple B mode lines acquired during rotation of the transducer through a 360° sweep at a rate of 800-1800

revolutions per minute. Immediately adjacent to the surface of the ultrasound transducer is a series of unresolvable 'ring down' signals constituting the so-called 'acoustic dead zone' that may obscure important wall surface details if excessively prominent. Incorporation of a mirror to lengthen the acoustic pathway within the catheter permits resolution of signals at the catheter surface. Mechanical catheters are advanced over an angioplasty guidewire by way of a monorail situated distal to the imaging element. A recently developed 2.9F catheter, operating at 30 MHz is devoid of guidewire and strut shadow artefacts. It consists of a transducer-tipped drive-shaft that runs in a distal sonolucent sheath. The sheath remains in situ within the vessel during image acquisition, thus preventing abrasive contact between the vessel wall and the transducer as it is advanced or withdrawn along the length of the vessel.

1.2.2. Electronic transducers

An electronic or solid state transducer is composed of a circular array of 32 or 64 rectangular elements, operating at a centre frequency of 20 MHz, situated around the circumference of the catheter shaft. The effective aperture is reduced by the necessarily curved geometry of the multi-element unit, as only a limited number of elements directly face the transmit / receive direction. A 'synthetic aperture focusing technique' has been developed whereby a pulse is transmitted by a group of adjacent elements and received by a single element at their centre. A 360° image is constituted following sequential activation of the subgroups around the circumference of the array. Despite this method of dynamic focusing of the electronically configured beam, the lateral resolution of this system is not significantly different to that of currently available mechanical systems [Benkeser, 1993]. Software advances have significantly improved the image quality of electronic systems in the recent past. However, whereas further improvement in lateral resolution of single element mechanical transducers is technically feasible [Lockwood, 1992], the greater number of elements operating at higher frequency

required by electronic transducers to achieve further improvements in lateral resolution may prove more difficult to achieve.

1.3. Arterial wall histology

The histological characteristics of arteries provide the basis for their ultrasonic appearance and a precise knowledge of their structure facilitates the interpretation and understanding of intravascular ultrasound images. Arteries may be categorised into two principal types on the basis of the histology of the media. The larger, central components of the arterial tree (the aorta, carotids, common iliac and pulmonary arteries) are 'elastic' arteries, so called because their media is composed of sheets of smooth muscle cells separated by multiple lamellae of elastin and collagen. On the other hand, connective tissue is relatively sparse in 'muscular' arteries, examples of which include the external iliac, femoral, renal, mesenteric and coronary arteries.

1.3.1. Histology of the coronary arteries

The coronary arteries are made up of three layers; the intima, the media and the adventitia (**figure 1.1**).

The intima consists of a superficial layer of endothelial cells and subendothelial tissue comprising connective tissue and smooth muscle cells. Its thickness increases with age, from a single cell layer at birth, to a mean of 60 μm from infancy to 5 years, 220 μm at 30 years and 250 μm at 40 years [Velican, 1981]. Further adaptive, physiological thickening of the intima occurs at points where wall tension is increased, such as arterial bifurcations and on the outer parts of bends, and may be either eccentric or diffuse [Stary, 1992]. Diffuse intimal thickening may also be seen in older patients, when it has been described as 'arteriosclerosis of the elderly' [Becker, 1985]. This is histologically distinct from atherosclerosis, a disease of the intima, that is comprised of smooth muscle cells, macrophages, foam cells,

fibroblasts and extracellular components including collagen, proteoglycans and extracellular lipid.

The internal elastic lamina, a sheet of elastic tissue that may naturally be duplicated or fragmented, separates the media from the intima. The external elastic lamina, separating the media from the adventitia is structurally similar, but thinner than the internal elastic lamina.

The muscular media of coronary arteries is predominantly composed of smooth muscle cells with smaller amounts of collagen, elastic tissue and proteoglycans. Fibrous degeneration of the media, particularly of the inner third, is not uncommon in patients with concomitant atherosclerotic disease [Porter, 1994]. The thickness of the media ranges from 125-350 μm (mean 200 μm) but thins (range 16-190 μm, mean 80 μm) and, indeed, may rupture in the presence of atherosclerotic disease.

The adventitia is composed of loose collagen and elastic tissue that merges with the surrounding peri-adventitial tissue and is 300-500 μm in width [Waller, 1989].

1.3.2. The interaction of ultrasound and histology

Identification of the outer border of the vessel with ultrasound depends on the presence of an ultrasonic interface between the outer layers of the vessel wall [Pignoli, 1986]. The media of muscular arteries appears as a distinct hypoechoic layer, sandwiched between the relatively more echodense intima and adventitia [Gussenhoven, 1989; Nishimura, 1990]. A high concentration of smooth muscle cells in the adventitia or fibrous degeneration of the media may lead to ultrasonic homogeneity and a poorly delineated outer border in muscular arteries [Di Mario, 1992]. In elastic arteries, the outer border of the vessel is usually ill-defined because of the high echogenicity of the elastic media and absence of an acoustic interface, unless generated by relatively hypoechoic adventitia composed of loose connective tissue [Nishmura, 1990].

A distinct ultrasonic interface represented by a strong, contiguous spectral signal is an important contributor to image interpretation. Although tissue constitution does influence the manner in which ultrasound is reflected (as scattered or spectral signals), the difference in acoustic impedance between adjacent tissues plays a particularly important role in this regard [Siegel, 1993; Peters, 1994a]. The leading edge of the intima (at the endoluminal interface between the blood-filled lumen and the endothelium) and the outer border of the media (at the junction of media/external elastic lamina and surrounding adventitia) are the most reliably determined vessel layer interfaces. The internal elastic lamina is composed of strongly echogenic elastic tissue, but fibrous change in the inner third of the media decreases the difference in acoustic impedance between these adjacent layers. Clear delineation of the internal elastic lamina, and consequently the inner border of the media, is thus frequently difficult or impossible to achieve. When the internal elastic lamina does generate a discrete spectral signal, a distal 'blooming' effect tends to artefactually widen the combined intima and internal elastic lamina thickness and diminishes medial thickness. Thus, in intravascular ultrasound images the thickness of the inner echogenic layer, conventionally interpreted as intima alone, correlates more closely with the combined thickness of intima and media [Porter, 1994]. Occasionally, the thickness of the media may be over- rather than under-estimated by limited grey scale assignation in ultrasound systems with a narrow dynamic range, leading to an artefactually wide sonolucent zone deep to the intimal leading edge [Fitzgerald, 1991]. In normal coronary arteries in young subjects, in which intimal thickness is less than the resolving power of the imaging system, no intimal layer may be evident [Fitzgerald, 1992a]. The absence of an acoustic interface between the adventitia and the surrounding peri-adventitial fat prevents the identification of the adventitia as a discrete, quantifiable entity.

In summary, the two strong and reliably identified acoustic interfaces in intravascular ultrasound images of the coronary artery correspond with the

endoluminal border and the external elastic lamina. The other histological interfaces produce more variable spectral signals or, in some cases, none at all. For these reasons, whereas the combination of plaque and media is readily appreciated, the individual vessel wall components, namely the intima (or plaque), the media, and the adventitia, cannot usually be identified (or measured) with confidence as discrete entities.

1.3.3. The role of image resolution

The resolving power of the imaging device, in addition to the acoustic properties of the tissue structures themselves, determine what can and cannot reliably be identified and quantified in intracoronary images. The axial resolution of a transducer operating at a centre frequency of 30 MHz is approximately 150 μm. Since the vessel wall layers are arranged circumferentially around the lumen, it might be anticipated that an intimal or medial layer measuring over 150 μm would be resolved by an intraluminal transducer operating at this frequency. This is rarely the case in practice, since the transducer is frequently located eccentrically within the lumen and thus it is the lateral rather than the axial resolution that determines whether or not the structure is resolved. The lateral resolution (and beam width) approximate the diameter of the transducer face in the near field of unfocused mechanical intravascular ultrasound transducers. The far field begins at 1-2 mm from the transducer face. Here the beam rapidly widens and consequently lateral resolution deteriorates. Effective lateral resolution is at least 300 μm in those parts of the imaging field that include many of the structures of interest.

1.3.4. The normal range of coronary artery dimensions

The normal range for the diameters of the coronary arteries in adults has been established in autopsy studies [Baroldi, 1983]. The left main coronary artery measures 2.0-5.5 mm (mean 4.0 mm); the left anterior descending artery 2.0-5.0 mm (mean 3.6 mm); the left circumflex artery 1.5-5.5 mm (mean 3.0 mm) and right

coronary artery 1.5-5.5 mm (mean 3.2 mm). The left anterior descending and left circumflex arteries taper along their length, but the calibre of the right coronary artery remains more or less constant as far as the origin of the posterior descending artery.

1.3.5. Cardiac cycle related change in vessel dimensions

The coronary arterial lumen cross-sectional area varies in relation to changes in the distending pressure during the cardiac cycle. The maximum lumen area occurs in mid- to late systole and the minimum area in late diastole. An exception to this pattern occurs in cases in which a 'tunnelled' artery runs under a muscle bridge, in which the artery is compressed during systole [Ge, 1994a]. The cross-sectional area of normal coronary arteries varies by 10% during the cardiac cycle, whereas pulsatile variation in the presence of plaque is reduced to 5% or less [Ge, 1994b].

By convention, the end-diastolic frames of angiograms are used for quantitative purposes, when cardiac motion and intraluminal contrast streaming are at a minimum. A number of arguments can be made for employing the opposite strategy of measuring intravascular ultrasound images at end systole. The maximum lumen dimensions during the cardiac cycle are clinically the more relevant measures for the purposes of sizing percutaneous interventional devices. After interventions, lumen dimensions at the site of minimum lumen area may vary during the cardiac cycle as friable tissue flaps move to-and-fro into the lumen from the vessel wall. The most practical approach in these circumstances may be to measure lumen dimensions when the size of any false lumen is minimised by the maximal distending pressure during the cardiac cycle. Furthermore, there is evidence to suggest that the beat to beat variability is less when measured in systolic compared to diastolic frames [Peters, 1994b].

1.4. Morphometric parameters

Intracoronary ultrasound allows a quantitative tomographic assessment of the coronary arteries that no other currently available technique can offer. In the following section, we describe the measurements, or morphometric parameters, that are commonly made on intracoronary ultrasound images (**figure 1.2**) and a number of specific considerations pertaining to each of these.

1.4.1. Lumen area

The lumen area is measured by tracing the leading edge of the circumferential interface between blood and intima. A suboptimal angle of incidence of the ultrasound beam [Di Mario, 1993], increased blood echogenicity, or a small acoustic impedance mismatch between the blood pool and an echolucent plaque may obscure this border. Thin, mobile intimal flaps may be difficult to distinguish from blood and are a further source of ambiguity in defining the lumen boundaries in post interventional images. Attempts to improve contrast between the lumen and surrounding tissue by adjusting post-processing, gross gain or time-gain compensation settings may unhelpfully diminish the outline of the endoluminal border. Edge detection may be facilitated on the real-time images by observing the dynamic alteration in speckle pattern characteristic of flowing blood compared to the more static pattern of adjacent tissue. The injection of contrast or saline into the coronary to temporarily clear bright blood signals may also facilitate edge detection. Experimental work has shown that intra-arterial contrast agents improve edge detection and the accuracy of lumen area measurements [Hausmann, 1994a], but no such agent is yet licensed for clinical use.

1.4.2. Vessel area

As the adventitia merges imperceptibly with the surrounding perivascular tissue, for the purposes of intravascular ultrasound measurements, the 'vessel area' is taken to mean the area enclosed by the outermost definable interface. This co-

incides with the external elastic lamina, between the media and adventitia, and is thus referred to as the 'external elastic lamina area'. Measurement of the internal elastic lamina allows the calculation of true plaque or intimal area, but, as previously discussed, is less reliably delineated. Occasionally, advanced fibrous degeneration of the media may obscure the interface between it and the surrounding adventitia [Nishimura, 1990]. Coronary stent implantation compresses the plaque, media and surrounding adventitia and in conjunction with the variable degree of acoustic shadowing cast by the stent struts may also give rise to difficulties in quantitating the vessel area. By convention, vessel area is considered unreliable when calcium induced acoustic shadowing obscures >60° of the vessel circumference[Hausmann, 1994b]. In cases of lesser degrees of shadowing, the vessel border is extrapolated from the identifiable sections of the media/adventitia interface.

1.4.3. Plaque area

The 'plaque' area, more accurately termed the 'plaque+media' area when the course of the external elastic lamina is traced to measure vessel area, is calculated as the difference between the vessel area and lumen area. As this measurement is derived from the vessel and lumen areas, similar considerations apply to difficulties in determining plaque area as apply to vessel area.

1.4.4. Percentage Vessel Area Stenosis

The percentage of the vessel area occupied by plaque is calculated using the formula: (1 - lumen area / vessel area x 100). This parameter is variably known as percent vessel area stenosis, the plaque burden, the percent obstruction or percent stenosis. As the latter two terms are also used to describe the ratio of the lumen area at the site of stenosis to the lumen area in the reference segment, these terms are probably best avoided. A number of investigators have taken the opposite approach and calculated the proportion of the vessel area occupied by

the lumen, termed the percentage lumen cross-sectional area [Nakamura, 1994]. Measurement of the plaque burden is closer to histological practice, and is the preferred approach. A simple but noteworthy distinction must be made between the difference between percentage vessel area stenosis and angiographically assessed 'percentage stenosis'. The latter is an expression of lumen narrowing at the stenosis relative to interpolated or reference segment lumen dimensions. The relationship between lumenographic and tomographic percent stenosis (as measured on ultrasound images or histological cross-sections) is neither linear nor predictable. Both compensatory vessel expansion and diffuse disease in the proximal reference segment tend to diminish the focal impact of atherosclerotic accumulation on the longitudinal profile of the lumen and account for the poor correlation noted between ultrasound and angiographic percent stenosis narrowing (**figure 1.3**) [Tobis, 1991a; Porter, 1993].

1.4.5. Diameters

A well-recognised limitation of coronary angiography as a means of assessing coronary disease is the inevitable restriction to measurements of luminal diameter which is an indirect, and sometimes misleading, measure of the haemodynamic significance of a stenosis. Flow relates in an exponential manner to the cross-sectional lumen area, which can be measured directly using intravascular ultrasound. Lumen diameter measurements nevertheless remain a central part of everyday clinical practice, as the appropriate size of interventional devices is chosen on the basis of the estimated diameter of the reference segments adjacent to a stenosis. In addition, the severity of a stenosis and the outcome of coronary interventions continue to be routinely evaluated in terms of the percentage diameter stenosis of the vessel judged from orthogonal angiographic views.

Lumen diameters may be measured from tomographic intravascular ultrasound images in a number of different ways: (A) a subjective assessment of maximum

and minimum diameter (the most widely applied method); (B) a mean diameter derived from the lumen area using the formula $d=2\pi^{1/2}$; (C) a minimum and maximum 'projected diameter' of the lumen (that includes fissures and dissections) identifiable if the silhouette of the vessel lumen is 'viewed' from all points around its circumference, and (D) diameters drawn through the geometric centre of the lumen.

The subjective choice of lumen diameters is subject to certain shortcomings. Whereas the maximum lumen diameter is usually readily identified, the selection of the minimum diameter may be difficult in cases in which the borders of the lumen are irregular and incorporate sections that protrude convexly into the lumen. Once the lumen boundary has been traced, it is a simple matter to apply an objective method, such as the automated determination of the minimum diameter through the geometric centre of the lumen. However, the geometric 'centre' of a crescentic lumen may lie outside the lumen boundaries, and so a modification of this approach (E) may be employed whereby the maximum diameter is determined, following which the minimum diameter is defined as the smallest diameter drawn through the mid-point of the maximum diameter.

1.4.6. Quantitative validation

Studies in phantoms and comparisons with histology have confirmed the accuracy of intravascular ultrasound measurements. A number of comparative studies have shown that direct measurement of lumen dimensions with intravascular ultrasound may disclose significant overestimation of lumen size by angiography. As outlined below, the data in this regard is inconsistent, and requires further clarification (**table 1.1**).

1.4.6.1. In vitro phantom correlations

In vitro ultrasound measurements of cylindrical phantoms of known dimensions are highly accurate although non-coaxial alignment of the catheter (not eccentric co-axial alignment) leads to geometrically predictable overestimation of lumen size

[Nishimura, 1990]. A further study has shown that ultrasound measurements of irregularly shaped phantom lumens are more accurate and smaller than quantitative angiographic measurements and correlate better with measured flow rates [Moriuchi, 1992].

1.4.6.2. In vitro histological correlations

Ultrasound and histological measurements of lumen area, vessel area and plaque area correlate closely [Nishimura,1990; DiMario, 1992; Potkin, 1990] but correlation analyses alone fail to convey the direction and extent of any measurement bias that exists. A more informative measure of agreement was applied by Anderson et al. who found that the intravascular ultrasound device markedly overestimated lumen area [Anderson, 1992]. The bias could not be accounted for by a small calibration error or tissue shrinkage and may have arisen from the narrow dynamic range and limited image quality of the ultrasound system employed in the study. Even when using state of the art scanning equipment, technical factors may confound exact comparison of ultrasound and histology measurements. Geometric distortion following sectioning of non-pressure perfused vessels reduces histological lumen area. Significant tissue shrinkage that occurs during histological processing may lead to an increase in lumen size following outward radial contraction of the wall [Potkin, 1990]. Formalin fixation, on the other hand, does not appear to affect vessel dimensions [Potkin, 1990].

1.4.6.3. Angiographic correlation

Comparisons between angiographic and intravascular ultrasound measurements of lumen dimensions have generally shown good agreement in normal vessels that deteriorates as lumen irregularity increases. The first systematic in vivo comparison between intravascular ultrasound and quantitative angiography, performed in canine peripheral arteries, demonstrated a close correlation for lumen dimensions measured by both techniques that worsened after balloon

angioplasty. Ultrasonically measured lumen dimensions tended to be slightly smaller, particularly after angioplasty [Nissen, 1990]. The same group found that the correlation between ultrasound and angiography was excellent in the circular lumina of normal human arteries, but deteriorated in diseased, eccentric lumina, where again ultrasound dimensions were smaller [Nissen, 1991]. Similar findings have recently been reported by De Scheerder et al. who found a clear bias toward overestimation of lumen dimensions by angiography in stenosed and post-angioplasty segments [De Scheerder, 1994]. De Franco et al. found that after a range of coronary interventions, ultrasound measurements of minimum lumen diameter were significantly smaller than angiographic measurements [De Franco, 1994].

A systematic bias in the opposite direction has also been documented. In angiographically normal arteries, St. Goar et al. found a close correlation between angiographic and ultrasound dimensions but 83% of ultrasound measurements were above the line of identity [St. Goar, 1991]. Porter et al. in a study of angiographically mildly diseased coronary arteries found a moderate linear correlation between angiographic and ultrasound measured diameters, (r=0.59), but ultrasound measurements tended to be larger [Porter, 1993]. Tobis et al. found a poor correlation between measurements made by both techniques for normal reference segments (r=0.26) that further deteriorated after angioplasty (r=0.12) [Tobis, 1991a]. Although frequently cited as an example of the marked discrepancy that may occur between angiographic and intravascular ultarsound assessments of irregular lumina, the ultrasound measured lumen area at the angioplasty site was inexplicably and illogically 33% larger than lumen area calculated from angiographic diameters. A similar pattern has been reported in a number of subsequent ultrasound studies of different coronary interventions [Mintz, 1992a; Davidson, 1991; Laskey, 1993]. Possible explanations for this bias are listed in **table 1.2**.

1.4.7. Quantitative reproducibility

Although many reports quote high correlation coefficients for intra- and interobserver agreement for measurement of vessel dimensions, more informative measures of agreement are infrequently reported and formal studies of the reproducibility of intravascular ultrasound measurements are few. In a recent report examining quantitative reproducibility in selected frames, no significant intra or interobserver bias or random variation was found for direct measurements (diameters, lumen area and vessel area), but a significant (>10%) bias was shown for plaque area (a derived measure) and random variability was >20% for both plaque area and percent area stenosis [Hausmann, 1994]. Peters et al. noted greater variability with decreasing absolute lumen size, and between sequential diastolic frames than between systolic frames [Peters, 1994b]. The long-term reproducibility of intravascular ultrasound. This issue requires clarification before intravascular ultrasound can confidently be applied in longitudinal studies to the study of restenosis, arterial remodelling and effects of lipid lowering therapy.

1.4.9. Qualitative validation

In an early in vitro study, Gussenhoven et al. noted that different plaque constituent tissue types appeared to have distinctive ultrasonic characteristics [Gussenhoven, 1989]. Lipid deposits were hypoechoic, fibromuscular lesions and fibrous lesions were of intermediate echogenicity and calcium was brightly echogenic with distal acoustic shadowing (**figure 1.4**). Intra-arterial thrombus has been reported to produce 'granular' echoes of variable echodensity [Pandian, 1990] and bright, finely speckled echoes [Comess, 1992; Lee, 1994]. Platelet rich thrombi are echolucent in contrast to whole blood thrombi that generate a characteristic fine speckled ultrasonic appearance [Frimerman, 1994].

Subsequent studies have confirmed that grey scale levels do correspond with tissue type, but with variable sensitivity and specificity (**table 1.3**). The

sensitivity for lipid deposit identification may be reduced by echogenic inclusions and its specificity reduced by a narrow system dynamic range giving rise to a subintimal echolucent zone regardless of tissue type [Fitzgerald, 1991]. Ultrasonic identification of lipid or calcification is also dependent on the radial thickness of the deposits which must be > 0.25 mm to be detectable [Peters, 1994c]. The ultrasonic appearance of thrombus described above does not appear to be specific [Siegal, 1991].

1.4.10. Qualitative reproducibility

The reproducibility of intravascular ultrasound qualitative analysis is also little studied. In classifying different plaque types, Hodgson et al. reported complete agreement between three observers in 47%, partial agreement in 38% and no agreement in 16% [Hodgson, 1993]. Low inter-observer error has been reported for recognition and measurement of plaque calcification [Mintz, 1992b; Fitzgerald, 1992b] and plaque dissection [Fitzgerald, 1992b]. On the other hand, Peters et al. demonstrated poor agreement for a number of qualitative features on intracoronary ultrasound images that were blindly evaluated in a number of reference centres (**table 1.4**) [Peters, 1994d].

1.5. Safety and feasibility

Reports to date indicate that despite its invasive nature, intracoronary ultrasound imaging is associated with a minor incidence of complications. Of 2207 ICUS studies performed in 22 centres, 92% of cases were free of complications and the commonest event was vasospasm, reported in 2.9% of cases [Hausmann, 1995]. Other procedural events attributable to the use of intravascular ultrasound, including dissection, thrombosis, embolisation, and acute occlusion, occurred in 0.3%. Myocardial infarction and emergency coronary artery bypass surgery, classified as major complications, occurred in 0.1%. Procedural and major complications of doubtful relation to the ultrasound examination occurred in 0.4%

and 0.2% respectively. Events were commoner in patients with unstable angina and acute myocardial infarction, but neither centre experience nor catheter size appeared to be predictive of complications.

In a further study, quantitative angiographic follow-up of patients who underwent intravascular ultrasound examination for assessment of transplant arterial status revealed no evidence to suggest accelerated intimal thickening in instrumented vessels [Pinto, 1993].

1.6. Clinical Observations with Intracoronary Ultrasound

1.6.1. Angiographically 'normal' arteries

Coronary angiography is an insensitive method for detecting early atheromatous thickening of the arterial wall, largely because of vascular remodelling whereby plaque occupies an average of 40% of coronary vessel cross section before luminal encroachment occurs. This phenomenon of so-called 'Glagovian' adaptive enlargement has been documented in vivo with ultrasound [Ge, 1993]. The plaque burden in the so-called 'normal reference segments' of vessels undergoing coronary intervention averages 35-40% [Tobis, 1989; Hodgson, 1993].

Angiographically normal or near normal left main coronary arteries are also commonly diseased. Atherosclerotic plaques were evident in 90% of a series of patients undergoing percutaneous coronary intervention [Hermiller, 1993] and in 45% of a mixed series undergoing diagnostic and post interventional study [Gerber, 1994]. It should be noted that the prognostic significance of patterns of coronary disease is largely based on the number of vessels in which 'significant' luminal stenoses (>50% lumen diameter reduction) have been angiographically documented in large series of patients. The prognostic significance of ultrasonically identified non-obstructive plaques has yet to be established.

1.6.2. Coronary wall pathology

Intravascular ultrasound characterises vessel wall morphology more accurately than angiography. Calcification is evident approximately twice as often on ultrasound as on fluoroscopy (76% vs. 48%) [Mintz, 1992b]. Lesion eccentricity is seen in 77% of lesions with ultrasound, (a figure similar to that documented at autopsy) in contrast to one third of angiographic stenoses [Waller, 1989; Fitzgerald, 1993].

1.6.3. Cardiac allograft arteriopathy

Allograft arteriopathy is the major cause of late cardiac transplant failure, but in its early stages luminal compromise is absent or too diffuse to be angiographically evident. Intravascular ultrasound is superior to angiography in determining the presence of graft arteriopathy [Pflugfelder, 1993]. Even when minimal irregularities on angiography were considered abnormal, intimal thickening was seen in twice as many patients with ultrasound (34%) as had angiographically evident disease (15%). Studies of vasomotion [Mills, 1992; Pinto, 1992; Anderson, 1993; Drexler, 1994] and combined 2D and Doppler ultrasound studies [Mills, 1992; Drexler, 1994] following pharmacologic provocation have been used to correlate the morphology and function of allograft arteries.

1.6.4. Acute coronary disease

Intravascular ultrasound is well suited to the in vivo study of acute coronary lesion morphology. Plaque rupture has been identified in vivo with ultrasound following myocardial infarction [Zamorano, 1994] and echolucent zones, possibly indicative of lipid deposits, occur more frequently in acute than in stable coronary lesions and are a more sensitive indicator of instability than angiographic criteria [Hodgson, 1993]. As described in chapter 4, a configuration of echo markers specific for unstable angina and highly suggestive of mural thrombus has been found on pre-interventional imaging of unstable lesions [Kearney, 1996]. These consist of a fine

echodense line running circumferentially within the lesion, suggestive of an acoustic interface between thrombus and the underlying plaque, and close conformation of the neolumen shape after intervention with the inner layer delimited by the line prior to intervention (**figure 1.5**).

1.6.5. Coronary vasomotor function

The vasomotor activity of the coronary arteries is readily assessed by real-time tomographic measurement of lumen area change [Ge, 1994a]. In combination with intracoronary Doppler, absolute coronary flow can be calculated and the differential effects of therapeutic agents on conductance and resistance vessels studied [Sudhir, 1993; Drexler, 1994]. The degree of change in lumen cross-sectional area during the cardiac cycle is a measure of vessel wall distensability. Increasing intimal thickness in coronary arteries correlates in a non-linear fashion with reduced distensability. Following balloon angioplasty and directional atherectomy, the distensability of heavily diseased vessel segments is comparable to normal vessels and greater than mildly diseased segments [Reddy, 1993].

1.7. The study of coronary interventions

1.7.1. Percutaneous Balloon Angioplasty

Until the introduction of intravascular ultrasound, in vivo study of coronary balloon angioplasty has been thwarted by the limitations of angiography in documenting changes within the vessel wall. Although autopsy data suggests a central role for intimal and medial dissection in successful angioplasty, dissections are evident on angiography in only 20-30% of cases. Angiographic dissection has been found to correlate with both lower [Hirshfeld, 1991] and higher [Guiteras, 1987] rates of restenosis, as well as having no apparent effect [Hermans, 1992]. The confusion may in part relate to the limitations of angiography in detecting, characterising, and quantitating dissections and also to the heterogeneity of angiographic appearances after PTCA that are described by the term 'dissection'. Ultrasound

identifies plaque tears twice as often as angiography [Davidson, 1991; Fitzgerald, 1993]. Detailed geometric analysis of intravascular ultrasound images of plaques prior to dilatation can identify stress points where plaque rupture is likely to occur [Lee, 1993]. The size and location of dissections relates to the presence of calcification, probably as a result of increased local shear stress within the plaque (**figure 1.6**) [Fitzgerald, 1992b]. The positive contribution of dissection to lumen gain is supported by data documenting a 30% greater increase in lumen area in lesions with tears compared to those that appear to have a smooth walled dilatation [Fitzgerald, 1993]. Per-interventional imaging using a combination balloon/ultrasound catheter in peripheral vessels has shown that plaques began to tear at low inflation pressure (≤2 atmospheres) and that elastic recoil (averaging 30%) occurs almost immediately following balloon deflation [Isner, 1991].

Plaque fracture does not lead to an increase in lumen area unless a concomitant increase in overall vessel size (vessel expansion) or decrease in plaque area (compression, axial remodelling or displacement) occurs. Vessel expansion or stretch is operative in most cases of coronary angioplasty and plaque area reduction appears to play a minor role [Braden, 1994] with the possible exception of unstable lesions [Kearney, 1996]. In contrast, plaque compression appears to be the major contributor to lumen gain in peripheral vessels [Losordo, 1992].

The proportion of patients reported to have dissection after angioplasty is very variable, ranging from 41% [Davidson, 1991] to 83% [Potkin, 1992]. Technical and methodological factors contribute to the variable findings between studies. False positive identification of dissection may arise from a limited dynamic range [Fitzgerald, 1991] and dissections may be missed because of calcific shadowing [Coy, 1992], an unfavourable angle of incidence [Di Mario, 1993] or wall wrapping by the imaging catheter. No definitions for plaque tear, rupture, fissure or dissection are uniformly applied, although two classifications of intravascular ultrasound

morphology after angioplasty have been proposed [Honye, 1992; Gerber, 1992]. Categorical classification of morphology on the basis of findings in one tomographic slice within the lesion is convenient but fails to take into account the longitudinal extent or the variability of changes within the lesion and the reproducibility of these classifications is not documented. Three dimensional reconstruction redresses some of these shortcomings by providing axial as well as cross-sectional assessment, volumetric analysis and a reproducible means of matching segments before and after intervention.

One of the most important observations made with intravascular ultrasound concerns the mechanism of restenosis following coronary intervention. Contrary to the widely held belief that restenosis results predominantly from neointimal proliferation, in vivo ultrasound studies have shown that the greater part of late lumen loss is due to 'negative remodelling' or contraction of the vessel, with a lesser contribution from neointimal growth [Mintz, 1994a; Di Mario, 1995]. In contrast to previous experimental work [Shwartz, 1991], the same process has been documented in a number of recent animal studies in Yucatan micropigs [Post, 1994] and in rabbits [Kakuta, 1994]. The SURE study (Serial Ultrasound in REstenosis) conducted by Nobuyoshi, Mintz and co-workers, has enlisted 70 patients of an intended 200 patients who undergo serial ultrasound studies at the time of intervention, at 24 hours, 6 weeks and again at 6 months.

1.7.2. Coronary stents

The metallic struts or coils of intracoronary stents are poorly visualised on fluoroscopy but are easily seen with ultrasound. Confirmation of full stent expansion and complete apposition of struts against the vessel wall, as well as accurate sizing of the balloon and positioning of the stent with respect to the lesion or adjacent dissections is afforded by ultrasonic guidance. A recent observational study has reported the acute outcome of ultrasound guided stent insertion

[Nakamura, 1994]. Despite angiographic success (comparable in absolute terms to that documented in previous stent trials), 80% of lesions were adjudged to be suboptimally dilated by ultrasound criteria and underwent repeat dilatation at higher pressures or with larger balloons. Minimum intrastent cross-sectional area increased by a third following repeat dilatation. An equivalent increase in angiographic minimum lumen diameter (MLD) of 14% was evident on post procedural quantitative angiography and reduction of residual stenosis from 9 to -4%, but importantly angiographic measurements were larger than ultrasound measured minor lumen diameters. Lumen eccentricity was not significantly improved after repeat dilatation and incomplete apposition of stent struts was infrequently documented. Sizing decisions based on vessel cross-sectional area have recently been abandoned by this group of investigators in favour of reference to lumen area proximal and distal to the lesion, as reference to vessel area in compensated segments may lead to balloon oversizing with adverse consequences. The rate of 'incomplete expansion' following angiographically guided stent deployment decreased to 40% following the change in the definition of optimal deployment [Colombo, 1995].

Mudra et al. found a substantial overestimation of minimum lumen diameter by quantitative angiography relative to intravascular ultrasound measurements both after initial stent insertion and after further dilatation as a result of lumen eccentricity and incomplete strut apposition [Mudra, 1994]. Minimum lumen diameter increased by 25% following ultrasound guidance. A retrospective comparison of the angiographic outcome in lesions undergoing ultrasound guided stenting with lesions undergoing standard stent insertion revealed a final minimum lumen diameter of 2.95 mm and -4% percent stenosis in the ultrasound guided group compared to 2.56 mm and 11% respectively in the standard group [Popma, 1994]. Transient distal vessel spasm occurred more frequently in the ulrasound guided group, but there was no increase in dissections or vessel wall perforation.

Despite these encouraging results, neither acute nor long term clinical outcome has been shown to be improved by ultrasound guidance of stent insertion. Larger intrastent dimensions and absence of intrastent stenosis provides the rheologic conditions that may reduce subacute thrombosis and possibly restenosis rates. A strategy of dispensing with anticoagulation following optimal stent insertion, associated with a low incidence of thrombotic and haemorrhagic complications, has been adopted both with [Colombo, 1995] and without ultrasound guidance [Morice, 1994]. A randomised trial (MUSIC) is currently underway to confirm that anticoagulation can be replaced by aspirin therapy in cases in which optimal stent deployment has been confirmed with ultrasound.

There are conflicting data concerning the mechanisms of stent restenosis. Results of one study suggested that stent collapse, possibly as a result of stent strut mechanical fatigue or extraneous tissue hyperplasia, contributes more to late loss of lumen area than does intimal hyperplasia [Keren, 1992]. Subsequently, more compelling data points to neointimal hyperplasia as the principal cause of late loss of lumen gain in coronary stents [Klauss, 1994].

1.7.3. Directional atherectomy

Knowledge of plaque constitution, shape and depth should help in assessing the suitability of a lesion for directional coronary atherectomy (DCA) and to safely maximise lumen gain. Superficial calcification (at or near the endoluminal surface of the plaque) is associated with a significantly lower tissue yield than either deep calcification or no calcification. De Lezo et al. also found that tissue yield was lower from echogenic than from echolucent plaques, although the latter appeared to have a higher rate of subsequent angiographic restenosis [De Lezo, 1993]. Contrary to the view that lumen gain results predominantly from lesion "Dottering", ultrasound has shown that plaque excision, manifest ultrasonically as plaque area reduction, is the predominant contributor to luminal enlargement [Braden, 1994].

A large residual plaque burden is frequently evident despite angiographically successful atherectomy (**figure 1.7a** and **1.7b**). The residual plaque burden was 43% of vessel cross-sectional area in the GUIDE trial [Fitzgerald, 1993], and 35% in de Leso's series [De Lezo, 1993] compared to angiographic residual diameter stenoses of 14% and 15 % respectively.

When using intravascular ultrasound to guide DCA procedures, the practical difficulty of determining radial and longitudinal orientation of the imaged segment would best be addressed by a combination device that would obviate the need for multiple passes of imaging and cutting catheters. Currently, sequential use of separate imaging and therapeutic catheters is required (adding approximately 15 minutes to procedure time) and radial and longitudinal orientation is achieved by referencing the target lesion to the origin of side branches [Kimura, 1992]. Three dimensional reconstruction will further facilitate the process.

1.7.4. Rotational atherectomy

A sharply delineated, uniformly cylindrical lumen is seen with ultrasound after rotational atherectomy [Mintz, 1992a]. A slightly larger lumen diameter relative to the largest burr used is attributed to off centre rotation of the burr during ablation, or to radial expansion of the vessel following a reduction in the circumferential and radial extent of vessel wall calcification. Fissures and dissections are infrequent and limited in their axial and radial extent and the principal mechanism of lumen enlargement is selective ablation of hard plaque [Kovach, 1993].

1.8. Clinical utility

No convincing evidence is currently available to support an indispensable role for intravascular ultrasound in routine clinical practice, but a number of large studies are addressing this issue at present and will report within the coming 2 years (**table 1.5**).

Intravascular ultrasound is of benefit in clarifying ambiguous diagnostic angiography in cases where an ostial location, branch overlap (**figure 1.8**), lumen eccentricity, or very short 'napkin ring' stenoses obscure the area of interest [White, 1992]. The proportion of diagnostic cases in which such clarification is required because of discordant angiographic and clinical findings is unreported, but is unlikely to be sufficiently high to warrant introduction of intravascular ultrasound into the laboratory for this indication alone. A plaque burden occupying ≥50% vessel cross sectional area was found in 10 of 20 patients with angiographically mild coronary disease [Porter, 1993], but in the absence of lumen compromise, the clinical relevance of non obstructive atheroma is not known and its identification does not at present necessarily aid clinical decision making.

A number of observational studies have assessed the extent to which intravascular ultrasound imaging influences decision making during coronary interventions. In GUIDE I, imaging after PTCA (112 lesions) or DCA (46 lesions) resulted in a change of therapeutic strategy (either with the same device or switching to a more appropriate device depending on lesion morphology) in 48% of cases [Fitzgerald, 1993]. In a multidevice environment, Mintz et al. found pre-interventional imaging influenced subsequent therapeutic strategy in 40% of cases [Mintz, 1994b]. This included revascularisation of doubtful lesions in 6%, deciding against revascularisation in 7%, and a change (6%) or selection (20%) of revascularisation strategy. Stone et al reported a change in therapeutic strategy in 30% of cases [Stone, 1993]. None of these observational studies permit evaluation of the impact of ultrasound guided decision making on short or long term outcome.

Intravascular ultrasound is a sensitive means of determining lesion shape, calcification and presence of dissection, variables that are poorly characterised by angiography and have each been ascribed conflicting predictive significance in

angiographic studies. A number of studies have correlated morphological and quantitative ultrasound findings with subsequent clinical outcome. In a series of 69 patients undergoing PTCA, DCA and excimer laser therapy, dissections evident on ultrasound were associated with a greater likelihood of an adverse outcome (principally restenosis) [Tenaglia, 1992a]. Honye et al. concluded that smooth walled dilatation was significantly more likely to lead to subsequent restenosis when compared to all other morphological patterns after PTCA, but only those who had recurrent symptoms (20%) underwent angiographic follow-up [Honye, 1992]. Mintz et al. have reported preliminary results of follow-up of 124 patients undergoing PTCA, DCA, rotational atherectomy, stent insertion and laser angioplasty [Mintz, 1994c]. Angiographic restenosis (defined as a >50% stenosis at 6 month angiographic follow-up), was associated with smaller minimum lumen area after intervention. Contrary to angiographic data, restenosis was commoner after less rather than more acute luminal gain, an observation consistent with the 'bigger is better' hypothesis [Kuntz, 1993]. Calcification and dissections were also more prevalent in those who restenosed. The PICTURE and GUIDE II trials are multicentre studies that have enrolled 200 and 250 patients respectively to assess the predictive utility of ultrasound morphology and quantitative findings immediately after intervention. Both studies are nearing completion and will report in 1996.

1.9. New developments

1.9.1. Longitudinal orientation and three dimensional reconstruction

Intravascular ultrasound imaging suffers from the lack of a systematic method of longitudinal orientation within the vessel. Following a slow transducer pullback at the start of the study, an operator generates a mental construct of vessel topography, both radially and longitudinally, by relating the image acquired at any given point to side branches, pericardium and landmarks in the vessel wall, and

by intermittent fluoroscopic documentation of transducer position during contrast injection. The variable morphology within atheromatous plaques [Fishbein, 1990] facilitates matching of lesion segments on repeat study. Perhaps because experienced intravascular ultrasound practitioners are accustomed to dealing with sequentially viewed 2D images in this manner, three dimensional reconstruction was assigned a low priority in a recent survey of perceived usefulness of specific future developments [Hodgson, 1994]. The importance of perfecting three dimensional reconstruction lies less in the provision of a readily assimilated display of the vessel (although this may prove useful) than in the development of a reproducible means of longitudinal orientation and capability for volumetric analysis. Inter-study reproducibility, and the feasibility of longitudinal studies of plaque regression or vessel remodelling after interventions depends on this advance. It may also serve to facilitate identification of the point of maximum lumen stenosis within a lesion or stent.

Longitudinal orientation may be achieved using a motorised timed pullback, a displacement sensing device to register catheter movement [Gussenhoven, 1993], or three dimensional roadmapping of the transducer using a simultaneously acquired biplane fluoroscopic recording during pullback [Koch, 1993; Evans, 1993]. Traction of the proximal end of the catheter does not relate in a linear fashion with transducer movement. This is attributable in part to the elasticity and variable stability of the guiding catheter which may straighten or move during the early part of the pullback or when there is increased friction between imaging catheter and the coronary wall. Catheter systems in which the transducer moves within a distal sonolucent sheath that remains in situ during pullback theoretically provide the basis for more accurate longitudinal positioning using either a timed pullback or a displacement sensing device.

Artefactual straightening of the imaged segment, an inevitable shortcoming of the reconstruction process, introduces quantitative and qualitative distortion, compressing the wall on the convexity of a curve and expanding that on its concavity. Restoration of the vessel's three dimensional spatial geometry may be achieved by plotting the ultrasound images along the course of the transducer, the passage of which may be plotted using simultaneously digitised biplane fluoroscopy [Koch, 1993]. Finally, in order to gate out the effect of axial and radial catheter movement during the heart cycle, a pullback speed <1.2 mm per second is required [Hodgson, 1994]. The effects of spiral rotation or prograde/retrograde movement of the catheter tip unrelated to cardiac rotation may still not be identifiable.

The quantitative accuracy of three dimensional reconstruction in depicting the depth and longitudinal extent of dissections in balloon disrupted coronary segments has been confirmed in vitro [Coy, 1992]. Substantial clinical experience in the application of three dimensional reconstruction is largely confined to peripheral vessel imaging. Rosenfield and colleagues reporting their experience using off-line [Rosenfield, 1991] and on-line [Rosenfield, 1992] three dimensional reconstruction of peripheral vessels, before and after angioplasty, noted that the course and depth of dissections was better appreciated on reconstructed segments. In vitro reconstuction of Palmaz-Shatz, Wiktor, Medinvent and Strecker stents produced detailed representations of each stent type [Mintz, 1993], but in vivo reconstruction of Palmaz-Shatz stents using the same algorithm was less successful, confounded by both motion artefact and the presence of echodense tissue indistinguishable from the stent struts. That such difficulties were encountered despite elimination of vessel pulsation highlights the problems that must be overcome before coronary reconstruction becomes accurate and reproducible.

1.9.2 Tissue characterisation

The differences in tissue structure that result in alterations in its ultrasonic backscattering properties may be capitalised on to develop an objective method of tissue characterisation. This has proved a difficult and frustrating task using transthoracic echo. The specific environment of intravascular imaging, in which high frequencies are used, interrogation distances are short and signal attenuation by the intervening blood is small, gives cause for optimism that such a system may be developed using intravascular ultrasound. Simple videodensitometric analysis has proved disappointing [Peters, 1994e]. The more sophisticated statistical methods of tissue classification, including such techniques as pattern recognition and texture analysis, may be more productive, particularly if applied to 'customised' images processed from the radiofrequency data in a more accurate manner than is performed by commercial scanners. The most promising approach involves direct study of radiofrequency parameters, including the frequency, amplitude and phase shift of the signal, to determine correlations between the different tissue types and their acoustic behaviour [Linker, 1989; Urbani, 1993; Spencer, 1995].

1.9.2. Other technical developments

Smaller transducers are being developed and a 0.035" imaging wire is currently undergoing clinical evaluation [Tenaglia, 1993]. Efforts to produce more sophisticated, focused transducers are actively being pursued. A micromotor is being developed to allow combination of the advantages of mechanical, single element transducers with optimal catheter shaft characteristics, and to eliminate rotation angle artefacts. The feasibility of forward-look imaging has been tested with a prototype 4.0 mm diameter catheter that provides B-mode images up to 2.0 cm anterior to the catheter tip [Evans, 1994]. If miniaturisation proves feasible, it may have an application in assessing the length of total occlusions or assessing highly stenotic segments through which a standard imaging catheter cannot be

passed or as an alternative strategy to produce a three dimensional reconstruction of the vessel [Ng, 1994]. Combined imaging and therapeutic catheters (both imaging balloons and atherectomy devices) are already available, but their widespread application awaits demonstration of the clinical utility of stand-alone intravascular ultrasound in the current set of clinical studies.

1.10. Conclusions

Intravascular ultrasound is an imaging modality that provides unique information concerning vascular morphology and function. It has already taught us a great deal concerning the mechanisms of coronary interventional procedures and promises to revolutionise our understanding of the process of restenosis. The changes that occur in allograft arteriopathy and coronary atheroma during lipid lowering therapy are currently under intensive investigation with intravascular ultrasound, promising to afford more effective preventive and therapeutic strategies. The precise role of intravascular ultrasound in clinical practice is currently being assessed in multicentre studies that will report in the near future. Its incorporation into regular practice is dependent on a convincing demonstration of cost-effectiveness as well as clinical utility. The lack of a common terminology is an unresolved problem that should be addressed by consensus agreement on standard definitions of the morphological and quantitative parameters encountered in intravascular ultrasound imaging. Improvements in image quality and catheter design appear now to be plateauing with similar image quality being offered by different systems. Likely future developments include three dimensional reconstruction, the ability to better characterise wall constituents using radiofrequency data and combination with Doppler analysis to fully characterise the functional status of the artery. It is clear that intravascular ultrasound will continue to be used as a powerful research tool in reference centres, but its more widespread application in the assessment and treatment of coronary disease depends on the outcome of current clinical trials.

Table 1.1 In vivo correlations of ultrasound and angiographic lumen diameter measurements

	correlation co-efficient	direction of bias	mean minimum diameter (mm) IVUS	angiography
"Normal segments"				
Nissen, 1990*	0.98	IVUS < angio	5.6	5.7
De Scheerder, 1994	0.92	IVUS < angio	3.5±0.7	3.6±0.7
Nissen, 1991	0.92	IVUS < angio	2.88±0.57	2.83±0.52
Alfonso, 1994	0.59	IVUS ≤ angio	3.5±1.0	3.6±1.0
Tobis, 1991b	0.26	IVUS > angio	3.0±11	3.0±1.0
St. Goar, 1991	0.86	IVUS > angio	3.8±0.9	3.4±0.8
Diseased segments				
De Scheerder, 1994	0.47	IVUS < angio	2.1±0.4	2.7±0.4
Nissen, 1991	0.77	IVUS < angio	3.11±0.76	3.17±0.83
Mintz, 1994b	0.83	IVUS > angio	1.6±0.6	1.1±0.8
Porter, 1993	0.59	IVUS > angio	3.3±0.9	2.7±0.8
Post intervention				
De Scheerder, 1994	0.28	IVUS < angio	1.9±0.3	2.1±0.5
Nissen, 1990*	0.86	IVUS ≤ angio	6.7	6.6
Tobis, 1991b	0.12	IVUS > angio	2.2±0.6	1.9±0.5
Davidson, 1991	0.28	IVUS > angio	-	-

* Canine peripheral arteries. All other studies were performed in living human subjects.

Table 1.2 Reasons for the discrepancy between angiographic and ultrasound measurements

Angiographic underestimation of lumen diameter
False lumen (dissection) not incorporated into angiographic measurement of diameter
Reduced contrast density at wall/lumen interface as a result of non-laminar flow
Intravascular ultrasound overestimation of lumen dimensions
Low dynamic range leading to weak intimal signal dropout
Scanner miscalibration
Rotation angle artefact in eccentrically positioned catheters
Non-coaxial alignment of catheter within the vessel (rare in the coronary arteries).
Direct splinting of disrupted vessel wall by catheter
Indirect splinting of vessel wall (increased intraluminal pressure and wall tension)
Observer bias

Table 1.3: Comparisons between IVUS tissue identification and histology

STUDY	TISSUE	SENSITIVITY	SPECIFICITY
Potkin, 1990	lipid	78% (7/9)	97% (100/103)
	fibrous	96% (81/84)	93% (26/28)
	calcific	100% (19/19)	100% (93/93)
Di Mario, 1992	lipid plaque	89% (32/36)	97% (62/64)
	fibrous plaque	67% (32/48)	100% (52/52)
	calcium	97% (35/36)	98% (63/64)
Peters, 1994c	lipid deposits	46% (16/35)	97% (67/69)
	calcific deposits	77% (20/26)	100% (78/78)
Siegel, 1991	normal	100% (12/12)	95% (58/61)
	stable atheroma	100% (18/18)	90% (52/58)
	disrupted intima	84% (26/31)	96% (44/46)
	thrombus	57% (8/14)	90% (51/57)

Table 1.4 Interobserver reproducibility of qualitative characteristics

Feature		Kappa	% Agreement
Intimal thickening	Circumferential	0.35	71
	Partial	0.31	60
	None	0.16	19
Lipid deposits	Present	-0.16	0.2
	Absent	-0.16	82
Calcium deposits	Present	0.86	97
	Absent	0.86	90

A kappa value of 1 indicates complete agreement, a value of -1.0 indicates complete disagreement, and a value of 0.0 indicates no agreement

Table 1.5a Observational studies (MC = multicentre)

Study	Devices	Patients	Centre	Aims (A) and Results (R)
GUIDE I	PTCA/DCA	187/187	Stanford (MC)	**A:** Angio vs. IVUS evaluation **R:** Significant discrepancy in assessment of plaque distribution, composition and morphology
GUIDE II	PTCA/DCA	425/500	Stanford (MC)	**A:** IVUS predictors of restenosis **R:** Post procedural plaque burden and IVUS MLD predict angiographic restenosis and clinical events
PICTURE	PTCA	200/200	Amsterdam (MC)	**A:** IVUS predictors of restenosis **R:** Plaque composition and morphology not predictive; absence of dissection, MLA, and plaque burden are
SURE	PTCA/DCA	50/100	Japanese (MC)	**A:** Restenosis mechanisms **R:** 'Negative remodelling' the predominant mechanism of restenosis. Occurs as a late event (1-6months)
WCC	All	>4000	Washington	**A:** Predictors of restenosis **R:** Plaque burden the most powerful predictor or restenosis
OARS	DCA	200/200	Boston (MC)	**A:** Acute gain/restenosis mechanisms **R:** Lumen gain due to tissue extraction-58%; VA increase-27%; adjunctive PTCA-15%. Most of late loss (86%) 2° to remodelling
Columbus	Stents	1183	Milan	**A:** IVUS vs. Angio evaluation of stents **R:** Despite a favorable angiographic appearances, 80% of stents are underexpanded. Omission of anticoagulation appears safe when certain criteria are met. Restenosis reduced to >20% when optimal adequate stent expansion achieved

Table 1.5b Hypothesis testing (uncontrolled) studies

Study	Devices	Patients	Centre	Aims (A) and Results (R)
INSPIRE	PTCA	123/500	Cleveland Clinic	**A:** Utility of IVUS guidance to select balloon and evaluate outcome **R:** N/A
MUSIC	Stent	98/200	Rotterdam	**A:** Safety of omitting anticoagulation following IVUS guidence **R:** N/A
RAVES	Stent	pilot/200	Washington	**A:** Safety of omitting anticoagulation following IVUS guidence in grafts **R:** N/A
ABACUS	DCA	103/200	Japanese (MC)	**A:** Aggresive debulking with IVUS guidence lowers restenosis **R:** Aggressive IVUS guided DCA leads to a residual plaque area of 48% (44% after adjunctive PTCA). Complications not increased

Table 1.5c Randomised trials

Study	Devices	Patients	Centre	Aims (A) and Results (R)
CLOUT	PTCA	65/500	Cleveland associated hospitals	**A:** IVUS measurement of vessel diameter to guide balloon upsizing **R:** Upsizing necessary in 86%. Further dilatation increases MLA by 40%, residual LD stenosis of 18%, without complications
ASSURE	PTCA/Stent	25/230	Edinburgh/Mainz	**A:** Selection of lesions for stent implantation following PTCA to reduce restenosis **R:** Successful pilot completed.

Figure 1.1 HIstological cross-section of a diseased coronary artery.

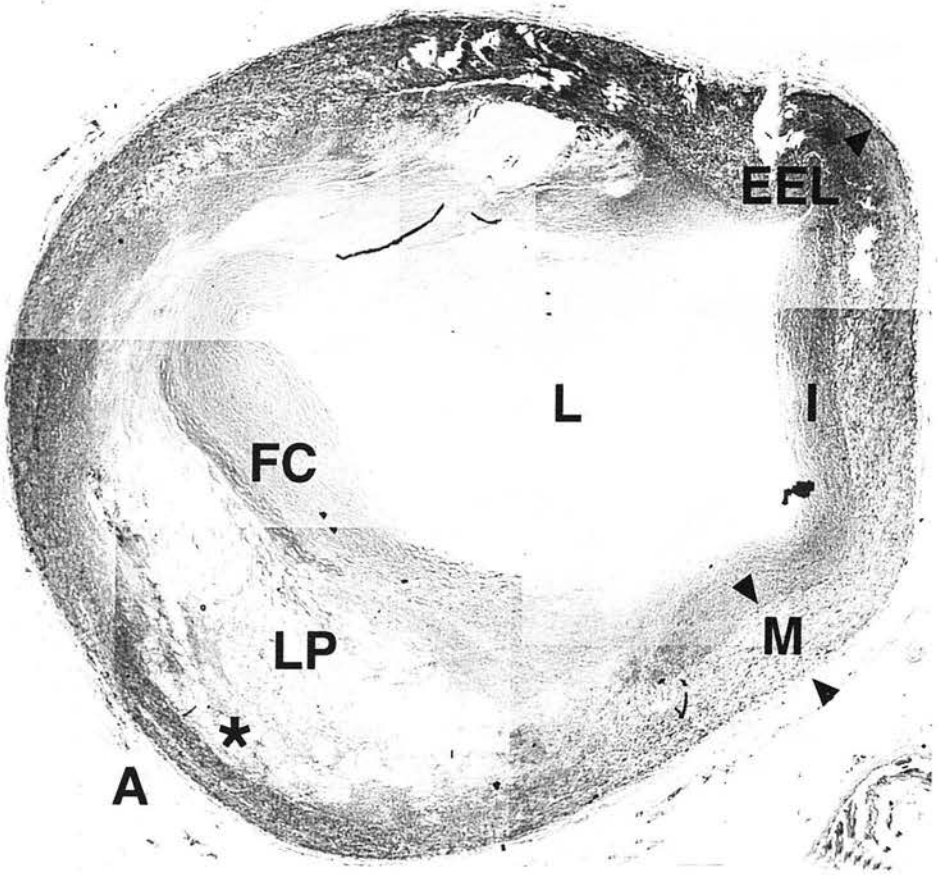

An eccentric plaque extending from 4 to 2 o' clock is made up of a fibrous cap (FC), and a central lipid pool (LP). Thinning of the media (M), indicated by the asterisk (*), is seen at the point of heaviest plaque formation. Mildly thickened intima (I) is seen from 2 to 4 o'clock. Although the external elastic lamina (EEL) is seen as a discrete dark line at 2 o'clock, the internal elastic lamina is not visible.

Figure 1.2 **Schematic diagram of the morphometric measurements made with intravascular ultrasound**

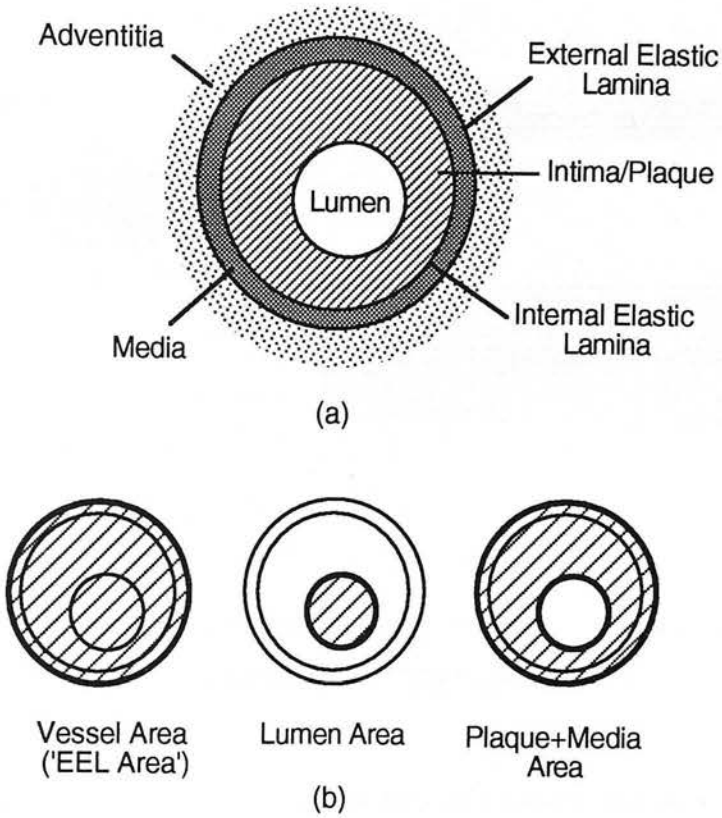

Upper panel (a): *Schematic of arterial wall structure.*

Lower panel (b): *Examples of IVUS measurements (outlined in bold) of vessel, lumen and plaque cross-sectional area are seen beneath. Vessel cross-sectional area is measured by tracing the outer perimeter of the echolucent layer (media), corresponding with the course of the external elastic lamina. The perimeter of the blood / intima interface is traced to measure the cross-sectional area of the lumen. 'Plaque', 'lesion' or 'intimal' cross-sectional area is calculated from the difference of vessel and lumen areas.*

Figure 1.3 **Basis for the discrepancy between angiographic and ultrasound measured 'percentage stenosis'**

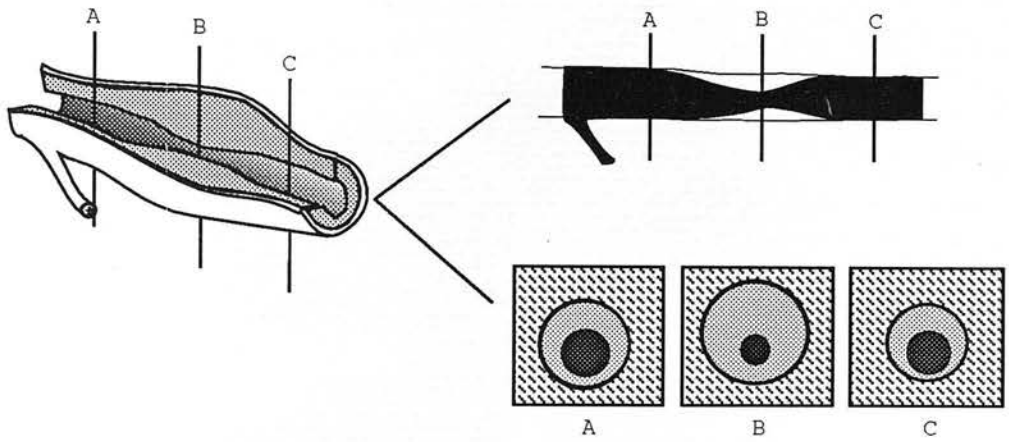

Left hand panel: *A schematic illustration of a focally stenosed coronary arterial segment. Line A transects the proximal lumen, B the point of minimum lumen dimensions, and C the distal lumen.*

Right upper panel: *The angiographic appearance of the same vessel, lines A and C transecting the 'normal' reference segments against which the diameter stenosis is evaluated by either caliper or automated edge detection systems.*

Right lower panel: *IVUS demonstrates diffuse intimal thickening at A and C, and vessel cross-sectional area expansion at the point of focal luminal stenosis B. Both factors explain the discrepancy between the >90% vessel cross-sectional area stenosis measured by IVUS and the angiographically derived calculated lumen cross-sectional area stenosis of 70% between points A/C and B.*

Figure 1.4 Ultrasound appearances of coronary artey tissue types

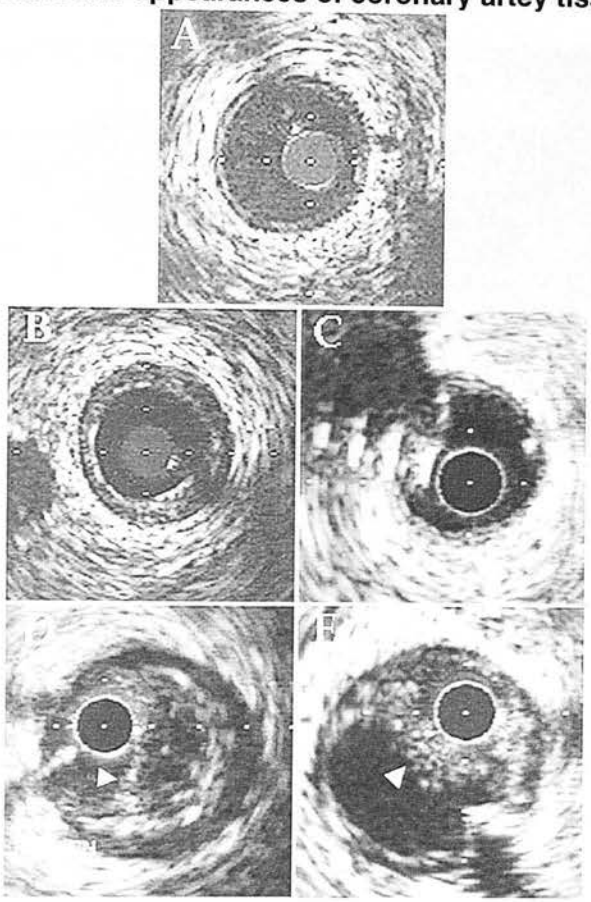

A. *Normal arteries are circular, and usually have a thin intimal leading edge giving rise to a 'three layer' appearance.*

B. *Moderately echodense circumferential intimal thickening is evident. This pattern usually corresponds to smooth muscle cells and fibrous tissue.*

C. *Calcium is distinguished by a highly echodense leading edge and distal acoustic shadowing. Reverberations are seen within the acoustic shadow.*

D. *Lipid pools may be identified as echolucent zones within the body of a plaque (11 to 7 o'clock). The catheter blank occupies much of a small, eccentrically placed lumen (7 to 11o'clock), and lies against a thin fibrous cap (arrow head).*

E. *Intracoronary thrombus may have a granular, finely speckled ultrasound appearance. Intraluminal thrombus lies between the catheter blank and the remainder of the lumen.*

Figure 1.5 'Inner layer' of thrombus in an acute coronary lesion

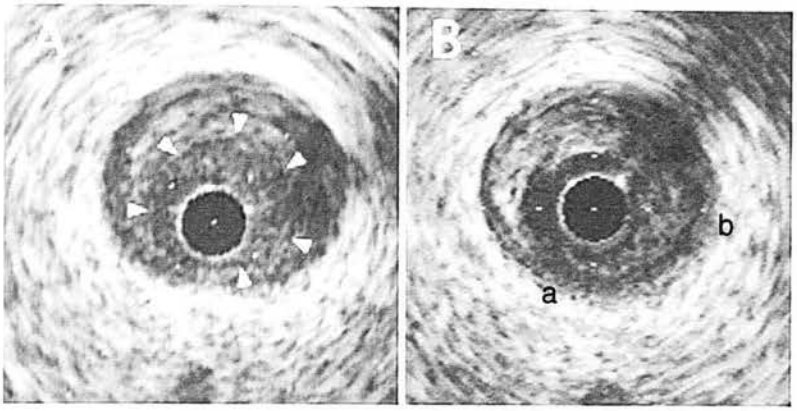

A set of echographic markers highly suggestive of thrombus has been identified in acute coronary lesions.

***A.** A subtle echographic interface (arrowheads) demarcates an inner layer of probable thrombus.*

***B.** Lumen area increase following angioplasty resulted from remodelling of the layer rather than vessel stretch. The plaque has torn at its thinnest point (a) and a subintimal dissection runs counterclockwise from 6 to 3 o'clock (as far as point b).*

Figure 1.6 Dissection commonly occurs adjacent to focal calcification

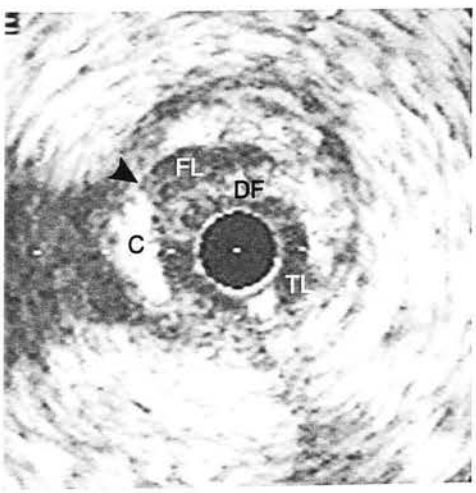

Dissection frequently occurs at the junction of fibrous plaque with focal calcific deposits, indicated in this image by the black arrowhead. TL: true lumen, FL: false lumen, DF: dissection flap, C: calcific deposit.

Figure 1.7a Subacute lesion before and after PTCA, and after DCA

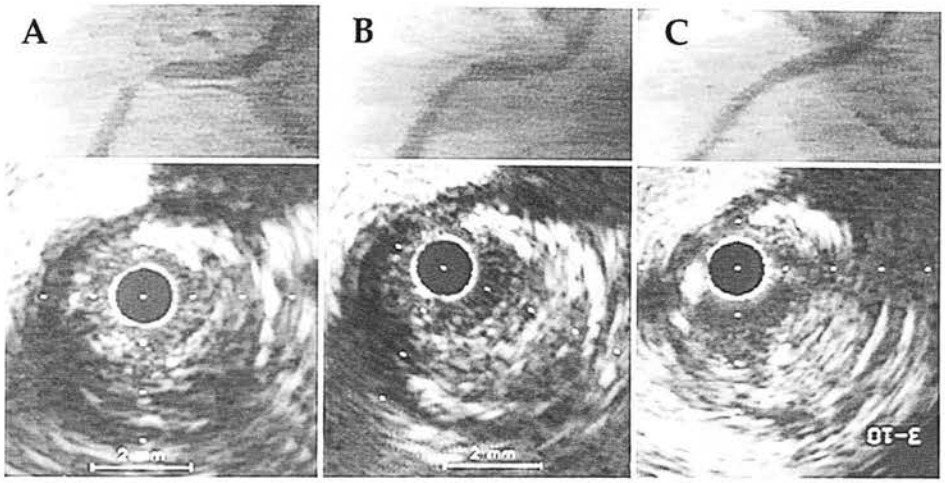

A. *In this patient 3 weeks after inferior wall myocardial infarction, angiography (upper left panel) revealed a high-grade, concentric stenosis in the proximal right coronary artery. Intravascular ultrasound at the stenosis (lower panel) revealed wedging of the catheter blank within a large, eccentric lesion. A demarcated layer of proable organising thrombus encircles the lumen. A focus of deep calcification is evident at 12 to 2 o'clock.*

B. *Following balloon angioplasty, angiography suggested a moderate residual stenosis.. Ultrasound revealed inadequate lumen gain that appeared to be the result of vessel stretch and incomplete remodelling of the inner layer.*

C. *Directional coronary atherectomy gave rise to an excellent angiographic appearance (upper panel). Although intravascular ultrasound confirmed a doubling of lumen area, and showed a number of discrete 'bites' into the plaque from the atherectomy device (3 and 6 o'clock) a residual plaque burden of >60% of vessel cross-sectional area was evident.*

Figure 1.7b Successful wall-wrap of a calcific flap distal to the treated lesion

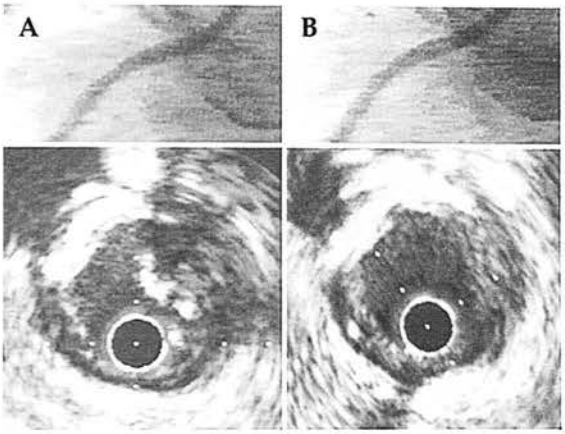

A. *Despite the excellent angiographic profile of the vessel, a discrete calcific flap was identified on ultrasound distal to the point of prior stenosis that was probably dislodged by the end of the atherectomy device.*

B. *A low pressure balloon inflation for 40 seconds tacked the flap back into place (right lower panel). The angiogram was not appreciably different after wall wrapping.*

Figure 1.8 Clarification of ambiguous angiography with IVUS

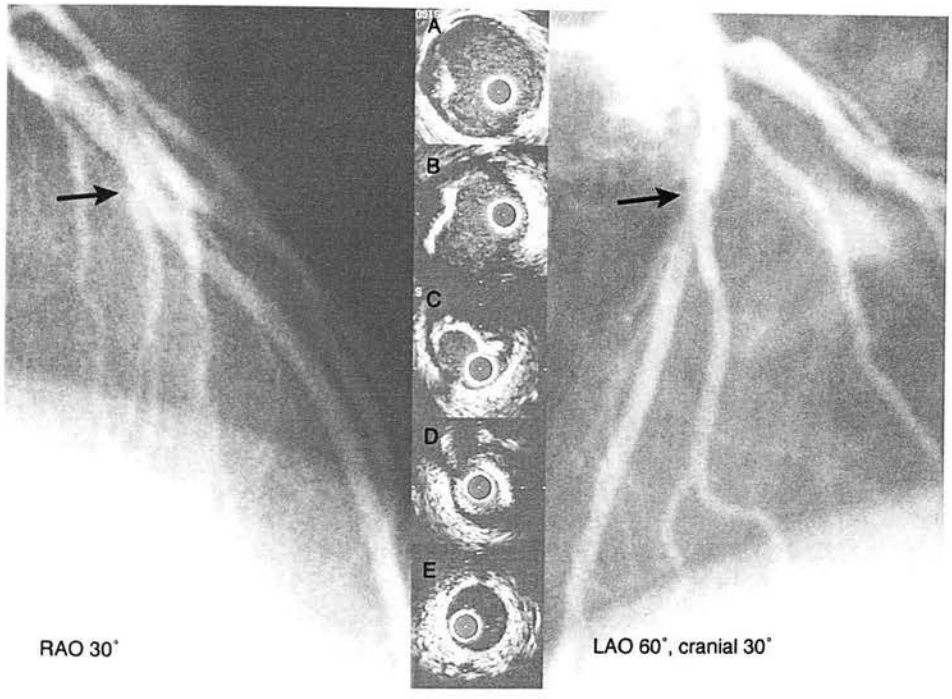

The angiogram of the left anterior descending artery of a 45 year old man who presented with a 6 month history of angina, and an exercise ECG positive for both symptoms and electrical changes. His coronary angiogram was reported as normal. A subsequent excercise thallium scintigram revealed a reversible anterior wall perfusion defect. In view of overlap of branches at the origin of the first septal perforator (black arrow), that were not separated in any angiographic projection, he was referred for intravascular ultrasound study.

A *There was a small, eccentric fibrous plaque in the left main coronary artery.*

B *At the origin of the left circumflex artery is a larger eccentric, and angiographically inapparent calcific plaque*

C *This 'silent' plaque extends into the proximal left anterior descending artery.*

D. *A tight and very focal 'napkin-ring' stenosis is clearly seen at the origin of a septal perforator*

E. *The distal vessel is both angiographically and ultrasonically normal.*

Chapter 2

A Comprehensive Analysis of the Short Term Reproducibility of Intravascular Ultrasound Quantitation

Contents *page*

2.1. Introduction

An imaging technique must be accurate, precise, and reproducible in order to document the small absolute changes in wall thickness and lumen dimensions that constitute coronary restenosis and atheroma regression or progression. For example, the absolute mean lumen diameter loss at 6 months after successful PTCA in 1445 lesions was 0.28±0.52 mm [Rensing, 1992]. The mean increase in the angiographic lumen diameter following 4 years of lipid lowering therapy in the Multicentre Anti-Atheroma Study (MAAS) study was just 0.08 mm (95% confidence interval 0.03-0.14 mm) [MAAS investigators, 1994]. These measurements were made using quantitative coronary angiography based on automated lumen edge detection algorithms that are known to be highly exact. Importantly, they have been shown to be reproducible in conditions that pertain during the routine acquisition of such data. Despite conforming with these rigorous requirements, quantitative coronary angiography, based as it is on contrast lumenography, is an indirect descriptor of the events that occur in the vessel wall. Intravascular ultrasound offers the advantage of directly documenting these changes. The accuracy of intravascular ultrasound quantitation has been established [Nishimura, 1990; Nissen, 1990], but the reproducibility of what is a manual, operator dependant method of measurement is not adequately defined. Similarly detailed information as has been acquired for quantitative angiography is needed for intravascular ultrasound before it is employed in large scale research protocols that involve longitudinal quantitative analyses. The one published study addressing this issue to date confined itself to the analysis of the reproducibility of measurements of single, pre-selected frames [Hausmann, 1994b]. In this study we investigated the short term reproducibility of intravascular ultrasound measurements in circumstances that closely approximate the conditions which operate in clinical practice.

2.2. Study Aims

We aimed to establish the short term reproducibility of measurements of coronary artery lesions made with intravascular ultrasound in the clinical setting.

2.3. Methods and materials

The short term reproducibility of morphometric measurements made in unselected frames at the site of operator defined minimum lumen area was assessed in a consecutive series of patients undergoing intracoronary ultrasound imaging employing a standardised examination protocol. Eighty-eight lesions were imaged in 82 intravascular ultrasound studies conducted in 46 patients. There were three lesion subtypes, the first consisting of coronary stenoses undergoing evaluation for diagnostic purposes or prior to intervention (36), the second consisting of lesions after balloon angioplasty (22) and the third consisting of coronary stents (30).

2.3.1. Intravascular ultrasound imaging protocol

Intravascular ultrasound studies were performed using a Hewlett Packard 'Sonos Intravascular' ultrasound scanner and Boston Scientific 'Sonicath' 3.5 F ultrasound catheters. All patients received either sublingual nitrate (1 milligram) immediately prior to the procedure or were on an intravenous infusion of nitrate. Having engaged the artery of interest with the guiding catheter, the intravascular ultrasound catheter was advanced over a 0.014 inch guide wire to a point within the vessel distal to the segment of interest. The catheter was manually withdrawn in a controlled manner at a rate of approximately 1 millimetre per second. After the transducer was withdrawn into the guiding catheter it was advanced a second time distal to the lesion and the pullback was repeated in the same manner. Further catheter passes were performed in cases where the operator felt that an area of interest required further scrutiny or imaging of a specific segment with a stationary

transducer was thought necessary. During IVUS imaging, a simultaneously acquired electrocardiogram was recorded and displayed beneath the video image.

2.3.1.1 Observers

Measurements were made by two observers. Both were experienced in the theory and practice of intravascular ultrasound. Observer #1 has performed >400 procedures, and observer #2 has been involved in >100 procedures.

2.3.1.2 Methods of measurement

Manual measurements were made off-line using the trackball and the integrated quantitation software of the ultrasound scanner. The quantitative analysis system is automatically calibrated for on-line measurements, but requires manual calibration using the millimetre grid on the screen for off-line analysis. Whenever possible, systolic frames (identified by the T wave of the ECG), were chosen for quantitation. The outer border of the vessel corresponding with the external elastic lamina was traced to measure vessel cross-sectional area (VA), and the endoluminal border was traced to measure lumen cross-sectional area (LA). Plaque cross-sectional area (PA) was calculated as the difference between the vessel and lumen cross-sectional area. Vessel area stenosis was calculated as (1 - LA/VA x 100). Lumen diameters were measured by marking each end of subjectively defined maximum and minimum diameters. Vessel area measurement was not performed in the stented lesions because of strut induced acoustic shadowing and/or loss of the plaque/adventitia demarcation following tissue compression by the stent. Vessel area could not be determined because of acoustic shadowing of more than 60° in 3/22 PTCA lesions and 14/36 diagnostic or pre-interventional lesions. Quantitative parameters computed indirectly from lumen and vessel area (plaque area and percentage stenosis) were not determined in those cases in which excessive calcification was present and following coronary stenting.

Measurements were automatically displayed on the console's screen and hard copies were printed from which the data was entered into a statistical analysis program spreadsheet. The time in hours, minutes and seconds and the frame count per second (1-24) is continuously displayed on the screen to allow precise identification of selected frames.

2.3.1.3 Reproducibility of measurements on unselected frames

The reproducibility of measurements made on unselected frames was assessed in three different ways. Firstly, the site of minimum lumen area was identified by one observer (observer #1) from sequential catheter pullbacks and time and frame number recorded and vessel dimensions measured at the site of minimum lumen area for each of the catheter passes. Secondly, in a separate analysis session at least 2 weeks after the first, the minimum lumen area was identified from any of the pullback sequences and the vessel measured a second time by observer #1 at that point. Thirdly, two observers were asked to individually identify the site of minimum lumen area during a pullback through a focal stenosis in separate analysis sessions. The time and frame number were noted and lumen dimensions measured by each observer.

2.3.1.4 Reproducibility of measurements on pre-selected frames

Single, pre-selected frame analysis was performed following the analysis of unselected frames. A frame on which the minimum lumen area was identified by observer #1 was analysed by that observer on two separate occasions 2 weeks or more apart to determine the degree of intraobserver variability and by observer #2 to determine interobserver variability.

2.3.1.5 Statistical analysis

Reproducibility was determined by calculating the mean difference between measurements as a measure of systematic bias and the standard deviation (SD) of the differences as a measure of random variation. Both are expressed as an

absolute value as well as a percentage of the average of each pair of measurements. The 95% limits of agreement were calculated as twice the standard deviation. Bland-Altman plots were constructed by plotting the mean difference against the average of paired measurements in order to assess the impact of absolute dimensions on variability and to visually assess the degree and direction of any bias [Bland, 1986]. The statistical significance of the bias between repeated measures was determined using paired student's t tests (significance defined as ≤0.01). Significant differences between the variability (measured as the standard deviation) of each analysis protocol was determined using Bartlett's test, with subsequent application of the 'F ratio' test to detect significantly different variability between any two of the groups. Statistical analysis was performed using a commercially available statistical programme (Statview v4.2).

2.4. Results

2.4.1. Intraobserver analysis - pre-selected frames (A)

There was no significant bias for any parameter measured on separate occasions from a pre-selected frame and in no case was the standard deviation > 10%. The mean difference and standard deviation for each of the quantitative parameters are given as absolute values and as a percentage of the mean of the repeated measurements (in brackets) in **table 2.1(A)** and are shown in **figures 2.1-2.6**.

2.4.2. Intraobserver analysis - sequential pullbacks (B)

Measurements made in unselected frames at the site of minimum lumen area were also highly reproducible. No significant bias was noted for any of the quantitative parameters, and the random variability was as low as that for the pre-selected intraobserver frame analysis. Random variability did not exceed 10% of the mean measurement of any parameter. The mean difference and standard deviation for each of the quantitative parameters, both as absolute values and expressed as a

percentage of the mean of the repeated measurements (in brackets) are given in **table 2.1(B)** and are shown in **figures 2.1-2.6**.

2.4.3. Intraobserver analysis - unselected frames (C)

The mean difference between measurements made at the site of minimum lumen area determined 2 weeks apart, although higher than that demonstrated in either of the previous analyses, were of negligible absolute proportions and not statistically significant. Random variability exceeding 10% was noted in the measurements of minimum lumen diameter (11.6%), lumen area (12.1%), vessel area (10.2%), and plaque area (13.8%). The mean difference (bias) and standard deviation for each of the quantitative parameters are given as absolute values and as a percentage of the mean of the repeated measurements in **table 2.1(C)** and are shown in **figures 2.1-2.6**.

2.4.4. Interobserver analysis - pre-selected frames (D)

The bias and random variability between measurements made by two observers were larger in all cases than those observed in both selected and unselected frame intraobserver analysis protocols. The measurements made by observer #2 were larger than those of observer #1 in the case of maximum lumen diameter (by 0.10 mm) and lumen area (by 0.18 mm^2), amounting to 5.4% and 8.3% of the average maximum lumen diameter and lumen area respectively. The standard deviation of the difference was greater than 10% of the average absolute measurement for all parameters apart from percent stenosis and was as high as 23% for lumen area and plaque area. The mean difference and standard deviation for each of the quantitative parameters are given as absolute values and as a percentage of the mean of the repeated measurements in **table 2.1(D)** and are shown in **figures 2.1-2.6**.

2.4.5. Interobserver analysis - unselected frames (E)

The variability between measurements made by separate observers in unselected frames at the site of MLA was of a similar order to that seen in pre-selected frames (analysis D). The mean difference and standard deviation for each of the quantitative parameters expressed in terms of absolute values and as a percentage of the mean of the repeated measurements are given in **table 2.1(E)** and are shown in **figures 2.1-2.6**.

2.4.6. Impact of lesion type

The impact of different lesion types on the reproducibility of measurements was analysed in the protocol in which other variables were least likely to have confounding effects, i.e. protocol A, the intraobserver analysis in selected frames. Bartlett's test indicated a difference in the variability of measurements of minimum lumen diameter and lumen area between pre-interventional/diagnostic, post PTCA and stented lesions but not for the other quantitative parameters (maximum lumen diameter, vessel area, plaque area or percentage stenosis). The variability of minimum lumen diameter in PTCA lesions (SD = 0.19 mm) was significantly greater than that for pre-interventional/diagnostic lesions (SD = 0.10 mm), but not that for stented lesions (SD = 0.13 mm). Measurements of lumen area were significantly more variable in stented lesions (SD = 0.30 mm^2) than in pre-interventional/diagnostic lesions (SD = 0.18 mm^2), but did not differ from post-angioplasty lesions (SD = 0.25 mm^2). When the absolute value of the standard deviation of repeated measurements of lumen area was plotted against the average lumen area, it was apparent that the absolute value increased as lumen area increased (**figure 2.7**). However, when expressed as a percentage of the average of the repeated measurements and plotted against lumen size, it was apparent that random variability, as measured by the standard deviation, was proportionately greater in smaller lumens (**figure 2.8**).

2.5. Discussion

2.5.1. The significance of unselected frame analysis

On a coronary angiogram, the maximum lumen stenosis is visible for the duration of the coronary injection as it contemporaneously opacifies the length of the coronary artery. In contrast, using intravascular ultrasound the minimum lumen area is identified from sequential tomographic images acquired during the longitudinal passage of the transducer through the segment of interest. At any time during the imaging sequence the vessel is imaged as a tomogram with a slice thickness equal to the lateral resolution of the transducer. The process of identifying the site of maximum stenosis from a sequential series of tomographic images requires observer registration and retention in memory of the vessel's changing dimensions and is clearly a different process to identifying a stenosis on a coronary angiogram. Selection of the site of minimum lumen dimensions is a potentially significant contributor to variability that is not considered in pre-selected frame analysis of reproducibility. Our study design of repeated measurements made at the site of minimum lumen area identified on sequential passes of the imaging catheter was devised to determine the reproducibility of measurements in different imaging sequences. This is allowed us to establish the short term quantitative reproducibility in unselected video frames that may be more applicable to clinically acquired data than studies based on selected frames.

2.5.2. Intraobserver variability

The intraobserver analysis performed on single, pre-selected video frames revealed no clinically significant bias. The relatively low levels of random variability were similar to the values found in a previous study [Hausmann, 1994b]. The variability of IVUS measurements of minimum lumen diameter in these circumstances (standard deviation = 0.15 mm) was very similar to that of

quantiative angiographic measurements of minimum lumen diameter in selected cine frames (standard deviation = 0.10 mm) [Reiber , 1985].

The variability of measurements made on sequential catheter withdrawals was unexpectedly found to be of a similar order to that of the selected frame analysis. We anticipated that the two part process of firstly selecting the frame showing the site of minimum lumen area followed by measurement of the various quantitative parameters would increase variability. However, the course of an ill-defined endoluminal boundary or external elastic lamina may more easily be interpreted by referring to the appearances in adjacent frames. Any tendency to increased variability in the 'unselected' frame analysis thus appeared to be offset by the advantages of sequential frame analysis. Random variability in this analysis protocol compares favourably to the short term variability reported for unselected cineangiographic recordings (the standard deviation of ultrasound measured minimum lumen diameter was 0.15 mm compared to 0.34 mm for cineangiography). Importantly, this part of our study also confirmed that the point of maximum lumen compromise is reproducibly identified in separate passes of the transducer within the vessel.

The greatest variability was demonstrated in the unselected analysis of lesions 2 weeks or more apart. Systematic bias remained small and the standard deviation for minimum lumen diameter of 0.22 mm compares favourably with the previously cited figure for short term variability using quantitative angiography of 0.34 mm. However, when considered as a proportion of the mean vessel size, the standard deviation for minimum lumen diameter (11.6%), lumen area (12.1%), vessel area (10.2%) and plaque area (13.8%) all exceed 10%. The 95% limits of agreement were as high as 2.08 mm^2, amounting to 27% of the average plaque area. The absence of a learning effect may have increased the variability noted in this analysis.

2.5.3. Interobserver variability

The interobserver variability in pre-selected frames, although no greater than that reported by other groups [Hausmann, 1994b; Peters, 1994b], proved to be greater than the variability associated with both pre-selected and unselected intra-observer analyses. Greater interobserver variability may relate to the selection of different sites within the vessel for quantitation, but a similar level of variability noted for both pre-selected and unselected interobserver analyses argues against this playing a major role. Differences in identifying the critical interfaces between lumen and plaque and the plaque/media and adventitia are almost certainly contributors to interobserver variability, but the absence of a consistent interobserver bias for measurements in our study do not point to systematic differences in image interpretation.

2.5.4. Impact of vessel dimensions on variability

No influence of size on the variability of measurements, manifest as divergence of data points from the zero line represented by the x-axis, can easily be discerned on the Bland Altman scattergrams (**figure 2.1-2.6**). However, when we plotted the standard deviation against groups of measurements divided according to lumen size, it was apparent that random variability tended to increase as lumen area increased (**figure 2.7**). The identification of the minimum lumen area is less easily discriminated as the difference between it and adjacent segments diminishes. Possibly for this reason, lumen area measurements in stented segments appeared to be more variable than in pre-interventional lesions. Although the absolute value of the standard deviation was smaller in smaller lumens, it was nevertheless proportionately greater in these circumstances (**figure 2.8**).

2.5.5. Potential impact of non-standardised quantitative definitions

Because no generally accepted definitions of vessel dimensions have as yet been proposed, systematic differences between measurements made by different individuals and/or institutions may arise, depending on the choice of quantitative definition. Lumen diameters may be measured in at least 5 different ways, as detailed in chapter 1, paragraph 1.4.5. The subjective choice of lumen diameters, the most frequently applied method, is subject to certain shortcomings. Whereas the maximum lumen diameter is usually readily identified, the selection of the minimum diameter may be difficult in cases in which the borders of the lumen are irregular and incorporate sections that protrude convexly into the lumen. In this study, the variability of minimum lumen diameter measurements was generally greater than that for maximum diameters (**figure 2.1, 2.2**). Use of an objective method, such as the automated determination of the minimum diameter through the geometric centre of the lumen, may be preferable. Similar inconsistencies may also apply in measuring the vessel area, which may be taken to mean an area enclosed by the outer boundary of the media (the 'external elastic lamina area' [Potkin, 1992]) or by the inner boundary of the media (the 'internal elastic lamina area' [Hausmann, 1994b]). Significant differences in the measurement of both vessel area and the derived measurement of plaque area may result, depending on the choice of the external or internal elastic lamina as the outer boundary of the vessel.

2.5.6. Previous studies

The one previous published study of the reproducibility of intravascular ultrasound measurements in selected frames found low intra- and interobserver variability for all measured parameters, although higher variability for derived parameters including plaque area and percent stenosis was noted [Hausmann, 1994b]. Our findings for intra- and interobserver reproducibility in the selected frame analysis are very similar to theirs. All systematic differences both within and

between observers were <10% of the mean measurement, and similar standard deviations were noted. Our study protocol extends these findings, confirming high reproducibility in the less predictable circumstances of sequential catheter passes and in unselected image sequences. Although lumen diameters were automatically determined following delineation of lumen area in the study of Hausmann et al. [Hausmann, 1994b], the reproducibility of subjectively chosen diameters in our single frame analysis was of a similar order.

Peters et al. determined both quantitative variability in single video frames and the beat to beat variability in sequential systolic and diastolic frames [Peters, 1994b] 10]. Greater random variability was observed in the inter - than in intra-observer comparisons. Variability appeared to increase with decreasing absolute lumen size and was greater between sequential diastolic frames than between systolic frames. We also found that if calculated as a percentage of mean vessel dimensions, variability, even if constant in absolute terms, proves to be larger in the case of smaller vessel dimensions.

No other formal analyses of the reproducibility of intravascular ultrasound have been reported. A number of clinical and experimental reports quote high intra- and interobserver quantitative reproducibility, frequently expressed as correlation coefficients >0.9 with low standard errors [Potkin, 1990; Moriuchi, 1990; St. Goar, 1992; Di Mario, 1992; Tenaglia, 1992b; Porter, 1993; Yamagishi, 1994]. The findings of these analyses are of limited applicability because of the small numbers studied and the omission of methodological details. The significant limitations of linear regression, the most frequently applied technique in these reports, as a method for measuring agreement have been pointed out by Bland and Altman [Bland, 1986]. A correlation coefficient of 1.0 may exist in the absence of true agreernent, and correlation coefficients increase as the range of true values measured increases, an important consideration in studies such as ours where the

full range of measurements typically encountered in clinical practice have been measured. In the present study, the regression coefficient for the interobserver comparison for vessel area in both selected and unselected frames (analyses D and E) was 0.92, despite considerable scatter evident on the Bland-Altman plots (**figure 2.4**).

2.5.7. Limitations

This study has characterised the short term reproducibility of IVUS measurements within and between observers in both selected and unselected video frames. It does not, however, allow conclusions to be drawn on the medium and long term reproducibility of IVUS quantitation. This information is required before quantitative IVUS data from longitudinal studies, including studies of the impact of lipid lowering trials and restenosis following percutaneous interventions, can meaningfully be interpreted.

The quantitative variability, particularly when expressed as 95% limits of agreement, appears to be high in a number of the analyses we performed, but was not significantly greater than that found by other experienced groups to which we have previously referred [Hausmann, 1994b; Peters, 1994b]. In order to determine the variability inherent in measuring unselected sites in a range of lumen sizes, we included both post-interventional and pre-interventional/diagnostic lesions in our analysis. Inclusion of the mean differences for all three lumen types is useful in providing data that are applicable to studies of restenosis in which lesions before intervention, after PTCA or stent, and at 6 month follow-up are included.

We did not use a mechanical pullback system because linearity of pullback cannot be relied upon unless catheters incorporating a distal sonolucent sheath in which the transducer travels are used. It is probable that use of a mechanical pullback system diminishes short term variability by ensuring an appropriately slow

pullback and may simplify the process of identifying the point of minimum lumen stenosis by permitting three dimensional reconstruction of vessel segments. Minimising long-term variability is dependent on the application of an objective means of longitudinal orientation as may be provided by such systems.

Despite these limitations, our study protocol relates closely to current clinical practice, and its findings, although at times possibly reflecting a 'worst case', are relevant to data acquired in clinical practice.

2.6. Conclusions

The short-term reproducibility of manual measurements of coronary arteries made on two dimensional intravascular ultrasound images is high. Variability is not significantly greater when performed in serial pullbacks of the imaging catheter, indicating that the site of maximum stenosis is reproducibly identifiable by intravascular ultrasound. Interobserver variability is somewhat greater, and when considered in terms of limits of agreement, may amount to a considerable proportion of the mean measurement in a given case. Although intravascular ultrasound is an accurate and largely reproducible method of quantitating the coronary arteries, the potential for clinically significant variability still exists. Systematic variability can be minimised by the widespread adoption of commonly agreed definitions of vessel dimensions. Random variability can be reduced by standardising methods of data acquisition and objectifying the process of quantitating vessel dimensions. This may depend on the development of reliable methods of tissue characterisation upon which automated border detection can be based. Efforts to improve the quantitative reproducibility of intravascular ultrasound should continue to allow it to achieve its full potential in the study of coronary disease.

Table 2.1 Bias and random variability for each parameter in each protocol

Analysis	Parameter	mean	(%)	SD	(%)
A	MLD (mm)	0.02	(1.0)	0.14	(7.0)
	MxLD (mm)	0.02	(1.2)	0.10	(4.7)
	LA (mm^2)	0.05	(2.2)	0.24	(7.1)
	VA(mm^2)	0.01	(0.5)	0.67	(5.9)
	PA (mm^2)	-0.06	(-1.9)	0.70	(8.7)
	%sten (%)	-1.04	(-1.0)	2.67	(4.9)
B	MLD (mm)	-0.02	(-1.1)	0.15	(7.9)
	MxLD (mm)	-0.01	(-0.5)	0.15	(6.2)
	LA (mm^2)	-0.02	(0.1)	0.37	(8.8)
	VA(mm^2)	-0.07	(-1.4)	0.81	(7.7)
	PA (mm^2)	-0.11	(-2.0)	0.74	(9.5)
	%sten (%)	-0.56	(-0.7)	2.51	(3.5)
C	MLD (mm)	0.01	(0.8)	0.22	(11.5)
	MxLD (mm)	0.01	(1.0)	0.14	(6.2)
	LA (mm^2)	0.07	(3.5)	0.34	(12.2)
	VA(mm^2)	-0.08	(-0.6)	0.96	(8.9)
	PA (mm^2)	-0.11	(-1.8)	0.74	(12.7)
	%sten (%)	-0.99	(-1.2)	3.81	(5.5)
D	MLD (mm)	-0.06	(-4.1)	0.30	(16.8)
	MxLD (mm)	-0.01	(-5.4)	0.31	(15.2)
	LA (mm^2)	-0.18	(-8.3)	0.64	(23.4)
	VA(mm^2)	0.09	(0.2)	1.92	(17.4)
	PA (mm^2)	0.27	(2.4)	1.82	(22.6)
	%sten (%)	2.01	(2.7)	6.5	(8.9)
E	MLD (mm)	-0.09	(-5.6)	0.28	(15.4)
	MxLD (mm)	-0.04	(-2.5)	0.30	(15.4)
	LA (mm^2)	-0.12	(-6.0)	0.67	(24.9)
	VA(mm^2)	0.21	(-0.7)	2.10	(20.0)
	PA (mm^2)	0.25	(0.6)	1.92	(26.1)
	%sten (%)	0.97	(1.3)	6.89	(9.5)

Figure 2.1 Scattergrams of repeated measures of minimum lumen diameter

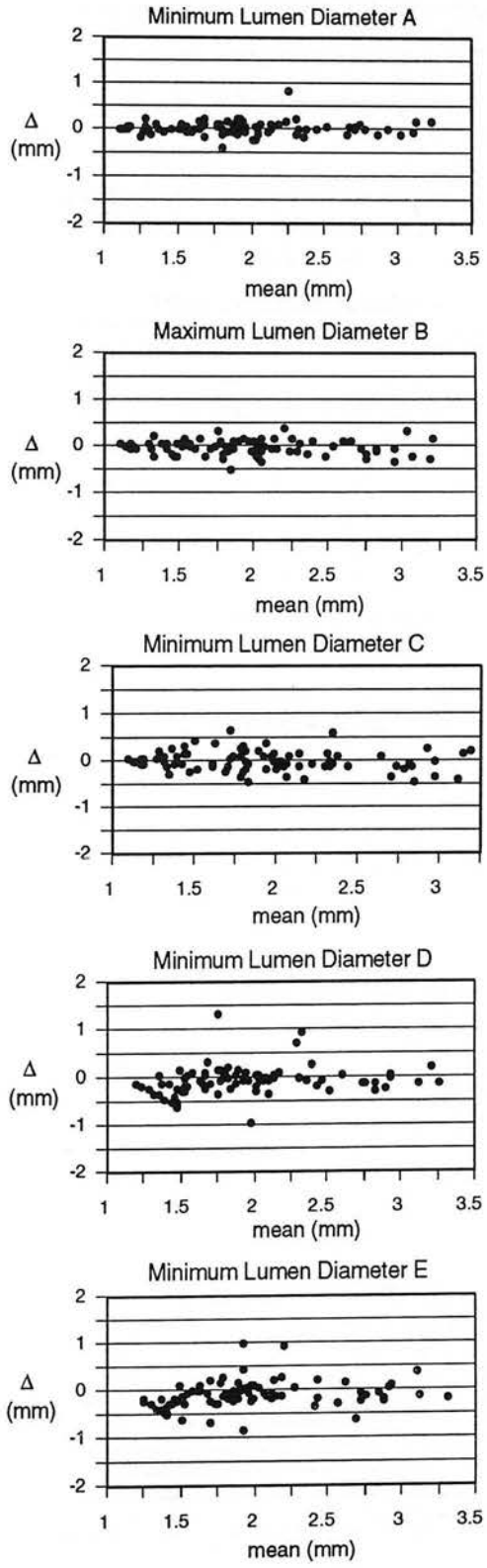

Figure 2.2 Scattergrams of repeated measures of maximum lumen diameter

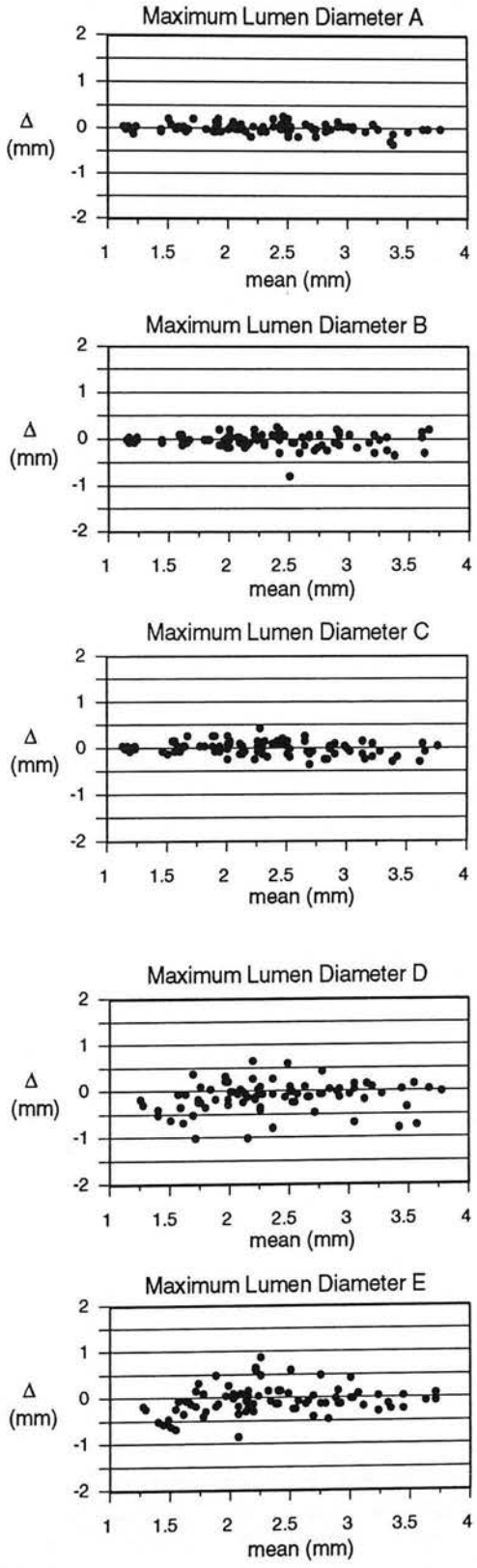

Figure 2.3 Scattergrams of repeated measures of minimum lumen area

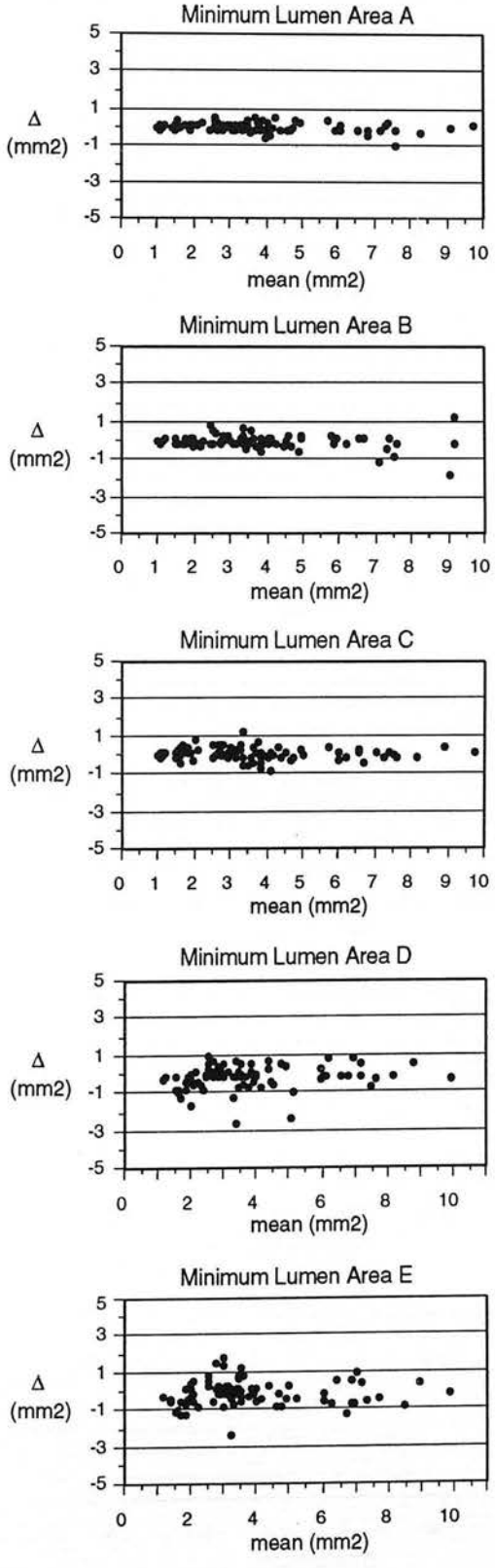

Figure 2.4 Scattergrams of repeated measures of vessel area

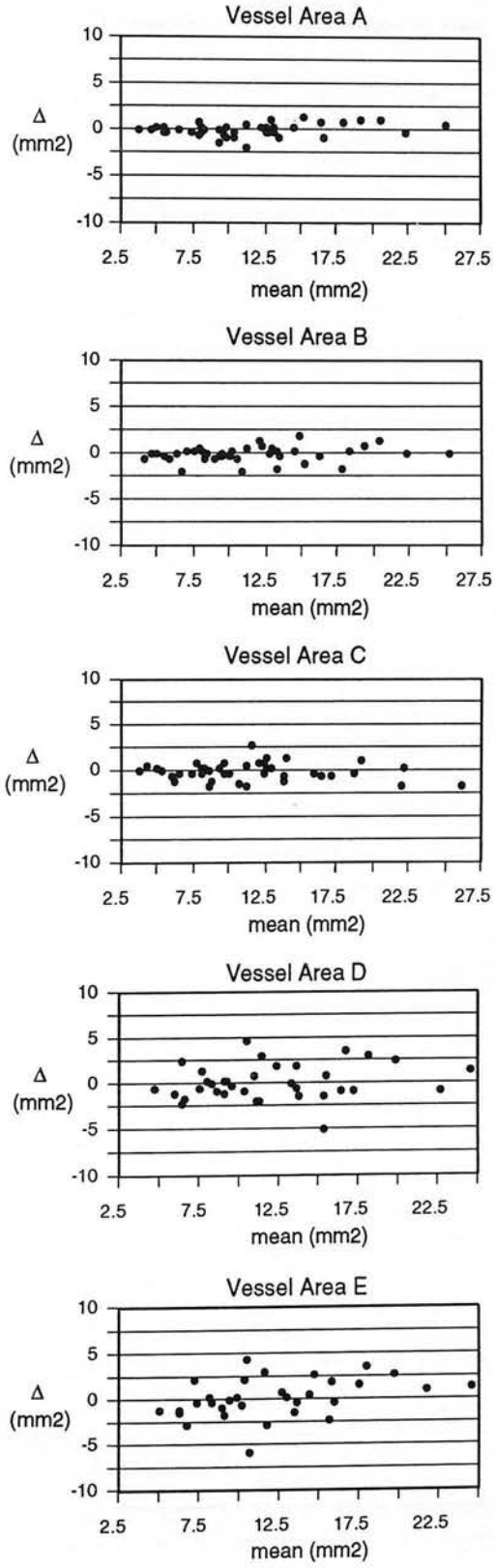

Figure 2.5 Scattergrams of repeated measures of plaque area

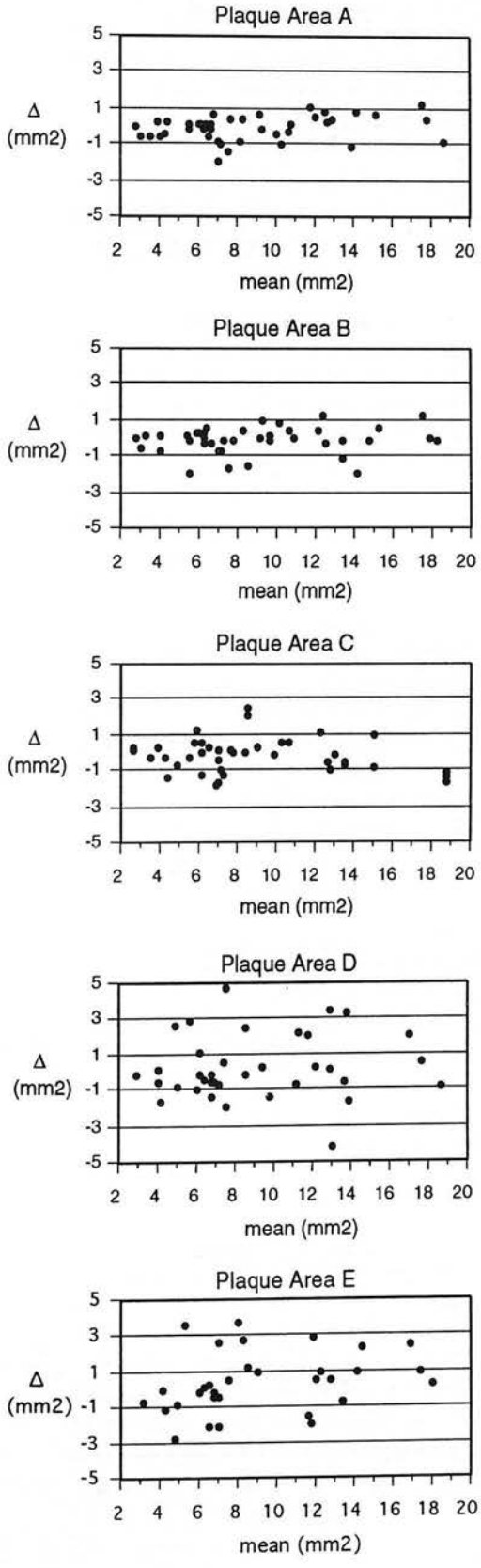

Figure 2.6 Scattergrams of repeated measures of percentage stenosis

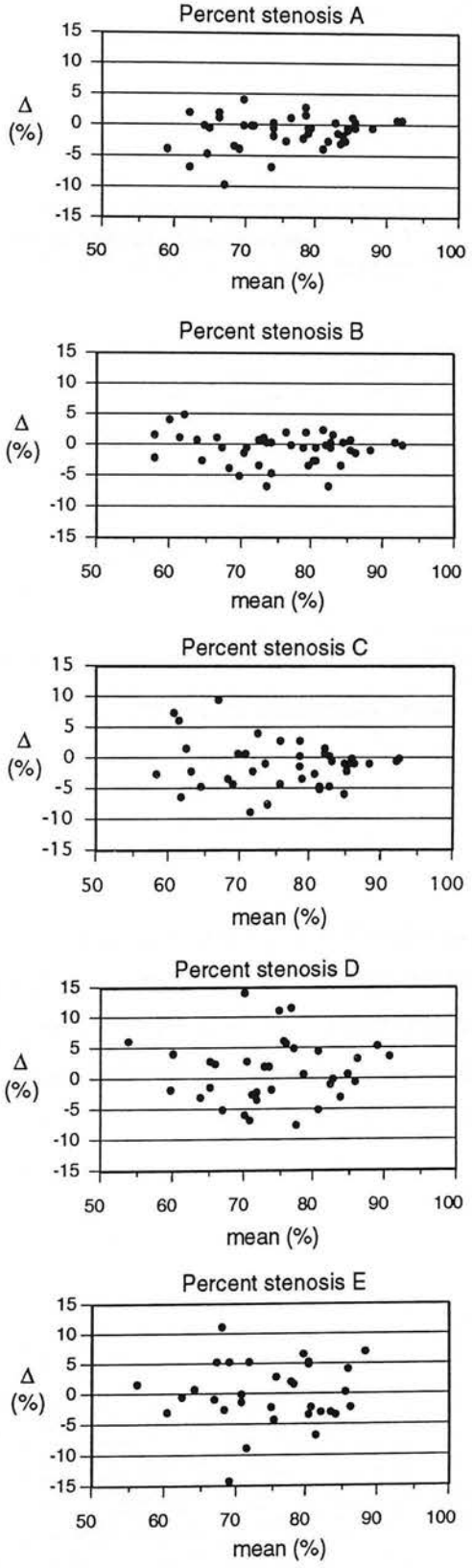

Figure 2.7 Random variability of lumen area measurement (absolute values)

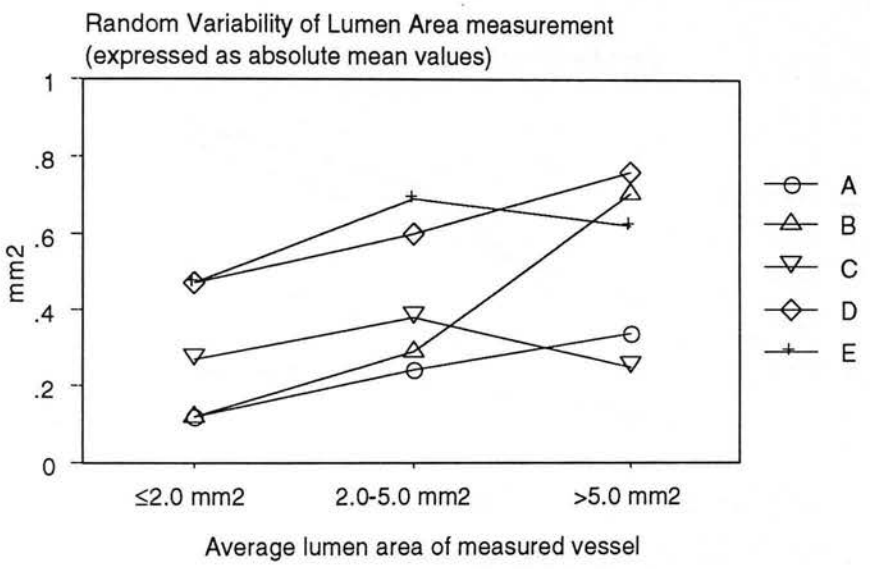

The absolute value of the standard deviation of the difference between repeated measurements (y axis), is plotted against 3 groups of measurements made in lumens ≤2.0 mm^2, 2.0-5.0 mm^2 and ≥5.0 mm^2 (average of the repeated measures). There is a trend toward a larger standard deviation as the lumen area increases (seen as a consistent feature in analyses A, C and D, and to a lesser extent in analyses B and E.

Figure 2.8 Random variability of lumen area measurement (% of mean area)

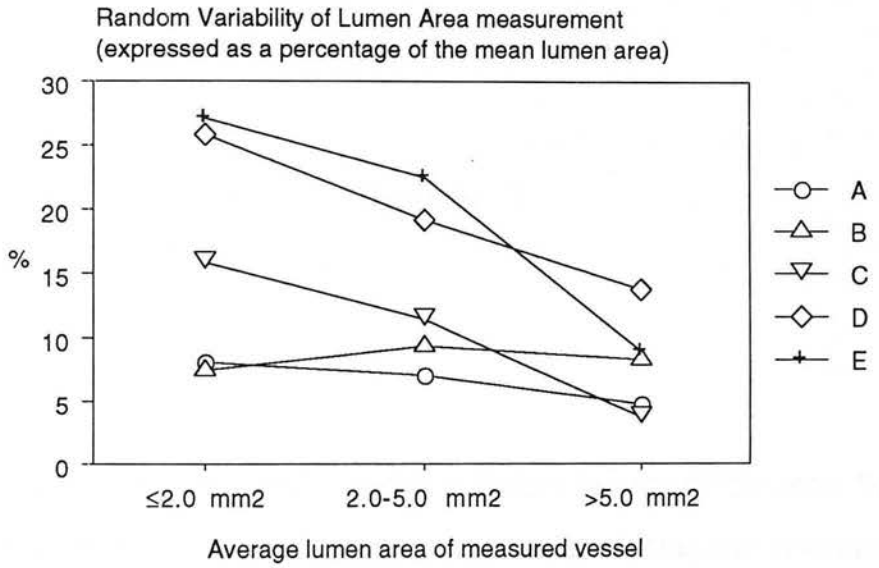

The standard deviation of the difference between repeated measurements is shown in this graph as a percentage of the average lumen area ((y axis). When plotted against the 3 groups of measurements made in lumens ≤2.0 mm^2, 2.0-5.0 mm^2 and ≥5.0 mm^2 (average of the repeated measures), it is apparent that in all analyses (A-E), random variability is proportionately greater in smaller lumens.

Chapter 3

A Study of the Quantitative and Qualitative Impact of Catheter Shaft Angulation in a Mechanical Intravascular Ultrasound System

and

A Review of Artefacts in Intravascular Ultrasound Imaging

Contents *page*

3.1. Introduction

Accurate image interpretation requires a recognition of the artefacts that are a feature of a particular imaging technique. The recognition of artefacts is facilitated by an understanding of their physical basis. Artefacts encountered in intravascular ultrasound imaging include both those familiar to general echocardiographers and also phenomena that are peculiar to intravascular ultrasound.

This chapter is divided into two sections. In the first, a study exploring the precipitating factors and the geometric and quantitative impact of the 'rotation angle artefact' is elaborated. The second section consists of a review of image artefacts and ambiguities that are encountered in intravascular ultrasound images.

3.2. Study aims

A study protocol was designed to systematically explore (1) the quantitative and qualitative impact of catheter shaft angulation of different degrees, at different sites and in different combinations on the geometric integrity of intravascular ultrasound images, and (2) the effect of catheter position within the phantom lumen on the manifestation of geometric distortion.

3.3. Materials and methods

3.3.1. In vitro phantom studies

A custom built perspex phantom was constructed (**figure 3.1**). This consisted of two square 1.5 x 1.5 cm, 0.4 cm thick perspex sections, in each of which a 4 mm circular central recess was fashioned. The sections were joined by four 1 cm long struts positioned at the outer corner of each section. Two 1.3 mm holes were precision drilled at central and eccentric positions within the central recess, to allow fixed positioning of the ultrasound catheter within the phantom lumen. Eight holes were drilled at near equidistant points around the circumference of the central lumen

in each section, allowing a length of 3.0 prolene suture to be threaded from one to the other to be provide 8 equidistantly positioned parallel lengths of suture between the two sections.

3.3.2. Catheter positioning

The length of the ultrasound catheter was positioned on a flat work surface on which a series of round pegs were positioned at set points. An acute angle was introduced into the catheter shaft by positioning it around the pegs. A wider curve was fashioned by drawing it around the outer circumference of a fixed upright cardboard tube with a 10 cm diameter. Appropriate positioning of the pegs and the larger tube allowed a series of angulations to be introduced into the course of the catheter, either alone or in combination. The bends were positioned to simulate the course of the catheter in vivo, running from the periphery, up the ascending aorta, around the aortic arch, and into the coronary arteries. A series of distal tip bends positioned over a short distance was designed to simulate the course of the catheter in more tortuous coronary arteries. The imaging element of the catheter was placed within the phantom in a water bath filled with normal saline and the catheter shaft outside the phantom was drawn through 20 different combinations of angles, in a set protocol, illustrated in **figure 3.2**. Sufficient tension was applied between the catheter tip and motor drive to remove all slack from the system. The catheter entered through the side of the water bath by way of a watertight valve, and the distal-most angulations were fashioned within the water bath itself.

3.3.3. Imaging equipment

Boston Scientific 3.5F, Sonicath ultrasound imaging catheters, operating at a centre frequency of 30 MHz, were used for imaging purposes, and were attached to a Hewlett Packard Sonos Intravascular ultrasound scanner. For each part of the 20 part protocol, the imaging element was positioned firstly within the lumen of the inwardly facing recess of the perspex section of the phantom, and then

immediately beyond this where the prolene sutures were visualised as 8 discrete point echodensities. A 5 second video recording and a thermal printer hardcopy were acquired at each of these sites for every variation of the 20 part protocol of catheter angulations. Images were acquired using 10 different catheters, 3 of which had been used for less than 10 minutes in a clinical study immediately prior to their use in the protocol and 7 that had been used ≥3 weeks beforehand. The 'fresh' catheters were irrigated with clean saline at the end of the clinical case, and did not dry out. The 'old' catheters, although flushed and cleaned after clinical use, had dried and required repeat flushing with saline prior to use in the study.

3.3.4. Quantitative and qualitative analysis

When all images had been acquired for each catheter tested, the video recording was reviewed and the qualitative and quantitative analyses performed. Measurements were made using the trackball driven integrated quantitative software package of the Hewlett Packard scanner. The system was calibrated using the cross-grid visible on the image. For each part of the protocol and for each catheter, the maximum and minimum diameter and lumen area of the phantom lumen was measured. Similarly, the distance between the 8 sutures was measured. All measurements were recorded on hardcopy and entered into a computer spreadsheet for later statistical analysis. A composite quantitative variable, known as the 'distortion index', was calculated to express the degree of distortion present in the image. Circularity was calculated as the ratio of maximum to minimum diameter. Change in lumen area, that can occur without detectable lumen shape distortion, was calculated as the modulus of the ratio of measured lumen area and true lumen area (12.57 mm^2) subtracted from 1, all added to 1. The values for circularity and change in lumen area were multiplied to give a composite measure of distortion. The formula for the 'distortion index' is shown below.

$$Distortion\ Index = \underbrace{(\max diam / \min diam)}_{\text{Circularity}} \times \underbrace{(1+|(1-area_{meas}/area_{true})|)}_{\text{Change in lumen area}}$$

A qualitative analysis of the degree of image distortion was also undertaken. A circular lumen shape was graded as 1, elliptical distortion as 2, more marked distortion resulting in the so-called 'kidney bean' or 'petal shaped' deformity as 3, and severe random distortion as 4. In addition, images were graded simply on the presence (1) or absence (0) of appreciable image distortion.

The influence of the catheter on quantitative accuracy and degree of distortion was assessed by plotting the measurements made by the each catheter in all catheter conformations in a cell plot that was then analysed for significant inter-catheter differences (**figure 3.3**).

The impact of the number of bends, the position of the bend, and the bend angle was determined by measuring the dimensions and calculating the distortion index for 3 sets of catheter conformations. The impact of the number of bends was assessed by comparing the measurements made in conformations 6 (a straight catheter) and 10 (4 bends). The influence of the position of the bend was assessed by comparing measurements made in conformations 11 (a straight catheter), 12 (proximal 90° bend), 13 (mid catheter 90° bend), 14 (distal 90° bend) and 15 (a distal tip 90° bend). The impact of the degree of angulation was assessed by comparing measurements made in conformations 11 (straight catheter), 16 (45° mid catheter angle), 13 (90° angle), 17 (180° angle) and 18 (a 360° loop).

We expected that the distortion of luminal shape induced by the rotation angle artefact would be apparent in the case of eccentrically placed catheters to a greater extent than concentrically placed catheters. This was tested by comparing measurements made in the same catheter conformations for each of the tested catheters from a central (conformations 1-5) and eccentric (conformations 6-10) location within the lumen.

In order to assess the accuracy of the radial geometry of the image, the distances between sutures were measured with the catheter in a central position in catheter positions 1-5, and the maximum and minimum distances recorded and their ratio calculated. A reduction or increase in the distance between sutures allowed the quantification of geometric distortion of the phantom wall even when no luminal distortion was evident.

3.3.5. Statistical analysis

The means and standard deviation were calculated for all continuous data. In the case of multiple comparisons between continuous variables, a repeated measures analysis of variance (ANOVA), with Bonferroni-Dunn post-hoc testing, was performed to test for significant differences. The data is presented in the form of bivariate scattergrams, in which the absolute data points and the mean and a single standard deviation (error bars) are shown for each x axis variable. The statistical analysis was performed using the commercially available statistics software package Statview v4.2®.

3.4. Results

3.4.1. The impact of the catheter

Analysis of the minimum and maximum lumen diameter, lumen area and the distortion index revealed that measurements made on images produced by catheter 6 were markedly aberrant (mean distortion index 1.47±0.31) (**figure 3.3**). This appeared to be due to a driveshaft kink. The mean distortion index for all other catheters was small (catheter 1: 1.11±0.89, catheter 2: 1.11±0.10, catheter 3 1.13±0.16, catheter 4: 0.11±0.11, catheter 5: 1.18±0.14, catheter 7: 1.11±0.10, catheter 8: 1.15±0.10, catheter 9: 1.11±0.07 and catheter 10: 1.08±0.05). ANOVA revealed a significant difference only between catheter 6 and the other catheters. When measurements made with catheter 6 were excluded, it was found that 94%

of minimum diameters, 87% of maximum diameters and 88% of lumen area measurements were accurate to within ±10% of their true dimensions.

In order to avoid other effects being obscured, the measurements made on images acquired with catheter 6 was excluded from further analyses apart from that examining the quantitative implications of discernible distortion. In this analysis, the 'random' distortions, almost completely confined to images from catheter 6, were usefully included.

3.4.2. The impact of the severity of catheter angulation

Measurements made with straight catheters were compared to measurements made with catheters with increasing degrees of mid-shaft angulation as described in paragraph 2.3.4. The mean and standard deviation of the minimum and maximum lumen diameter, lumen area and distortion index are shown in **table 3.1**. The minimum diameter measured with a 360° catheter loop was significantly smaller than measurements made with catheters in the other conformations. No significant increase in the maximum diameter was noted, although there was a trend towards a larger diameter in the case of measurements made with a mid-catheter loop. The lumen area did not differ significantly between different degrees of catheter angulation, although a larger standard deviation was noted in the case of mid-catheter loop measurements. The trend toward an increased distortion index was also evident as angulation increased (**figure 3.4**).

3.4.3. The impact of bend position

No significant differences were noted between measurements made with straight catheters and those made with 90° bends at different points along the length of the catheter. The lumen dimensions and distortion indices are given for each bend position in **table 3.1**, and plots of the distortion index and lumen area for each position shown in **figure 3.5**.

3.4.4. The impact of the number of bends

The impact of the number of bends was assessed by comparing values obtained with straight catheters with those obtained using catheters with multiple bends. There was no significant difference between the minimum or maximum diameter, or lumen area measured from the images acquired with the straight catheters and those from the catheter with multiple bends. The distortion index, although tending to be larger in the catheters with multiple bends, was not significantly different. The measurements and distortion index for both catheter conformations are given in **table 3.1**, and the lumen area and distortion index plots shown in **figure 3.6**.

3.4.5. Eccentric vs. Concentric luminal position

The mean maximum diameter measured 4.14±0.15 mm on images acquired by eccentrically placed catheters. This was significantly larger than the 4.00±0.10 mm maximum diameter measured with centrally positioned catheters, $p<0.001$. Similarly, the mean lumen area of 12.85±0.71 mm^2 measured by eccentrically placed catheters was larger than the mean area of 12.44±0.60 mm^2 measured by concentrically placed ones, $p=0.004$. The distortion index was slightly but significantly greater in eccentrically placed catheters (eccentric 1.14±0.07 vs. concentric 1.06±0.03, $p<0.0001$). The minimum diameter did not differ significantly according to the intraluminal location of the catheter (3.91±0.14 mm with eccentric catheters vs. 3.91±0.10 mm with concentric catheters, $p=0.84$). The dimensions measured in eccentric and concentric locations, and the distortion indices are given in **table 3.1**, and the plots of the lumen areas and distortion indices shown in **figure 3.7**.

3.4.6. Qualitative classification of images

All images were classified according to the lumen shape into circular, elliptical, kidney shaped, or random, and graded from 1 to 4 respectively. The distortion index increased in relation to the grade of image deformity, and was associated

with a larger standard deviation as the grade increased. The mean lumen area increased as distortion grade increased (from 12.68±0.67 mm^2 to 12.77±0.99 mm^2 (elliptical) to 12.96±1.33 mm^2 (kidney) to 15.85±0.21 mm^2 (random), although only the area of random shaped lumina was significantly greater than the other lumen shapes (**figure 3.8**). Perceptible lumen distortion was very infrequent in images from concentrically positioned catheters (6%), whereas it was noted in 70% of images from eccentrically located catheters. Whereas lumen area measurements were accurate to within ±10% of true lumen area in 97% of images where no distortion was noted, this was true in only 81% of lumen area measurements in images in which distortion was recognised.

3.4.7. Wall distortion in the absence of lumen distortion

The inter-suture distance was measured in all the conformations of concentrically located catheters (conformations 1-5), and the maximum and minimum distance noted. The proportional decrease in the smallest distance from the true minimum distance (2.0 mm) and increase in the maximum distance from the true maximum distance (2.6 mm) was then calculated. Although significant distortion in lumen shape or size was very infrequent in images acquired with a central catheter location (paragraph 2.4.5.), we did detect a significant reduction in minimum inter-suture distance between straight catheters (conformation 1) and those with a series of bends (conformation 5) (**figure 3.9**). Similarly, the maximum inter-suture distance was greater when measured by catheters in conformations 4 and 5, than in the straighter conformations. There was no correlation between the change in intersuture distance (either maximum or minimum) and the distortion index. This indicates the presence of geometric distortion of the wall, in the absence of lumen distortion.

3.4.8. Impact of catheter age

The age of the catheter did not have a significant bearing on the distortion index (new 1.11±0.09 vs. old 1.13±0.12). However, a significantly greater number of images acquired with older catheters were classified as distorted ($p<0.001$), and the distortion grade was higher in older catheters (new 1.46±0.62 versus old 1.82±0.77).

3.5. Discussion

Although it is widely recognised that images acquired with mechanical intravascular ultrasound scanners are subject to a varying degree of geometric distortion as a result of non-uniform transducer rotation, the extent of the problem and its quantitative impact have been little studied. The present in vitro study was designed to determine the factors contributing to the occurrence of the 'rotation angle' artefact, and to establish its quantitative impact. In the next section of this chapter describing intrasvascular ultrasound artefacts, the physical basis of the artefact is discussed.

3.5.1. The impact of bend severity, number and location

Increasing catheter angulation led to a greater degree of image distortion and a significant reduction in minimum diameter in the case of a 360° loop in the catheter. There was a trend towards increasing distortion and quantitative inaccuracy with an increasing number of catheter bends and in bends adjacent to the catheter tip relative to more proximal ones. The quantitative differences were small, however, and these factors did not appear to separately contribute in a significant way to the degree of image distortion.

3.5.2. Intraluminal catheter position

Subjectively apparent geometric distortion was present in the majority of images acquired with eccentrically located catheters (70%), but were evident in only 6%

of images from centrally located catheters. In addition, lumen dimensions were overestimated by catheters situated eccentrically within the lumen and were significantly larger than measurements made with centrally located catheters. In the presence of a rotation angle artefact, no appreciable change in lumen shape or size is evident in images acquired with centrally located catheters, but as our analysis of inter-strut distances shows, geometric distortion of the wall may nevertheless occur in these circumstances. In clinical practice, a rotational angle error occurring in a centrally located catheter may thus not impact on the geometry or dimensions of the lumen and hence be difficult to recognise, but may nevertheless lead to misrepresentation of vessel wall anatomy.

3.5.3. Frequency of identifiable image distortion

The high frequency of appreciable lumen shape distortion was greater than is thought to occur in clinical practice. In our study, we employed previously used catheters, a proportion of which had dried out between their initial use and their use in the study. The build-up of small amounts of rust, calcium or coagulated proteinaceous debris on the drive shaft of these catheters increased the probability of angular errors occurring. In most centres, new catheters, in which drive shaft rotation should be relatively unimpeded and uniform, are employed for each clinical case. In the present study, identifiable distortion was less frequent in images from 'fresh' catheters than older catheters. The true rate of image distortion in clinical practice is, however, unknown, as it may be difficult to identify in a naturally irregular diseased coronary arterial lumen

3.5.4. The quantitative impact of image distortion

Our findings indicate that the quantitative accuracy of an image cannot be relied upon when geometric distortion as a result of a rotational angle error is identified. The direction of the quantitative error cannot be confidently predicted in any given

case, although our results indicate that the mean lumen area tends to increase as the grade of distortion increases.

3.5.5. Implications for clinical practice

When geometric distortion is recognised during a clinical study, the quantitative accuracy of images is questionable and caution should be exercised in basing important clinical decisions upon them. When it does occur, attempts can be made to reduce or prevent image distortion induced by rotational angle errors by ensuring that the extra-arterial course of the catheter is as straight as possible. In the absence of recognisable lumen distortion, most images, even in this study employing previously used catheters, were found to be quantitatively accurate. Greater accuracy should be achieved in images acquired with previously unused imaging catheters.

3.6. Conclusions

Both as a clinical and a research tool, the quantitative accuracy of intravascular ultrasound images is of central importance, and is arguably more critical to the efficacy of this technique than for any of the other, to date more qualitative applications of ultrasound. The size and direction of the quantitative error induced by non-uniform rotation of mechanical transducers is unpredictable and when the catheter is located centrally within the lumen, is difficult to identify. Although relatively infrequent when using new, optimally performing imaging catheters, the use of older, previously used catheters carries a greater risk of rotation angle errors occurring. This should be borne in mind when previously used catheters are used for in vitro work, or, following resterilisation, are used for further clinical examinations.

3.7. A Review of Artefacts in Intravascular Ultrasound imaging

When considering the many potential sources of ambiguity and image distortion that are encountered in intravascular ultrasound imaging, it is helpful to think in terms of (a) those artefacts directly relating to the imaging equipment itself and (b) artefacts that are a function of the environment in which the images are acquired. In the first group, we consider (1) the rotation angle artefact, (2) the spatial resolution of the device, (3) the 'dynamic range', and (4) the so-called 'ring-down' effect. In the second group, the impact of (1) the angle of incidence of the ultrasound beam, (2) catheter position within the vessel and (3) shadow artefacts are considered.

3.7.1. Technical factors

3.7.1.1. The Rotation Angle Error Artefact

The so-called 'rotation angle error' artefact, recognised since intravascular ultrasound scanning was first introduced, is a problem peculiar to mechanical intravascular ultrasound devices. In the first section of this chapter, we report our findings concerning its quantitative impact and precipitating factors. In this section, we begin by reviewing a number of theories put forward to explain its occurrence.

Finet et al., referring to the phenomenon as the 'petal-shaped deformation', propose that this form of image distortion arises when the transducer, situated eccentrically against the imaged lumen wall, vibrates at the same frequency as the pulse repetition frequency [Finet, 1993]. As illustrated in **figure 3.10**, assuming that point zero of the transducer rotation occurs when the transducer is adjacent to the vessel wall, the imaging element moves back and forth from the vessel wall as a result of catheter vibration at a similar frequency to the rotation of the element through its 360° cycle. The net effect of concordant transducer vibration and rotation frequencies is that early and late in the cycle the leading edge echoes from

the lumen boundary are more distant from the centre of the image, and in mid cycle are closer to it, than would occur were the transducer in a stable luminal position throughout the cycle. The familiar petal- or kidney-bean shaped representation of a circular structure results. Although theoretically plausible, this course of events clearly does not operate in all cases in which the artefact is manifest. In the experimental investigation of the rotation angle artefact described in the first section of this chapter the transducer was fixed in a concentric or eccentric position within the phantom lumen at all times.

A theory that may operate more frequently has been elaborated by Chae et al. [Chae, 1992]. Accurate reconstruction of the radiofrequency data returning from the rotating transducer requires a constant and predictable relationship between the element and the drive-shaft motor, from which radial orientation of the scan line is determined. Torsional flexibility of the drive shaft can lead to a discrepancy arising between the radial course of the motor-drive and that of the transducer. The angle between the actual direction of the ultrasound beam and its assumed radial orientation, registered from the motor-drive, is known as the azimuth angle, and may be constant or variable during each cycle. A uniform angular discrepancy over a complete rotation of the catheter does not introduce geometric distortion, but offsets the image around its central axis. This effect is typically seen if a constant constraint is placed on drive shaft rotation, such as when the 'O' ring of the Tuohy-Borst valve is tightened excessively around the operating catheter. If tightened further, gradual rotation of the image around its central axis is seen, that will, unless the 'O' ring is loosened, increase in velocity and result in the catheter 'binding' and a knot forming in the proximal segment of the imaging catheter, outside the guiding catheter.

Non-uniform angular discrepancies typically occur as 'sinusoidal' angular errors during which catheter tip rotation slows and accelerates from the uniform velocity of

the motor. Clinical examples of the rotation angle error arterfact are shown in **figure 3.11**. The way in which such an angular discrepancy produces the 'rotation angle artefact' is shown in the schematic diagram in **figure 3.12**. A slowing of the transducer's rotation from point 'a' to point 'b' leads to a disproportionate number of scan lines being emitted and received for this anatomical segment of vessel wall. Conversely, subsequent acceleration of the transducer's rotation from 'b' to 'a' leads to fewer scan lines being emitted and received during this part of the transducer's course than would be the case if the transducer were rotating at a uniform velocity. As a uniform rotation velocity is assumed in the image reconstruction algorithm, the 240 scan lines are distributed evenly through 360° in the reconstructed image without regard to the anatomical source of each line. Whereas cyclic variations in transducer rotational velocity have no apparent distorting effects on the lumen when a transducer is centrally placed in a circular vessel or phantom (**figure 3.12 (a)**), distortion of the lumen shape may be seen in the case of eccentric transducer positioning and in the presence of irregular vessel or phantom lumen contours(**figure 3.12 (b)**). Furthermore, although geometric distortion of the lumen contour is limited by a central transducer position, distortion of the vessel wall geometry may nevertheless occur in these circumstances.

Non-uniform rotation of the transducer results from friction between the rotating driveshaft and its polyethylene housing. In previously used catheters, this arises from an accumulation of rust, calcium, or coagulated proteinaceous material. In new catheters, minor kinks in the driveshaft, as a result of manufacturing error or following forceful handling during advancement of the catheter are potential causes. Reversible but important friction can also be induced by severe bends in the catheter that may be encountered as the transducer is advanced into an acutely angled ostium or branch origin. Bends may also form in the catheter between the motor drive connection and the guiding catheter. In our experience, severe stenoses are an uncommon cause of rotational angle artefacts. If very hard and

unyielding, the catheter is unlikely to pass in the first instance, and if composed of softer material, it is likely to be Dottered by the catheter and subsequently to offer less resistance.

The effect of the rotation angle error artefact on lumen area quantitation was also explored by Chae et al. using 5F CVIS (Cardiovascular Imaging Systems) catheters [Chae, 1992]. The lumen area of phantoms and fixed vessels were over- and underestimated by ±10% when old catheters (used clinically for more than 30 minutes) were placed eccentrically within the lumen. Geometric distortion was not seen with new catheters. A systematic pattern of quantitative error was noted depending on the radial orientation of this particular catheter. Overestimation of lumen area occurred when the support strut running to the distally fixed transducer was adjacent to the vessel wall, and underestimation when it faced towards the lumen. No such pattern was discernible in our study with 3.5F Boston Scientific Sonicath imaging catheters.

Angle artefacts may be avoided or minimised by (1) avoiding bends in the imaging catheter between the motor drive and the guiding catheter, (2) avoiding a tight grip of the catheter or an excessively tightened Touhy-Borst valve. Changing the rotational frequency of the driveshaft is occasionally helpful if an error persists despite the above measures. If an error is evident on initial testing of the catheter in a fluid filled syringe prior to clinical use, a manufacturing error can reasonably be assumed and a different catheter should be used.

More definitive remedies to the problem require further technical advances in mechanical catheter system design. Work continues on developing the optimal drive shaft conformation, that combines optimal handling and flexibility with maximal torsional rigidity. The spiral wound design on which the present generation of catheters is based has not been improved upon [Martin, 1989]. A servo system might be developed whereby the increased torsional friction to

which the driveshaft is subject during each rotation is sensed and compensated for by the motor. It is not clear whether such exquisitely fine adjustments to motor speed, rotating at an average of 1800 rpm, would be feasible, or whether these changes would predictably translate to uniform rotation at the end of the driveshaft, given the above considerations concerning limited torsional rigidity. The most promising solution is offered by the development of a micromotor that can be placed at the distal end of the catheter and thus obviate the need for a driveshaft. Prototype imaging catheters incorporating a micromotor are currently undergoing initial clinical testing [Bom, 1995].

3.7.1.2. Spatial resolution

The spatial resolution of intravascular ultrasound systems is a potential source of ambiguity and image artefact. It can be discussed in terms of the axial resolution and lateral resolution.

3.7.1.2.1. Axial resolution

The smallest distance between two point reflectors along the axis of an ultrasound beam at which they can be separately discerned is the axial resolution. The axial resolution is determined by the wavelength and the pulse duration. Theoretically the shortest pulse duration is half a wavelength, but in practice axial resolution measures at least twice the wavelength. In the high frequency transducers used for intracoronary imaging (2.9F, 3.0F and 3.5F operating at 25 to 30 MHz centre frequencies) it typically measures ~150 μm. It does not change significantly as a function of distance from the transducer and thus does not give rise to the variations in image appearance that arise from variable lateral resolution.

3.7.1.2.2. Lateral resolution

The lateral resolution, defined as the smallest distance between two point reflectors on a line perpendicular to the beam path at which the reflectors are identifiable as separate, is a function of beam width. An object that lies off the

centre of the primary beam produces a lower amplitude reflection than is generated by an object insonated by the centre of the beam, and is represented on the image as a point on a line corresponding with the central axis of the beam. In order that closely apposed structures lying parallel to the beam be identifiable as separate entities, they must be separated by more than the one beam width. Beam width, traditionally measured as the width of the centre-lobe at the -6dB or the 'one-half maximum' amplitude point, is itself a function of the transducer's aperture diameter, as well as its shape, frequency and focusing profile.

Unlike axial resolution, lateral resolution varies as a function of distance from the transducer. Within the so-called 'near field' or Fresnel zone, where the ultrasound beam is theoretically non-divergent, lateral resolution is approximately equal to the aperture diameter. The near field ends at the 'transition point', at a distance of $d2/4\lambda$ from a circular transducer and $d2/2\lambda$ from a square transducer (where d = the aperture diameter, and λ = the centre frequency wavelength). At this point, the Fraunhofer zone or 'far field' begins in which the ultrasound beam diverges rapidly. The smaller the aperture, the greater the divergence of the beam, as evident from the formula $\sin \theta = 0.61/r$, where θ = the angle of divergence, and r = the radius of the beam at the transition point.

The lateral resolution is increased by (1) reducing the size of the aperture and/or by (2) increasing the centre frequency, both physical characteristics that have successfully been incorporated into the design of intracoronary transducers. However, by decreasing the size of the aperture, its power output and sensitivity are reduced, as is the length of the 'near field' where lateral resolution is maintained.

A number of problems relating to limited lateral resolution are encountered in clinical practice. The transducer is usually situated eccentrically within the lumen, and in large arteries, the opposite vessel wall lies within the zone in which a significant deterioration in lateral resolution occurs. Ultrasound speckles become splayed and

the appreciation of fine anatomical details is reduced. An important example of image ambiguity induced by poor lateral resolution is encountered when imaging stents. Stent struts are highly echo-reflective and if situated in the far field of the ultrasound beam may appear as broad, flat echoes. In certain circumstances, depending on the angle of insonation and position of the strut relative to the transducer, this may give the appearance of incomplete apposition and prompt further high pressure balloon inflations where none are indicated (**figure 3.13**). An understanding of the phenomenon of declining lateral resolution as a function of distance from the transducer is important to avoid such interpretative errors.

3.7.1.3. Dynamic range

The dynamic range of an ultrasound system is a critical determinant of the image quality it delivers. By dynamic range we mean the range of perceptible signal intensities that are assigned to a distribution of grey levels (255 levels in an 8 bit system). It determines the smallest difference in the signal amplitude reflected from different tissue elements that can be distinguished [Weyman, 1994]. A limited dynamic range thus contributes to the inability of a system to detect interfaces between differing tissue constituents.

As a limited system dynamic range implies a narrow range of signal strengths across which grey levels are assigned, its effect is to increase image contrast. As a consequence, specifically in the context of intravascular ultrasound imaging, endoluminal definition is decreased and artefactual intralesional echo dropout may occur that may be misinterpreted as lipid pools, dissections or tears (**figure 3.14**). Fitzgerald et al. studied the effect of different dynamic ranges on image interpretation and quantitation [Fitzgerald, 1991]. In vitro images of a post-mortem femoral artery were acquired with the instrument's dynamic range set to its maximum (55 dB) and at a number of levels down to 20 dB. An appreciable reduction in the range of image grey levels and significant overestimation of lumen

area occurred when the dynamic range was set to <30 dB. Many of the earlier intravascular ultrasound systems produced with which much of the early published work was performed, suffered from an unacceptably low dynamic range (**figure 3.14**).

3.7.1.4. "Ring-down artefact"

In the immediate vicinity of the transducer, sound waves are poorly resolved. Contributing to the chaotic behaviour of sound waves in this part of the near field adjacent to the transducer is the so-called 'ring-down' effect. Following electrical stimulation of a piezoelectric transducer, and generation of an ultrasound beam, the transducer requires a finite amount of time to become silent. During this 'ring-down' period, noise is generated that is visible on the ultrasound image as an area of bright signals immediately adjacent to the transducer. The amount of ring-down noise is a function of the excitatory pulse width, the physical characteristics of the transducer, and its matching layer and backing material. It was a prominent feature in images generated by the first generation of intravascular ultrasound scanners (**figure 3.14**) and resulted in the acoustic diameter of a transducer being up to 0.5 mm greater than the outer diameter of the catheter [Nissen, 1990]. Improvements in the design of both mechanical and electronic transducers (the multiple elements in the most recent generation of electronic catheters are embedded beneath the catheter surface) have minimised the impact of this artefact.

The distinction between the 'ring-down' artefact and the 'catheter blank' (which is circular in shape) has been a persistent source of confusion. The blacked out central circle seen in all intravascular ultrasound images, known as the catheter blank, is an electronically configured and arbitrarily sized area in the centre of the image that indicates the catheter's position within the lumen. In mechanical scanners it is usually sized by the manufacturer to have the same diameter as the catheter. The ring-down effect, although seen in intravascular ultrasound images

as a thin, echodense halo of 'noise' around the circumference of the catheter blank, is actually a linear phenomenon, constituting the proximal portion of the ultrasound beam immediately adjacent to the transducer. Following the circular reconstruction of the image, the combined ring-down noise of each beam assumes a circular shape.

Contributing to this outer ring of noise are echoes generated by the polyethylene housing of the catheter. Mechanical catheters require flushing of the polyethylene housing with water to acoustically couple the transducer with the blood filled lumen. Inadvertent injection of microbubbles around the transducer impairs acoustic coupling, further increasing the prominence of the echodense halo around the catheter blank and degrading image quality. Although adjusting the time gain compensation nearest the transducer to zero obliterates this area of noise, potentially important near field information may be lost. In the electronic (Endosonics®) system the catheter blank is manually sized by the operator at the start of a study in order to obscure the ring-down noise as completely as possible and is thus slightly larger than the known outer dimensions of the catheter.

3.7.2. 'Environmental' factors

3.7.2.1. Angle of incidence

Specular echoes are generated at the interface of two acoustically distinct materials or tissues. The amplitude of the reflected signal received by the transducer is maximal for interfaces that are insonated at right angles to their surface, as the reflection angle is zero, and the sound waves are reflected directly towards the transducer. As the angle of incidence approaches 180°, the amplitude of the returning signal diminishes and the videodensity of the ultrasound image is reduced by up to 50% [Di Mario, 1993]. A suboptimal angle of incidence in intravascular images impairs endoluminal border definition and lead to inaccuracies in the

delineation of the lumen boundary. Difficulties also arise in determining the presence or absence of wall tears or dissections (**figure 3.15**).

Peters et al. have studied the impact of insonation angle in a detailed investigation of the phenomenon of echodense lines or layers observed at the intima-media junction [Peters, 1994a]. They did not find a histological basis for the phenomenon. Neither specific patterns of the internal elastic lamina (linear, corrugated, duplicated, fragmented or absent) nor plaque thickness or subtype (fibrous, lipid or mixed) appeared to affect the presence or absence of an echodense layer. Rather it appeared to depend on catheter position within the vessel or phantom, seen almost solely when the angle of incidence was 90°.

3.7.2.2. Transducer orientation

The shape of a vessel imaged by an intraluminal imaging catheter varies in a predictable pattern as its alignment with the long axis of the vessel varies. Non-coaxial or non-orthogonal alignment results in an oblique imaging plane. The elliptical representation of a circular lumen produced in such circumstances is not a distortion, but rather an accurate rendition of the data acquired from that imaging plane. Coaxial alignment of the catheter, whether centrally or eccentrically positioned within the lumen, produces an orthogonal tomogram of the vessel in which true cross-sectional diameters and areas can be measured.

It has wrongly been believed that the elliptical shape encountered during non-coaxial alignment of the transducer was due to non-uniform transducer or mirror rotation, i.e. the rotation angle artefact [Coy, 1991]. Although severe catheter angulation may give rise to a rotation angle artefact, non-coaxial alignment does not. Moreover, although elliptical distortion resulting from non-uniform transducer rotation may appear similar to that arising from non-coaxial alignment, the two have very different physical bases; the first a genuine artefact arising from impaired catheter function, the second an accurate representation of an oblique imaging

plane. McKay et al. reported that marked degradation of image quality associated with non-coaxial catheter alignment was not improved by increasing gross gain [McKay, 1989]. Declining lateral resolution, which is not responsive to alterations in the power output of the transducer, is the most probable explanation for their findings.

An oblique imaging plane inevitably leads to quantitative overestimation of the imaged vessel. The major diameter and cross-sectional area increase as the transducer assumes a non-coaxial position, whereas the minor diameter does not change. Non-coaxial catheter alignment is recognised as a contributor to the tendency towards overestimation of vessel dimensions by ultrasound. McKay et al. observed an increase in measurements with transducer angulation of ≥10° [McKay, 1989]. Chae et al. showed that a 30° deviation of the ultrasound catheter from the long axis of the vessel introduced a ~15% error in lumen area quantitation [Chae, 1992]. This can be predicted from geometric theory that states that the area increases in proportion to the inverse of the cosine of the angle from orthogonal alignment. A study comparing ultrasound and quantitative angiographic dimensions in angiographically normal coronary arteries revealed that the mean deviation of the ultrasound catheter from the long axis of the vessel was 15° (range 0 - 29°) [St. Goar, 1991]. Predictably, the more the catheter deviated from the vessel long axis, the greater was the discrepancy between the ultrasound and angiographic diameters. At 83% of the sites where matched measurements were made, ultrasound measured diameters exceeded angiographic diameters, and the mean difference was 0.5±0.4 mm. An axially eccentric catheter position, for reasons elaborated above, did not influence the shape or correlate with differences between ultrasound and angiographic diameter measurements. The small diameter of coronary arteries (measuring 2.0 to 5.2 mm in this series) limits the scope for significant non-orthogonal alignment of intravascular ultrasound catheters and

minimises its quantitative impact when it does occur. Elliptical tomograms are most likely to be acquired in large vessels, ectatic segments or grafts.

3.7.2.3. Acoustic shadowing

Echogenicity is dependent on the density, compressibility and viscosity of a material. Very dense matter gives rise to intense, bright echoes at its leading edge and if acoustically impenetrable, to an anechoic acoustic shadow. In certain circumstances (sufficiently intense reflected signal strength, low signal attenuation and sensitive transducer), returning echoes may generate a secondary signal from the transducer that in turn is reflected by the acoustic interface. The duration between the transmission of the primary signal and reception of the secondary signal by the transducer is twice that of the primary signal's transmission-receive time, giving rise to a secondary echo in the image twice the distance from the transducer as the first. Such reverberations may be single or multiple depending on the conditions outlined above and the pulse repetition frequency of the transducer (**figure 3.16**).

Acoustic shadowing, with or without reverberations, is often a useful marker of calcific or very dense fibrous tissue deposits in intravascular ultrasound images. Dystrophic calcification of atheromatous deposits in the arterial wall is a frequently encountered and clinically relevant finding [Mintz, 1992b; Fitzgerald, 1992b]. Its characteristic echographic appearance makes it the most accurately (**table 1.3**) and reproducibly identifiable tissue type (**table 1.4**) [Peters, 1994d]. Acoustic shadowing is occasionally observed in the absence of calcification. Dense fibrotic or elastic tissue, particularly when insonated by an eccentrically placed transducer abutting against the vessel wall, may have a highly echodense leading edge and strongly attenuate the ultrasound signal. Increasing power output, gross gain, or adjusting time gain controls may clarify the nature of such regions. Additionally, observing the anechoic area as the transducer moves away from the vessel wall

during the cardiac cycle or with manipulation may reveal more distal penetration of ultrasound.

Angioplasty guidewires, over which most currently used ultrasound catheters are run into the coronary artery, are echodense and acoustically impenetrable. If lying at a distance from the transducer, as is frequently the case with the Boston Scientific 3.5F (and 4.8F) Sonicath catheter design, the acoustic shadow is small and its impact on the image is slight. When situated close to the catheter housing, the guidewire casts a broader acoustic shadow that may be associated with reverberations (**figure 3.16**). The 5.0F CVIS Insight catheter design incorporates a rotating acoustic mirror to lengthen the ultrasound transmission path within the catheter housing, so that very near field noise does not interfere with imaging at the catheter surface. The distally situated transducer faces back towards the tilted, rotating mirror, that reflects the ultrasound signal through 90° out to the vessel wall. The electrical connection to the transducer consists of a metal strut that lies within path of the reflected ultrasound. This gives rise to a prominent acoustic shadow or 'pie-slice' artefact that occupies up to 90° of the circumferential extent of the image [Peters, 1994c]. Although the catheter can be rotated to expose sections of the vessel wall obscured by this shadow, this and guidewire artefacts can occasionally interfere significantly with imaging.

The guidewire artefact is not encountered with electronic catheters (Endosonics), in which the multiple transducer elements are set circumferentially on the outer surface of the over-the-wire catheter. The problem has also been overcome in newer mechanical catheter designs (CVIS 2.9F, Boston Scientific 3.0F). Both have a common distal lumen within a sonolucent sheath into which the transducer tipped drive shaft is advanced following withdrawal of the guidewire to a more proximally situated double-lumen section of the catheter. When imaging is completed, the

transducer is withdrawn, replaced by the guidewire and the ultrasound catheter withdrawn using a monorail technique.

Acoustic shadows cast by stent struts frequently prevent identification of the outer vessel boundary and measurement of vessel and plaque area following the implantation of the stent. Compression of the plaque material and surrounding adventitia also obscures the interface at the external elastic lamina (**figure 3.15**).

3.7.2.4. Spontaneous contrast

Spontaneous contrast, encountered frequently in transoesophageal, and to a lesser extent in transthoracic, echocardiography, is reflected from slowly flowing blood. De Kroon et al. have shown that intravascular spontaneous contrast is proportional to rouleaux concentration, and increases in intensity as blood flow velocity decreases and rouleaux form [De Kroon, 1993]. The natural echodensity of blood flowing at normal flow rates within the coronary arteries imaged at high frequency can be suppressed by adjustment of post-processing and time gain controls. A degree of blood echodensity should be maintained for a number of reasons. Setting the near field time gain controls to low levels reduces blood signal intensity at the cost of obscuring important data arising from structures adjacent to the transducer. Not infrequently, the endoluminal border lies within this zone. The bright speckles generated by blood may diminish the contrast between the lumen and the vessel wall and thus obscure the endoluminal border in still frames. Nevertheless, the blood pool is readily identified on real-time imaging by the dynamic variation of speckle intensity characteristic of flowing blood (**figure 3.17**). This may act as a useful 'contrast' medium in identifying dissections within a plaque or ambiguous edges in an irregular or disrupted lumen. The phenomenon of the dynamic variation in speckle density of flowing blood has been capitalised upon to develop a system of gated image averaging whereby the blood filled areas of the artery are differentiated from adjacent tissues [Li Wenguang, 1993].

When uncertainty concerning the edge of the lumen, presence of a dissection or differentiation of prominent contrast from thrombus remains, intracoronary injection of contrast medium or saline transiently introduces an anechoic region in the distribution of the displaced the blood. Microbubbles in the injectate are seen as focal, (or confluent, if present in high concentration) echodensities during the coronary injection (**figure 3.17a** and **3.17b**).

3.7.2.5. Vasopasm

Coronary spasm is the commonest side-effect or 'complication' of intracoronary ultrasound, observed in 8.4% of arteries undergoing intravascular ultrasound study for detection of cardiac allograft arteriopathy [Pinto, 1993]. Its incidence may have been underestimated in a retrospective multicentre registry, in which it was reported in only 4% [Hausmann, 1995]. Although not strictly speaking an artefact, if not recognised it may lead to significant image misinterpretation and quantitative error. Vasospasm is rare if sublingual glyceryl trinitrate is administered prior to the intravascular ultrasound study. Intracoronary glyceryl trinitrate is used in circumstances when exact quantitation is required, a follow-up study is anticipated or in cases of recognised spasm despite sublingual GTN. An example of severe spasm, reversed by intracoronary GTN, in the distal 'reference segment' of an artery after angioplasty is illustrated in **figure 3.18**.

3.7.3. Conclusions

The accurate interpretation of images is a prerequisite for the safe and useful application of intravascular ultrasound in clinical practice and clinical research. There is no substitute for the experiential process of learning by exposure to the many appearances that are encountered in clinical imaging and by the frequent analysis of off-line images. Nevertheless, an understanding of the physical basis of the artefacts and the ways in which the physics of ultrasound may impact on image presentation, is an important means of improving interpretation skills.

Table 3.1 Absolute measurements (mean±1SD) and distortion index

Degree of Angulation	Max Diameter (mm)	Min Diameter (mm)	Lumen area (mm^2)	Distortion index
Straight catheter (11)	4.10±0.12	3.97±0.9	12.78±0.82	1.09±0.07
45° bend (16)	4.16±0.12	3.90±0.16	12.93±0.68	1.12±0.07
90° bend (13)	4.17±0.14	3.94±0.10	13.33±0.91	1.14±0.08
180° bend (17)	4.19±0.20	3.91±0.17	12.99±1.05	1.15±0.09
360° bend (18)	4.33±0.38	3.62±0.34	12.52±2.35	1.39±0.21
Bend Position				
Straight catheter (11)	4.10±0.12	3.97±0.90	12.78±0.82	1.09±0.07
Proximal 90° bend (12)	4.21±0.36	3.97±0.11	13.56±1.29	1.16±0.22
Mid shaft 90° bend (13)	4.17±0.14	3.94±0.10	13.33±0.91	1.14±0.08
Distal 90° bend (14)	4.19±0.21	3.94±0.11	13.40±1.07	1.15±0.16
Distal tip 90° bend (15)	4.25±0.46	3.94±0.16	13.39±1.32	1.20±0.30
Number of bends				
Straight catheter (6)	4.10±0.12	3.97±0.90	12.78±0.82	1.09±0.07
Multiple bends (10)	4.16±0.11	3.86±0.16	13.00±0.77	1.15±0.07
Concentric vs. Eccentric				
Concentric straight (1)	4.10±0.12	3.97±0.09	12.78±0.82	1.06±0.03
Concentric 1 bend (2)	4.11±0.08	3.90±0.16	12.79±0.54	1.06±0.04
Concentric 2 bends (3)	4.12±0.07	3.93±0.10	13.02±0.57	1.06±0.03
Concentric 3 bends (4)	4.19±0.28	3.89±0.16	12.68±0.86	1.07±0.03
Concentric 4 bends (5)	4.16±0.11	3.86±0.16	13.00±0.77	1.06±0.04
Eccentric straight (6)	4.01±0.11	3.94±0.13	12.56±0.69	1.09±0.07
Eccentric 1 bend (7)	3.99±0.10	3.91±0.11	12.33±0.54	1.09±0.05
Eccentric 2 bends (8)	4.00±0.11	3.94±0.11	12.54±0.68	1.10±0.04
Eccentric 3 bends (9)	4.01±0.86	3.88±0.09	12.33±0.56	1.14±0.10
Eccentric 4 bends (10)	3.99±0.09	3.90±0.11	12.37±0.60	1.15±0.07

Figure 3.1 Schematic drawing of the perspex phantom

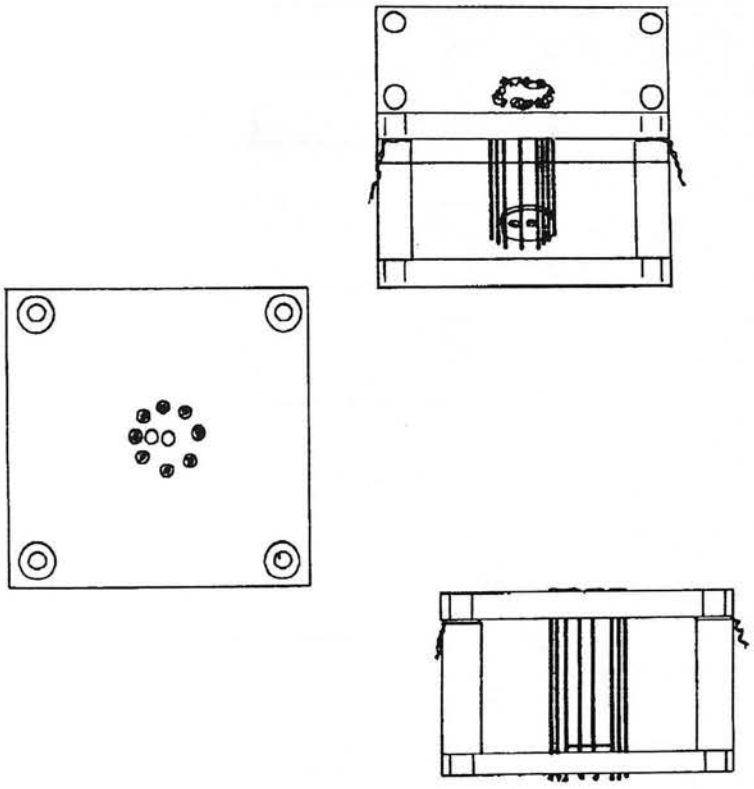

A complete description of the perspex phantom is given in paragraph 3.3.1

Figure 3.2 Catheter conformations

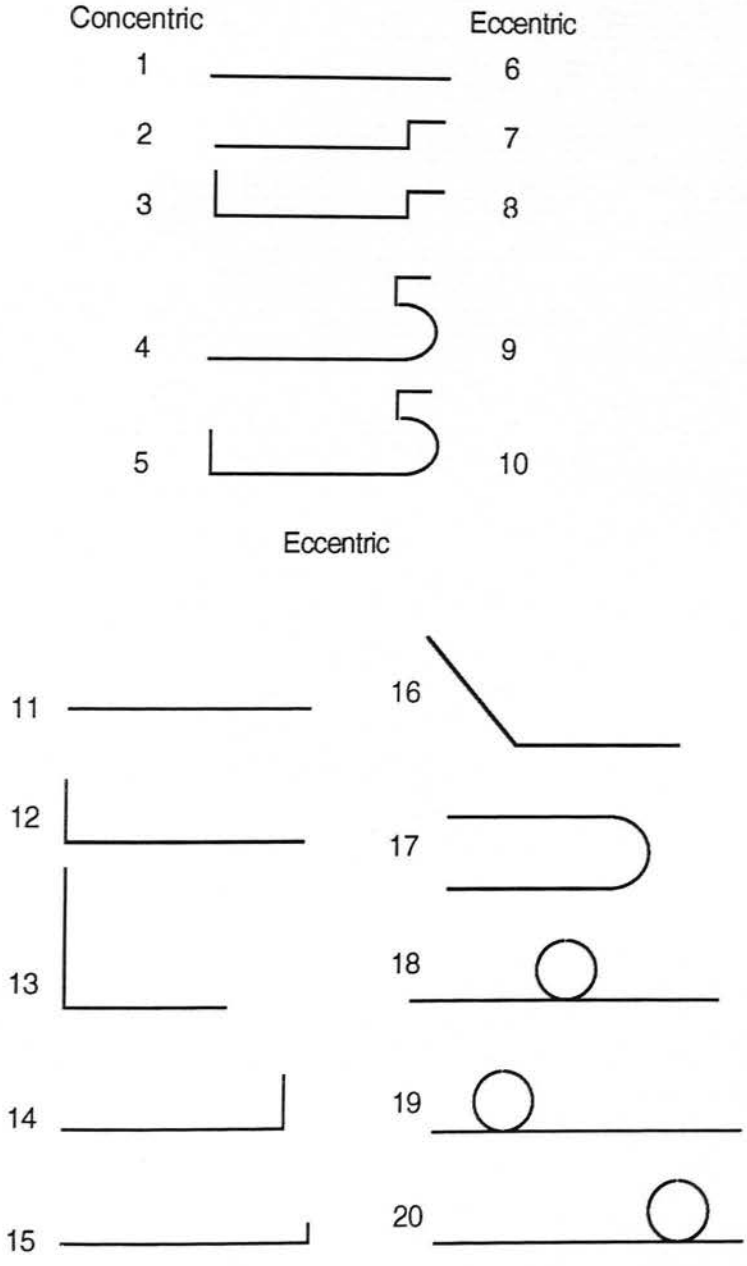

Figure 3.3 Bivariate scattergrams for individual catheters

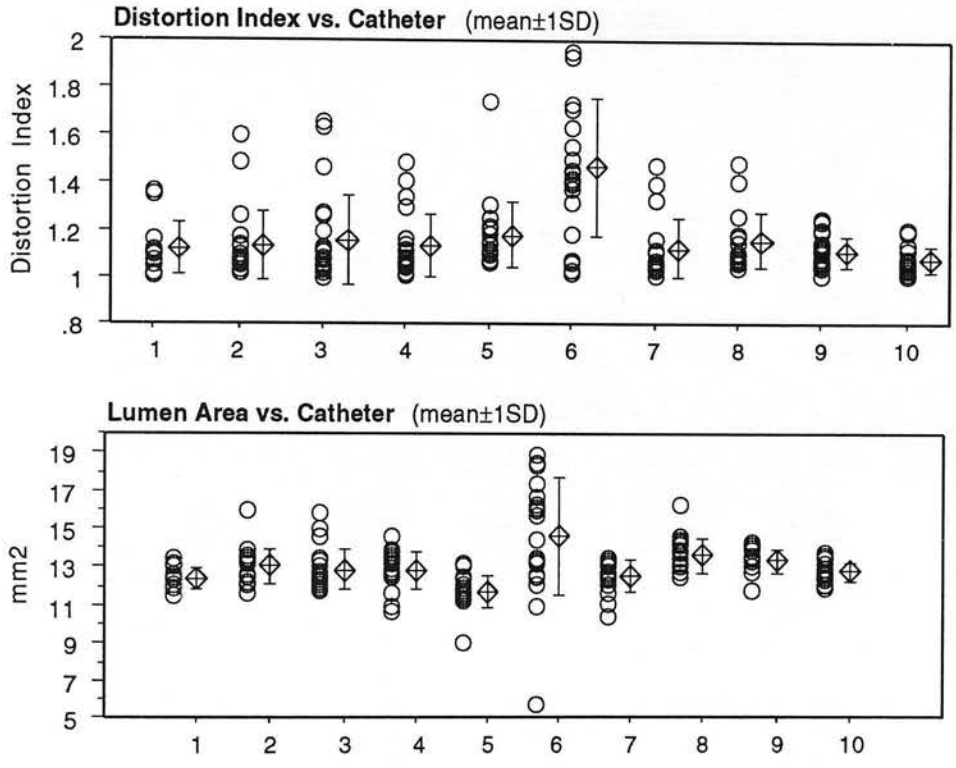

Figure 3.4 Bivariate scattergrams for degree of angulation

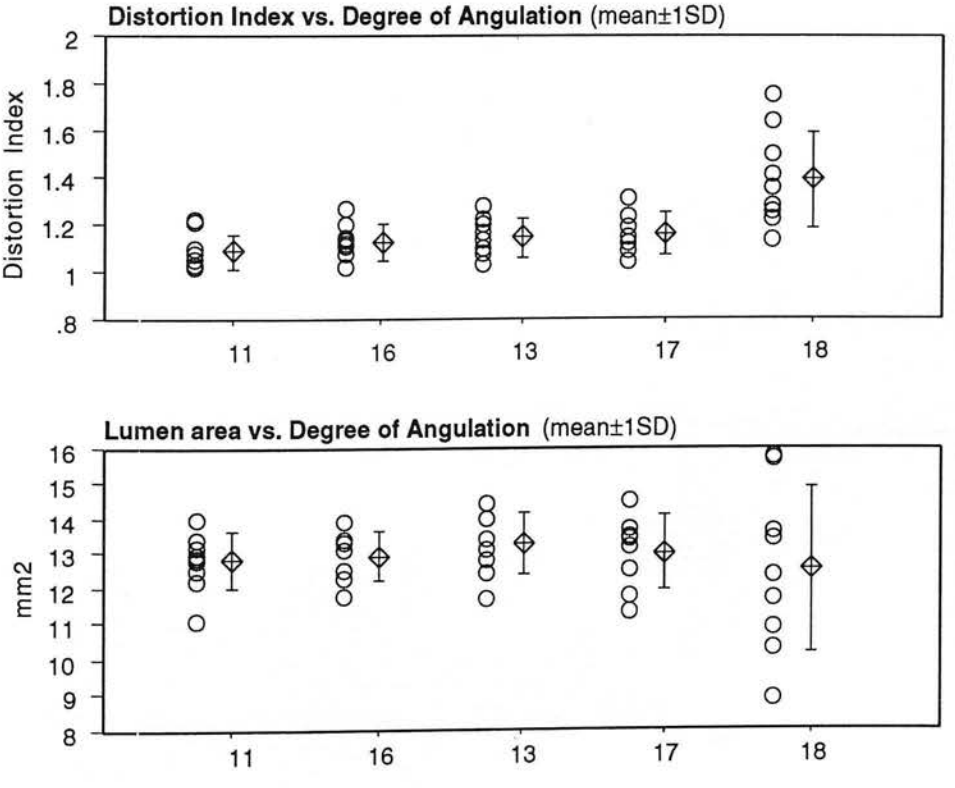

Figure3.5 Bivariate scattergrams for bend location

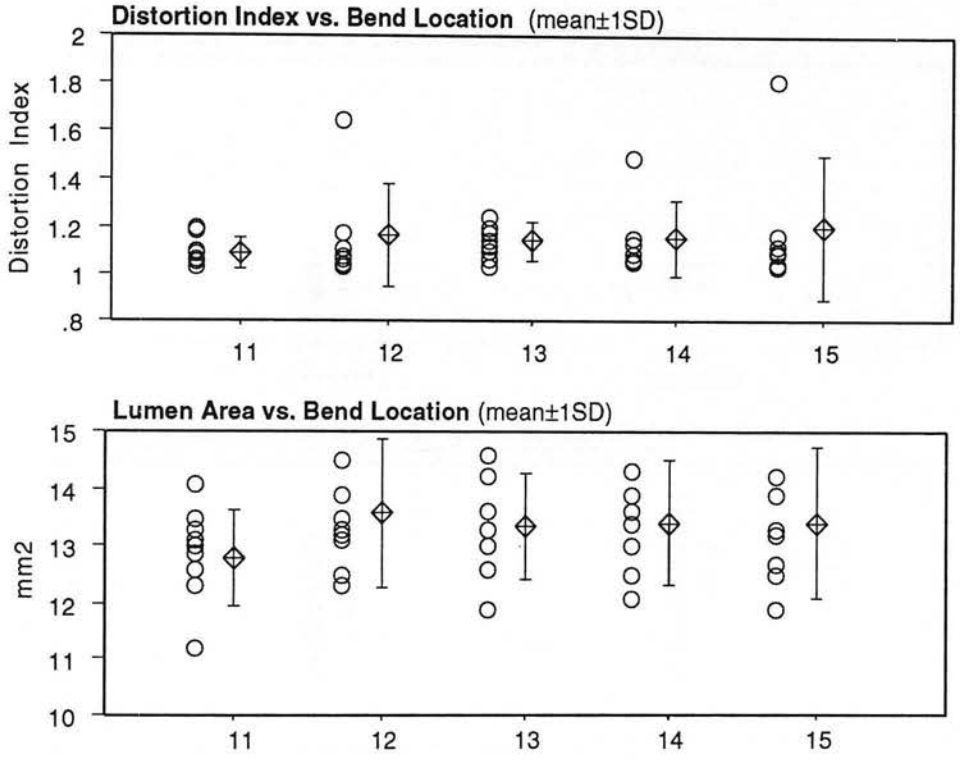

Figure 3.6 Bivariate scattergrams for number of bends

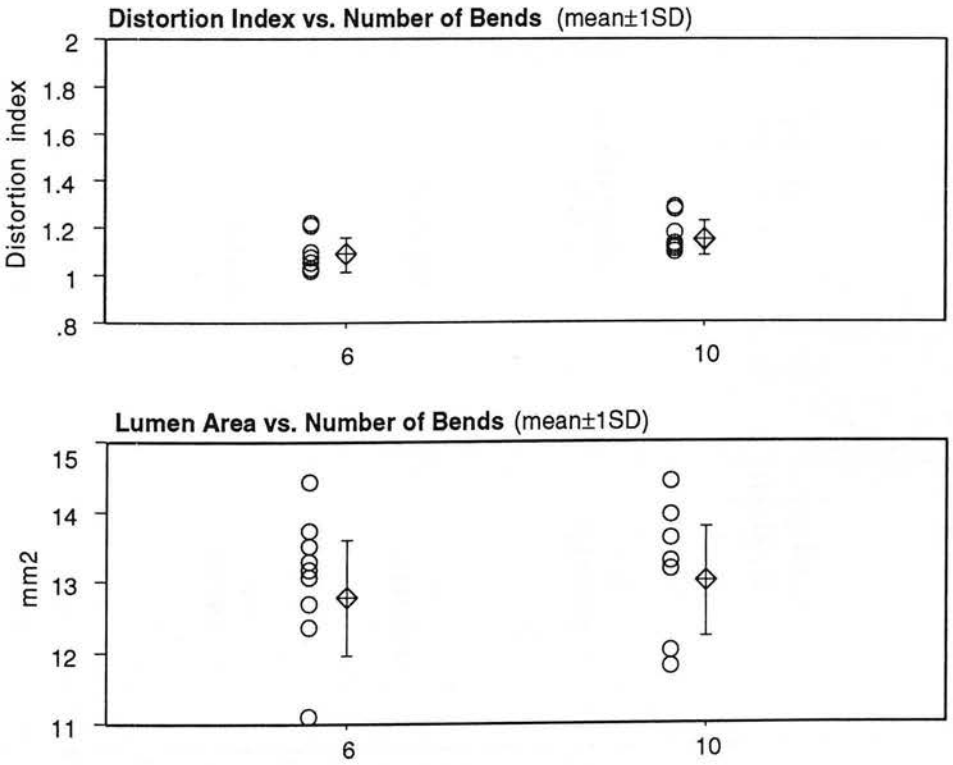

Figure 3.7 Bivariate scattergrams for catheter position

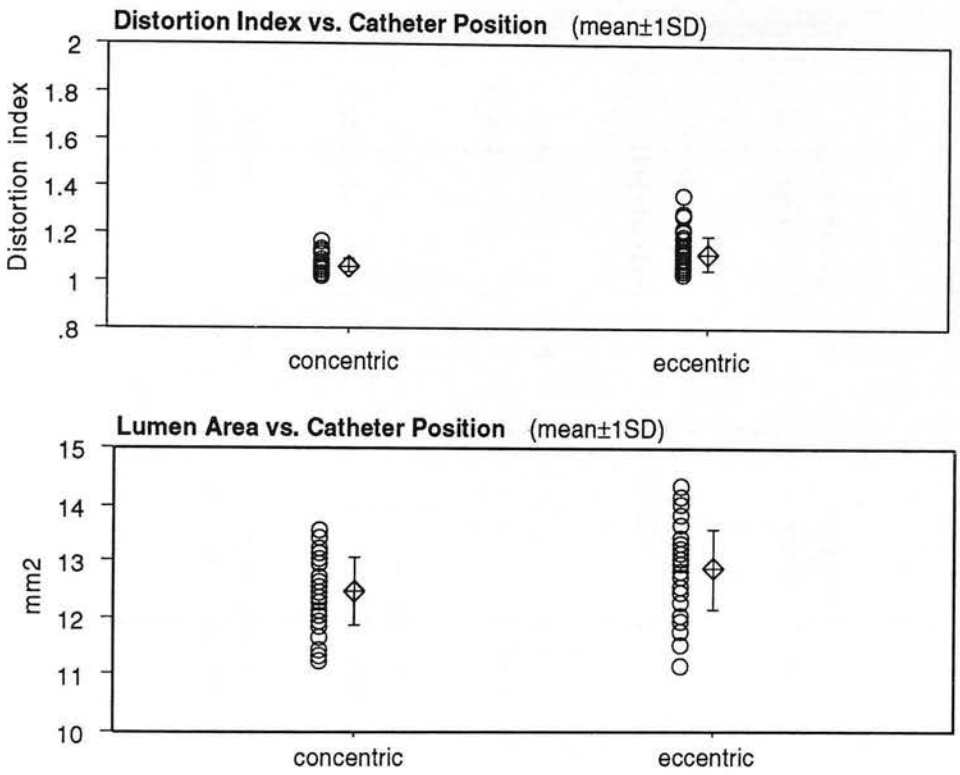

Figure 3.8 Bivariate scattergrams for lumen shape

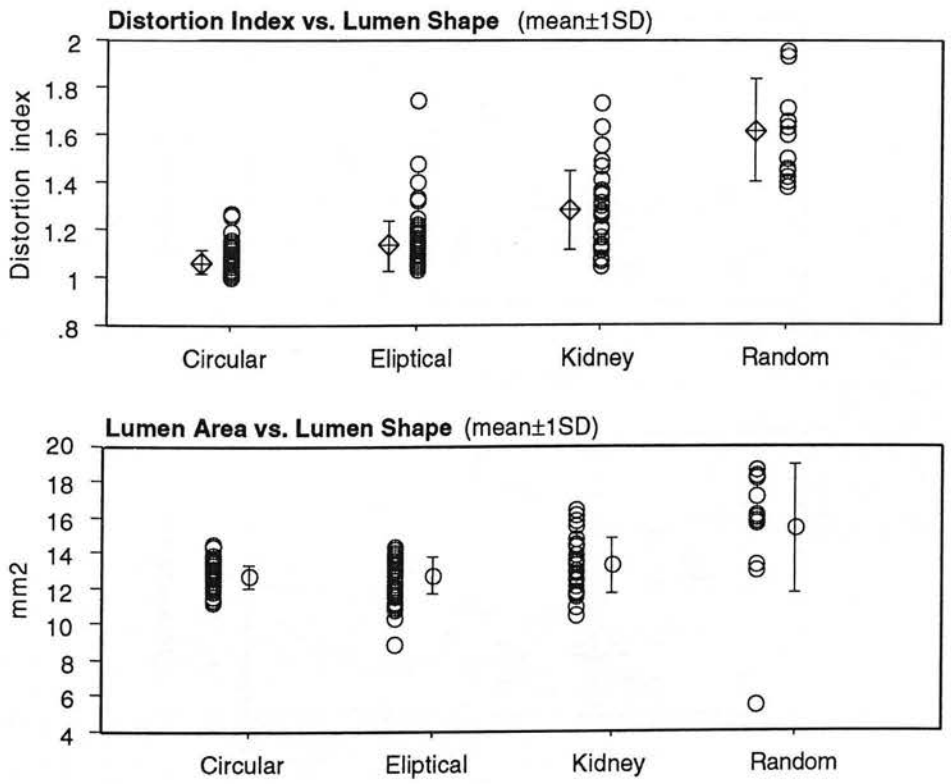

Figure 3.9a Bivariate scattergrams for strut distance Δ vs. number of bends

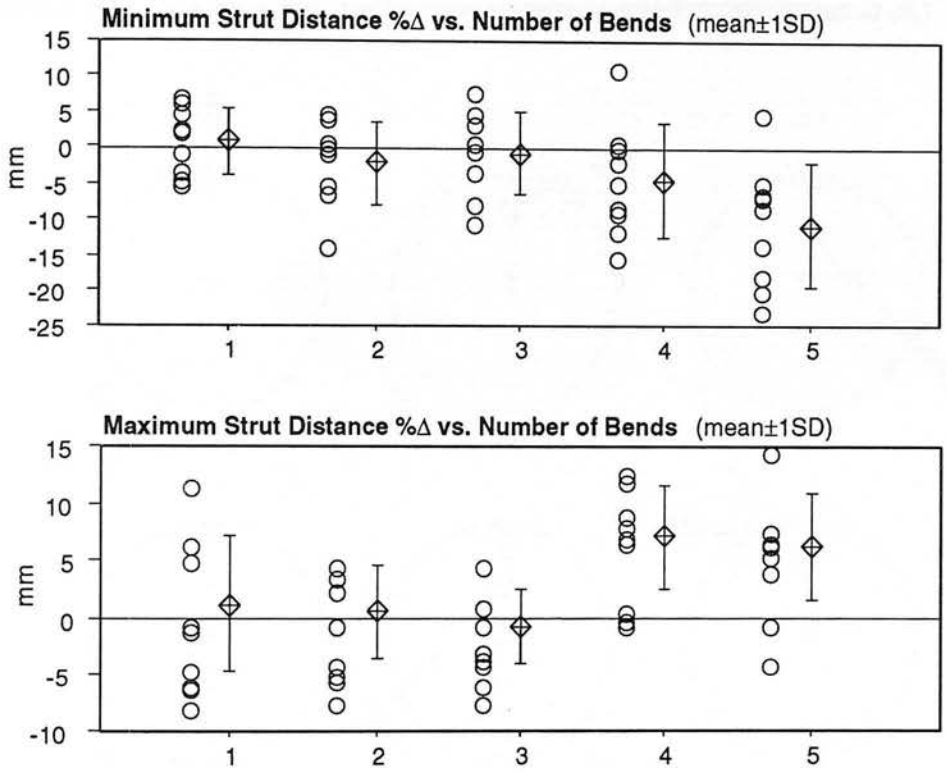

Figure 3.9b Regression of distortion index vs. max and min strut distance Δ

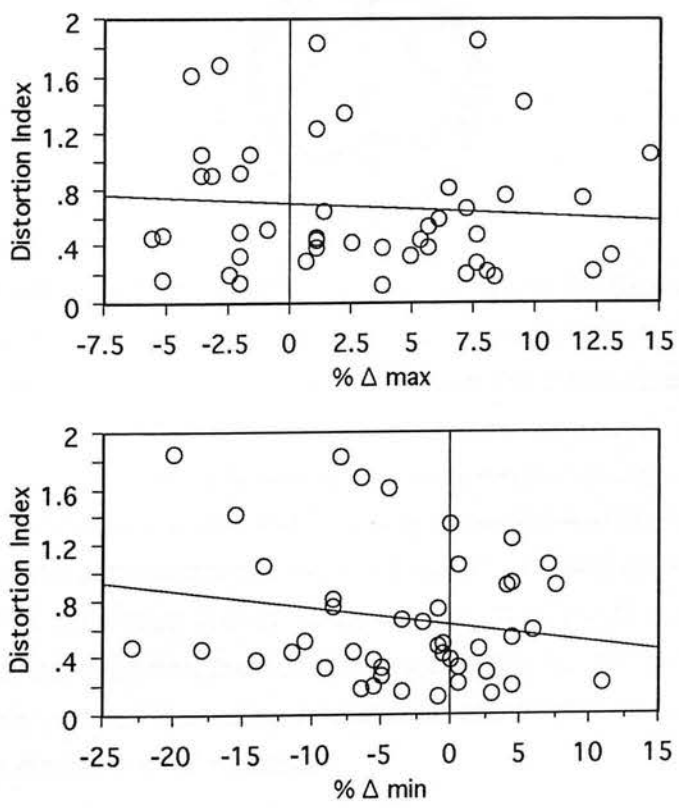

Figure 3.10 Basis for the 'petal-shaped deformation' (after Finet et al.)

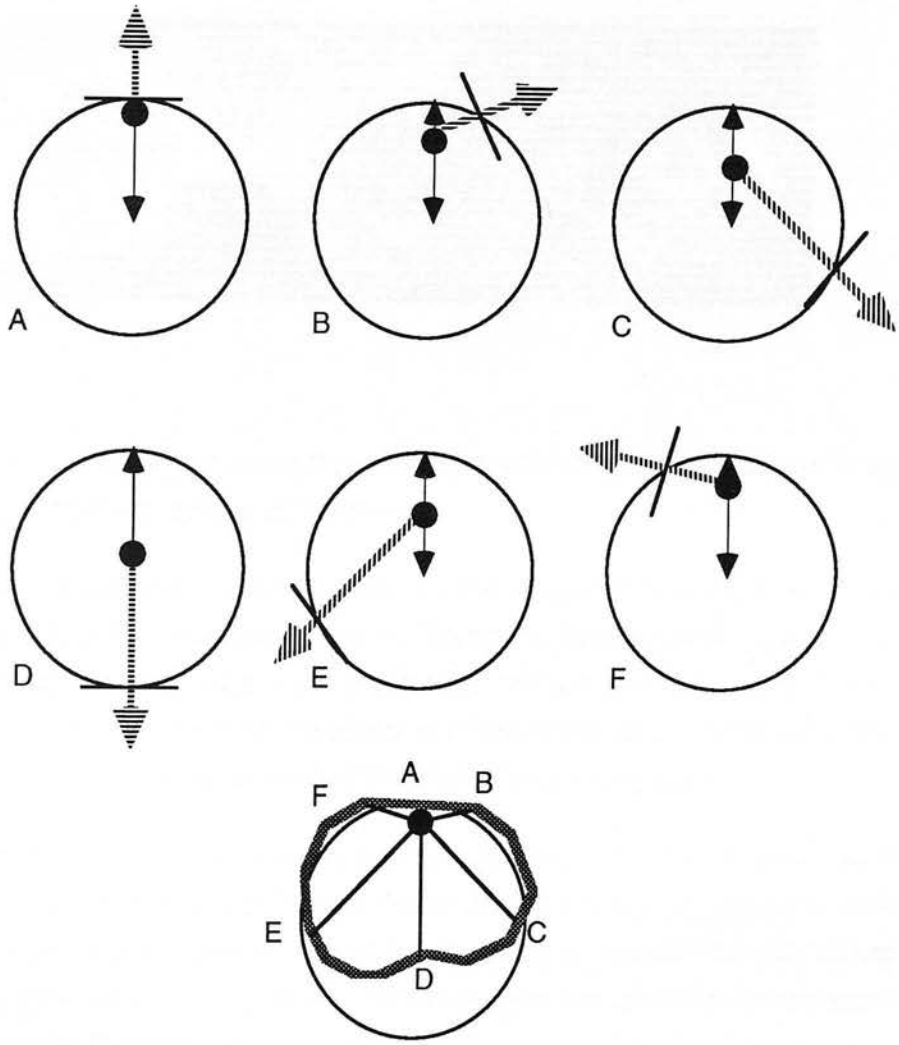

At point A, the transducer lies against the vessel wall, and the ultrasound beam is aimed directly at the vessel wall (indicated by the cross-hatch arrow). As the transducer rotates, it also moves to and fro within the lumen (indicated by the double headed arrow). The net effect of concordant transducer vibration and rotation frequencies is that early and late in the cycle the leading edge echoes from the lumen boundary (indicated by the right angled line at the interface of beam and wall) are more distant (for points B and F), and in mid cycle are closer to the centre of the image (points C, D, and E), than would occur were the transducer in a stable luminal position throughout the cycle. The familiar petal- or kidney-bean shaped representation of a circular structure is thus produced, as shown in the lower part of the schematic.

Figure 3.11 Examples of the rotational angle error artefact

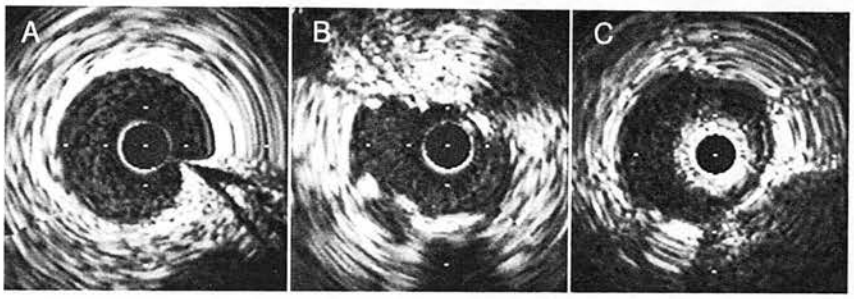

A *A severe rotation angle artefact produces readily identifiable distortion of an image of a normal segment of coronary artery.*

B *A rotation angle error was identified in the image of this stent, in which bunching of echoes is seen from 11 to 1 o'clock, and splaying of the speckles in the lower half of the image. An erroneous interpretation of stent lumen asymmetry, and, depending on the direction of the associated quantitative error, stent underexpansion, may be made if the artefact is unrecognised.*

C *Manufacturing errors in the recently introduced 3.0F 'Spy'® ultrasound catheter has resulted in a peculiar manifestation of the rotation angle error, with evidence of repeated 'stick-slip' behaviour occurring at regular intervals during the transducer's cycle. In this image, 7-8 discrete areas of scan line bunching are identified around the vessel wall circumference .*

Figure 3.12 The basis for the rotation angle artefact

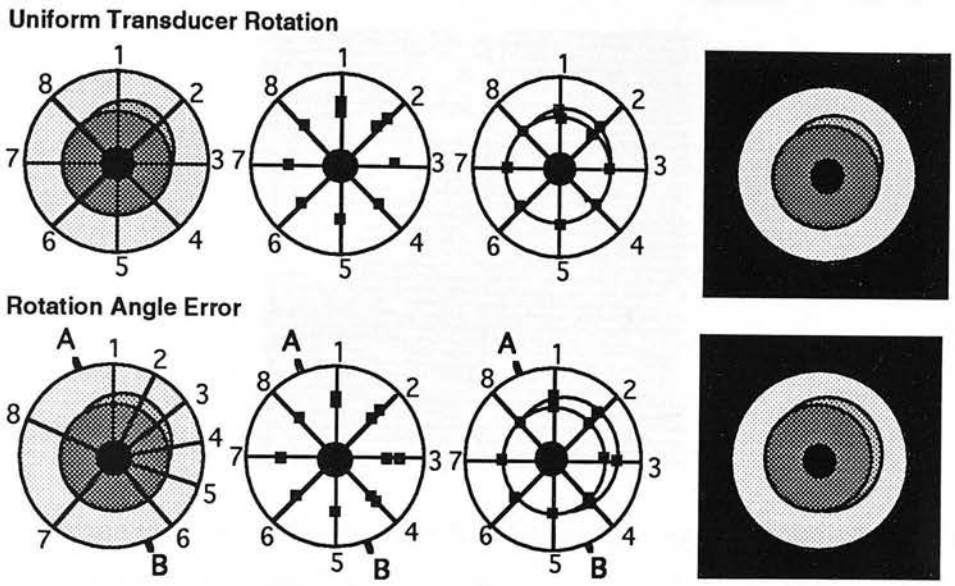

(a) Central Catheter Location

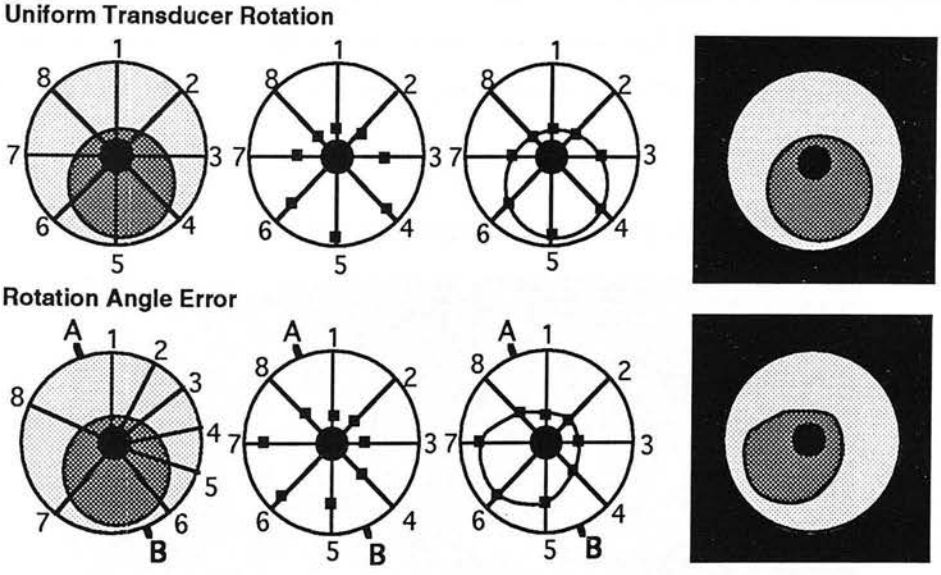

(b) Eccentric Catheter Location

The basis of the rotation angle artefact is shown in the schematic diagram, and detailed in section 3.7.1.1. of the text. In (a), an accurate reconstruction of a vessel is shown from ultrasound data generated by a concentrically placed, uniformly rotating transducer. Non-uniform rotation of a centrally located transducer leads to distortion of the wall, but not lumen, geometry.

In the lower panel (b), the impact of a rotation angle error in an eccentrically located transducer. i.e. distorted lumen and wall geometry, is shown.

Figure 3.13 Splaying of stent strut as a result of failing lateral resolution

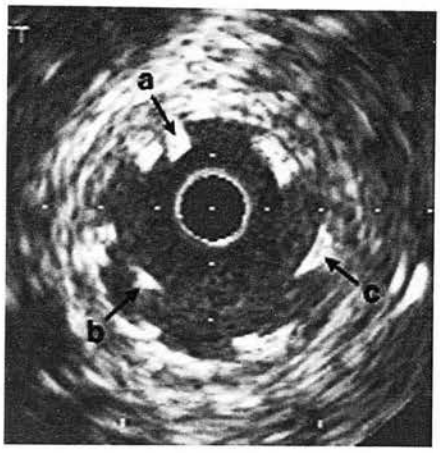

A number of struts of this Palmaz-Schatz stent are poorly apposed to the vessel wall, most notably that labelled 'a'. Despite appearances, the strut at position 'c' was relatively well apposed, but splaying of the intense signal as a result of failing lateral resolution gave the impression of malapposition. The guidewire, labelled 'b', was distinguished from a strut as it was mobile within the lumen, and was seen to extend either side of the stent on the catheter pullback sequence.

Figure 3.14 Poor quality images characteristic of early IVUS scanners

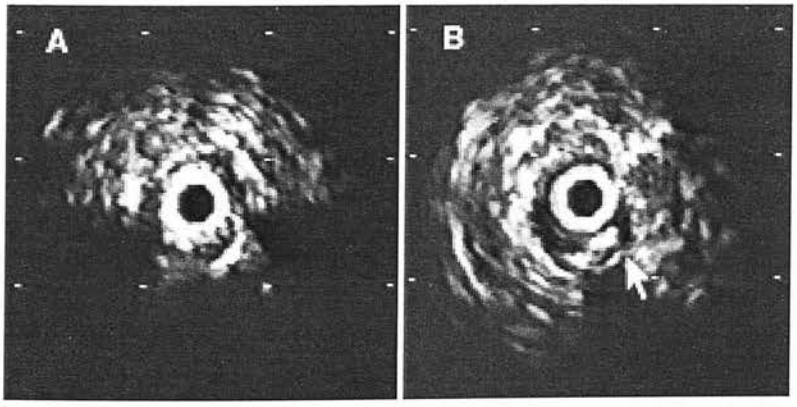

These images were acquired with a Diasonics intravascular ultrasound scanner and 4.8F Boston Scientific imaging catheters. A prominant ring-down artefact surrounds the catheter blank, and obscures much of the lumen.

*In **B**, the arrow points to a possible dissection behind a focal area of calcification. The lesion had not been dilated, however, and these appearances may simply have been the consequence of the limited dynamic range of the imaging system.*

Figure 3.15 The impact of a suboptimal angle of ultrasound insonation

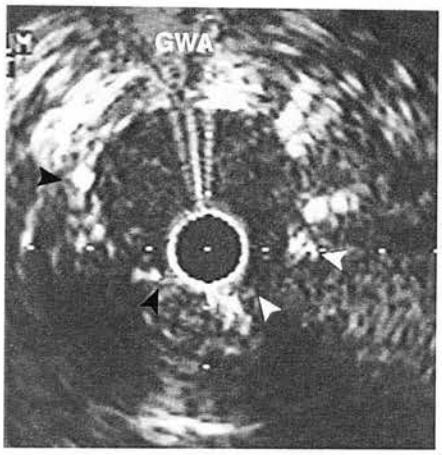

The deleterious effects of a suboptimal angle of incidence of the ultrasound beam with the insonated tissue is illustrated in this image of a well apposed AVE Microstent at the ostium of the posterior descending branch of a right coronary artery. A reduction of videodensity of the vessel wall, not attributable to interposed struts, is evident from 7 to 9 o'clock, where the angle of incidence varies from ~120-180°. The course of the sidebranch, arising between the white arrows, is typically indistinct, as the angle of insonation of both endoluminal borders approximates 180°, but is evident to a limited degree from the blood generated spontaneous contrast within its lumen.

Figure 3.16 Reverberations generated by calcification and guidewires

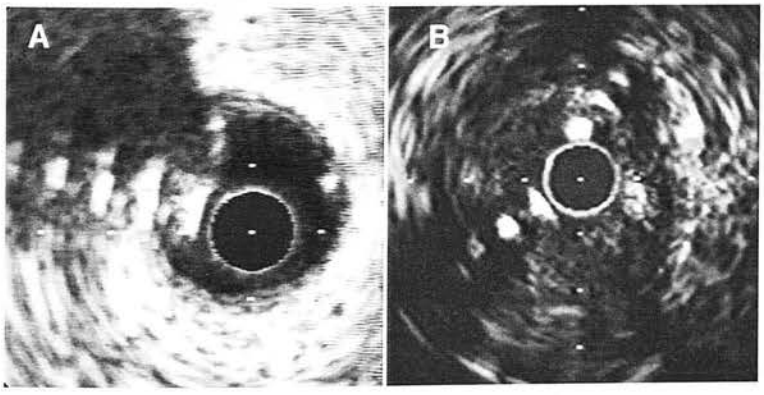

*In panel **A**, a focus of calcification is seen from 7 to 12 o'clock. It is reliably identified by the strong leading edge echo, and serial reverberations propagating into the acoustic shadow.*

*In panel **B**, acoustic shadowing and reverberations are generated by guidewires at 7 and 1 o'clock.*

Figure 3.17 Spontaneous contrast in an unstable lesion following PTCA

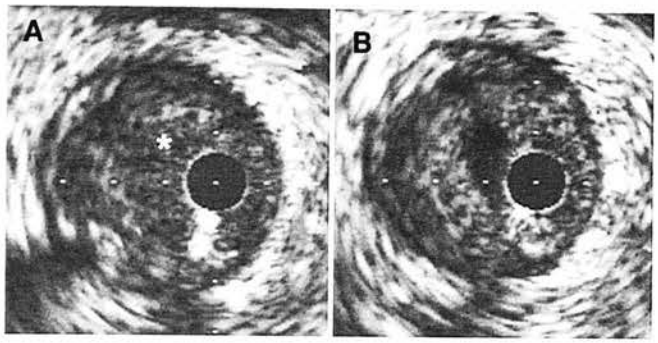

A. *Spontaneous contrast may obscure the borders of the lumen, particularly on still images. In these images, an irregular lumen of an unstable lesion following angioplasty is filled by spontaneous contrast (asterisk).*

B. *The endoluminal border is not discernible until the blood is displaced during radiographic contrast injection.*

Figure 3.18 Vasospasm reversed by intracoronary glyceryl trinitrate

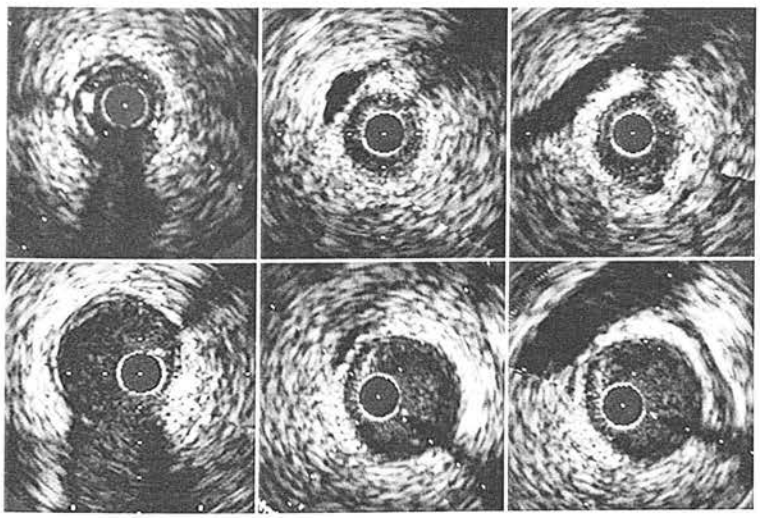

In the upper panels, the catheter blank is closely enveloped by a vessel in which marked vasospasm has occurred.

In the lower panels, at matched sites following the administration of glyceryl trinitrate, the true dimensions of the vessel are appreciated. Following the nitrate injection vasodilatation of the right ventricular branch (arising at 6 o'clock in the left-hand panels) and surrounding veins is also seen.

Chapter 4

Differences in the morphology of unstable and stable coronary lesions and their impact on the mechanisms of angioplasty

An in vivo study with intravascular ultrasound

Contents *page*

4.1. Introduction

As a tomographic technique that provides insight into the underlying plaque morphology and tissue substrate of coronary lesions, intravascular ultrasound (IVUS) has great promise as an imaging modality for studying acute coronary disease. In accordance with pathological studies, echolucent zones, possibly corresponding with lipid pools, are seen more frequently in unstable lesions studied with IVUS [Hodgson, 1993]. The potential of the technique to reveal more detailed information concerning the acute coronary syndromes has, however, been curtailed by difficulties encountered in identifying thrombus. It is widely recognised that despite considerable improvements in image resolution and dynamic range in the current generation of scanners, videodensitometric parameters alone are neither sufficiently sensitive nor specific to identify intraluminal or mural thrombus with any degree of certainty.

4.2. Study Aims

The aims of this observational study were twofold. Firstly, we aimed to characterise the echomorphology of unstable coronary lesions using intravascular ultrasound prior to coronary angioplasty, and, by comparing them to stable coronary lesions, determine whether there were specific features that might be used to distinguish them apart. Secondly, by performing intravascular ultrasound examinations before and after angioplasty, and by comparing matched pre- and post-interventional images within the lesion, we sought to determine and compare the mechanisms of angioplasty in stable and unstable lesions.

4.3. Methods

4.3.1. Patients

An intravascular ultrasound examination was performed in haemodynamically stable patients in patients undergoing percutaneous transluminal coronary

angioplasty before and after intervention. All patients gave informed consent prior to intravascular ultrasound imaging and the study protocol was approved by the institutional ethics review committee. Stable angina was defined as exercise induced chest pain, Canadian Cardiovascular Society (CCS) grades I-IV, which was stable for the preceding two months. Patients were diagnosed as having unstable angina if they experienced new onset angina within the 2 months prior to catheterisation, had angina of a crescendo pattern, constituting an abrupt worsening of their angina by at least 2 CCS grades within 2 months of their catheterisation, or post-infarction angina characterised by recurrent ischaemic pain within two weeks of their myocardial infarction. Patients who went on to develop acute myocardial infarction (formation of q waves and/or a rise in cardiac enzymes) were excluded from analysis.

4.3.2. Coronary angiography and angioplasty - procedural aspects

Coronary angiography was performed using either a Siemens HICOR or Cardoscop U angiographic system. Arteriography and subsequent angioplasty were conducted in a standard fashion using the Judkins approach following right femoral artery puncture. An intravenous infusion of glyceryl trinitrate was set up and the patient was systemically heparinised. A 0.014 inch guide wire (Advanced Cardiovascular Systems, California) was advanced across the lesion to be dilated. Following IVUS imaging as described below, serial balloon dilatations were performed until an optimal angiographic result was obtained. An intracoronary bolus of 5000 IU of heparin and 200 μg of glyceryl trinitrate were injected through the guide catheter after balloon dilatation was completed. The guide wire was left in situ after removal of the balloon catheter and post-interventional IVUS imaging was performed.

4.3.3. Coronary angiography - analysis

Qualitative assessment of the angiographic appearance of lesions before angioplasty was performed by two experienced angiographers and lesions were classified according to the classification of Ambrose et al. [Ambrose, 1985]. The immediate angiographic outcome of the procedure was visually assessed by the operator.

4.3.4. Intravascular ultrasound procedures

Intravascular ultrasound examinations were performed using a Diasonics intravascular ultrasound scanner for 15 cases and a Hewlett Packard Intravascular Sonos for 18 cases. Low profile, 3.5F Sonicath ultrasound catheters (Boston Scientific Corporation) were used, operating at a centre frequency of 20 MHz in the case of the Diasonics device and at 30 MHz in studies performed with the Hewlett Packard Intravascular Sonos. Images were continuously recorded on 0.5 inch S-VHS videotape for later off-line analysis. The ultrasound transducer was advanced over the guide wire to a point distal to the lesion and then slowly withdrawn. The video recording of the ultrasound images acquired during pullback was numbered to coincide with numbered, short cineangiographic recordings of the catheter in the vessel in order to provide more precise longitudinal orientation of the ultrasound images. In addition, an audio recording of the operator's commentary describing the transducer position was recorded on videotape. As the lesion became apparent on the ultrasound images, an injection of radiographic contrast medium was simultaneously documented on the cineangiogram in order to document the exact position of the transducer in the vessel and to improve endoluminal border definition in the ultrasound images. In the majority of cases, once this 'orientating pullback' was completed, the lesion was again crossed with the transducer in order to permit further analysis of the target lesion. The duration of intracoronary imaging was typically 2-3 minutes, each study adding 8-10 minutes in all to the procedure time.

4.3.5. Ultrasound image analysis - methodological aspects

Each videotape examination was dubbed onto a second S-VHS tape and both were simultaneously viewed using twin Panasonic video recorders and monitors. Longitudinal orientation and accurate matching of sites before and after dilatation were achieved in a number of ways. Longitudinal orientation, both before and after intervention, was provided by the numbered stop-frames on the video recording of the IVUS pullback matched against the numbered cineangiographic film runs. More precise pairing of the pre- and post-interventional images could be achieved by matching arterial branch points and specific morphological features of the vessel wall and surrounding echographic features, including focal calcification, adjacent veins and pericardium.

A systematic approach was adopted in choosing the site within the lesion for quantitative analysis. The video frame of the minimum lumen area in the lesion after dilatation and the matching frame from the pre-interventional recording were chosen for analysis. When a match could not be found for the post-interventional image in which the minimum area was apparent, the nearest matching set of images from pre- and post-PTCA IVUS examinations were analysed. The chosen frames were digitised using a Leutron Vision frame grabber and transferred to the hard disc of a Sun Sparc II workstation.

4.3.6. Qualitative IVUS analysis

4.3.6.1. Lesion echodensity

Qualitative analysis of the off-line IVUS video recordings was performed by two observers. The echodensity of each lesion was evaluated as previously described [Gussenhoven, 1989], where lesions were classified as echolucent when areas of minimal or no echo reflections (black or dark grey) were reproducibly evident within the vessel wall and echodense when bright echoes with distal

acoustic shadowing were noted in a part or whole of the lesion. Any other distinguishing echographic features were also noted.

4.3.6.2. PTCA mechanisms

The mechanisms of PTCA were determined from matched pre- and post-interventional images in which the most marked morphological changes in the lesion after PTCA were seen. Vessel stretch was considered to have occurred when a ≥ 10% increase in vessel cross-sectional area (CSA) was evident. Remodelling was said to be present when lesion (or 'plaque)' CSA was reduced by ≥ 10%. Wall tears were classified as minor or major. Minor tears were defined as tears confined to the intima and/or subtending an arc of less than 90° and major tears defined as tears reaching or penetrating the media and/or extending circumferentially more than 90°. Lesion morphology and the mechanism of dilatation were compared in patients with stable and unstable angina.

4.3.7. Quantitative IVUS assessment

Quantitative IVUS analysis of the digitised IVUS images was performed using a quantitation program (Mainz), which calculates distances and areas from pixel counts between and within operator defined computer-mouse delineated points and boundaries respectively. Calibration was performed using the millimetre grid on the IVUS images. Maximum and minimum lumen diameters drawn through the geometric centre of the lumen were determined automatically by the quantitation program following manual tracing of the lumen boundary. Lumen cross-sectional area (the area enclosed by the interface of intimal leading edge and lumen), vessel cross-sectional area (incorporated within the external elastic membrane) and lesion cross-sectional area (vessel area minus lumen area) were measured at the point of minimum lumen dimensions after dilatation and at the corresponding site before dilatation, or at the nearest adjacent points at which matching of images was

possible. We chose to use the term 'lesion' cross-sectional area in preference to 'plaque' cross-sectional area as this measurement may include regions of mural thrombus as well as atheromatous plaque. Images were rejected for quantitative analysis if more than 60° of the vessel wall circumference was obscured by acoustic shadowing from calcific deposits. In cases of minor degrees of acoustic shadowing, the outer border of the vessel was circumferentially extrapolated as previously described [Potkin, 1992].

4.3.8. Statistical analysis

Continuous data are expressed as means ± one standard deviation. Categorical data are expressed as percentages with absolute counts given in brackets. Comparisons between continuous variables were performed using the two tailed paired and unpaired Student's t-test as appropriate. Differences in categorical variables were evaluated using chi square testing. Significance was defined as a probability (p) value of less than 0.05. Statistical analyses were performed using Statview® v4.2.

4.4. Results

4.4.1. Clinical details

Thirty-three patients underwent IVUS imaging before and after coronary angioplasty. Fifteen patients had stable angina and 18 patients had unstable angina. Of those with unstable angina, 10 had new onset angina (9 of whom suffered from rest pain). A further 4 patients had crescendo angina and 4 had post infarction angina. Sixty-one percent (11/18) of patients with unstable angina experienced rest pain within the week preceding their catheterisation, and in 44% (8/18) this occurred within the 48 hours immediately preceding catheterisation. Demographic and clinical details are summarised in **table 4.1**.

4.4.2. Lesion morphology

A specific ultrasonic appearance was observed in the majority of unstable lesions prior to angioplasty. This consisted of an inner layer of homogeneous echodensity demarcated from the outer part of the lesion by a fine circumferential line (**figures 4.1-4.3**). The line was echodense in parts, consistent with a spectral echo at the interface between two tissues of differing acoustic impedance. At other points the interface between the inner and outer layer was echolucent or evident as a line of dynamic speckles during the on-line examination or on video playback, consistent with flowing blood. The echodensity and speckle pattern of the inner layer frequently did not differ noticeably from the surrounding lesion, but, in a proportion of cases was more readily appreciated because of an abrupt interface of differing echodensity or speckle pattern at the demarcating line. In these instances, it typically had a finer speckle pattern, and was usually more echolucent than the surrounding lesion. Following angioplasty, the layer appeared to be largely or completely obliterated and close conformation was noted between the shape of the neolumen with that of the inner layer prior to intervention (**figures 4.1, 4.2**). A thin circumferential or fragmented remnant of the layer was seen around the edge of the neolumen in four cases. A demarcated inner layer was seen at some point in the target lesion in 77% (14/18) of patients with unstable angina and in only one stable lesion ($p<0.01$). The latter was a case of restenosis in which an echolucent demarcating line was evident in a number of frames. Unlike the majority of unstable lesions in which layering was evident, no evidence of remodelling was noted in this lesion after angioplasty (see angioplasty mechanisms).

4.4.3. Lesion echodensity

Areas of low echodensity were more prevalent in unstable lesions than in stable lesions, present in 72% (13/18) compared to 46% (7/15), $p=0.13$. An example of an echolucent zone within an unstable plaque is shown in **figure 4.3**. Highly echodense areas with acoustic shadowing (lesion calcification) was evident in

61% (11/18) of unstable lesions and 80% (12/15) of stable lesions, p=0.24. A summary and comparison of morphological findings in both groups is shown in **table 4.2a**.

4.4.4. Angioplasty mechanisms

Lesion remodelling, compression or displacement was seen in 77%(14/18) of the unstable lesions including all but two in which layering was evident. Increase in lumen area was predominantly the result of vessel stretch in one of these cases and was negligible in the other, neither remodelling nor stretch occurring to any extent. Significant lesion CSA reduction was seen in only 2 stable lesions (13%). On the contrary, vessel stretch was frequently seen in patients with stable angina (73%, 11/15) compared to those with unstable disease (22%, 4/18) $p<0.01$ An example of vessel wall stretch and tear in a stable lesion is shown in **figure 4.4** and the differences in angioplasty mechanisms between stable and unstable lesion highlighted in **figure 4.5**. Lesion tear was present to a similar degree in both groups of patients. Minor tears were found in 53% (8/15) of unstable lesions and 39% (7/18) of stable lesions, p=0.41. Major tears were present in 17% (3/18) of unstable lesions and 13% (2/15) of stable lesions, p=0.8. **Table 4.2b** summarises the differences in angioplasty mechanisms found between both groups.

4.4.5. Quantitative analysis

Lesion CSA was reduced to a greater extent in patients with unstable angina, $-14.8 \pm 8.3\%$ (2.1 ± 1.3 mm^2) than in patients with stable angina, $-4.1 \pm 8.4\%$ (0.42 ± 0.9 mm^2), $p<0.01$. Moreover, whereas the reduction in lesion CSA in unstable lesions was highly significant ($p<0.01$), the lesion CSA of stable lesions did not change significantly after angioplasty (p=0.07). The increase in vessel area after angioplasty resulting from vessel wall stretch in the dilated segment was less marked in patients with unstable angina, $+5.5 \pm 5.6\%$ (0.8 ± 0.9 mm^2) than in stable lesions, $+13.5 \pm 6.8\%$ (1.6 ± 0.9 mm^2), $p<0.01$. Lesion dimensions before

and after angioplasty in the stable and unstable lesions are shown in **table 4.3** and the differences in vessel and lesion CSA change in **figure 4.5**.

4.4.6. Angiographic analysis

Type II eccentric lesions were commoner in unstable patients (39%, 7/18 vs. 7%, 1/15, $p<0.05$). In the unstable group, 4/18 patients had concentric smooth walled stenoses, 5/18 had eccentric, type I (smooth walled) stenoses, 7/18 had eccentric, type II (complex) stenoses and 2/18 demonstrated diffuse irregularity. In the stable group, 4/15 culprit lesions were concentric and smooth walled, 9/15 were eccentric and smooth walled, 1/15 were eccentric, type II and 1/15 consisted of multiple irregularities. The distribution and number of vessels that were diseased and a summary of the angiographic lesion morphology is given in **table 4.4a** and **4,4b**.

4.5. Discussion

4.5.1. The basis of the 'layered' appearance

The principal finding of this study is the observation that unstable coronary lesions are frequently characterised by a previously unreported echographic appearance consisting of a 'layered' appearance within the lesion. Without concomitant angioscopy or a tissue diagnosis from atherectomy cuttings, the histological basis of this echographic appearance is uncertain but on the basis of the following observations we believe that the most plausible explanation for echographic lesion layering is mural thrombus apposed to an underlying atheromatous plaque. First, these markers were seen predominantly in unstable lesions, the majority of which are known to be thrombotic in nature [Davies, 1984; Falk, 1985]. The pattern we describe is more readily explained by a closely apposed layer of thrombus than by other histological features, such as plaque fissuring or lipid collections, that are also known to occur more commonly in this group of patients. Second, the echo characteristics of the inner layer corresponded

with published descriptions of experimentally induced intra-arterial thrombus (fine, scintillating speckle). The echodense line demarcating the outer border of the layer may be a specular echo resulting from an acoustic interface between tissues of differing acoustic impedance, such as plaque and thrombus. Third and very suggestively, in unstable lesions the shape and size of the neolumen following intervention corresponded closely with those of the delimited inner layer prior to angioplasty, with a thin layer of residual material evident in a number of cases (**figures 4.1, 4.2**). The likelihood that this arises from displacement or remodelling of a circumferentially distributed inner layer of thrombus was supported by the significant reduction in lesion cross-sectional area seen in unstable but not stable lesions. Compression of other plaque components, including lipid atheroma, has not been found to occur in an experimental angioplasty model [Casteneda, 1980], increasing the probability that a readily deformable tissue, such as thrombus, was present in those lesions in which a marked reduction in cross-sectional area occurred and in which a layer was identified.

4.5.2. Angioplasty mechanisms

Prior to the introduction of smaller transducers and pre- and post interventional IVUS imaging, direct determination of coronary artery wall stretch or compression was not possible. In this study in which all patients underwent pre-interventional imaging, differences between the mechanism of angioplasty in stable and unstable lesions are described for the first time. Previous studies have shown that lumen gain at angioplasty results from plaque rupture in combination with vessel stretch [Block, 1981; Sanborn, 1983], and that the original theory of a 'cold flow' compression of soft atheroma [Dotter, 1964; Grüntzig, 1977] is an improbable basis for lumen gain [Casteneda, 1980]. In agreement with these findings, we found no evidence to suggest compression of plaque in stable lesions in which vessel stretch was the more prominent angioplasty mechanism (**figure 4.4**). A distinctive dilatation mechanism appeared to operate in unstable plaques,

involving compression or longitudinal remodelling of a central portion of the lesion. Despite these differences, the post-angioplasty minimum lumen area was similar in both unstable and stable lesions and plaque tears, both minor and major, were observed with similar frequency in both groups.

4.5.3. Other studies

To date, little has been published concerning intravascular ultrasound findings in the acute coronary syndromes. In the one previous report of IVUS findings in a series of patients with unstable angina, echolucent plaques, thought to correspond with 'soft' or lipid laden collections, were found significantly more often in unstable angina, and were a more sensitive indicator of an unstable lesion than was the angiographic appearance [Hodgson, 1993]. Echolucent zones were found more frequently in the unstable lesions that we studied (**figure 4.3**), but the difference did not reach statistical significance. A higher prevalence of lipid plaques in acute coronary lesions is pathophysiologically plausible [Falk, 1983], but an overview of validation studies shows that lipid plaque is the histological subtype identified with least accuracy by videodensitometric analysis of IVUS images [Kearney, 1995]. Until technical advances make more precise and reproducible tissue characterisation feasible, the usefulness of markers of plaque instability based on echodensity alone thus remains problematic. In case reports describing the ultrasound findings in unstable lesions, thrombus was diagnosed on the basis of a 'granular' echographic appearance, as first described in an experimental report of the ultrasonic characteristics of intravascular thrombus [Mintz, 1992c; Siegal, 1991]. In our study, the inner layer in unstable lesions was characterised in a proportion of cases by a fine granular appearance and/or difference in echodensity from surrounding tissue, but in no case did the identification of a layer rely solely on these characteristics. The need for a more accurate set of diagnostic markers to identify thrombus has been highlighted by reports of the poor sensitivity [Seigal, 1991] and specificity [Jain, 1992] of IVUS in this regard when relying solely upon

the speckle pattern. That others do acquire images in which lesion layering is evident, but have not appreciated its significance appears likely. An example in the published literature is seen in an IVUS image of a layered unstable lesion before directional coronary atherectomy, a pattern that is not alluded to by the authors and is not depicted on an accompanying graphic of an homogenous plaque [Weissman, 1994].

Previous reports of the mechanisms of angioplasty based completely on pre- and post-interventional IVUS imaging are confined to the peripheral circulation [Losordo, 1992]. To our knowledge there are no previous reports of the mechanisms of angioplasty in unstable lesions or comparisons between angioplasty mechanisms in stable and unstable disease. Previous studies of angioplasty mechanisms based on post-interventional imaging alone identified vessel stretch indirectly (by comparing the dilated segment vessel CSA to the vessel CSA in the proximal segment), a method that may be subject to significant error in view of the adaptive enlargement of diseased arterial segments. Lesion CSA reduction is not identifiable without pre-interventional imaging and the assumption that the absence of tears or dissections indicates smooth stretch of the vessel wall takes no account of the possibility of the remodelling process which we describe.

4.5.4. Implications of the study findings

At a practical level, our findings have implications for the acquisition and interpretation of IVUS images of coronary lesions. Pre-interventional imaging is shown to be important both to allow accurate characterisation of the lesion and to determine the true mechanism of angioplasty, e.g. in order to distinguish between layer displacement from simple stretch. A controlled, slow pullback of the catheter is essential to ensure complete characterisation of the lesion, as tissue features

such as layering may be subtle and easily missed if confined to a small number of frames on the video playback sequence.

Our findings have a number of clinical and theoretical implications. If these markers prove to be a reliable means of detecting mural thrombus, intravascular ultrasound will provide a highly informative means of studying in vivo the role of thrombus in the acute coronary syndromes, the natural history of coronary atheroma and the short and long-term outcome of coronary interventions. The role and efficacy of new antithrombotic agents, including hirudin and GP IIb, IIIa receptor antagonists are currently being evaluated in the peri-interventional setting. A method of accurately identifying and quantifying the thrombotic burden, as may be provided by IVUS assessment using these markers, may prove useful in selecting patients who are likely to gain from adjunctive antithrombotic therapy. Prediction of the mechanism and short term outcome of angioplasty with IVUS, although theoretically promising [Lee, 1993], has not as yet been realised. Apart from the observation that wall tears occur more frequently at the junction between calcific deposits and more compliant plaque tissue [Fitzgerald, 1992b], no other predictors of the mechanism of angioplasty have been reported. Identification of lesion layering in unstable patients may prove to be a means of predicting acute lesion remodelling as the likely angioplasty mechanism in lesions in which it is found. The impact of lesion layering on restenosis is an interesting issue for future study. At a practical level, our findings have implications for the acquisition and interpretation of IVUS images of coronary lesions. Pre-interventional imaging is seen to be crucially important both to accurately characterise the lesion and to determine the true mechanism of angioplasty, e.g. in order to distinguish between layer displacement from simple stretch. A controlled, slow pullback of the catheter is essential to ensure complete characterisation of the lesion, as tissue features such as layering may be subtle and easily missed if confined to a small number of frames on the video playback sequence.

4.5.5. Technical considerations and limitations

A number of technical artefacts may introduce apparent layering within a lesion and were specifically excluded during morphological analysis. A discrete circular line centred on the catheter blank may be seen when adjacent time gain controls are set to different levels, but is recognised by its unnatural symmetry and position with respect to the centre of the image. Second, temporal averaging of images obtained at the border of the lesion with a segment of less stenosed adjacent lumen can produce a 'layered' appearance but can be excluded by switching off the averaging process and by the demonstration of the phenomenon at different points throughout the lesion. Third, the increased reflectivity of blood imaged at 30 MHz, particularly as flow becomes sluggish and rouleaux form, can be mistaken for a discrete tissue layer rather than the blood filled lumen. We systematically excluded this phenomenon by (1) injecting a contrast or saline flush to clear the lumen of blood speckle, and (2) by distinguishing between the dynamic speckle generated by flowing blood on real-time viewing from the relatively static speckle of adjacent tissues or thrombus.

As our ultrasound imaging was limited to two dimensions, we were not able to determine whether the reduction in lesion cross-sectional area was the result of displacement, remodelling or compression of the inner layer. No symptomatic or electrocardiographic sequelae were noted in these patients to suggest that embolisation of material was operative. More detailed analysis of angioplasty mechanisms will be possible when an accurate method of volumetric plaque analysis has been developed.

Although all clinical subtypes of unstable angina were studied, the majority of patients suffered chest pain at rest, underwent urgent angiographic examination and required coronary angioplasty, all factors that may have selected a group with more severe disease. A layered morphology was seen in lesions underlying all

three subtypes of unstable angina considered, but in just one stable lesions. We have observed a layered morphology and layer obliteration following angioplasty in patients with acute myocardial infarction and in patients studied some weeks following acute infarction. Layering may thus be a marker of the acute coronary syndromes more generally, but this issue was not addressed by this study and the specificity of echographic lesion layering requires further study.

4.6. Conclusions

In this observational study, a set of echographic morphological markers that may reflect the presence of mural thrombus was found in a majority of patients with unstable angina. We furthermore describe differences in the mechanisms of angioplasty between stable and unstable lesions, with vessel stretch seen to a greater extent in stable lesions and remodelling of a central layer seen in unstable lesions. We anticipate that further improvements in image quality of intravascular ultrasound devices and advances in tissue characterisation techniques will make the detection of fine histological features within coronary lesions more reliable, but in the interim, the markers we describe should be taken into account when analysing IVUS images. Further studies are required to determine the prevalence and specificity of this echographic pattern and to determine its histological basis.

Table 4.1 Demographic and clinical details

	Stable	Unstable			
Patients	15	18			
Age	53.2±8.9	56.2±10.3			
Male/female	11/4	15/3			
CCS*	2.0±0.5	3.6±0.8			
Unstable angina category			**rest pain <48 hrs**	**rest pain >48 hrs**	**no rest pain**
New onset	-	10	6	3	1
Crescendo	-	4	1	0	3
Post infarction	-	4	1	2	1

Table 4.2 Ultrasonic lesion morphology (a), and PTCA mechanisms (b)

(a) IVUS Morphology	Stable	Unstable	χ^2 p
Echolucent	7/15 (46%)	13/18 (72%)	0.13
Echodense + acoustic shadow	12/15 (80%)	11/18 (61%)	0.24
Layering*	1/15 (7%)	14/18 (77%)	<0.01
(b) Angioplasty mechanisms	**Stable**	**Unstable**	χ^2 p
Stretch	11/15 (73%)	4/18 (22%)	<0.01
Remodelling	2/15 (13%)	14/18 (77%)	<0.01
Minor Tear	8/15 (53%)	7/18 (39%)	0.41
Major Tear	2/15 (13%)	3/18 (17%)	0.79

Table 4.3 Dimensions before and after PTCA in stable and unstable lesions

	Pre PTCA		Post PTCA	
	Stable	Unstable	Stable	Unstable
Max lumen diameter (mm)	1.9±0.5	1.6±0.4	2.9±0.7	2.7±0.6
Min lumen diameter (mm)	1.6±0.4	1.5±0.3	2.1±0.5	2.4±0.5
Lumen CSA (mm^2)	2.3±1.0	1.8±0.7	4.4±1.7	4.7±1.9
Vessel CSA (mm^2)	12.4±3.8	16.7±6.6	14.0±4.3	17.7±6.6
Lesion CSA (mm^2)	10.1±3.5	14.8±6.1	9.7±3.6	12.8±5.9
Percentage stenosis (%)	80.8±8.0	88.7±3.3	68.7±10.2	71.8±9.1

Table 4.4 Lesion distribution and angiographic morphology

(a) Lesion distribution and number of diseased vessels	Stable	Unstable	
Vessel: LAD	13	9	
RCA	2	6	
LCx	0	3	
One vessel disease	9	13	
Two vessel disease	5	5	
Three vessel disease	1	0	
(b) Angiographic Morphology	**Stable**	**Unstable**	**χ^2 p**
Concentric	4/15 (26%)	4/18 (22%)	NS
Eccentric type I	9/15 (60%)	5/18 (28%)	NS
Eccentric type II	1/15 (7%)	7/18 (39%)	<0.05
Multiple irregularities	1/15 (7%)	2/18 (11%)	NS

Figure 4.1 Inner layer in an unstable RCA lesion before and after PTCA

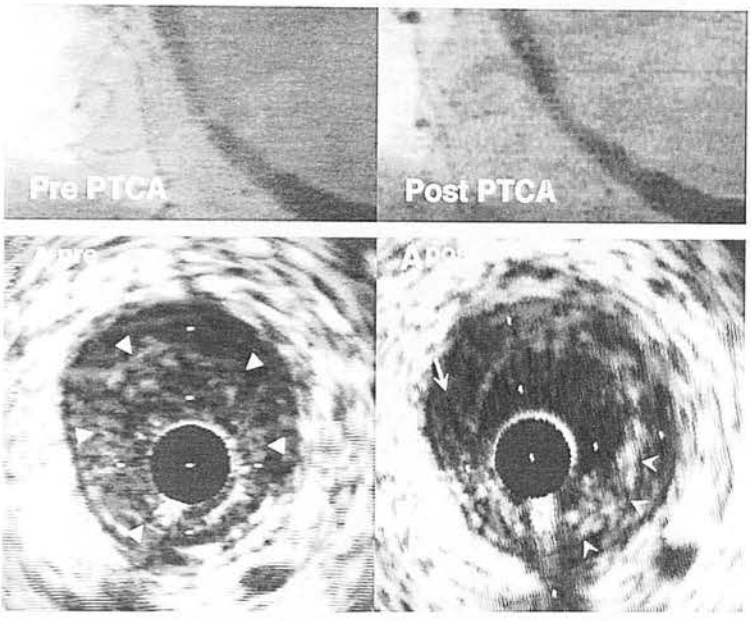

The upper panels show angiograms before and after angioplasty of a lesion in the right coronary artery of a 56 year old woman with new onset unstable angina. The lower panels show the corresponding IVUS images at the lesion before and after PTCA.

A pre. *Aa large eccentric lesion surrounds the catheter blank. Within the lesion, a fine circumferential line (arrowheads), echodense from 6 o'clock to 12 o'clock and echolucent for the remainder of its course, demarcates an outer from an inner layer.*

A post. *After PTCA, the neolumen at the site of minimum lumen area conforms closely in shape with that of the inner layer prior to intervention. Although minor vessel stretch is evident, the increase in lumen size appears to be predominantly the result of remodelling or 'compression' of the inner layer. Some residual material (possibly mural thrombus) is seen in the lower right hand edge of the lumen (hollow arrowheads) at 5 o'clock. A minor plaque tear is indicated by the white arrow.*

Figure 4.2 Inner layer in an unstable lesion

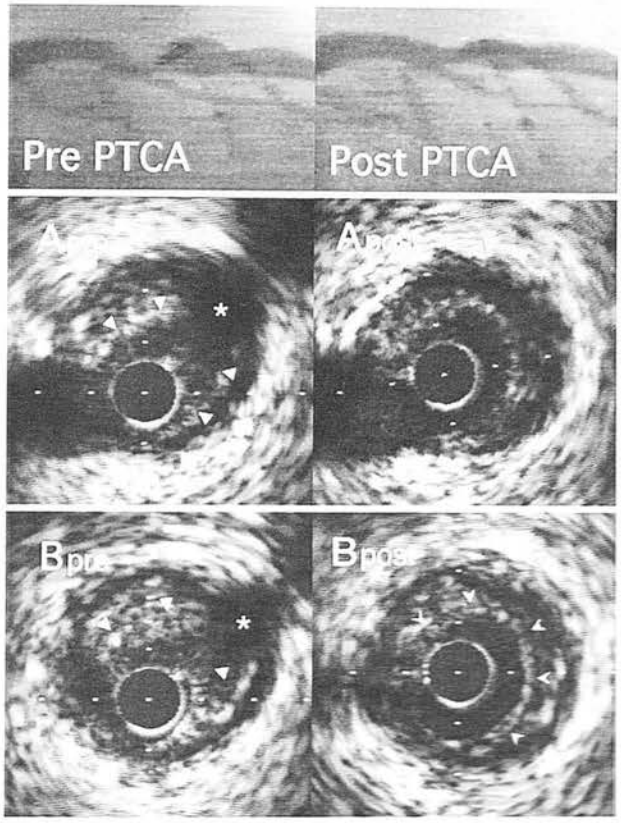

The angiograms before and after PTCA of a proximal LAD stenosis causing unstable angina are seen in the upper panels. The lower panels show matched IVUS images of the lesion before and after PTCA.

A pre. *The catheter blank, situated at the origin of the first diagonal branch, is wedged in an eccentric lesion (9 to 7 o'clock), that is divided into outer and inner layers, separated by an echodense line (arrowheads).*

A post. *After PTCA the neolumen corresponds in area and shape with the demarcated inner layer prior to dilatation. Little stretch and no significant change in dimensions of the underlying plaque has occurred.*

B pre. *At a point proximal to the diagonal origin, a layer is again evident (arrowheads) obscured by the guide-wire artefact at 2 o'clock (asterisk).*

B post. *The neolumen corresponds in dimensions and shape with the layer evident prior to intervention, but a thin remnant of the layer is evident from 9 to 6 o'clock (hollow arrowheads).*

Figure 4.3 An example of a 'vulnerable plaque'

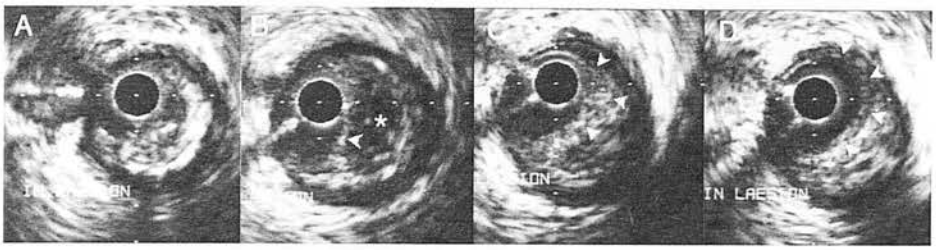

An example of a probable pool of lipid rich material or 'atheroma' underlying a critical stenosis in a patient with unstable angina (a "vulnerable plaque"). The series of images, A-D, are taken from a catheter pullback through the stenosis.

***A.** A diagonal branch (10 o'clock) arises at the distal end of the lesion. The catheter blank sits in a small, eccentrically placed lumen, the unoccupied portion of which is seen on its lower, left side.*

***B**. The large eccentric plaque is made up of an echolucent core (asterisk) separated from the lumen by a thin cap (arrowhead).*

***C**. Subtle layering (possibly representing mural thrombus) is evident from 1-6 o'clock., the inner layer separated from the underlying lesion by a thin echolucent line (arrowheads).*

***D**. The thin layer is better seen (arrowheads), appearing echolucent relative to the underlying plaque.*

Figure 4.4 Angioplasty of a stable lesion

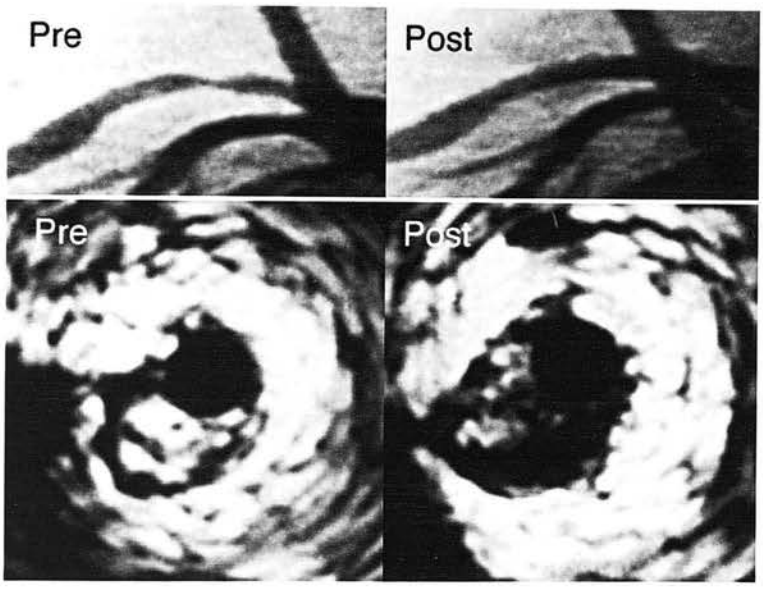

The angiograms (upper panels) show a concentric stenosis in the proximal left anterior descending artery before and after angioplasty. The angiographic appearances suggest satisfactory lumen gain, without visible dissection.

In the lower panels, intravascular ultrasound demonstrates a highly eccentric echodense plaque at the point of maximum stenosis, the area of which does not change following angioplasty. The lumen is completely occupied by the catheter blank before angioplasty. The eccentric plaque extends from 3-9 o'clock.

The lower right hand panel shows the lesion after angioplasty. The increase in lumen size is seen to be the result of a sub-intimal dissection and moderate vessel stretch. (The impact of the limited dynamic range of the Diasonics scanner, with which this study was performed, is evident in these high contrast images).

Figure 4.5 Lesion area change (a) and vessel area change (b) after PTCA

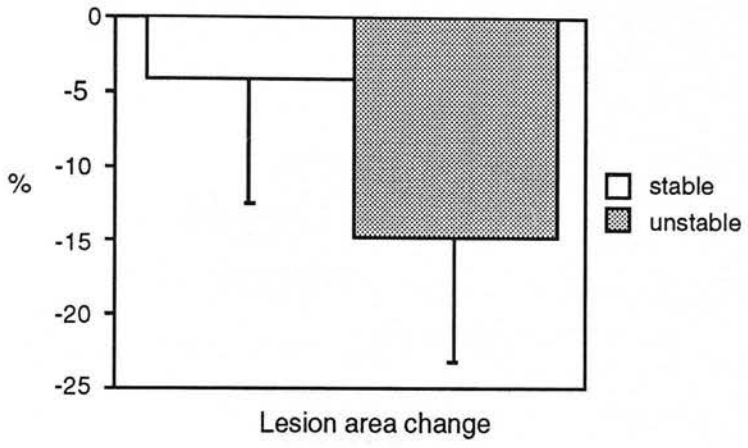

(a)

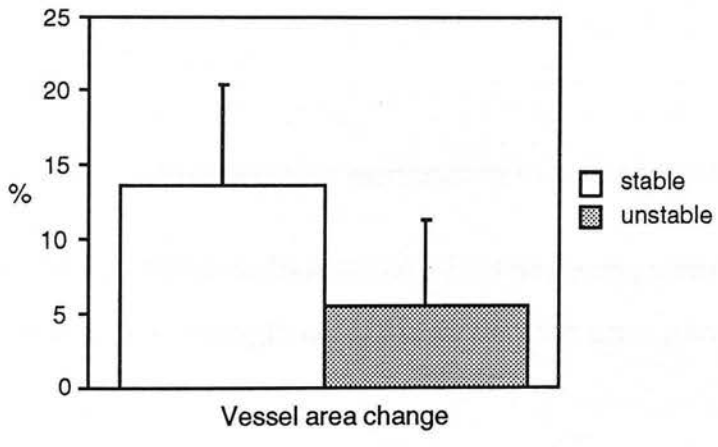

(b)

Bar graphs of relative changes in vessel dimensions following balloon angioplasty in stable and unstable lesions. Error bars indicate one standard deviation. ***(a)*** *The relative reduction in lesion cross-sectional area in stable lesions, -4.1 ± 8.4%, was significantly less than the reduction that occurred in unstable lesions, -14.8±8.3%.* ***(b)*** *The relative increase in vessel cross-sectional area, indicative of vessel wall stretch, was +13.5±6.8% in stable lesions, significantly greater than the +5.5±5.6% in unstable lesions.*

Chapter 5

The application of intravascular ultrasound in coronary stenting

Observations in a consecutive series of ultrasound guided stent implantations in a single centre over an 18 month period

Contents *page*

5.1. Introduction

In view of its potential to improve both the acute and long-term outcome of coronary stenting, the guidance of coronary stent deployment by intravascular ultrasound is currently a subject of great interest. Potential benefits including cost-savings generated by a simpler and safer post implantation therapeutic regimen that allows early patient discharge are particularly appealing in the current climate of cost constraint. For those working in the field of intravascular ultrasound, the guidance of stent implantation is seen as one of the most promising clinical applications of the technique. So far, however, there is no data to suggest that ultrasound guidance is necessary in all cases. It may transpire to be the case that, having revealed the deficiencies of current practice, appropriate solutions might be applied without ultrasound or that its use be confined to specific indications. In this chapter and the next, a number of aspects of the application of intravascular ultrasound in stent implantation are explored.

5.2. Study Aims

The aim of this study was to document the ultrasound findings in a series of patients undergoing coronary stenting in which balloon inflation pressures of 10 atmospheres and over were used to dilate the deployed stent. The proportion of angiographically successful cases fulfilling the criteria for ultrasound success was determined. The impact of a routine policy of a moderate to high final balloon inflation pressure was evaluated in terms of the proportion of cases fulfilling the different ultrasound criteria for 'optimal' deployment. The differences in deployment strategy between those fulfilling these criteria and those not were assessed, and the nature and impact of further intervention in those cases judged to be suboptimally deployed was determined.

5.3. Methods and materials

5.3.1. Patients and procedures

Included in this study were consecutive cases who received coronary stents that were examined wtih intravascular ultrasound following angiographically guided optimisation, and a final balloon inflation pressure within the stent of ≥10 atmospheres had been applied. Stents were implanted for four different indications, i.e. elective, bail-out, for a suboptimal angiographic result, and as a part of a clinical trial. Elective procedures were pre-planned. Bailout procedures were carried out for threatened or actual acute closure of the vessel. A suboptimal angiographic result prompted stent implantation when the residual stenosis after balloon angioplasty was estimated to exceed 30-40%, with or without a dissection ≤ type B. The procedures were conducted over an 18 month period at a single centre (Western General Hospital, Edinburgh) during which time there were 533 balloon angioplasty procedures, in 75 of which coronary stents were implanted.

5.3.2. Catheterisation protocol

Coronary angiography was performed using a digital angiographic system (Siemens HICOR). French 8 guiding catheters were used in the majority of cases and French 6 guiding catheters in 2 cases. A 0.014 inch floppy guide wire was advanced to the distal coronary artery and balloon angioplasty performed in the standard fashion.

5.3.3. Stent implantation protocol

In the case of elective stenting, pre-dilatation was performed with an undersized balloon or more frequently a definitively sized, but underinflated, balloon prior to delivery of the stent on a definitively sized balloon. Stents were hand crimped onto the balloon of the operator's choice prior to delivery to the treated lesion, except in 2 instances in which pre-mounted stents were employed. In all cases, prior to imaging with intravascular ultrasound, an effort was made to optimise stent

deployment by using an inflation pressure of at ≥10 atmospheres of an appropriately sized balloon, chosen on the basis of a visual assessment of the adjacent reference lumen diameters on the angiogram. The angiographic appearances indicative of optimal stent deployment were defined as the absence of visually appreciable residual stenosis within the treated segment, uniform contrast density proximal, within and distal to the deployed stent, and complete coverage of dissection flaps. In stented segments judged to be incompletely or suboptimally treated on the basis of the ultrasound findings, a number of alternative strategies were adopted. These included further dilatations of the same balloon at higher pressures, a change to a larger or less compliant balloon, or implantation of further stents in the case of uncovered dissections.

5.3.4. Anticoagulant and antiplatelet therapy

A bolus dose of 10,000 units of heparin was administered after the coronary artery was engaged by the guiding catheter, and a further 5,000 units given one hour later if the procedure was still underway. In those cases in which warfarin anticoagulation was instituted following stent implantation, the arterial sheath was removed at approximately four hours after the procedure (when the activated partial thromboplastin time (APTT) measured <1.5:1). Four hours after sheath removal, a bolus intravenous injection of 2,000 units of heparin was given, and a heparin infusion running at 1,000 units per hour was started. The dose of heparin was adjusted following a further check of the APTT 6 hours later, in order to maintain an APTT of 2.5-3.0:1. The infusion was continued until warfarin anticoagulation, started on the evening of the procedure, had achieved an international normalised ratio (INR) of 2.5-3.0:1. Warfarin therapy was continued for 2 months. Three hundred milligrams of soluble aspirin was administered in the catheterisation laboratory prior to stent implantation, and was continued in a dose of 300 mg of an enteric coated preparation per day.

The patients not anticoagulated following stent implantation (8 cases in the last 6 months of the study, excluding bailout cases, in whom an optimal ultrasound result was documented), were discharged the day after the procedure on 300 mg of enteric coated aspirin alone. Ticlopidine was not used.

5.3.5. Intravascular ultrasound

An intravascular ultrasound study was performed following stent deployment using Boston Scientific/Scimed 3.5 F Sonicath ultrasound catheters (and in one case a 3.0 F 'Spy' catheter) connected to a Hewlett-Packard Sonos Intravascular Ultrasound scanner. The catheter was advanced over the wire distal to the stented segment of vessel and withdrawn slowly through the lesion. This was repeated at least once and a third pass was performed if judged necessary to allow study of areas of interest with a stationary transducer position. Each study was stored on S-VHS videotape and measurements made off-line from the video images. In cases in which the ultrasound findings revealed suboptimal deployment, a repeat ultrasound study was performed to re-assess the response of the treated segments to further intervention whenever possible.

5.3.5.1. Quantitative analysis

The standard morphometric parameters previously described (maximum and minimum lumen diameter, lumen cross-sectional area, vessel cross-sectional area, plaque cross-sectional area and percentage vessel cross-sectional area stenosis) were measured within the stent at (1) the site of minimum lumen area, (2) the site of maximum lumen area, (3) the proximal end of the stent and (4) the distal end of the stent. The same measurements were made at the proximal and distal reference sites (points adjacent to the stent chosen by the operator as being most representative of 'normal' lumen size for that part of the treated vessel). The mean reference dimensions were calculated as the mean of proximal and distal reference dimensions [Nakamura, 1994]. In cases in which two or more stents were

implanted serially in a single lesion, they were treated as one for the purposes of quantitative analysis, and a single proximal and distal reference segment measured.

Three indices of stent expansion, in which the minimum lumen area within the stented segment is related to three different reference segment morphometric parameters, were calculated. The first, known hereafter as the 'mean reference lumen area index', is the minimum lumen area within the stent expressed as a percentage of the mean reference lumen area. The second is the 'distal reference lumen area index', in which the minimum stent lumen area is expressed as a percentage of the distal reference lumen area. In the third, the 'mean reference vessel area index', the minimum intrastent lumen area is expressed as a percentage of the mean reference vessel cross-sectional area (**figure 5.1**).

A symmetry index, defined as the ratio of minimum to maximum lumen diameter within the stent, was determined in each case at the point of maximum asymmetry.

5.3.5.2. Qualitative analysis

The position of each of the stent struts relative to the vessel wall was assessed throughout the length of the stented segment, and malapposition identified if any strut was surrounded by blood (i.e. to lie within the lumen). Care was taken to avoid misinterpretation of the effect of failing lateral resolution and mistaking the guide wire for a malapposed strut. Potentially flow limiting plaque or uncovered dissections adjacent to the stent were specifically sought. The presence of calcification was noted within the stented segment and was graded according to its radial extent (1 = ≤90, 2 = 90-180° and 3 = 180-360°), and according to its axial distribution as focal or diffuse.

5.3.5.3. Ultrasound criteria for successful implantation

During each case, on-line intrasvascular ultrasound guidance was used for clinical purposes to evaluate the acute outcome of the procedure. Four specific ultrasound criteria were assessed.

(1) Optimal stent expansion was judged to be present when the minimum lumen cross-sectional area within the stent was ≥80% of the mean reference lumen area (i.e. <20% intrastent stenosis relative to the mean reference lumen area).

(2) Adequate symmetry was defined as a symmetry index >0.7 at the site of maximum asymmetry within the stent.

(3) Complete apposition of all stent struts against the vessel wall.

(4) Absence of potentially flow limiting uncovered dissections or plaque either side of the stent.

5.3.6. Statistical analysis

Absolute measurements are expressed as mean values ± 1 standard deviation. Proportions are expressed as percentages, with the absolute values in brackets. Comparisons between groups of continuous variables were made using the student's t test and the unpaired test as appropriate. The Chi square test was used to test the significance of differences detected between groups of nominal variables. Significance was defined as a p value <0.05.

5.4. Results

5.4.1. Demographic and clinical details

Forty-four patients underwent intravascular ultrasound investigation following stent implantation in which a final dilatation pressure of 10 atmospheres or more had been applied. The demographic and clinical details of the patients included in the study are shown in **table 5.1**. The group of patients whose clinical status is

described as 'post-procedure' include three patients who underwent repeat intervention following balloon angioplasty performed within the previous 24 hours. A fourth patient, in whom 2 stents had been implanted for bailout purposes 4 days previously (without ultrasound guidance), required a third stent to wall-wrap a proximal segment of uncovered dissection. Cases in which the procedure was terminated following the initial ultrasound study are described as Group A and those undergoing further intervention as Group B. In the tables in which the absolute measurements for the cases in groups A and B are shown, individual cases are denoted by a number from 1-22 in group A, and from 23-44 in group B. In group B, quantitative and qualitative ultrasound results are reported as 'initial', denoting the findings of the first ultrasound study performed after attempted optimisation using angiographic guidance, and 'final', denoting the findings of the last ultrasound study performed in the case.

5.4.2. Technical details

5.4.2.1. Stent numbers

A single stent was implanted in 24 cases, two stents in separate lesions in 1 case, one and a half Palmaz-Schatz stents in one case, two contiguous stents in 13 cases, and 3 contiguous stents in 5 cases. A total of 63.5 stents were deployed.

5.4.2.2. Stent types

Three different types of stent were used. The majority (54.5) were Palmaz Schatz stents (Johnson and Johnson, Inc.) of different sizes: twenty articulated 15 mm (PS-153) stents, one half PS-153, twenty-five 14 mm (PS-154) stents, six 18 mm (PS-204) stents, one 10 mm (PS-104) stent and two 8 mm (PS-084) stents. Eight Microstents (Applied Vascular Engineering, Inc.) were implanted (five 3.5 mm x 8 mm and two 4.0 mm x 8 mm stents, and one 3 mm x 4 mm stent) and one 3.5 mm x 20 mm Gianturco-Roubin stent (Cook, Inc.). The echographic appearances of a

well-deployed Palmaz-Schatz stent, a Microstent, and a Gianturco-Roubin stent are shown in **figure 5.2**.

5.4.2.3. Balloon characteristics

The maximum balloon size used in an effort to achieve optimal deployment prior to ultrasound examination was 3.4±0.4 mm, range 2.5-4.0 mm. The maximum balloon pressure was 13.0±2.4 atmospheres, range 10 to 18 atmospheres. In group A, the balloon size prior to the ultrasound study was 3.6±0.5 mm, range 2.5 to 4.0 mm, and the maximum inflation pressure was 13.4±2.6 atmospheres, range 10 to 18 atmospheres. Although slightly greater, these values were not significantly different from those in group B in which the maximum balloon size was 3.3±0.4 mm, range 3.0 to 4.0 mm, and the maximum inflation pressure was 12.5±2.1 atmospheres, range 10-16 atmospheres. The maximum balloon size used during re-intervention in group B was 3.6±0.5 mm, range 3.0 to 5.0 mm, and the maximum balloon pressure was 16.3±2.7 atmospheres, range 10 to 20 atmospheres, both significantly greater than the size ($p=0.03$) and inflation pressures ($p<0.0001$) used in group B in the initial attempt to optimise deployment

There were significant differences in the compliance characteristics of the balloons used in groups A and B. Compliant balloons were used almost twice as often in group B compared to group A (10 vs. 6), and moderately compliant balloons were also used more frequently (11 vs. 7). Minimally compliant balloons, on the other hand, were used more frequently in group A than in group B (9 vs. 1), $p<0.05$. Prior to the initial ultrasound study, there was no significant difference in the frequency with which short balloons were used in both groups (4 in group A vs. 1 in group B), $p=0.15$. In group B, significantly more minimally compliant balloons were used during repeat intervention than were used during the initial efforts to deploy the stent (19 vs. 1), $p<0.0001$. Furthermore, whereas short balloons were used in only one case prior to ultrasound examination in this group of patients,

they were used in 12 cases during follow-on intervention, p<0.0001. The specific details of balloon diameter, length and compliance characteristics are shown in **table 5.2a** for group A, and in **table 5.3a** for group B. The latter table also details the ultrasound findings prompting re-intervention, and the details of the balloon catheters used in both the initial and follow-on intervention.

5.4.3. Procedural outcome

5.4.3.1. Angiographic outcome

The angiographic result obtained prior to the initial IVUS assessment was judged to be optimal in 39/44 cases and satisfactory in a further 3 cases, in 2 of which there was a suspicion of a filling defect within the stented lumen and in the third, a suspicion of distal stent malapposition. Two further cases described below were evidently unsuccessful.

5.4.3.2. Ultrasound outcome

In 50% of cases, the angiographic and ultrasound findings concurred in demonstrating optimal stent implantation. The ultrasound findings either prompted or contributed to the decision to intervene further in the remaining 50% of cases (22/44) and in 46% (18/39) of cases in which stent deployment had appeared optimal on angiography. The IVUS findings that prompted re-intervention were (1) inadequate stent expansion in 17 cases, (2) malapposition of stent struts in 6 cases (5 of which were also underexpanded), (3) obstructive intraluminal material in 3 cases, and (4) in one case, an uncovered, potentially obstructive dissection flap adjacent to the stent.

5.4.3.3. Further intervention

The changes instituted in cases undergoing further intervention were as follows: an increase in balloon inflation pressure in 86% (19/22) of cases, a switch to a less compliant balloon in 77% (17/22) of cases, a switch to a short balloon in 59%

(13/22) of cases, and balloon upsizing in 27% (6/22) of cases. A further stent was implanted in one case and an infusion catheter placed in order to infuse tPA into a vein graft in another case.

5.4.3.4. Failure to repeat IVUS examination

Following repeated balloon dilatation instigated by the ultrasound findings, a second ultrasound examination was successfully performed in 15 cases. In 7 cases, imaging was not repeated following re-intervention for the following reasons. A 3.5F Sonicath probe would not pass through a stent in a right coronary artery, its distal tip apparently snagging against the outer aspect of the proximal part of the stent. Another Sonicath could not be passed for a second time through a 6F guiding catheter used to allow a radial artery approach, probably as a result of inadequate cleaning of the surface of the imaging catheter between the studies. A third attempted repeat study failed when the drive-shaft of a 3.0F 'Spy' catheter would not pass for a second time into the common distal sonolucent segment of the catheter, apparently as a result of a manufacturing error. The final 4 cases were not restudied for logistical reasons.

The impact of repeat intervention is detailed below in the sections describing the quantitative and qualitative findings.

5.4.3.5. Clinical outcome

Acute success was achieved in 95% (42/44) of cases. There was one case (2%) of acute occlusion of a stent. This was implanted in a failed attempt to open a thrombotic occlusion occurring four hours after balloon angioplasty of an unstable lesion causing post-infarction angina. Recurrent myocardial infarction was not prevented. In a second case, there was a large amount of debris within a stented segment of a vein graft, some of which was thought to represent acute thrombus; an infusion catheter was positioned within the graft and tPA infused and the patient studied the next day, by which time a reduction in the number and extent

of filling defects was evident. This patient suffered a small non-q wave myocardial infarction. There were 2 subacute occlusions (4%): one confirmed case of subacute thrombosis in a small vessel stented for bailout purposes using a 2.5 mm balloon, and a presumed subacute thrombosis of a stented unstable lesion in a left circumflex artery leading to an inferior myocardial infarction in the second case. Haemorrhagic complications occurred in 2 cases; one pseudoaneurysm successfully treated by compression and frank haematuria in a second case. No adverse events occurred during intravascular ultrasound investigation nor during the follow-on interventions prompted by the ultrasound findings.

5.4.4. Quantitative findings

5.4.4.1. Reference dimensions

The measurements of the proximal, distal and mean reference sites are shown in **table 5.4**. In all cases, a distal reference segment was identifiable and measurable. A proximal reference segment could not be identified in 8 cases as a result of the very proximal location of the stent within the vessel. Excessive calcification or inadequate delineation of the course of the external elastic lamina prevented measurement of the vessel area (and hence calculation of the plaque area and percentage vessel area stenosis) in 4 cases at the distal reference site and in 4 cases in the proximal reference. The reference dimensions increased slightly but significantly following further intervention, from 7.7±2.2 mm^2 to 8.7 mm^2 ($p=0.05$), presumably as a result of a 'tenting' effect of a fully expanded stent. The change in the reference segment dimensions is shown in **figure 5.3a**.

5.4.4.2. Stent dimensions

The maximum lumen area within the stented segment at the initial ultrasound study in all cases was significantly larger than that of the proximal, distal or mean reference segments, measuring 122±29% of the mean reference lumen area. On the other hand, the minimum stent lumen area remained significantly smaller (on

average 79±13%) than that of the mean reference segment. The minimum stent lumen area on initial ultrasound examination was 6.0±1.8 mm^2 in all patients, 6.6±1.9 mm^2 in group A and 5.5±1.6 mm^2 in group B (p=0.06). Following further intervention in group B, this increased significantly by 1.5 mm^2 (27%) to 7.2±2.2 mm^2, p<0.001. If an outlier (no. 35) is excluded, the change measured 1.2 mm^2 to 6.7±1.4 mm^2, an increase of 22%, and was still significant to p<0.001. The final minimum lumen area in group B was slightly greater than in group A, but not significantly so (p=0.12). In those undergoing re-intervention, the minimum lumen area increased in all cases but one (no. 29), in which deployment of a second stent to cover a dissection flap distal to the originally deployed stent produced a smaller lumen area within the stented segment when quantitatively evaluated as one.

The vessel area was measurable at the distal end of the stent in 21 cases (50%), at the proximal end in 16 cases (38%) and within the stent in only 11 cases (26%). The mean stent dimensions for all cases on initial ultrasound assessment, and separately for groups A and B (the latter both before and after re-intervention) are shown in **table 5.4**. The absolute values of the minimum stent lumen area and the mean reference lumen area are shown in **table 5.2b** for group A, and in **table 5.3b** for group B. A plot of the change in minimum stent lumen area in cases undergoing re-intervention in group B is shown in **figure 5.3b**.

The expansion indices relating the minimum intrastent lumen area to a number of different reference segment dimensions, described above, were calculated for each of the cases. At the initial ultrasound study, the mean reference lumen area index measured 79±13%, range 50-115%. It measured <80% in almost half of the cases (46%, 20/44) and <90% in 82% (36/44) of cases. The distal reference lumen index was 84±18%, range 54-153%, being <80% in 39% (17/44) of cases and <90% in 68% (30/44) of cases. The mean reference vessel area index was 45±10%, range

27-71%. In 95% (38/40) of the cases in which measurements were possible, this index measured <60%, the limit thought to represent the lower limit of adequate stent expansion [Nakamura, 1994]. The minimum lumen area in the stent measured 67±15% (range 28-91%) of the maximum lumen area. Plots of the distribution of the values for these three indices are shown in **figure 5.4 (a-c)**, and comparing the distribution of each index in groups A and B are shown in **figure 5.5 (a-c)**. The change in each of the ratios achieved in patients undergoing re-intervention in group B is shown in **figure 5.6 (a-c)**.

5.4.4.2.1. Group A

In those patients in whom no further intervention was undertaken on the basis of the initial ultrasound study, the mean reference lumen area index was 86±10% (63-114%), the distal reference lumen area index was 92±13% (64-123%), and the mean reference vessel area index was 52±8% (40-71%). The minimum lumen area within the stent measured 72±10% (54-90%) of the maximum lumen area. During the procedure, a mean reference lumen area index (the index used to guide the clinical procedures) of <80% was accepted in three cases (in 2 native arteries and in one vein graft). In all three cases, there was considerable disparity in the dimensions of the proximal and distal reference segments (the proximal considerably larger than the distal in case nos. 7 and 22, and vice versa in case no. 3), such that further expansion was thought neither necessary nor wise.

5.4.4.2.2. Group B

For those patients in whom a suboptimal ultrasound result prompted a repeat study, the initial mean reference lumen area index was 71±11% (50-92%), the distal reference lumen area index was 77±20% (54-153%), and the mean reference vessel area index was 40±8% (27-56%). The minimum stent lumen area measured 62±17% (28-91%) of the maximum stent lumen area. In the 15 cases in which data was acquired following re-intervention, these values increased

significantly to 89±12% (69-111%), 98±29% (70-197%), 49±10% (37-81%) and 69±15% (33-92%) respectively.

In 4 cases, further intervention was performed despite a mean reference lumen area index of >80%. In the first case (no. 29), an uncovered dissection flap was revealed. Further stent expansion was of no benefit in case no. 39, in which acute thrombosis occurred. Re-intervention was performed in an effort to minimise the impact of intrastent debris in case no. 40 and to correct strut malapposition in case no. 42.

In three cases, a mean reference lumen area index of <80% was accepted as the final result. In case no. 28, the mean reference lumen area was large at 10.3 mm^2, and as the lesion was relatively calcified and a minimum intrastent lumen area of 7.5 mm^2 had been achieved, it was decided not to attempt further stent expansion. In case no. 30, lesion calcification was also the reason for limited extra lumen gain following a switch to a less compliant, larger balloon inflated to higher pressures. As the distal lumen diameter measured 3.1 mm, 0.4 mm smaller than the balloon size used, it was decided not to risk distal dissection and to accept this result as adequate. In case no. 32, a mass of tissue within the stent was successfully wall-wrapped using a less compliant balloon at higher pressure, but its stenotic impact was not abolished.

5.4.4.3. Stent-to-Reference and Balloon-to-Reference ratios

The minimum intrastent lumen area measured at the first ultrasound examination was 64±14 (34-109)% of the nominal cross-sectional area of the largest balloon used prior to the ultrasound study. The balloon to reference lumen area ratio was 1.3±0.3 (0.7-2.0), and balloon to artery diameter ratio 1.1±0.1 (0.8-1.3).

5.4.4.3.1. Group A

In those in whom a satisfactory ultrasound result was documented at the initial study, the minimum stent lumen area was 65±9% (45-82%) of the nominal inflated balloon cross-sectional area, the balloon to lumen area ratio was 1.3±0.1 (1.1-1.6) and the balloon to lumen diameter ratio was 1.1±0.1 (1.0-1.2).

5.4.4.3.2. Group B

In those undergoing re-intervention, the initial minimum stent lumen area was 63±18% (34-109%) of the inflated balloon area, the balloon to reference lumen ratio 1.2±0.3 (0.7-2.0), and the balloon to lumen diameter ratio 1.0±0.1 (0.8-1.3). These increased to 73±15% (41-100%), 1.2±0.2 (0.7-1.7) and 1.1±0.2 (0.9-1.6) respectively following re-intervention.

5.4.4.4. Symmetry Index

The symmetry index, the ratio of minimum to maximum lumen diameter, was calculated at the point of maximum asymmetry within the stent. It was slightly lower at the site of the minimum lumen diameter (0.87±0.07) than at the proximal (0.89±0.08) and distal ends (0.90±0.05) and at the site of maximum stent lumen area (0.91±0.07). A markedly asymmetric lumen (symmetry index <0.7) was noted in just 4 cases (0.61, 0.66, 0.67, 0.68) at the time of initial ultrasound study, so that 93% (40/44) of cases had a symmetry index >0.7 and 64% (28/44) had an index ≥0.8. Although one of the markedly asymmetric cases underwent further intervention that led to an improvement in the symmetry index from 0.67 to 0.73, there was no significant difference between the index at initial or final ultrasound examination in the 15 patients restudied. The direction of change of the index was unpredictable, some cases showing greater symmetry and others greater asymmetry following further intervention (**figure 5.3c**). One case (no. 32) in which marked deterioration in the symmetry index occurred following follow-on intervention had a large mass of intrastent debris that, although effectively wall-

implantation which had since resorbed. In view of the acute nature of the lesion, this may have represented a layer of partially organised thrombus.

5.4.5.2. Impact of calcium

Calcification of the stented segment was classified as occupying one, two or more quadrants (graded 1 to 3), and as being focal or diffuse. Neither the simple presence or absence, nor the degree of calcification correlated with the perceived need for re-intervention or the occurrence of strut malapposition.

5.4.5.3. Stent debris

Tissue within the stented lumen was documented in six cases (2 in group A, and 4 in group B). Intraluminal debris was identified in 2 cases in which stents were implanted into degenerative vein grafts. This was minor in one case, and thought to represent soft, degenerative fibrous tissue. In the second case, presenting with unstable angina, there was proliferation of the filling defects over a short period of time, suggesting the presence of acute as well as organised thrombus (**figure 5.10**). The filling defects were angiographically apparent in this case, which was treated with an infusion of tPA down the graft. A third example occurred in an unstable lesion in a left anterior descending artery. It was not clear whether this represented soft tissue or thrombotic debris. In a fourth case, friable tissue intruded through the struts of a stent implanted into a segment of recanalised proximal left anterior descending artery. Although the stenotic impact of this tissue was reduced by further inflations, the lumen remained highly eccentric and its area was moderately stenotic relative to the distal reference lumen. The intrastent material in the fifth case was clearly thrombus that, following initially successful stent implantation for complete occlusion occurring four hours after angioplasty, rapidly re-accumulated. This lesion had caused a limited anterior myocardial infarction 1 week previously and subsequent postinfarction unstable angina. The sixth case was that of a patient who had undergone implantation of 2 stents for bailout

purposes 5 days previously, but because of ongoing chest pain was restudied and found to have a semi-occlusive tissue flap that also required stenting at the proximal end of the treated segment. An angiographically inapparent crescent of tissue, possibly representing a layer of mural thrombus, was noted within the distal stent (**figure 5.11**). This patient required repeat catheterisation for recurrent angina 3 months later, and was found to have a long restenosis in the distal 2 stents. A repeat intravascular study performed prior to stent angioplasty showed profuse echolucent neointima formation within the stented lumen, with no change in the stent dimensions (**figure 5.11**). Following successful angioplasty, the stents had clearly undergone further expansion, and the neointima appeared as a thin, disrupted layer of tissue, some of which may have been extruded through the stent struts.

5.5. Discussion

5.5.1. Background

Coronary stenting was introduced into clinical practice in the late 1980s in order to achieve two primary goals: (1) to wall-wrap occlusive dissections and tissue flaps that had caused or were threatening to cause acute vessel closure during balloon angioplasty, and (2) to prevent restenosis [Sigwart, 1987]. Although recent randomised trials have confirmed that stents do reduce the rate of restenosis [Serruys, 1994; Fischman, 1994] and compelling observational data exists to support their efficacy in treating acute vessel closure [George, 1993; Serruys, 1993], the high rates of thrombotic and haemorrhagic complications experienced in the years after their initial introduction led to doubts being cast on their potential to safely fulfil these roles [Serruys, 1991]. The first patients in whom Palmaz-Shatz stents were implanted were not treated with anticoagulants. Following reports of subacute thrombosis occurring in apparently well deployed stents, usually at 5-10 days after implantation, it became common practice for all patients to undergo

purposes 5 days previously, but because of ongoing chest pain was restudied and found to have a semi-occlusive tissue flap that also required stenting at the proximal end of the treated segment. An angiographically inapparent crescent of tissue, possibly representing a layer of mural thrombus, was noted within the distal stent (**figure 5.11**). This patient required repeat catheterisation for recurrent angina 3 months later, and was found to have a long restenosis in the distal 2 stents. A repeat intravascular study performed prior to stent angioplasty showed profuse echolucent neointima formation within the stented lumen, with no change in the stent dimensions (**figure 5.11**). Following successful angioplasty, the stents had clearly undergone further expansion, and the neointima appeared as a thin, disrupted layer of tissue, some of which may have been extruded through the stent struts.

5.5. Discussion

5.5.1. Background

Coronary stenting was introduced into clinical practice in the late 1980s in order to achieve two primary goals: (1) to wall-wrap occlusive dissections and tissue flaps that had caused or were threatening to cause acute vessel closure during balloon angioplasty, and (2) to prevent restenosis [Sigwart, 1987]. Although recent randomised trials have confirmed that stents do reduce the rate of restenosis [Serruys, 1994; Fischman, 1994] and compelling observational data exists to support their efficacy in treating acute vessel closure [George, 1993; Serruys, 1993], the high rates of thrombotic and haemorrhagic complications experienced in the years after their initial introduction led to doubts being cast on their potential to safely fulfil these roles [Serruys, 1991]. The first patients in whom Palmaz-Shatz stents were implanted were not treated with anticoagulants. Following reports of subacute thrombosis occurring in apparently well deployed stents, usually at 5-10 days after implantation, it became common practice for all patients to undergo

vigorous anticoagulation with heparin and dextran during the procedure, and subsequently to be orally anticoagulated for a period of at least 8-12 weeks, in addition to antiplatelet therapy with aspirin and dipyridimole [Schatz, 1991]. Despite these measures, subacute thrombosis continued to be a problem. In the recently reported BENESTENT trial, subacute thrombosis occurred in 3.5% of elective cases. In bail-out circumstances, in which marked vessel wall disruption and/or the presence of thrombus is assumed to have an important procoagulant effect, the reported rate of subacute thrombosis varied from 7% to 16% [Sutton, 1994; Hermann, 1992]. The aggressive anticoagulant regimes in turn led to haemorrhagic complications in 13.5% of electively stented patients in BENESTENT [Serruys, 1994] and as much as 26% of cases in the initial report of bailout stenting using the Palmaz-Schatz stent [Hermann, 1992].

The recent exponential growth in coronary stenting is ascribable to two principal factors. The first was the publication in 1994 of evidence from two controlled trials that a reduction in restenosis could be achieved by the elective implantation of Palmaz-Schatz stents. A 10% absolute reduction, from 32 to 22%, equivalent to a 31% relative reduction was documented in the BENESTENT trial [Serruys, 1994] and an absolute reduction of 10.5%, from 42.1 to 31.6%, equivalent to a relative reduction of 25%, was reported by the STRESS investigators [Fischman, 1994].

The second major contributor to the increased use of coronary stents has been the significant reduction in the rate of serious thrombotic and haemorrhagic complications associated with stent implantation, as a result of modifications to deployment and post-deployment practice.

The potential role of stent under-expansion in generating subacute thrombosis was commented upon in the report of major events following Gianturco-Roubin stent implantation [Sutton, 1994]. Prior to the publication of this report, studies with intravascular ultrasound had revealed incomplete stent expansion in a high

proportion of cases following 'standard' implantation techniques [Goldberg, 1993]. On the basis of these findings, Colombo and colleagues developed a strategy of ultrasound guided stent optimisation using high pressure balloon inflation of appropriately sized balloons within the stent to safely maximise lumen size. It was argued that optimising the rheology, or restoring laminar blood flow characteristics, within the treated segment minimised the risks of platelet activation, aggregation and subsequent occlusive thrombus formation, and that having achieved optimal stent deployment, the need for anticoagulation was obviated. Having omitted anticoagulation, a cumulative stent thrombosis rate (to 6 months) of 1.4% and haemorrhagic event rate of 0.6% was achieved [Colombo, 1995].

Just as intravascular ultrasound data concerning incomplete deployment prompted the widespread adoption of a strategy of high pressure 'post-dilatation' of deployed stents, changes in the pharmacological approach were being advocated by others. The role of platelets in the generation of subacute thrombosis was identified by Palmaz et al. in an experimental canine model [Palmaz, 1989]. Moreover, 4 of the 7 patients in whom subacute thrombosis occurred in the first reported series of Palmaz-Shatz stents, occurred following the withdrawal of aspirin therapy for a variety of reasons [Schatz, 1991]. Ironically, this 18% subacute thrombosis rate led to the development of aggressive coumadin based anticoagulation regimes, which appeared to reduce the risk of thrombosis, but at the cost of significantly greater risk of haemorrhagic complications. A conviction concerning the importance of platelet aggregation in the aetiology of subacute thrombosis prompted a number of French investigators to use ticlopidine, either alone or in combination with aspirin, to treat stented patients [Barragan, 1994; Morice, 1995]. This agent inhibits adenosine diphosphate and thrombin induced platelet aggregation [Robert, 1991], and in combination with aspirin in healthy volunteers has been found to have a synergistic effect against collagen induced platelet aggregation [De Caterina, 1991]. Data from a number of French stent

registries showed that in combination with subcutaneous low-molecular weight heparin, ticlopidine use during the acute and sub-acute phase of coronary stenting was associated with a low subacute thrombosis rate (4.2% in one series [Barragon, 1994] and 1.2% in another [Morice, 1995a]). The use of low-molecular weight heparin has since been abandoned without apparent adverse effect [Morice, 1995b]. Ultrasound guidance was not used in these series of patients.

Given the uncontrolled nature of the data, it is unclear as to which element or combination of elements of the above stratagems are the key components that have reduced the risks of subacute thrombosis. Although ultrasound guidance and high balloon inflation pressures are emphasised as being of central importance by the Milan group, ticlopidine was used as the sole antiplatelet agent in the majority of the cases constituting their published series. Similarly, the French investigators have, to a variable extent, also employed a strategy of high pressure post-dilatation of the deployed stent, albeit without ultrasound guidance. Thus, whereas intravascular ultrasound guidance is currently relied upon by some to achieve safe maximisation of stent lumen size prior to early discharge without anticoagulation, it is viewed by others as an unnecessary and expensive research tool extraneous to the needs of the everyday practice of coronary stenting. Current data would suggest that subacute thrombosis rates can be maintained at a very low level by adopting a strategy of routine high pressure post dilatation of the stent in combination with antiplatelet therapy, and that the incremental advantage of ultrasound guidance in improving the acute result is likely to be small. The recent introduction of heparin coated stents may further minimise the advantage that ultrasound guidance confers in the short-term. It may be that the extra lumen gain achieved using ultrasound will translate into lower rates of restenosis, but this issue requires formal assessment in a controlled trial. Ideally, the effect of high pressure dilatation, the compliance characteristics of the balloon, the antiplatelet agent used, and the impact of intravascular ultrasound guidance would each be

assessed in a factorial design study. At that point, if no advantage associated with its routine use was shown, it could fairly be stated that intravascular ultrasound, having provided the insights that have formed the basis of current deployment strategies, should remain a research tool in specialist centres with an interest in developmental work in coronary intervention.

5.5.2. The findings of the present study

In this series of patients, we sought to determine with intravascular ultrasound the impact of a routine policy of moderate to high pressure balloon inflation, and what further intervention, prompted by the ultrasound findings, could achieve.

5.5.2.1. Angiographic vs. ultrasound 'success'

Although the angiograms of the majority of cases in this study portrayed a 'successful result', with no appreciable residual stenosis and uniform contrast density throughout the treated segment, subsequent intravascular ultrasound investigation revealed incomplete or suboptimal deployment in almost 50% of cases. The principal explanation for this marked discrepancy is that angiography appears to systematically overestimate lumen dimensions following coronary stent implantation. In a number of comparisons between intravascular ultrasound and quantitative angiographic measurement of the minimum dimensions of implanted coronary stents, measurements made by intravascular ultrasound have consistently been smaller compared to quantitative coronary angiography (**table 5.5**) [Mudra, 1994; Nakamura, 1994; Colombo, 1995]. This finding is all the more striking given the opposite bias observed in many previous comparisons of IVUS and angiographic measurements in other contexts, as detailed in Chapter 1 (**table 1.1**). Angiographic overestimation may result from tracking of contrast around struts that are embedded into the vessel wall. The outer edge of the angiographically depicted lumen, determined by the presence of contrast, is thus situated to a variable extent outwith the anatomic endoluminal border constituted by tissue

protruding between the stent struts. The lumen border is identified by automated quantitative angiographic systems between the first and second derivatives of grey level density change, and stent struts themselves, being variably echodense, may confound edge detection algorithms that rely on subtle differences in contrast levels. Thirdly, the angiographic projections chosen to study the treated segment after stent deployment may not profile the lumen in its smallest dimension (**figure 5.12**). Finally, very short segments of stent stenosis (due to tissue prolapse or an underlying resistant 'napkin-ring' stenosis), may be obscured by foreshortening of the vessel.

The tendency for subjective overestimation of the degree of lumen gain achieved by a balloon angioplasty is well documented [Bertrand, 1993]. An accurate visual assessment of a minor residual stenosis is even less likely following stent deployment. The discrepancy between visual assessment of the angiogram and the quantitative ultrasound data is better understood when the above technical factors are taken into account, and it is remembered that an area stenosis of 20% is equivalent to a 10% diameter stenosis and a 10% area stenosis equivalent to just 6% diameter stenosis. This minor level of narrowing, particularly when present in stents that are otherwise overtly 'overexpanded' elsewhere along their length may easily be missed.

Angiographically unrecognised stent underexpansion revealed by intravascular ultrasound was first described by the Milan group in abstract form in 1993 [Goldberg, 1993]. A subsequent report from the same group indicated that underexpansion was found in 80% of cases, despite the prior application of routine high pressure post-dilatation of the stents that aimed to achieve a 'negative' angiographic residual stenosis [Nakamura, 1994]. In a more recent and complete description of a larger cohort of patients by the same group, it was observed that following the adoption of different criteria for ultrasound 'success',

the proportion of cases found to be 'underexpanded' dropped from 88% to 40% [Colombo, 1995]. In a carefully studied group of 16 patients, Mudra et al again found that 94% of stents that appeared to be fully deployed on angiographic assessment were incompletely expanded when evaluated by ultrasound. The inflation pressures used to initially deploy the stent in this series (7.4±1.7 atmospheres) were considerably lower than are routinely used today.

In our study, further intervention following ultrasound detected underexpansion led to a 22% increase in lumen area within the stent. Colombo et al reported a 28% increase in stent lumen size [Colombo, 1995], and Mudra a 40% increase in lumen size [Mudra, 1994]. Evidently, the amount of lumen gain on re-intervention that is both required and possible will depend on the initially adopted deployment strategy.

5.5.2.2. Definitions of adequate expansion

Although striking, these findings, and our own, beg the question as to what constitutes 'adequate stent expansion'. Clearly, the specific quantitative criteria for successful expansion, although all aiming to ensure minimal residual intrastent stenosis in order to optimise stent rheology, are each empirically defined (**table 5.6**). The initial definition of adequate expansion proposed by the Milan group [Goldberg, 1993] was a minimum stent lumen area ≥80% of inflated balloon cross-sectional area. The second definition proposed by the same group [Nakamura, 1994] stipulated that the stent minimum lumen area should equal or exceed 60% of the mean reference vessel cross-sectional area. Since on average 40% of the vessel cross-sectional area in the reference segments is occupied by plaque, this was thought to be a suitable criterion to minimise luminal stenosis and to reconstitute a smooth luminal profile. When the dangers of excessive balloon oversizing that may result from this strategy were recognised, the same group advocated a more conservative goal of a minimum intrastent lumen area that

exceeded that of the distal lumen area, emphasising the importance of unimpeded run-off of blood flow through the stent in the prevention of thrombus formation [Colombo, 1995]. The MUSIC investigators and Mudra and co-workers advocate that minimum stent lumen area be ≥90% of mean reference lumen area or that it be greater than the distal reference lumen area. In the ASSURE study, and during the acquisition of the data presented in this chapter, we have aimed to achieve a stent lumen area ≥80% of the mean reference lumen area.

There is no data to support one specific figure over another. A target that is unattainable in the majority of cases is unhelpful, as it is likely to lead to excessive balloon oversizing and risks of vessel dissection or rupture. In **figure 5.4**, distribution plots of the various indices relating minimum stent lumen area to mean reference lumen area, distal reference lumen area and mean reference vessel area are shown for the present series. The target of a minimum stent lumen area ≥ the mean reference lumen area, and ≥60% of the mean reference vessel area is almost never achieved following a policy of moderately high pressure balloon inflation during stent deployment. From the plots documenting the change in lumen area of stents undergoing repeat intervention (**figure 5.6**), it can be seen that although the majority of stents can be expanded to ≥80% of the mean reference lumen area, and almost all cases be expanded to ≥80% of the distal reference lumen area, the proportion of cases judged successful by the more rigorous criteria falls to 50% for a 90% cut-off and to a negligible number for a 100% cut-off point. The criterion of a minimum stent lumen area that measures ≥60% of reference vessel area is almost never reached, despite further intervention. Mudra et al. reported that whereas the majority of their small series (15/16) had a minimum stent lumen area of ≥80% of the reference lumen area, 25% failed to reach their stipulated cut-off of 90%, despite efforts to achieve full expansion. Unusually, following repeat intervention, Colombo et al. reported optimal expansion, judged in the initial 339/452 lesions as a minimum stent lumen area ≥60% of vessel area and in the remainder of the series

(113/452) as a minimum stent lumen area ≥ the distal lumen area, in 96% of cases [Colombo, 1995]. The validity of Colombo's approach is currently being assessed by the MUSIC trial investigators.

5.5.2.3. Symmetry index

The unpredictable direction of change in the geometry of the stented lumen following repeated intervention is well illustrated in the change in symmetry index in the 15 cases in group B in whom repeated measurements were made. This observation has been made by others [Nakamura, 1994], and has prompted the abandonment of this criterion by most groups. The potential for increased asymmetry following re-intervention should be borne in mind, and if an adequate cross-sectional area has been achieved, further efforts to achieve a more symmetric lumen with further dilatation avoided. Presumably, such asymmetry arises from differences in the compliance characteristics of different portions of the vessel wall circumference, that react in an unpredictable fashion to balloon inflation.

5.5.2.4. Strut malapposition

The relative radiolucency of most stents, and the difficulties of discerning intraluminal structures using contrast angiography, explain the difficulties in identifying malapposition of stent struts on the angiogram. In contrast, malapposition is identified with ease using intravascular ultrasound, as the location of the echodense struts relative to the vessel wall is readily identifiable. In view of the insensitivity of angiography for detecting this phenomenon, two key questions arise if intravascular ultrasound guidance is not available. Firstly, how often does malapposition occur, and secondly what can be done to avoid it?

In our study, strut malapposition was observed in 6 cases. In one case, there was a suspicion from the angiographic appearances, borne out by the ultrasound study, that the distal portion of the stent might not be fully apposed to an ectatic portion of vessel (**figure 5.8**). In the remaining 5 cases, 12% of the total study

group, the angiographic appearances suggested full expansion and complete apposition of the stent to the vessel wall. In the first series reported by the Milan group, malapposition appeared to be a very rare phenomenon, observed in only 5% of cases [Nakamura, 1994]. However, malapposition was documented in 28% of cases in the STRUT study registry [Fitzgerald, 1995]. In these patients, malapposition occurred far more frequently in heavily calcified lesions (50%) than in minimally or non-calcified lesions (11%). We did not observe any differences in the quantitative or qualitative variables in calcified lesions relative to non-calcified lesions, but did not perform pre-interventional imaging. The identification of vessel wall constituents, including calcium, is less easily performed following stent deployment, as a result of the vessel wall compression and the shadowing effect of the stent struts.

In none of the cases in which malapposition was noted in our series were non-compliant or minimally compliant balloons used prior to ultrasound imaging, and the mean inflation pressure was relatively low at 12.7 atmospheres. Further intervention with minimally compliant balloons corrected the problem in all case but one, in which the distal end of a rigid stent (an AVE Microstent), was undersized relative to the lumen at the proximal end of the lesion. High pressure inflation of a non-compliant, oversized balloon (3.5 mm in a 3.0 mm stent) did achieve significantly greater expansion of the stent and near complete apposition (**figure 5.8**). A policy of truly high pressure inflation with non-compliant balloons may minimise the risk of strut malapposition.

5.5.2.5. Stent debris

The presence of a filling defect within the stent may be seen as a readily apparent, discrete mass, or more frequently may present as an ill-defined loss of contrast density. Intravascular ultrasound clearly demonstrates the location, circumferential and longitudinal extent of such tissue masses and their stenotic

impact. Differentiation of the tissue type is not possible, but the circumstances and behaviour of the tissue mass within the stent may provide some indication of its likely constitution.

Neither the prognostic significance, nor the most appropriate approach to tackling intrastent stent debris is clear. When thought likely to be thrombotic, it is our empirical practice to administer intracoronary tPA using an intracoronary infusion catheter. When thought to be fibrous or degenerative material, we have attempted to minimise its stenotic impact by performing repeat balloon dilatations at high pressure to wall-wrap, and potentially extrude the material through the stent struts. The implantation of further stents within the stent has been advocated by some, and the use of perfusion balloons for prolonged inflations by others, but the effectiveness of either practice remains unknown.

5.5.2.6. Deployment strategy

The beneficial impact of certain stent deployment practices is suggested by our findings. Although the balloon size and pressures were not significantly different between those found to have fulfilled the ultrasound criteria for successful deployment and those not, significantly more non-compliant and minimally compliant balloons were used in the initially successful group. A significant improvement in lumen dimensions was achieved by a change to less compliant balloons and higher pressure. The considerable variability of stent dimensions, attested to by an average stenosis of 21% despite an average maximum stent lumen area amounting to 122% of the mean reference lumen area, reflects the variable distensability of the underlying lesion resulting from different degrees of plaque burden and tissue density. These discrete segments of under-expansion may best be corrected using short balloons, that also have the advantage of avoiding detrimental over-expansion of adjacent vessel segments. The empirical and routine use of high pressure inflations of minimally compliant, but appropriately

sized or slightly oversized balloons may prove to the most effective strategy to obviate the need for ultrasound guidance.

5.5.2.7. Study limitations

The small size of the study group, the heterogeneity of the indications for stent implantation, as well as the variable pharmacological regime used following stent implantation, make it impossible to draw any conclusions concerning the clinical impact of ultrasound guidance on the acute outcome in this group of patients. The study was not designed as a study of clinical efficacy, but rather to document morphological and morphometric findings of intravascular ultrasound in this series of patients.

Quantitative coronary angiography was not available to allow a formal comparison between ultrasound and angiographic quantitation. Quantitative angiography has to date proved to have a limited role in clinical practice, used as an aid to choose the appropriate balloon size, but generally not to assess the outcome of an intervention. The difficulties encountered in acquiring accurate measurements in a substantial proportion of cases [Gurley, 1992] leads us to believe that visual assessment of the angiographic result, as employed in this study, will remain the basis for clinical decision making for most interventionalists for the foreseeable future. It is nevertheless acknowledged that the absence of objectively determined angiographic criteria for a successful outcome is a shortcoming of this and all other series of observational studies comparing intravascular ultrasound and angiographic outcomes in coronary stenting. It is likely that future studies will incorporate efforts to compare on-line quantitative angiographic outcome with the ultrasound findings.

5.6. Conclusions

The findings of this study confirm that intravascular ultrasound demonstrates incomplete stent deployment in a substantial proportion of cases despite a satisfactory angiographic appearance. The application of a final inflation as high as was judged necessary to achieve an optimal angiographic result, in all cases >10 atmospheres, was nevertheless associated with inadequate stent expansion in over 40% of cases. Unrecognised stent strut malapposition was found in over 10% of cases. There appeared to be greater stent expansion following the use of non- or minimally compliant balloons, and strut malapposition was associated with the use of relatively low inflation pressures. Following further intervention, the majority of cases demonstrated an increase in stent dimensions and correction of strut malapposition. The choice of a particular expansion index is seen to impact significantly on the ultrasound evaluation of the outcome of a procedure.

The clinical utility of intravascular ultrasound in guiding coronary stent deployment is supported by data such as these. Its use does, however, lead to longer and more expensive procedures. The empirical application of high pressure dilatation, the use of non-compliant or short balloons, and the merit of one or other antiplatelet agent, are also supported by suggestive but uncontrolled data. A controlled trial is required to disentangle the various components of stent deployment and post-deployment practice and determine the optimal strategy. It will prove a difficult task to show that intravascular ultrasound guidance can reduce further an already very low rate of acute and subacute complications. A more realistic hypothesis is that the safe maximisation of lumen gain achieved with ultrasound guidance may translate into lower rates of stent restenosis. Whatever its clinical role, our observations illustrate well how intravascular ultrasound continues to provide us with detailed and otherwise unavailable insights.

Table 5.1 Demographic and clinical details

Cases		44
Age		56.3±10.5
Sex	Male	32
	Female	12
Clinical status	Stable angina	21
	Unstable angina	19
	Post procedure	4
Indication	Elective	15
	Suboptimal angiogram	14
	Bailout	11
	Clinical trial	4
Treated vessel	RCA	17
	LAD	16
	LCx	4
	Vein grafts	7

Table 5.2a Balloon size, compliance and inflation pressure (Group A)

	Balloon size (mm)	Balloon Compliance	Inflation pressure (atm)
1	4.0-20	C	10
2	3.0-20	MC	15
3	3.5-20	MC	16
4	4.0-10	LC	14
5	4.0-10	LC	15
6	3.5-20	LC	14
7	2.5-20	MC	14
8	4.0-20	MC	12
9	4.0-20	LC	16
10	3.0-20	LC	18
11	3.5-20	MC	12
12	4.0-20	C	10
13	4.0-20	C	10
14	3.0-10	LC	16
15	4.0-20	MC	12
16	4.0-20	C	10
17	3.0-20	LC	16
18	3.0-20	MC	12
19	3.5-10	LC	12
20	3.5-20	C	12
21	4.0-20	LC	18
22	3.0-20	MC	11
Mean	3.55		13.4
SD	0.50		2.6

Group A

C=compliant; MC=moderately compliant; LC=low compliance

Table 5.2b Quantitative findings (Group A)

	Minimum Stent Lumen Area (mm^2)	Mean Reference Lumen Area (mm^2)	Min Stent LA / Mean Ref LA %	Min Stent LA / Dist Ref LA %	Min Stent LA / Mean Ref VA %
1	8.1	9.8	83	93	56
2	4.7	5.6	84	98	59
3	5.0	7.6	66	73	40
4	7.1	8.9	80	85	50
5	9.1	10.4	88	101	-
6	6.0	7.1	85	85	-
7	3.1	3.8	79	94	52
8	6.8	8.0	86	80	49
9	7.6	8.9	86	64	47
10	4.3	4.5	96	100	52
11	7.2	7.6	95	89	51
12	8.6	9.7	89	123	60
13	9.5	11.3	84	99	50
14	4.0	4.7	85	85	-
15	8.5	9.9	86	80	44
16	7.6	8.1	94	103	46
17	5.3	6.2	86	86	71
18	5.2	5.4	96	96	-
19	7.3	6.4	114	114	57
20	7.9	8.7	91	92	46
21	8.0	9.3	86	78	60
22	3.2	5.1	63	100	41
Mean	6.6	7.6	86	92	52
SD	2.0	2.2	11	14	8

Group A

Table 5.3a Balloon characteristics and reason for re-intervention (Group B)

	Reason for Reintervention	Initial			Final		
		Size (mm)	Compl.	Press. (atm)	Size (mm)	Compl.	Press. (atm)
23	Underexpansion	3.5-20	C	10	3.5-10	LC	18
24	Underexpansion, malapposition	2.5-20	MC	14	3.0-10	LC	16
25	Underexpansion	3.5-20	C	10	3.5-20	NC	14
26	Underexpansion	3.0-20	MC	16	3.0-10	LC	18
27	Underexpansion	4.0-20	C	12	4.0-10	LC	16
28	Underexpansion	3.5-20	MC	12	3.5-20	LC	14
29	Uncovered dissection	3.0-20	MC	10	3.0-20	C	16
30	Underexpansion	3.0-20	MC	11	3.5-20	LC	16
31	Underexpansion	3.5-20	C	11	3.5-10	LC	16
32	Underexpansion, debris	3.0-20	C	12	3.0-20	LC	18
33	Underexpansion	3.5-20	MC	10	3.5-10	LC	18
34	Underexpansion	3.5-20	C	16	4.0-10	NC	12
35	Underexpansion, malapposition	4.0-20	C	12	5.0-20	MC	10
36	Underexpansion	3.5-20	MC	15	3.5-10	LC	20
37	Underexpansion, malapposition	3.5-20	MC	12	3.5-10	LC	18
38	Underexpansion	3.0-20	MC	10	3.5-10	LC	11
39	Acute thrombosis	3.0-20	MC	14	3.0-10	LC	17
40	Debris	3.5-20	C	12	3.5-20	LC	19
41	Underexpansion, malapposition	4.0-20	C	10	4.0-10	LC	16
42	Malapposition	3.0-20	MC	12	3.0-10	LC	18
43	Underexpansion, malapposition	3.0-20	C	16	3.5-20	LC	18
44	Debris	3.0-20	C	12	3.5-10	LC	18
Mean		3.3		12.4	3.6		16.3
SD		0.4		2.0	0.5		2.6

Group B

Compl,=Compliance characteristics; C=compliant; MC=moderately compliant; LC=low compliance

Table 5.3b Minimum stent and mean reference lumen area change (Group B)

	Minimum Stent Lumen Area (mm^2)		Mean Reference Lumen Area (mm^2)	
	Initial	Final	Initial	Final
23	5.9	-	8.6	-
24	2.8	-	3.9	-
25	4.6	6.5	7.0	8.0
26	3.3	3.9	4.8	5.8
27	6.7	8.4	9.5	10.6
28	7.1	7.5	10.3	10.0
29	6.1	5.9	6.6	6.1
30	3.5	4.8	7.0	7.3
31	4.8	-	6.6	-
32	4.5	5.1	6.7	7.2
33	5.3	6.9	7.0	7.5
34	7.9	-	11.4	-
35	8.6	13.7	14.1	15.3
36	6.8	8.4	10.5	9.85
37	6.0	7.4	8.7	10.2
38	4.1	7.5	6.8	6.3
39	4.7	-	5.8	-
40	5.3	6.3	6.5	7.1
41	6.1	-	11.4	-
42	5.5	7.1	6.4	9.55
43	7.7	8.1	9.8	9.25
44	3.8	-	7.0	-
Mean	5.5	7.2	7.8	8.7
SD	1.6	2.2	2.3	2.4

Group B

Table 5.3c Changes in reference indices (Group B)

	Minimum Stent LA Mean Reference LA (%)		Minimum Stent LA Distal Reference LA (%)		Minimum Stent LA Mean Reference VA (%)	
	Initial	Final	Initial	Final	Initial	Final
23	67	-	71	-	53	-
24	72	-	72	-	54	-
25	66	93	59	83	31	44
26	69	82	73	87	46	55
27	71	89	68	86	30	37
28	69	73	66	70	44	47
29	92	89	88	86	55	54
30	50	69	67	92	32	43
31	66	-	77	-	40	-
32	67	76	82	93	34	39
33	76	99	62	81	35	46
34	69	-	68	-	43	-
35	61	98	64	102	34	54
36	65	80	81	100	34	42
37	69	85	78	96	39	48
38	60	110	60	110	44	81
39	81	-	87	-	37	-
40	82	98	87	103	45	53
41	92	-	92	-	50	-
42	86	111	153	197	35	46
43	79	83	85	89	39	41
44	54		54		27	
Mean	71	89	77	98	40	49
SD	11	12	20	29	8	10

Group B

Table 5.4 Morphometric parameters and symmetry index

	Min LD (mm)	Mx LD (mm)	LA (mm^2)	VA (mm^2)	PA (mm^2)	% sten (%)	SI
Reference							
Distal	2.9±0.5	3.2±0.5	7.4±2.4	12.8±5.0	5.4±3.5	39.2±13.2	0.92±0.05
Proximal	3.1±0.5	3.5±0.5	8.5±2.5	16.0±4.7	7.4±2.8	45.2±8.9	0.90±0.08
Mean	3.0±0.5	3.3±0.5	7.7±2.2	13.7±4.5	6.0±2.8	41.3±10.1	-
Stent (All)							
Minimum	2.6±0.4	3.0±0.5	6.0±1.8	19.7±3.7	12.6±3.2	63.6±6.2	0.87±0.07
Maximum	3.3±0.5	3.6±0.5	9.1±2.3	18.6±3.9	9.9±2.6	53.4±7.5	0.91±0.07
Proximal	3.0±0.5	3.4±0.5	7.9±2.3	19.4±4.5	11.0±3.6	56.0±9.3	0.89±0.08
Distal	3.0±0.5	3.3±0.5	7.9±2.3	17.2±3.9	9.1±2.7	52.1±8.5	0.90±0.06
Stent (A) n=22							
Minimum	2.7±0.4	3.1±0.5	6.6±1.9	21.2±3.9	13.5±3.8	62.5±6.1	0.86±0.07
Maximum	3.2±0.5	3.6±0.5	9.1±2.5	17.7±3.9	9.0±2.3	50.4±5.7	0.91±0.07
Proximal	3.1±0.5	3.4±0.6	8.2±2.5	19.8±4.3	10.8±3.2	54.0±7.2	0.89±0.08
Distal	3.0±0.5	3.4±0.5	8.2±2.4	16.5±3.9	8.1±2.7	48.5±8.9	0.91±0.07
Stent (B) initial n=22							
Minimum	2.5±0.4	2.8±0.4	5.5±1.6	17.8±2.8	11.6±2.3	57.2±10.1	0.87±0.08
Maximum	3.3±0.5	3.6±0.4	9.1±2.0	19.4±3.8	10.9±2.5	56.4±8.2	0.91±0.08
Proximal	2.9±0.5	3.3±0.5	7.6±2.1	19.1±5.0	11.2±4.0	56.6±10.8	0.89±0.09
Distal	2.9±0.5	3.2±0.5	7.5±2.2	18.0±4.0	10.1±2.5	56.1±6.3	0.90±0.05
Stent (B) final n=15							
Minimum	2.8±0.6	3.2±0.4	7.2±2.2	19.2±4.7	11.1±3.8	57.2±10.1	0.88±0.10
Maximum	3.4±0.4	3.9±0.4	10.5±2.3	20.8±3.7	11.9±2.6	56.7±4.9	0.89±0.08
Proximal	3.6±0.4	3.2±0.5	9.1±2.2	20.3±3.4	10.7±2.3	52.8±7.4	0.89±0.08
Distal	3.6±0.6	3.1±0.5	8.9±2.8	16.7±3.8	8.9±2.9	52.7±8.3	0.89±0.07

Table 5.5 Discrepancy between QCA and IVUS MLD measurements

Study	pts.		QCA MLD	IVUS MLD
Mudra, 1994	n=16	Initial	2.6±0.3	2.2±0.2
		Final	2.9±0.3	2.6±0.3
Nakamura, 1994	n=64	Initial	3.1±0.5	2.7±0.4
		Final	3.6±0.5	3.1±0.5
Colombo, 1995	n=359	Initial	-	2.7±0.5
		Final	3.4±0.5	3.1±0.5

Table 5.6 Quantitative definitions of adequate stent expansion

Study/Centre	Reference	Definition
Columbus I	[Colombo, 1993]	Stent MLA>80% of balloon CSA
Columbus II	[Nakamura, 1994]	Stent MLA>60% of mean reference VA
Columbus III	[Colombo, 1995]	Stent MLA>100% of distal reference LA
Mudra	[Mudra, 1995]	Stent MLA>90% of mean reference LA
MUSIC	[MUSIC protocol]	Stent MLA>90% of mean reference LA Stent MLA>100% of lowest reference LA
ASSURE	[ASSURE protocol]	Stent MLA>80% of mean reference LA

Figure 5.1 Schematic diagram illustrating the sites at which measurements are made to calculate the expansion indices

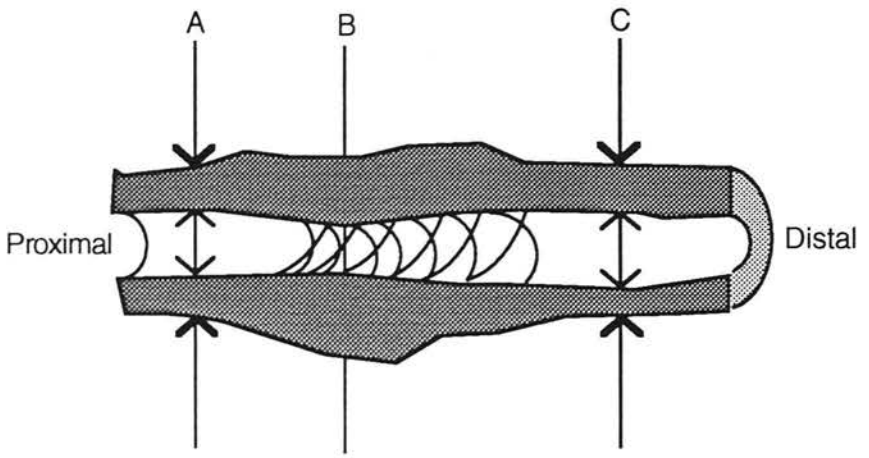

The sites at which measurements are made to calculate the expansion indices are illustrated in this schematic. The minimum lumen area is measured at the point within the stent indicated by line B. Lines A and C mark the proximal and distal reference sites respectively. The vessel area is measured at proximal and distal reference sites (indicated by the bold arrowheads on lines A and C) and the mean vessel area calculated as the sum of the proximal and distal reference vessel area divided by two. The lumen area is measured at the proximal and distal reference sites (at the points indicated by the light arrowheads on lines A and C) and the mean reference lumen area calculated as the sum of proximal and distal reference lumen area divided by two. The ***mean reference lumen area index*** *= [lumen area B / ((lumen area A + lumen area C) / 2)] x 100. The* ***distal reference lumen area index =*** *the (lumen area B / lumen area C) x 100. The* ***mean reference vessel area index*** *= [lumen area B / ((vessel area A + vessel area C)) / 2] x 100.*

Figure 5.2 The echosignatures of a Palmaz-Schatz stent, an AVE Microstent, and a Gianturco-Roubin stent

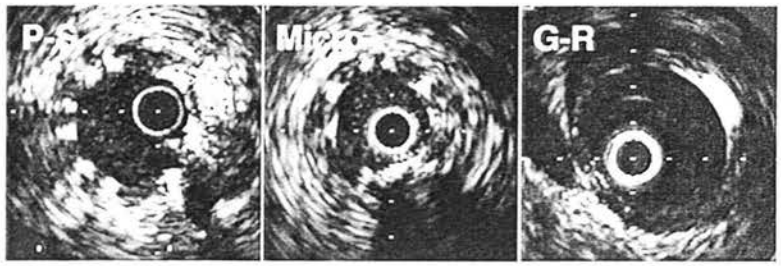

Three different types of stent were used in this series of patients. Each has a slightly different echographic signature, illustrated in this set of images.

P-S. *A Palmaz-Schatz stent is seen in the left hand panel. The fully apposed struts of this PS-154 stent are represented by discrete point echodensities arranged symmetrically around the endoluminal border.*

Micro. *In the middle panel, an AVE Microstent is seen. The 8 point echodensities representing the struts of the this 3.0 mm diameter, 8 mm long stent are again seen to be fully apposed to the vessel wall.*

G-R. *This panel shows an ultrasound image of a Gianturco-Roubin stent. The image plane typically incorporates a short longitudinal segment of the stent coil, seen as a short arc against the vessel wall at 2 to 3 o'clock.*

Figure 5.3 Quantitative changes in cases undergoing re-intervention

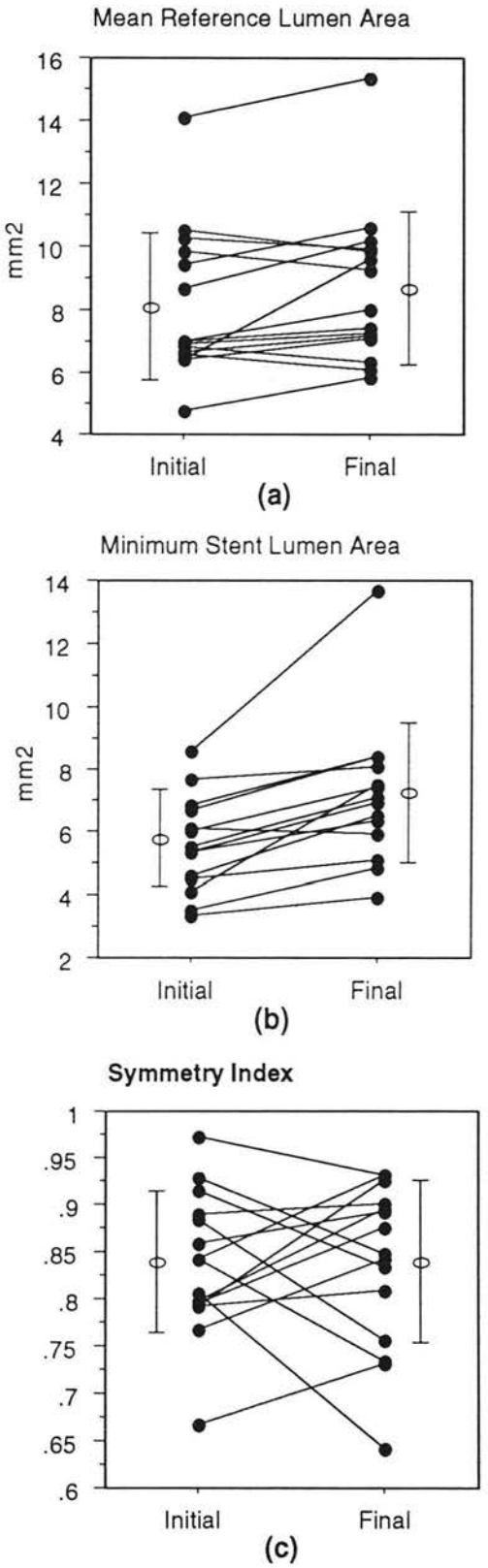

Figure 5.4 Cell plots of the reference indices after initial intervention

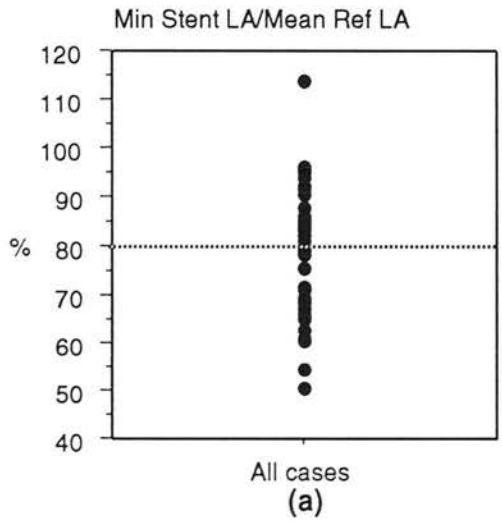

(a)

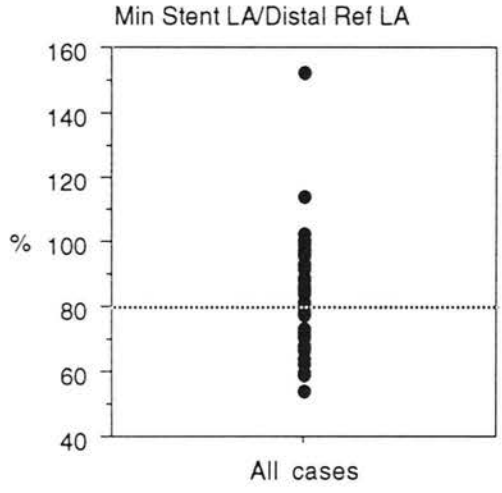

(b)

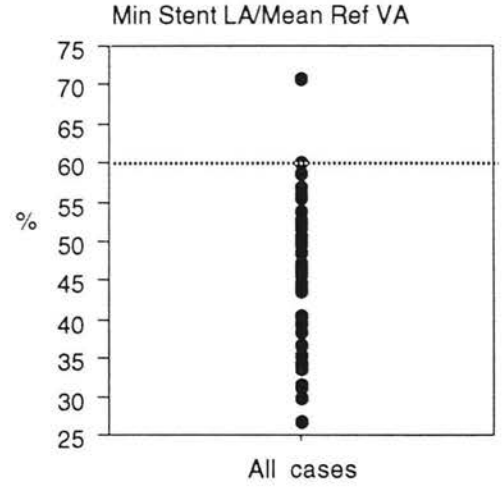

(c)

Figure 5.5 Cell plots of the reference indices in groups A and B

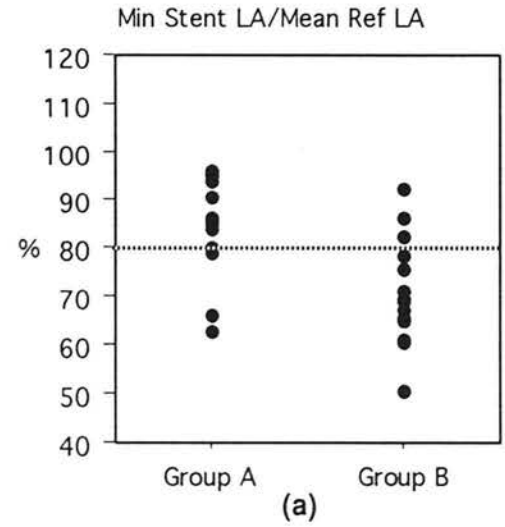

(a)

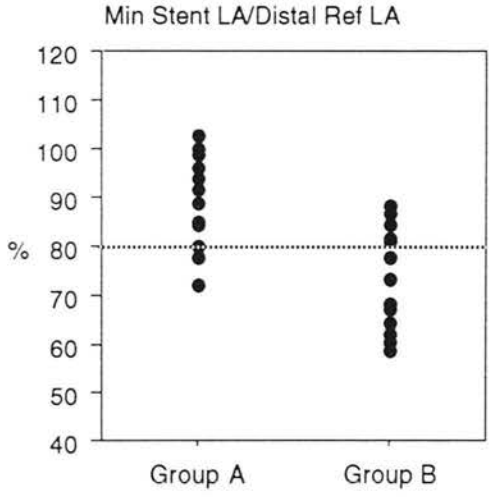

(b)

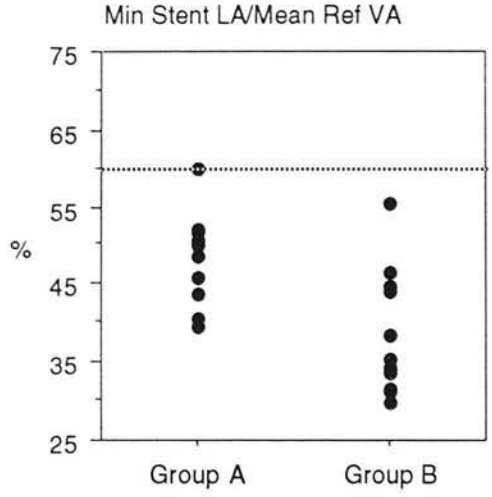

(c)

Figure 5.6 Changes in the reference indices after re-intervention in group B

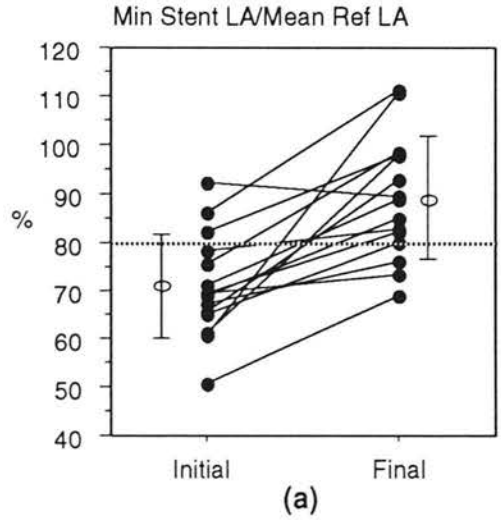

(a)

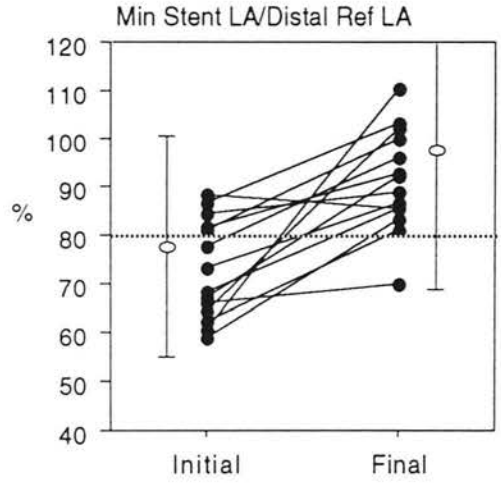

(b)

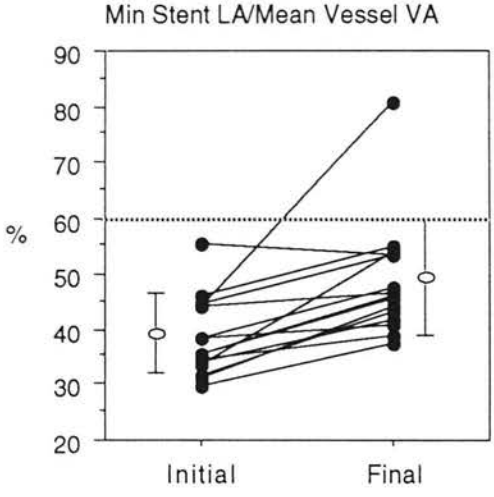

(c)

Figure 5.7 Prolapsed tissue in a stent treated by attempted wall-wrapping

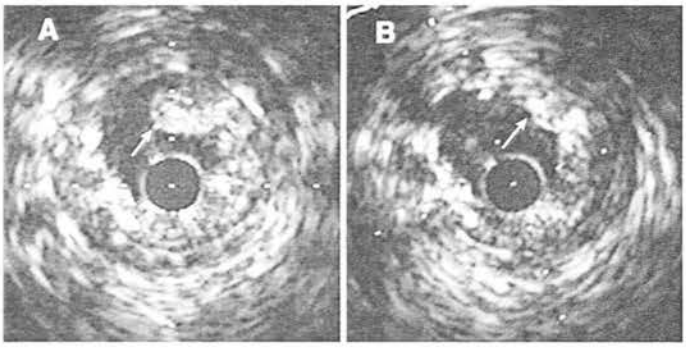

A large eccentric mass of intrastent debris was identified (from 12 to 7 o'clock, arrow) in the proximal segment of a PS-204 implanted into a recanalised proximal LAD occlusion. A high pressure inflation wall wrapped the tissue against the inner border of the stent, but did not satisfactorily abolish its stenotic impact. The final cross-sectional lumen profile was asymmetrical.

Figure 5.8 Correction of stent strut malapposition

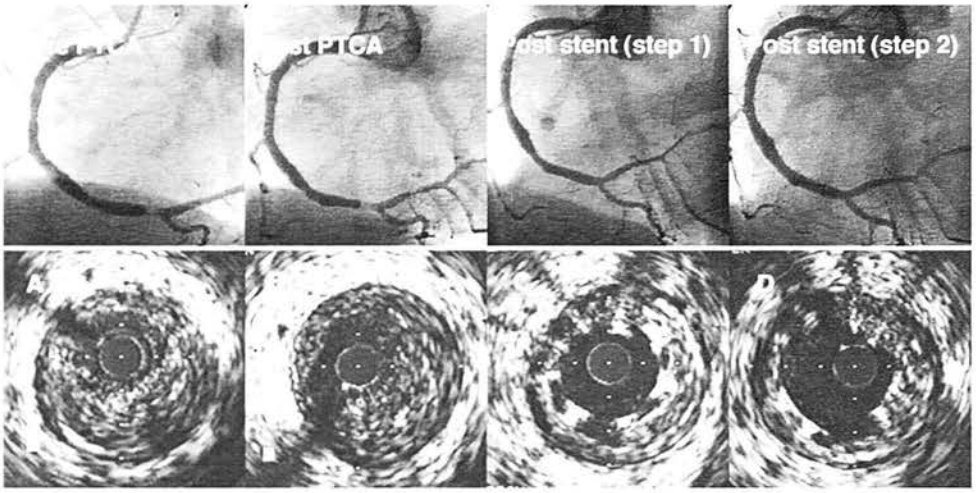

Pre PTCA. *Angioplasty of an eccentric stenosis proximal to the origin of the posterior descending artery gave rise to a hazy angiographic appearance and an ultrasound appearance that was interpreted as a combination of disrupted soft tissue and intraluminal thrombus (**A**).*

Post PTCA. *Following intracoronary thrombolysis the angiographic appearances did not change significantly, although the ultrasound did suggest some clearance of intraluminal debris. A large eccentric tissue flap remained (**B**) and so it was decided to implant a PS-084 stent. This could not be advanced beyond the mid pars descendens, where it was deployed. An 8 mm long, 3.0 mm diameter AVE microstent was delivered to the lesion without difficulty and deployed with a high pressure inflation of the pre-mounted balloon.*

Post stent (step 1). *Despite favorable angiographic appearances, ultrasound clearly demonstrated poor strut apposition in the proximal portion of the lesion (**C**).*

Post stent (step 2). *High pressure dilatation of a 3.5 mm short, minimally compliant balloon led to improved if not complete strut apposition (**D**), emphasising the importance of using a flexible stent that can conform to variable lumen size over short distances in circumstances such as these.*

Figure 5.9 'Late onset' malapposition of stent struts

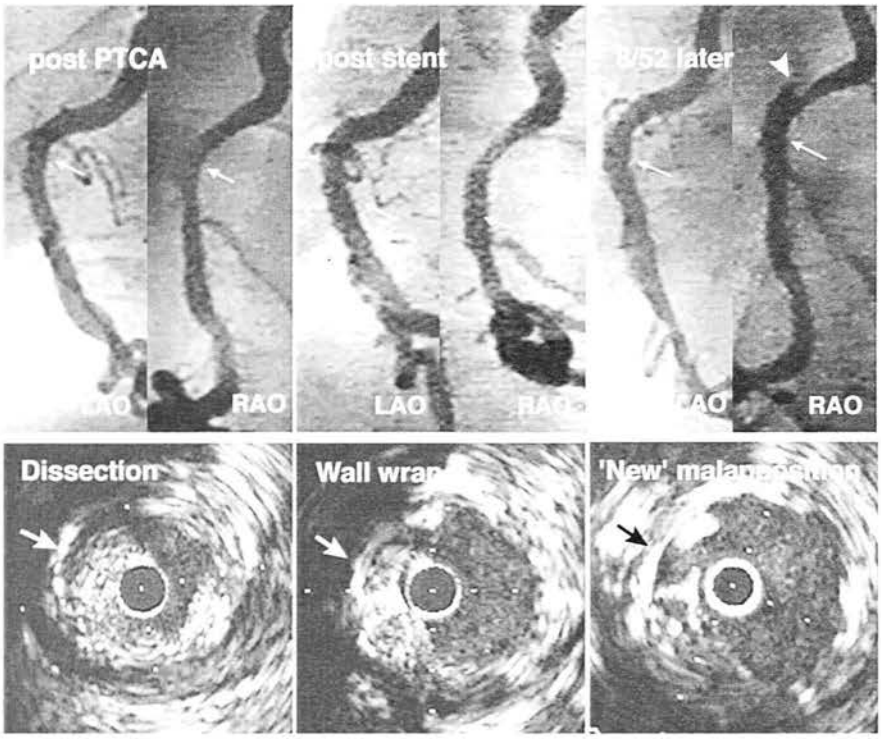

Post PTCA. *Balloon angioplasty of a focal stenosis in the mid right coronary artery of a man presenting with post-infarction unstable angina led to angiographically hazy appearance. Intravascular ultrasound study confirmed the presence of a large 'tissue flap' (arrow) and significant residual lumen stenosis.*

Post stent. *A PS-154 was implanted and both angiographic and ultrasound criteria indicated a successful result.*

8/52 later. *The patient returned 8 weeks later with atypical chest pain and unexplained dypsnoea for a further study. Angiography demonstrated an eccentric protrusion of tissue at the proximal end of the stent (arrow). Intravascular ultrasound showed a satisfactory lumen area of >6.0 mm^2 at the most stenotic point and that the tissue mass was situated proximal to the stent. Unexpectedly, incomplete apposition of the proximal stent struts was found (black arrow). On review of the original study, it became apparent that no strut retraction had occurred, but rather remodelling of the vessel wall, with apparent resorption of the 'tissue flap' that had been wall-wrapped by the stent. This may have consisted of organised thrombus rather than fibrous tissue.*

Figure 5.10 Intrastent debris in an unstable vein graft stenosis

This PS-154 was implanted into an unstable, irregular lesion at the proximal end of an LAD vein graft. An angiographically evident filling defect proliferated rapidly. Intravascular ultrasound study showed satisfactory expansion of the stent throughout its length relative to the distal reference segment, seen in the right hand panel, (the proximal location of the stent had prevented measurement of a proximal reference). Diffuse mural and intraluminal debris was evident throughout the stented segment (seen in the 5 left hand panels). In view of the unstable nature of the lesion, the rapid proliferation of the intraluminal tissue, and to a lesser extent its ultrasound characteristics, it was felt that this was at least partly thrombotic in nature. An infusion of thrombolytic was given by way of an intracoronary infusion catheter, and some improvement in the angiographic appearances was evident the following day. The patient suffered a small non-q wave myocardial infarction, but remained well thereafter.

Figure 5.11 Stent restenosis caused by neo-intima formation

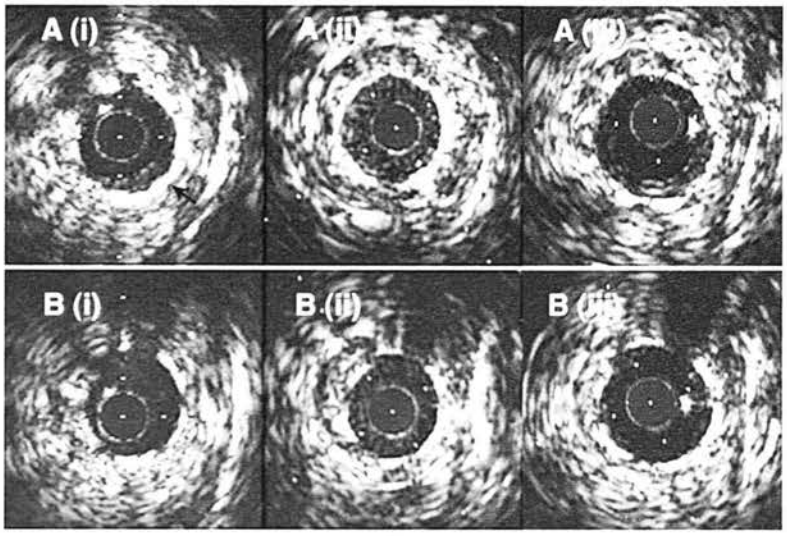

A/B (i). *Four days after the original procedure, a third PS-154 was required to treat a proximal dissection flap that had not been recognised when two other PS-154 stents were implanted for bailout repair of a long mid LAD dissection. Intravascular ultrasound guidance of the third stent implantation ensured complete coverage of the dissection and adequate expansion of the stent. On ultrasound study of the previously implanted 2 stents, a small crescent of tissue (from 4 to 7 o'clock) was noted at a point of stent strut overlap (**A(i)**), identified as an uninterrupted arc of echodense struts underlying the crescent of tissue. In view of the short time since stent implantation, this more probably consisted of mural thrombus deposition than neointima. At an adjacent site within the distal stent, at the origin of a small sidebranch (**B**), no such tissue was seen.*

A/B (ii). *The patient returned 2 1/2 months later and was found to have severe restenosis in the distal stents. Ultrasound showed this was the result of profuse neointima formation, seen as a relatively echolucent tissue completely surrounding the catheter blank.*

A/B (III). *Stent angioplasty disobliterated the stent lumen by further expanding the stent area, compressing/remodelling the neointimal tissue and possibly by extruding it to a limited extent through the stent.*

Figure 5.12 Stent lumen eccentricity was not angiographically apparent

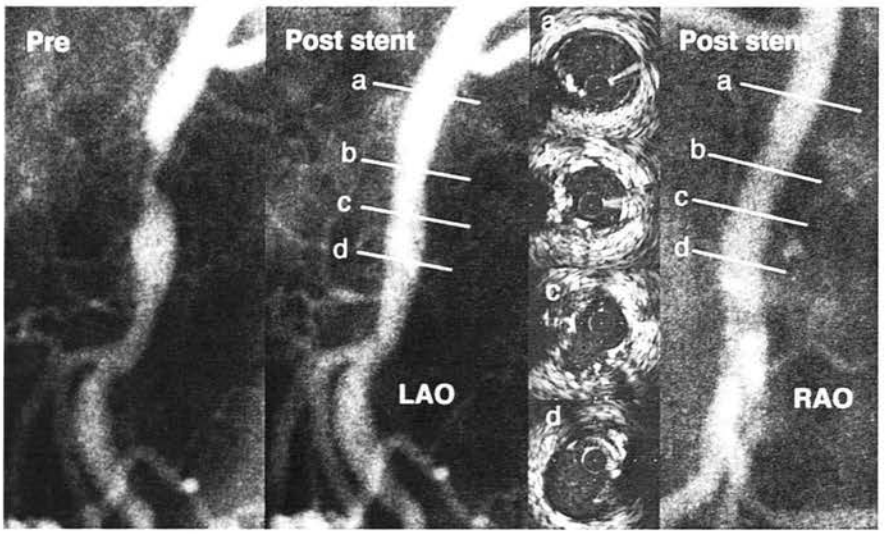

*Neither significant stent underexpansion (ultrasound panel **b**), nor marked lumen asymmetry (ultrasound panel **d**) demonstrated by ultrasound was evident in the 2 angiographic projections obtained following primary stent implantation in this right coronary artery. A third projection (in this case an anteroposterior) might have revealed the narrow lumen profile of the stented lumen seen in panel **c**.*

*Although incomplete expansion, seen in panel **b**, does frequently respond to further balloon dilatation, the response of asymmetric segments of stent to further balloon inflations is unpredictable.*

Chapter 6

An Analysis of the Reproducibility of Reference Lumen Quantitation with Intravascular Ultrasound in Stented Coronary Arteries

Contents *page*

6.1. Introduction

Intravascular ultrasound is currently used to achieve optimal coronary stent deployment and to allow an informed decision to omit anticoagulation in cases in which certain quantitative and qualitative criteria have been met [Colombo, 1995]. Larger stent lumen dimensions that are achieved using IVUS guidance [Mudra, 1994; Popma, 1994] may additionally lead to reduced rates of restenosis, on the basis that greater lumen gain, regardless of the interventional technology used to achieve it, is associated with lower rates of significant lumen renarrowing [Kuntz, 1993]. A variety of quantitative criteria for successful stent deployment have been proposed [Nakamura, 1994; Mudra, 1994; Colombo, 1995]. Regardless of the specific criterion chosen, a central part of the quantitative evaluation of a deployed stent with intravascular ultrasound is the comparison of minimum intrastent dimensions with the dimensions of the reference segments. These are the lumen segments adjacent to the stenosis that appear angiographically normal and 'appropriately sized' for that particular portion of the artery. The selection and measurement of reference sites using ultrasound are both operator dependant processes and potential sources of variability. The variability of such measurements must be sufficiently low for quantitative ultrasound evaluation to be a useful and objective contribution to the decision making process.

6.2. Study aims

The study was designed to determine the variability of reference segment quantitation using intravascular ultrasound.

6.3. Methods and materials

6.3.1. Clinical IVUS examinations

The videotaped IVUS examinations of 24 patients following coronary stent deployment were used to determine the reproducibility of repeated measurements of vessel dimensions at the reference segments. In a separate analysis, the impact of sequential interventions on the reference segment dimensions in a given vessel was studied. In 24 cases the treated segment was studied sequentially following angioplasty and then stent implantation, in 14 cases following initial stent deployment and again after post-dilatation and in 9 cases following angioplasty, initial stent deployment and post dilatation.

6.3.2. Cardiac catheterisation

Cardiac catheterisation was performed by way of the femoral artery. Appropriately selected 8F guiding catheters were used to engage the ostium of the coronary artery and 0.014 inch guide wires were advanced to a distal position in the artery following the intra-arterial administration of 10,000 units of heparin. A range of PTCA balloon catheters was used to perform coronary angioplasty. In the patients included in this study, only Palmaz-Shatz stents, manually crimped onto a balloon of the operator's choice, were used. Following stent deployment, every effort was made to achieve an optimal angiographic result, using, when judged necessary, either the same balloon at higher pressure, a similarly sized non- or minimally compliant balloon, a short high pressure balloon or a larger diameter balloon. When the operator was satisfied that the stent was optimally deployed on the basis of its angiographic appearance, intravascular ultrasound imaging was performed.

6.3.3. Intravascular ultrasound examination

A Hewlett Packard 'Sonos Intravascular' ultrasound scanner and Boston Scientific 'Sonicath' 3.5 F catheters were used in all cases. The intravascular ultrasound

catheter was advanced to a point distal to the segment of interest and then manually withdrawn in a slow, controlled pullback at a rate of approximately 1 mm per second. In all cases, after the transducer was withdrawn into the guiding catheter it was advanced a second time distal to the lesion and the pullback was repeated in the same manner. During IVUS imaging, a simultaneously acquired electrocardiogram was recorded and displayed beneath the video image. The study was recorded on S-VHS videotape and later analysed off-line.

6.3.4. Vessel measurement technique

On review of the videotaped ultrasound examinations, sites distal and proximal to the stented segment, identified during the transducer pullbacks, were chosen by the observer as representative of the 'normal' reference vessel. When a proximal reference segment was not present (ostial lesion or very proximally deployed stent), a distal reference only was selected. Whenever possible, measurements were made on systolic frames (peak of T wave on the ECG), in order to record the maximum vessel dimensions at the selected site. Measurements were made manually using the trackball and the integrated quantitation software of the ultrasound scanner. Luminal diameter (minimum (MLD) and maximum (MxLD)), was subjectively determined by the observer. The outer border of the vessel corresponding with the external elastic lamina was traced to measure vessel cross-sectional area (VA), and the endoluminal border was traced to measure lumen cross-sectional area (LA). Vessel area stenosis was calculated as (1 - LA/VA x 100). Measurements were automatically displayed on the console's screen and hard copies were printed from which the data was entered into a statistical analysis programme spreadsheet.

6.3.4.1. Analysis of variability protocols

Three different analysis protocols were employed to determine reproducibility of measurements on the unselected frames.

6.3.4.1.1. Intraobserver analysis in separate catheter pullbacks (analysis A)

Distal and proximal reference sites were chosen by observer #1 on both the first and second catheter pullback video sequences. Vessel dimensions were measured at these sites and recorded.

6.3.4.1.2. Intraobserver analysis in separate analysis sessions (analysis B)

Observer #1 analysed the same video recordings in a separate analysis session at least 2 weeks later, and again selected distal and proximal reference sites at which vessel quantitation was performed.

6.3.4.1.3. Interobserver analysis on unselected frames (analysis C)

A second observer (#2) was asked to select, quantify and record the distal and proximal reference sites in each case in a separate analysis session.

6.3.5. Statistical analysis

Systematic bias was determined by calculating the mean difference between measurements, and the standard deviation (SD) of the differences was calculated to measure random variation. Both are expressed as an absolute value as well as a percentage of the average of each pair of the absolute measurements. The 95% limits of agreement were calculated as twice the standard deviation. Bland-Altman plots were constructed for each of the quantitative parameters by plotting the mean difference on the y axis against the average of paired measurements on the x axis in order to assess the impact of absolute dimensions on variability and to visually assess the degree and direction of any bias [Bland, 1986] (**figures 6.1-6.3**). The statistical significance of the bias between repeated measures was determined using paired student's t tests and significance was defined as ≤ 0.01.

Bartlett's test was applied to detect a difference in the variability between any of the three sets of measurements from analyses A, B and C. The 'F ratio' test was subsequently applied to detect different variability between any two of the groups. Statistical analysis was performed using a commercially available statistical programme (Statview v4.2).

6.4. Results

6.4.1. Analysis of Reproducibility

A distal reference segment was identified in all cases by both observers. A proximal reference could not be identified in 6 cases because of the proximal location of the stent within the treated vessel.

6.4.1.1. Analysis A

The mean difference, standard deviation and the confidence intervals for each morphometric parameter at proximal, distal and mean reference sites are shown in **table 6.1** and the scattergrams are shown in **figures 6.1-6.3**. In the following paragraphs, the standard deviation of the difference of the repeated measurements is given both in absolute terms and in brackets as a proportion of the average of the two measurements of each parameter.

No significant bias was evident between measurements made on any of the quantitative parameters at the proximal and distal reference segments on sequential pullbacks of the catheter through the stented segment and its absolute value was small in all cases. On the contrary, random variability was greater than 10% of the average of the measured dimensions, being 0.88 mm^2 (12.3%) in the case of proximal lumen area, 0.86 mm^2 (14.94%) for proximal plaque area and 6.28% (14.5%) for proximal percentage stenosis. In the distal reference, random variability exceeded 10% of the average absolute dimension for all parameters excluding the diameters. It measured 0.92 mm^2 (12.94%) for lumen area, 1.53 mm^2

(13%) for vessel area, 1.31 mm^2 (28.3%) for plaque area and 8.21% (23.1%) for percentage stenosis. The random variability of the mean lumen area was 0.8 mm^2 (11%).

6.4.1.2. Analysis B

The results of this analysis are shown in **table 6.2**, and the scattergrams in **figures 6.1-6.3**. No significant bias was detected for any quantitative parameter either at the proximal or distal reference site, and the mean difference was again small in all cases. Random variability was >10% of the mean vessel dimension in the proximal reference segment for the following parameters: 1.06 mm^2 (14.8%) for lumen area, 1.54 mm^2 (27.5%) for plaque area and 8.98 mm^2 (21.0%) for percentage stenosis. Distally, random variability was >10% for all parameters except the maximum lumen diameter, for which it was 0.22 mm (7.2%). The random variability for the minimum lumen diameter was 0.29 mm^2 (10.5%), lumen area 1.06 mm^2 (15.3%), vessel area 1.86 mm^2 (16.0%), plaque area 1.45 mm^2 (30.8%) and percentage stenosis 8.35% (22.8%). The mean lumen area random variability measured 0.80 mm^2 (11.4%).

6.4.1.3. Analysis C

The results of this analysis are shown in **table 6.3**, and the scattergrams are shown in **figures 6.1-6.3**. Again, no significant bias was detected between repeated measurements made in this analysis by the two observers. Measures of random variability were >10% for all morphometric parameters, at proximal and distal reference sites except proximal and distal maximum lumen diameter. At the proximal reference site the random variability of the minimum diameter was 0.32 mm (11.3%), for lumen area 1.28 mm^2 (17.9%), vessel area 2.15 mm^2 (16.8%), for plaque area 1.91 mm^2 (34.7%) and for percentage stenosis 10.25% (24.1%). At the distal reference, the random variability of the minimum lumen diameter was 0.42 mm (15.0%), for lumen area 1.23 mm^2 (18.0%), for vessel area 2.9 mm^2 (25.4%),

for plaque area 2.4 mm^2 (52.8%) and for percentage stenosis 13.86 % (37.3%). The random variability of the mean reference lumen area measured 0.94 mm^2 (13.4%).

6.4.2. Comparison between analysis protocols

Random variability was greater in the interobserver analysis than in the intraobserver analyses. This difference was significant for repeated measures of vessel area, plaque area, and percentage stenosis at proximal and distal reference segments. The maximum lumen diameter was the most consistently measured parameter at both reference sites and in all analysis protocols. Although the random variability of measurements of proximal and distal reference lumen area tended to be greater in the interobserver analysis, that for the mean reference lumen area was lower and of a similar order in both inter- and intraobserver analyses.

6.5. Discussion

6.5.1. Criteria for successful stent deployment

The qualitative criteria for optimal stent deployment include (1) complete apposition of the stent against the vessel wall, and (2) absence of flow limiting lesions (dissection flaps or stenotic plaques) that might compromise run-off from the stented segment. The quantitative criteria include (1) adequate stent expansion and (2) adequate intrastent lumen symmetry (a ratio of minimum diameter to maximum diameter >0.7 throughout the stent) [Nakamura, 1994]. Whereas strut apposition, flow-limiting lesions limiting run-off from the stent and marked stent lumen asymmetry are recognised with little difficulty, the identification of adequate stent expansion is a quantitative process that depends on the selection of an appropriate reference segment against which to compare minimum stent lumen dimensions. The stipulation that reference measurements be made 0.5-1.0 centimetre proximal or distal to the end of the stent [Nakamura, 1994] can at best

be crudely estimated from fluoroscopic evaluation of the transducer in the vessel. The most 'representative' reference segment may not lie within these specified limits, and in reality this process is performed on a more ad hoc basis.

The definition of what constitutes 'adequate expansion' is empirically defined and has evolved over the last 2 years. When referencing to ultrasonically determined vessel dimensions, the Milan group reported vessel rupture in 4 of 359 patients (1.1%) as a consequence of balloon oversizing [Colombo, 1995]. Recognition of the variability of plaque burden in the reference segment, and the potential for very large vessel dimensions and plaque accumulation in the presence of preserved lumen area as a result of adaptive vascular remodelling, has led to the abandonment of this criterion. The same group of investigators now advocate the more straightforward approach of ensuring that the minimum intrastent lumen area exceeds that of the distal reference area. The criteria for optimal expansion advocated by other groups is shown in **table 5.5**.

6.5.2. Findings of the present study

6.5.2.1. Quantitative characteristics of the reference segments

The mean vessel dimensions were slightly larger at proximal than at distal reference sites, as a result of vessel tapering. Minimum and maximum lumen diameters were almost equal, indicating near circularity. Although this is usually a feature of relatively non-diseased vessels, the mean vessel area occupied by plaque (measured as percentage vessel area 'stenosis') in this group of patients was 43% in the proximal segment and 35% in the distal reference. The diffusely diseased nature of angiographically normal reference segments has been consistent finding in vessels undergoing coronary intervention [Tobis, 1989; Hodgson, 1993].

6.5.2.2. Reproducibility of the reference segment quantitation

Mean vessel dimensions were highly consistent across the different analysis protocols (**tables 6.1-6.3**). The negligible mean difference between repeated measures indicates an absence of systematic bias either within or between observers. In contrast, random variability reached a clinically significant level for many of the measured parameters. The least variability was evident in measurements made on sequential catheter pullbacks, in which a learning effect may have occurred. However, even in this analysis, the 95% confidence limits for the proximal and distal lumen area amounted to 25% of the mean proximal and distal lumen area. Marked variability was noted in the interobserver analysis, in which the 95% confidence intervals for proximal and distal lumen areas amounted to over 35% of the mean measured lumen area.

6.5.2.3. Variability as a function of morphometric parameter

Variability was highest in the case of measurements of vessel and plaque area and percentage stenosis, particularly in the interobserver analysis. A moderate degree of wall thickening was found in the reference segments in which an angiographically 'normal' luminal profile was maintained by adaptive vessel enlargement. The distribution and degree of wall thickening vary considerably over short distances within the coronary arteries [Fishbein, 1990] and the large variability of these morphometric parameters probably reflects the selection of different vessel segments for quantitation.

The maximum lumen diameter was the most reproducibly measured parameter. Variability attributable to differences in image interpretation, edge detection and the measurement process is likely to be lowest for the maximum diameter which is the least ambiguous of morphometric parameters. It is also possible that the maximum diameter was more consistent throughout the reference segments than other parameters. The maximum diameter of the reference segment is clinically important,

as it guides the choice of balloon size (and/or inflation pressure in compliant balloons) when incomplete stent expansion has been demonstrated.

In determining the adequacy of stent expansion, intrastent dimensions are most frequently compared to lumen area measurements in the reference segments. Although the interobserver 95% confidence limits for proximal and distal reference segments were ±35%, they were 10% less for the mean reference lumen area, a pattern that was also seen in the other analysis protocols. The mean reference area may thus be a preferable quantity against which to compare the stent area than the distal reference alone in an effort to reduce variability.

6.5.3. The findings of other studies

The reproducibility of reference segment measurements made with IVUS has not previously been formally studied. Mudra et al refer briefly to an analysis of repeated measurements made at 23 sites, including proximal and distal reference sites and the most stenotic site within the stent on repeated pullback sequences [Mudra, 1994]. They found a mean difference and standard deviation of 0.02±0.13 mm for minimum lumen diameter and 0.04±0.33 mm^2 for cross-sectional lumen area. The correlation co-efficient for the lumen diameter was 0.88 and for lumen area 0.97. The significance of these figures is unclear, as they are composite values for measurements of sites that are subject to different degrees of variability (the site of maximum intrastent stenosis is more readily identifiable than the 'correct' reference site either side of the stent). Moreover, the proportion of different sites included in the analysis is not stated. In a separate study (chapter 3) we found a standard deviation of the difference between repeated measurements of 0.13 mm for minimum diameter and 0.3 mm^2 for lumen area at the most stenotic site within stents. In the same study, we noted a trend toward increasing interobserver variability as lumen area increased, possibly as a result of greater difficulty in discriminating specific sites for quantitation in the absence of the cue of discernible

differences in lumen size. The corresponding standard deviations for mean reference lumen diameter and area in the present study were 0.2 mm and 0.80 mm^2 respectively.

Colombo et al. [Colombo, 1995] studied the interobserver and intraobserver reproducibility of measurements made at 30 'randomly selected sites' within stented and reference segments. Although correlation coefficients were all >0.93, and standard error of the estimate low, an analysis of variability on selected frames does not reflect the variability operating in clinical practice, to which the selection of the site for quantitation is a major contributor. In addition, the use of linear regression analysis does not adequately characterise variability [Bland, 1986].

6.5.4. Implications for clinical practice

This study demonstrates that although the process of reference segment quantitation is not subject to systematic bias, random variability is high. This is most marked for those morphometric parameters that tend to be variable within the reference segments (i.e. vessel and plaque area and percentage vessel area stenosis) and are thus highly sensitive to selection of different tomographic sections for analysis. Of concern, we found that the intraobserver and interobserver 95% confidence intervals for the mean reference lumen area were over ±20% of average measured reference lumen area, a level of variability that clearly has the potential to impact on the classification of a given case as being adequately treated or otherwise. The average of the proximal and distal reference lumen areas was less variable than either one alone, suggesting that there may be advantages in using this particular parameter in an effort to improve the reproducibility of the technique.

6.6. Conclusions

IVUS guidance provides useful additional qualitative and quantitative information to the operator during stent implantation. Nevertheless it should be recognised that the quantitative information it provides is subject to at least moderate variability, and the quality of such data is thus contingent upon the clinical experience and interpretative skills of the operator. Should specific, objective quantitative ultrasound criteria be shown to be important (an issue requiring much future study to be resolved), then efforts will have to be made to improve the reproducibility of IVUS quantitation in these circumstances. Such measures may include objective methods of vessel quantitation based on automated edge detection techniques and three dimensional reconstruction to permit the determination of interpolated reference lumen dimensions against which stent dimensions can be compared.

Table 6.1 Bias and random variability - Analysis A

	Average Dimension	Mean Δ	$mean\Delta/av.dim$ (%)	SD Δ	$SD\Delta/av.dim$ (%)	C.I. Δ	$C.I.\Delta/av.dim$ (%)
Prx MLD (mm)	2.84	0.03	(1.0)	0.17	(5.9)	0.34	(11.9)
Prx MxLD (mm)	3.16	0.06	(1.9)	0.24	(7.7)	0.48	(15.3)
Prx LA (mm^2)	7.16	-0.06	(-0.9)	0.88	(12.3)	1.76	(24.6)
Prx VA(mm^2)	13.18	-0.41	(-3.1)	0.97	(7.4)	1.94	(14.7)
Prx PA (mm^2)	5.77	-0.29	(-5.0)	0.86	(14.9)	1.72	(29.9)
Prx %sten (%)	43.33	-0.74	(-1.7)	6.28	(14.5)	12.56	(29.9)
Dist MLD (mm)	2.81	0.00	(0.1)	0.27	(9.6)	0.47	(19.3)
Dist MxLD (mm)	3.09	0.05	(-1.6)	0.24	(7.7)	0.47	(15.4)
Dist LA (mm^2)	7.11	-0.23	(-3.2)	0.92	(12.9)	1.84	(25.9)
Dist VA (mm^2)	11.76	-0.29	(-2.5)	1.53	(13.0)	3.07	(26.1)
Dist PA (mm^2)	4.62	0.01	(0.1)	1.31	(28.3)	2.61	(56.5)
Dist %sten (%)	35.61	0.12	(0.3)	8.21	(23.1)	16.42	(46.1)
Mean LA (mm^2)	7.25	-0.08	(-1.1)	0.8	(11.1)	1.61	(22.2)

The mean difference, standard devation and 95% limits of agreement of repeated measurements of each morphometric parameter in proximal and distal reference sites, and for the mean reference lumen area are shown for analysis A. In brackets in the adjacent column, each of these is also given as a proportion of the average dimension.

Table 6.2 Bias and random variability - Analysis B

	Average Dimension	Mean Δ	$mean\Delta / av.dim$ (%)	SD Δ	$SD\Delta / av.dim$ (%)	C.I. Δ	$C.I.\Delta / av.dim$ (%)
Prx MLD (mm)	2.82	0.05	(1.8)	0.21	(7.4)	0.42	(14.9)
Prx MxLD (mm)	3.19	0.01	(0.4)	0.23	(7.2)	0.46	(14.5)
Prx LA (mm^2)	7.14	-0.02	(0.3)	1.06	(14.8)	2.11	(29.6)
Prx VA(mm^2)	12.79	-0.18	(-1.4)	1.23	(9.6)	2.46	(19.3)
Prx PA (mm^2)	5.61	-0.11	(-1.9)	1.54	(27.5)	3.09	(55.0)
Prx %sten (%)	42.72	0.55	(1.3)	8.98	(21.0)	17.96	(42.0)
Dist MLD (mm)	2.79	-0.04	(-1.4)	0.29	(10.5)	0.58	(20.9)
Dist MxLD (mm)	3.02	-0.01	(-4.3)	0.22	(7.2)	0.43	(14.4)
Dist LA (mm^2)	6.91	-0.24	(-3.4)	1.06	(15.3)	2.12	(30.7)
Dist VA (mm^2)	11.61	-0.31	(-2.7)	1.86	(16.0)	3.72	(32.1)
Dist PA (mm^2)	4.70	-0.30	(-6.4)	1.45	(30.8)	2.89	(61.6)
Dist %sten (%)	36.65	0.70	(1.9)	8.35	(22.8)	16.7	(45.6)
Mean LA (mm^2)	7.06	-0.07	(-1.0)	0.80	(11.4)	1.61	(22.8)

The mean difference, standard devation and 95% limits of agreement of repeated measurements of each morphometric parameter in proximal and distal reference sites, and for the mean reference lumen area are shown for analysis B. In brackets in the adjacent column, each of these is also given as a proportion of the average dimension.

Table 6.3 Bias and random variability - Analysis C

	Average Dimension	Mean Δ	$mean\Delta/_{av.dim}$ (%)	SD Δ	$SD\Delta/_{av.dim}$ (%)	C.I. Δ	$C.I.\Delta/_{av.dim}$ (%)
Prx MLD (mm)	2.87	0.04	(1.5)	0.32	(11.3)	0.65	(22.6)
Prx MxLD (mm)	3.20	0.05	(1.6)	0.29	(9.2)	0.59	(18.3)
Prx LA (mm^2)	7.17	0.25	(3.4)	1.28	(17.9)	2.57	(35.8)
Prx VA(mm^2)	12.84	0.15	(1.2)	2.15	(16.8)	4.31	(33.6)
Prx PA (mm^2)	5.50	-0.08	(-1.5)	1.91	(34.7)	3.82	(69.5)
Prx %sten (%)	42.47	-1.01	(-2.4)	10.25	(24.1)	20.51	(48.3)
Dist MLD (mm)	2.77	0.00	(0.1)	0.42	(15.0)	0.83	(30.0)
Dist MxLD (mm)	3.02	-0.01	(-0.4)	0.28	(9.2)	0.55	(18.4)
Dist LA (mm^2)	6.87	-0.17	(-2.5)	1.23	(18.0)	2.47	(35.9)
Dist VA (mm^2)	11.42	-0.10	(-0.9)	2.9	(25.4)	5.8	(50.8)
Dist PA (mm^2)	4.62	0.10	(2.1)	2.44	(52.8)	4.88	(105.7)
Dist %sten (%)	37.12	-0.26	(-0.7)	13.86	(37.3)	27.72	(74.7)
Mean LA (mm^2)	7.04	-0.04	(-0.6)	0.94	(13.4)	1.89	(26.8)

The mean difference, standard devation and 95% limits of agreement of repeated measurements of each morphometric parameter in proximal and distal reference sites, and for the mean reference lumen area are shown for analysis C. In brackets in the adjacent column, each of these is also given as a proportion of the average dimension.

Figure 6.1a Scattergrams for repeated measurement of proximal reference dimensions

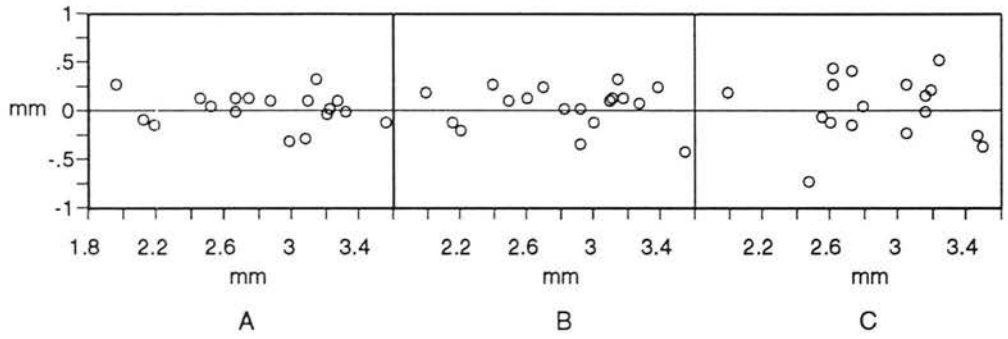

Proximal Minimum Lumen Diameter

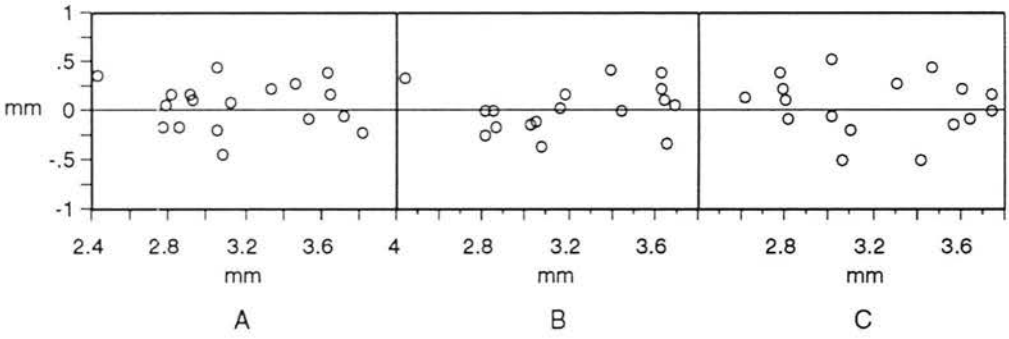

Proximal Maximum Lumen Diameter

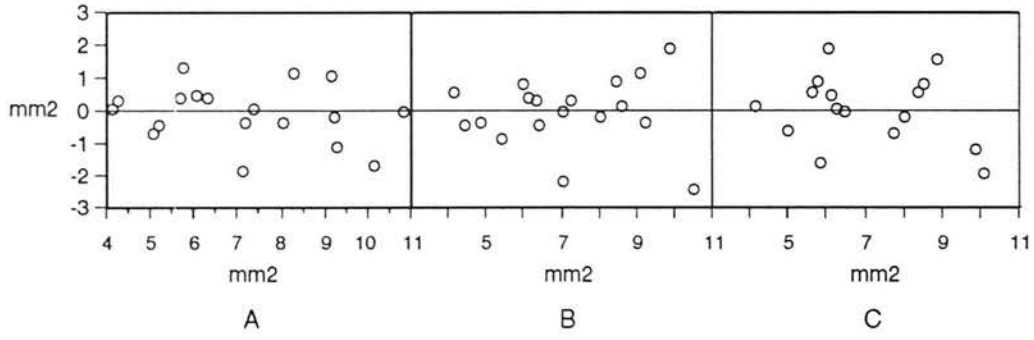

Proximal Lumen Area

Figure 6.1b Scattergrams for repeated measurement of proximal reference dimensions

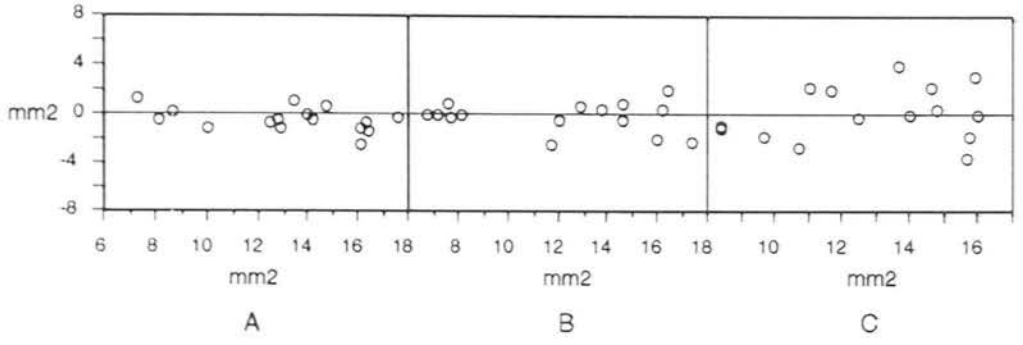

Proximal Vessel Area

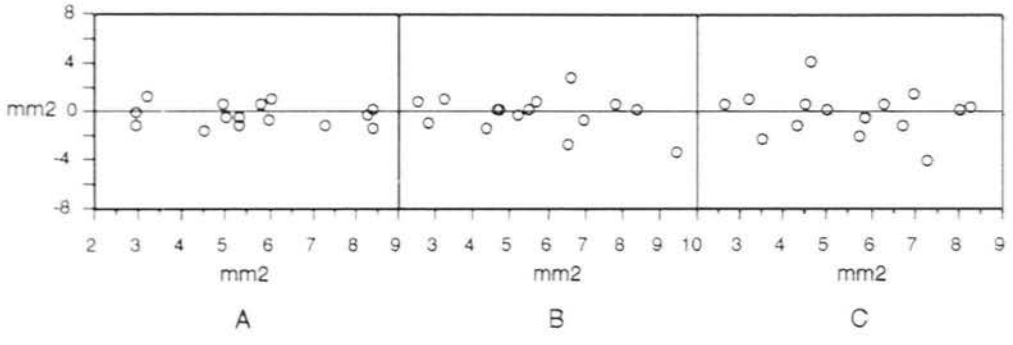

Proximal Plaque Area

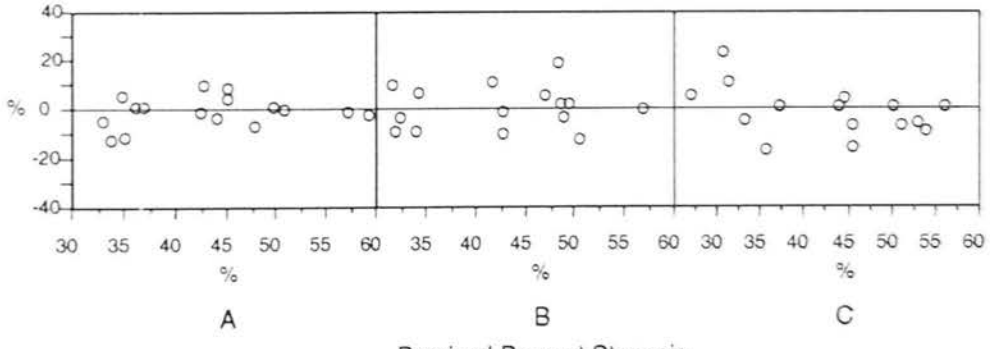

Proximal Percent Stenosis

Figure 6.2a Scattergrams of repeated measurements of distal reference dimensions

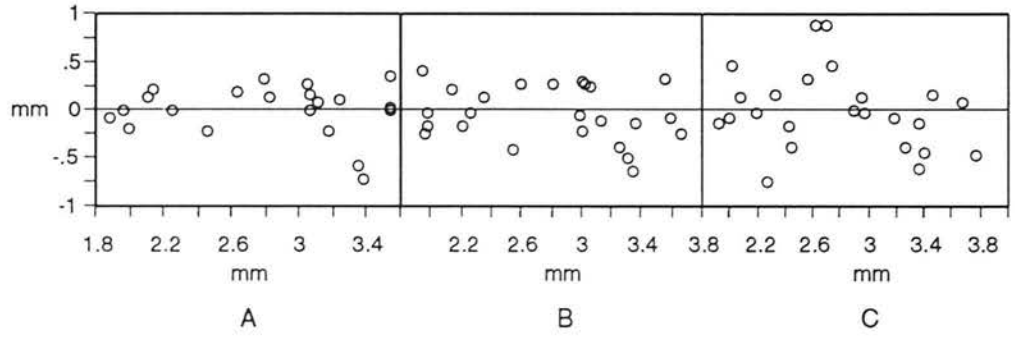

Distal Minimum Lumen Diameter

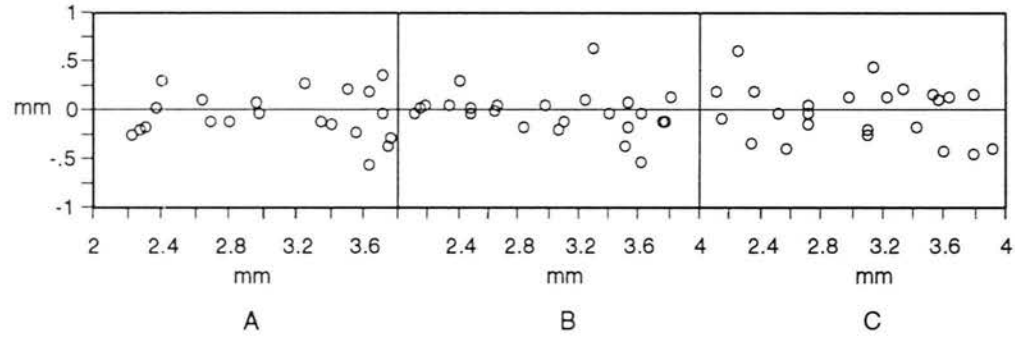

Distal Maximum Lumen Diameter

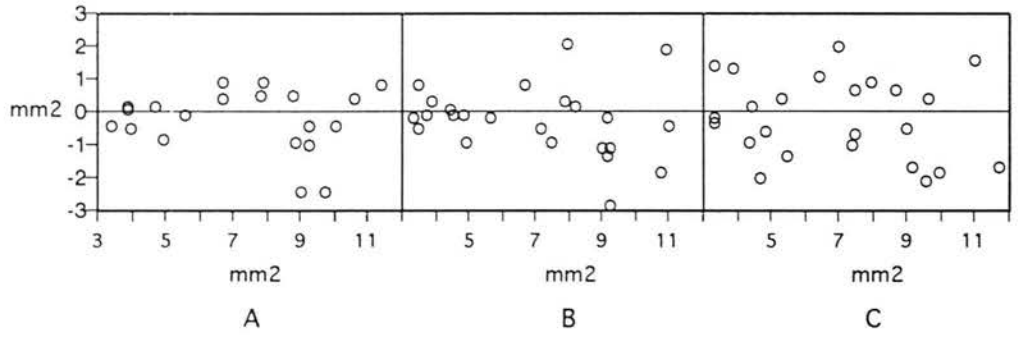

Distal Lumen Area

Figure 6.2b Scattergrams of repeated measurements of distal reference dimensions

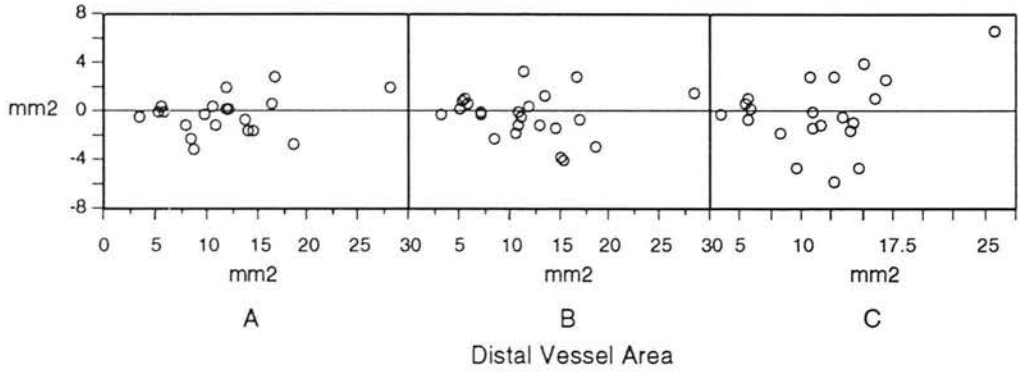

Distal Vessel Area

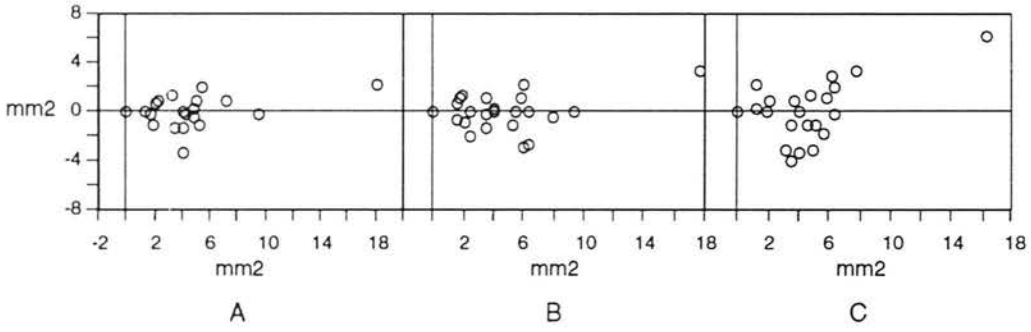

Distal plaque area

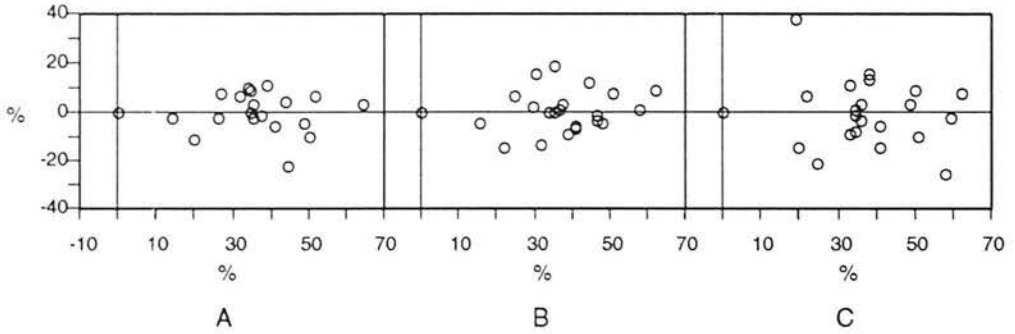

Distal Percent Stenosis

Figure 6.3 Scattergrams of repeated measurements of mean reference dimensions

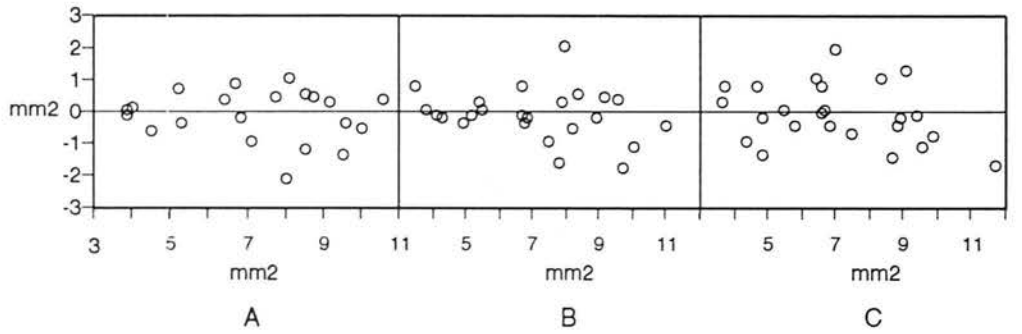

Mean Reference Lumen Area

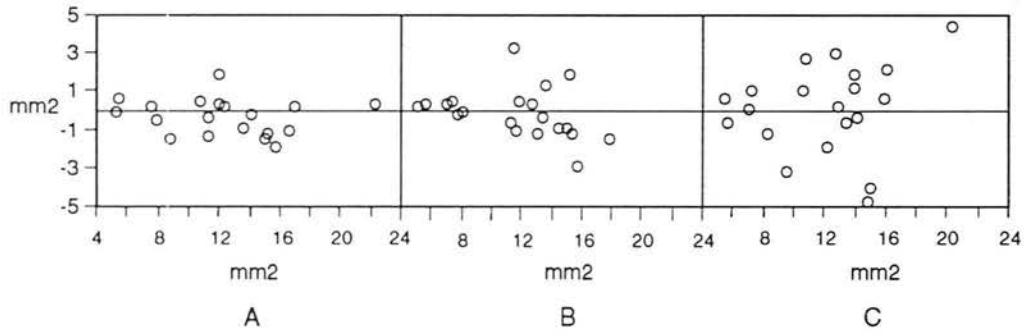

Mean Reference Vessel Area

Chapter 7

Summary and Conclusions

The first chapter outlines the advantages of intravascular ultrasound as a research technique. A brief technical and methodological overview is given and a number of the methodological difficulties that are addressed in later chapters are highlighted.

In Chapter 2, the reproducibility of measurements made with intravascular ultrasound is examined. Previous studies have confirmed satisfactory short-term reproducibility in selected video frames. We adopted a new approach of assessing the variability of measurements made on unselected frames and in separate catheter passes. Intraobserver variability was low in these circumstances, and did not differ between selected and unselected frame analyses. Moreover, the random variability of the measurements of unselected frame minimum diameters was slightly less than that previously documented for quantitative coronary angiography (0.22 mm vs. 0.34 mm respectively). The intraobserver random variability of minimum lumen area measurements was impressively low at 0.37 mm^2. The interobserver variability was greater (0.67 mm^2 for lumen area measurement), and was equivalent in both selected and unselected analyses. For most morphometric parameters, it was of a scale that might confound the detection of changes in the dimensions of the coronary arteries. We concluded that further efforts are required to ensure greater reproducibility of ultrasound measurements.

In chapter 3, we examined the quantitative and qualitative impact of the rotation angle error artefact on mechanical intravascular ultrasound images. Severe catheter bends induced quantitative inaccuracy, apparently as a result of a rotation angle error artefact. The position of the transducer within the lumen was important. When the transducer was located centrally within the lumen, a rotation angle error artefact did not impact significantly on the lumen shape or size (and hence may not be recognisable), but did effect the geometry of the vessel wall.

The direction of the quantitative error induced by a rotation angle error artefact was unpredictable, although an overall trend towards increasing lumen area was noted. Older catheters generated a greater level of image distortion. In the absence of recognisable lumen distortion, most images, even in this study employing previously used catheters, were found to be quantitatively accurate. When geometric distortion is recognised during a clinical study, the quantitative accuracy of images is questionable and caution should be exercised in basing important clinical decisions upon them.

In chapter 4, an issue of interpretative methodology is addressed. Intravascular ultrasound's wall-viewing capacity makes it particularly attractive as a means of studying acute coronary disease. However, the non-specific grey level characteristics of thrombus and of lipid-rich plaques have limited its application in this area of research. We found a distinctive echographic pattern in unstable coronary plaques. The morphology of this 'inner layer' within the lesion, and its behaviour following balloon angioplasty, led us to propose that it represented mural thrombus. Having characterised the echographic appearance of stable and unstable lesions, we also found significant differences in the mechanism of angioplasty between both groups. Stable lesions underwent greater stretch and little if any 'plaque' area reduction, whereas the opposite was true of unstable lesions.

In chapter 5, we report the detailed observations made in a consecutive group of cases who underwent ultrasound guided stent implantation. Despite the use of moderate to high pressure balloon dilatation and achievement of a subjectively satisfactory angiographic result, almost 50% of cases did not fulfil the ultrasound criteria for successful stent deployment and 10% of cases demonstrated incomplete apposition of the stent struts. The proportion of stents judged to be underexpanded varied according to the specific expansion index applied. Only

18% of our cases fulfilled the more rigorous criteria for stent expansion, widely applied by other groups, on initial ultrasound assessment. It is not clear what degree of stent expansion is necessary to optimise acute and long-term outcome, but an expansion index should be chosen that can realistically be obtained without jeopardising the patient. In our series, a further 22% increase in lumen area was achieved in suboptimally expanded stents following ultrasound prompted re-intervention. The use of non-compliant balloons appeared to be associated with a greater likelihood of greater expansion and a successful outcome.

In chapter 6, we looked at the quantitative reproducibility of the reference segment. The unselected intraobserver random variability of the mean reference lumen area measured 0.8 mm^2, over twice the variability of minimum lumen area within a lesion. The interobserver variability was larger, measuring 0.94 mm^2. The 95% limits of agreement thus amounted to 27% of the mean reference lumen area (7.0 mm^2). Clearly, this level of reproducibility has implications for the ability of different individuals or groups to aim for a specific quantitative outcome, even if they operate with the same criteria. As the observations made in the series of patients reported in chapter 5 attest to, ultrasound assessment is not just a means of quantitating the outcome of a procedure but also provides important qualitative information. Those who argue for the central importance of the quantitative ultrasonic criteria should bear in mind the variability inherent in selecting and measuring the reference segments.

All the studies reported in this thesis point to the need for efforts to improve intravascular ultrasound technology and practice. Developments in catheter design are needed to overcome the problem of the rotation angle error artefact. Adoption of standard definitions and guidelines concerning the interpretation of images will help to reduce the variability associated with qualitative evaluation. Both qualitative and quantitative evaluation are currently operator dependant. To significantly improve the reproducibility of the technique, development of automated tissue identification that also provides the basis for reliable boundary detection is required. The development of such a system of radiofrequency based tissue characterisation, which it is believed may provide the solutions to many of the shortcomings outlined in this work, is the area to which our group is currently devoting much its energy.

Chapter 8

Bibliography

Alfonso F, Macaya C, Goicolea J, Iniguez A, Hernandez R, Zamorano J, Perez-Vizcayne MJ, Zarco P. 1994
Intravascular ultrasound imaging of angiographically normal coronary segments in patients with coronary artery disease. Am Heart J 1994;127:536-44

Ambrose J, Winters S, Stern A, Eng A, Teichholz L, Gorlin R, Fuster V. 1985
Angiographic morphology and the pathogenesis of unstable angina. J Am Coll Cardiol 1985, 5:609-616

Anderson MH, Simpson IA, Katritsis D, Davies MJ, Ward DE. 1992
Intravascular ultrasound imaging of the coronary arteries: an in vitro evaluation of measurement of area of the lumen and atheroma characterisation. Br Heart J 1992;68:276-81

Anderson TJ, Meredith IT, Uehata A, Mudge GH, Selwyn AP, Ganz P, Yeung AC. 1993
Functional significance of intimal thickening as detected by intravascular ultrasound early and late after cardiac transplantation. Circulation 1993;88:1093-100

Baroldi G. 1983
Disease of the coronary arteries. In Cardiovascular Pathology. Vol. 1. (Ed. Silver MD) Churchill Livingstone, New York (1983) 317-391

Barragan P, Sainsous J, Silvestri M, Bouvier JL, Comet B, Simeoni JB, Charmasson C, Bremondy M. 1994
Ticlopidine and subcutaneous heparin as an alternative regimen following coronary stenting. Cathet Cardiovasc Diagn 1994;32:133-138

Becker. 1985
Atherosclerosis - A lesion in search of a definition. Int J Cardiol 1985;8:375-7

Benkeser PJ, Churchwell AL, Lee C, Abouelnasr DM. 1993
Resolution limitations in intravascular ultrasound imaging. J Am Soc Echocardiogr 1993;6:158-65

Bertrand M, Lablanche M, Bauters C, Leroy F, MacFadden E. 1993
Discordant results of visual and quantitative estimates of stenosis severity before and after coronary angioplasty. Cathet Cardiovasc Diagn 1993;28:1-6

Bland M, Altman G. 1986
Statistical methods for assessing agreement between two methods of clinical measurement. Lancet 1986;i:307-310

Block P, Myler R, Stertzer S, Fallon J. 1981
Morphology after transluminal angioplasty in human beings. N Engl J Med 1981;305:382-85

Bom N. 1995
Intravascular ultrasound. Technical update 1995. In: Abstracts of the 11th Symposium on Echocardiology, Rotterdam, The Netherlands: page 3

Braden GA, Herrington DM, Downes TR, Kutcher MA, Little WC. 1994
Qualitative and quantitative contrasts in the mechanisms of lumen enlargement by coronary balloon angioplasty and directional coronary atherectomy. J Am Coll Cardiol 1994;23:40-8

Casteneda-Zuniga W, Formanek A, Tadavarthy M, Vlodaver Z, Edwards J, Zollikofer C, Amplatz K. 1980
The mechanism of balloon angioplasty. Radiology 1980;135:565-71

Cieszynski T. 1960
Intracardiac method for the investigation of structure of the heart with the aid of ultrasonics. Arch Immunol Ter Dosw 1960;8:551-7

Chae JS, Brisken AF, Maurer G, Siegel RJ. 1992
Geometric accuracy of intravascular ultrasound imaging. J Am Soc Echocardiogr 1992;5:577-87

Colombo A, Hall P, Nakamura S, Almagor Y, Maiello L, Martini G, Gaglione A, Goldberg SL, Tobis JM. 1995
Intracoronary stenting without anticoagulation accomplished with intravascular ultrasound guidance. Circulation 1995;91:1676-88

Comess K, Fitzgerald P, Yock P. 1992
Intracoronary ultrasound imaging of graft thrombosis. N Eng Med J 1992;327:1691-2

Coy KM, Maurer G, Siegel RJ. 1991
Intravascular ultrasound imaging: A current perspective. J Am Coll Cardiol 1991;18:1811-23

Coy K, Park J, Fishbein M, Laas T, Diamond G, Adler L, Maurer G, Siegel R. 1992
In vitro validation of three-dimensional intravascular ultrasound for the evaluation of arterial injury after balloon angioplasty. J Am Coll Cardiol 1992;20:692-700

Davidson CJ, Sheikh KH, Kisslo KB, Phillips HR, Peter RH, Behar VS, Kong YH, Krucoff M, Ohman EM, Tcheng JE, Stack RS. 1991
Intracoronary ultrasound evaluation of interventional technologies. Am J Cardiol 1991;68:1305-9

Davies MJ, Thomas A. 1984
Thrombosis and acute coronary artery lesions in sudden cardiac ischemic death. N Engl J Med 1984;310:1137-40

De Caterina R, Sicari R, Bernini W, Lazzerini G, Buti SG, Giannessi D. 1991
Benefit/risk profile of combined antiplatelet therapy with ticlopidine and aspirin. Thromb Haemost 1991;65:504-510

De Franco AC, Tuzcu ME, Moliterno DJ, Elliot J, Berkalp B, Franco I, Raymond RE, Whitlow PL, Guyer S, Nissen SE. 1994
Overstimation of lumen size after coronary interventions: Implications for randomised trials of new devices. Circulation 1994;90:I-550

De Kroon MG, van der Heiden MS, Bom N, Borst C. 1993
Quantitative characterisation of arterial tissue and blood: complications and perspectives. In: Intravascular ultrasound. 3rd edition. Edited by Roelandt J, Gussenhoven E, Bom N. Dordrecht, The Netherlands: Kluwer Academic Publishers; 1993:109-118

De Lezo JS, Romero M, Medina A, Pan M, Pavlovic D, Vaamonde R, Hernandéz E, Melián F, Rubio F, Marrero J, Segura J, Irurita M, Cabrera JA. 1993
Intracoronary ultrasound assessment of directional coronary atherectomy: immediate and follow-up findings. J Am Coll Cardiol 1993;21:298-307

De Scheerder I, De Man F, Herregods MC, Wilczek K, Barrios L, Raymenants E, Desmet W, De Geest H, Piessens J. 1994
Intravascular ultrasound versus angiography for measurement of luminal diameters in normal and diseased coronary arteries. Am Heart J 1994;127:243-51

Di Mario C, The S, Madretsma S, von Suylen R, Wilson R, Bom N, Serruys P, Gussenhoven E, Roelandt J. 1992
Detection and characterisation of vascular lesions by intravascular ultrasound: an in vitro study correlated with histology. J Am Soc Echocardiogr 1992;5:135-146

Di Mario C, Madretsma S, Linker D, The S, Bom N, Serruys P, Gussenhoven E, Roelandt J. 1993
The angle of incidence of the ultrasonic beam: a critical factor for the image quality in intravascular ultrasonography. Am Heart J 1993;125:442-448

Di Mario C, Gil R, Camenzind E, Ozaki Y, von Birgelen C, Umans V, de Jaegere P, de Feyter PJ, Roelandt JRTC, Serruys PW. 1995
Quantitative assessment with intracoronary ultrasound of the mechanisms of restenosis after percutaneous transluminal balloon angioplasty and directional coronary atherectomy. Am J Cardiol 1995;75:772-777

Dotter C, Judkins M. 1964
Transluminal treatment of ateriosclerotic obstruction: description of a new technique and a preliminary report of its application. Circulation 1964;30:654-70

Drexler H, Fischell TA, Pinto FJ, Chenzbraun A, Botas J, Cooke JP, Alderman EL. 1994
Effect of L-arginine on coronary endothelial function in cardiac transplant recipients. Relation to vessel wall morphology. Circulation 1994;89:1615-23

Evans JL, Ng K, Vonesh M, Cusick D, Morales R, Tommaso C, Meyers S, Roth S, Kramer B, McPherson D. 1993
Spatially correct three dimensional reconstruction of intracoronary ultrasound: Further validation and initial patient studies. J Am Coll Cardiol 1993;21:181A

Evans JL, Ng KH, Vonesh MJ, Kramer BL, Meyers SN, Mills TA, Kane BJ, Aldrich WN, Jang YT, Yock PG, Rold MD, Roth SI, McPherson DD. 1994
Arterial imaging with a new forward-viewing intravascular ultrasound catheter, I. Initial studies. Circulation 1994;89:712-7

Falk E. 1983
Plaque rupture with severe pre-existing stenosis precipitating coronary thrombosis. Characteristics of coronary atherosclerotic plaques underlying fatal occlusive thrombi. Br Heart J 1983;50:127-34

Falk E. 1985
Unstable angina with fatal outcome: Dynamic coronary thrombosis leading to infarction and/or sudden death. Autopsy evidence of recurrent mural thrombosis with peripheral embolization cluminating in total vascular occlusion. Circulation 1985;71:699-708

Finet G, Maurincomme E, Tabib A, Crowley RJ, Magnin I, Roriz R, Beaune J, Amiel M. 1993
Artifacts in intrascular ultrasound imaging: analyses and implications. U I Med Biol 1993;19:533-47

Fischman D, Leon M, Baim D, Schatz R, Savage MP, Penn I, Detre K, Veltri L, Ricci D, Nobuyoshi M, Cleman M, Heuser R, Almond D, Teirstein P, Fish D, Colombo A, Brinker J, Moses J, Shaknovich A, Hirshfeld J, Bailey S, Ellis S, Rake R, Goldberg S on behalf of the STRESS investigators. 1994
A randomised comparison of coronary-stent placement and balloon angioplasty in the treatment of coronary artery disease. N Engl J Med 1994;331:496-501

Fishbein M. 1990
Coronary artery plaque morphology after balloon angioplasty. J Am Coll Cardiol 1990;15:1430-1431

Fitzgerald PJ, Brisken AF, Brennan JM, Hargrave VK, MacGregor JS, Yock PG. 1991
Errors in ultrasound image interpretation and measurement due to limited dynamic range. Circulation 1991;84:II-438

Fitzgerald P, St. Goar F, Connolly A, Pinto F, Billingham M, Popp R, Yock P. 1992a
Intravascular ultrasound imaging of coronary arteries. Is three layers the norm? Circulation 1992;86:154-158

Fitzgerald P, Ports T, Yock P. 1992b
Contribution of localized calcium deposits to dissection after angioplasty: an observational study using intravascular ultrasound. Circulation 1992;86:64-70

Fitzgerald PJ, Yock PG. 1993
Mechanisms and outcomes of angioplasty and atherectomy assessed by intravascular ultrasound imaging. J Clin Ultrasound 1993;21:579-88

Fitzgerald PJ, on behalf of the STRUT Registry Investigators. 1995
Lesion composition impacts size and symmetry of stent expansion: Initial report from the STRUT registry. J Am Coll Cardiol 1995; abstract suppl:49A

Frimerman A, Miller HI, Hallman M, Laniado S, Keren G. 1994
Intravascular ultrasound characterization of thrombi of different composition. Am J Cardiol 1994;73:1053-1057

Ge J, Erbel R, Zamorano J, Koch L, Kearney P, Görge G, Gerber T, Meyer J. 1993
Coronary artery remodeling in atherosclerotic disease: an intravascular ultrasonic study in vivo. Coron Artery Dis 1993;4:981-6

Ge J, Erbel R, Rupprecht HJ, Koch L, Kearney P, Görge G, Haude M, Meyer J. 1994a
Comparison of intravascular ultrasound and angiography in the assessment of myocardial bridging. Circulation 1994;89:1725-32

Ge J, Erbel R, Gerber T, Görge G, Koch L, Haude M, Meyer J. 1994b
Intravascular ultrasound imaging of angiographically normal coronary arteries: a prospective study in vivo. Br Heart J 1994;71:572-578

George B, Voorhees W, Roubin G, Fearnot N, Pinkerton C, Raizner A, King S, Holmes D, Topol E, Kereiakes D, Hartzler G. Multicentre investigation of coronary stenting to treat acute or threatened closure after percutaneous transluminal coronary angioplasty: Clinical and angiographic outcomes. J Am Coll Cardiol 1993;22:135-43

Gerber T, Erbel R, Görge G, Ge J, Rupprecht H-J, Meyer J. 1992
Classification of morphologic effects of percutaneous transluminal coronary angioplasty assessed by intravascular ultrasound. Am J Cardiol 1992;70:1546-1554

Gerber T, Erbel R, Gorge G, Ge J, Rupprecht HJ, Meyer J. 1994
Extent of atherosclerosis and remodeling of the left main coronary artery determined by intravascular ultrasound. Am J Cardiol 1994;73:666-71

Glagov S, Weisenberg E, Zarins C, Stankunavicius R, Kolettis G. 1987
Compensatory enlargement of human atherosclerotic arteries. N Engl J Med 1987;316:1371-75

Grüntzig A, Senning Å, Siegenthaler W. 1977
Non operative dilatation of coronary-artery stenosis - percutaneous transluminal coronary angioplasty. N Engl J Med 1977;301:61-68

Guiteras Val P, Bourassa MG, David PR, Bonan R, Crépeau J, Dyrda I, Lespèrance J. 1987
Restenosis after successful percutaneous transluminal coronary angioplasty: the Montreal Heart Institute experience. Am J Cardiol 1987;60:50B-55B

Gurley J, Nissen S, Booth D, DeMaria A. 1992
Influence of operator- and patient-dependent variables on the suitability of automated quantitative coronary arteriography for routine clinical use. J Am Coll Cardiol 1992;19:1237-1243

Gussenhoven E, Essed C, Lancée C, Mastik F, Frietman P, van Egmond F, Reiber J, Bosch H, van Urk H, Roelandt J, Bom N. 1989
Arterial wall characteristics determined by intravascular ultrasound imaging: an in vitro study. J Am Coll Cardiol 1989;14:947-52

Gussenhoven E, van der Lugt A, van Strijen M, Kroeze H, The S, van Egmeond F, Honkoop J, Peters R, de Feyter P, van Urk H, Pieterman H. 1993
Displacement sensing device enabling accurate documentation of catheter tip position. In: Intravascular ultrasound. 3rd edition. Edited by Roelandt J, Gussenhoven E, Bom N. Dordrecht, The Netherlands: Kluwer Academic Publishers;1993:257-162

Hausmann D, Sudhir K, Mullen WL, Fitzgerald PJ, Ports TA, Daniel WG, Yock PG. 1994a
Contrast-enhanced intravascular ultrasound: validation of a new technique for delineation of the vessel wall boundary. J Am Coll Cardiol 1994 15;23:981-7

Hausmann D, Lundkvist A-J, Friedrich GJ, Mullen WL, Ftagerald PJ, Yock PG. 1994b
Intracoronary ultrasond imaging: Intraobserver and interobserver variability of morphometric measurements. Am Heart J 1994;128:674-80

Hausmann D. on behalf of the SAFETY in ICUS group. 1995
The safety of intracoronary ultrasound. A multicentre survey of 2207 examinations. Circulation 1995;91:623-630

Hermans WR, Rensing BJ, Foley DP, Deckers JW, Rutsch W, Emanuelsson H, Danchin N, Wijns W, Chappuis F, Serruys PW, on behalf of the MERCATOR study group. 1992
Therapeutic dissection after successful coronary ballon angiplasty: no influence on restenosis or on clinical outcome in 693 patients. J Am Coll Cardiol 1992;20:767-80

Hermiller J, Buller C, Tenaglia A, Kisslo K, Phillips H, Bashore T, Stack R, Davidson C. 1993
Unrecognised left main coronary artery disease in patients undergoing interventional procedures. Am J Cardiol 1993;71:173-178

Hirshfeld JW, Schwartz JS, Jugo R, MacDonald RG, Goldberg S, Savage MP, Bass TA, Betrovec G, Cowley M, Taussig AS, Whitworth HB, Margolis JR, Hill JA, Pepine CJ, and the M-HEART investigators. 1991
Restenosis after coronary angioplasty: a multivariate statistical model to relate lesion and procedure variables to restenosis. J Am Coll Cardiol 1991;18:647-56

Hodgson J, Reddy D, Suneja R, Nair R, Lesnefsky E, Sheehan H. 1993
Intracoronary ultrasound imaging: Correlation of plaque morphology with angiography, clinical syndrome and procedural results in patients undergoing coronary angioplasty. J Am Coll Cardiol 1993;21:35-44

Hodgson J McB. 1994
Intracoronary ultrasound. In: Faxon DP, Holmes DR, Sandborn TA, Schatz RA (Eds): Interventional Cardiology Newsletter(2)1994, Elsevier Science, New York; 12-13

Honye J, Mahon D, Jain A, White C, Ramee S, Wallis J, Al-Zarka A, Tobis J. 1992
Morphological effects of coronary balloon angioplasty in vivo assessed by intravascular ultrasound imaging. Circulation 1992;85:1012-1025

Isner J, Rosenfield K, Losordo D, Rose L, Langevin Jr E, Rasvi S, Kosowsky B. 1991
Combination balloon-ultrasound imaging catheter for percutaneous transluminal angioplasty - validation of imaging, analysis of recoil and identification of plaque fracture. Circulation 1991;84:739-754

Jain A, Ramee S, Mesa J, Collins T, White C. 1992
Intracoronary thrombus: chronic urokinase infusion and evaluation with intravascular ultrasound. Cathet Cardiovasc Diagn 1992;26:212-14

Kakuta T, Currier JW, Haudenschild CC, Ryan TJ, Faxon DP. 1994
Differences in compensatory vessel enlargement, not intimal formation, account for restenosis afte angioplasty in the hypercholesterolemic rabbit model. Circulation 1994;89:2809-2815

Kearney P, Starkey IR, Sutherland GR. 1995b
Intracoronary ultrasound: Current state of the art. Br Heart J 1995;73 (supplement 3): 16-25

Kearney P, Erbel R, Rupprecht HJ, Ge J, Koch L, Voigtländer T, Stähr P, Görge G, Meyer J. 1996
Differences in the morphology of unstable and stable coronary lesions and their impact on the mechanisms of angioplasty. An in vivo study with intravascular ultrasound. Eur Heart J 1996; May issue

Kimura BJ, Fitzgerald PJ, Sudhir K, Amidon TM, Strunk BL, Yock PG. 1992
Guidance of directed coronary atherectomy by intracoronary ultrasound imaging. Am Heart J 1992;124:1365-9

Klauss V, Blasini R, Regar E, Krötz M, Rieber J, Theisen K, Mudra H. 1994
Serial intravascular ultrasound studies for assessment of morphologic changes of coronary Palmaz-Schatz stents. Eur Heart J 1994;15(abstract supplement):535

Koch L, Kearney P, Erbel R, Roth Th, Ge J, Brennecke R, Meyer J. 1993
Three dimensional reconstruction of intracoronary ultrasound images: roadmapping with simultaneously digitised coronary angiograms. In: Proceedings of IEEE, Computers in Cardiology. Durham NC, USA. 1993: 89-91

Kovach JA, Mintz GS, Pichard AD, Kent KM, Popma JJ, Satler LF, Leon MB. 1993
Sequential intravascular ultrasound characterization of the mechanisms of rotational atherectomy and adjunct balloon angioplasty. J Am Coll Cardiol 1993;22:1024-32

Kuntz RE, Baim D. 1993
Defining coronary restenosis. Circulation 1993;88:1310-1323

Laskey WK, Brady ST, Kussmaul WG, Waxler AR, Krol J, Hermann HC, Hirshfeld JW Jr, Sehgal C. 1993
Intravascular ultrasonographic assessment of the results of coronary artery stenting. Am Heart J 1993;125:1576-83

Lee DY, Eigler N, Fishbein MC, Bhambi B, Maurer G, Siegel RJ. 1994
Identification of intracoronary thrombus and demonstration of thrombectomy by intravascular ultrasound imaging. Am J Cardiol 1994;73:522-3

Lee R, Loree H, Cheng G, Lieberman E, Jaramillo N, Schoen F. 1993
Computational structural analysis based on intravascular ultrasound imaging before in vitro angioplasty: prediction of plaque fracture locations. J Am Coll Cardiol 1993;21:777-82

Li Wenguang, Bouma CJ, Gussenhoven EJ, ter Haar Romeny, Pasterkamp G, Rijsterborgh H, Pieterman H. 1993
Computer-aided intravascular ultrasound diagnostics. In: Intravascular ultrasound. 3rd edition. Edited by Roelandt J, Gussenhoven E, Bom N. Dordrecht, The Netherlands: Kluwer Academic Publishers; 1993:79-90

Linker D, Yock P, Grønningæther Å, Angelsen B. 1989
Analysis of backscattered ultrasound from normal and diseased arterial wall. Int J Card Imaging 1989;4:177-185

Lockwood G, Ryan L, Gotlieb A, Lonn E, Hunt J, Liu P, Foster S. 1992
In vitro high resolution intravascular imaging in muscular and elastic arteries. J Am Coll Cardiol 1992;20:153-60

Losordo D, Rosenfield K, Pieczek A, Baker K, Harding M, Isner J. 1992
How does angioplasty work? Serial analysis of human iliac arteries using intravascular ultrasound. Circulation 1992;86:1845-58

MAAS investigators. 1994
Effect of simvastatin on coronary atheroma: the Multicentre Anti-Atheroma Study (MAAS). Lancet 1994;344:633-38

Martin RW, Johnson CC. 1989
Design characteristics for intravascular ultrasonic catheters. Int J Cardiac Im 1989;4:201-216

McKay CR, Griggith J, Kerber RE, Marcus ME. 1989
Factors influencing intraluminal ultrasound image quality and arterial wall morphology. Circulation 1989;80:II-2305

Mills RM, Billett JM, Nichols WW. 1992
Endothelial dysfunction early after heart transplantation. Assessment with intravascular ultrasound and Doppler. Circulation 1992;86:1171-1174

Mintz GS, Potkin BN, Keren G, Satler LF, Pichard AD, Kent KM, Popma JJ, Leon MB. 1992a
Intravascular ultrasound evaluation of the effect of rotational atherectomy in obstructive atherosclerotic coronary artery disease. Circulation 1992, 86:1383-1393

Mintz GS, Douek P, Pichard AD, Kent KM, Satler LF, Popma JJ, Leon MB. 1992b
Target lesion calcification in coronary artery disease: an intravascular ultrasound study. J Am Coll Cardiol 1992;20:1149-55

Mintz GS, Potkin BN, Cooke RH, Stark KS, Kent KM, Satler LF, Pichard AD, Leon MB. 1992c
Intravascular ultrasound imaging in a patient with unstable angina. Am Heart J 1992;123:1692-4

Mintz GS, Pichard AD, Satler LF, Popma JJ, Kent KM, Leon MB. 1993
Three-dimensional intravascular ultrasonography: reconstruction of endovascular stents in vitro and in vivo. J Clin Ultrasound 1993;21:609-15

Mintz GS, Pichard AD, Kent KM, Satler LF, Popma JJ, , Leon MB. 1994a
Intravascular ultrasound comparison of restenotic and de novo coronary artery narrowings. Am J Cardiol 1994;74:1278-1280

Mintz GS, Pichard AD, Kovach JA, Kent KM, Satler LF, Javier SP, Popma JJ, Leon MB. 1994b
Impact of preintervention intravascular ultrasound imaging on transcatheter treatment strategies in coronary artery disease. Am J Cardiol 1994;73:423-30

Morice MC, Zemour G, Benveniste E, Biron Y, Bourdonnec C, Faivre R, Fajadet J, Gaspard P, Glatt B, Joly P et al. 1995a
Intracoronary stenting without comadin: one month results of a French multicenter study. Cathet Cardiovasc Diagn 1995;35:1-7

Morice MC, Commeau P, Monassier JP, Riou P, Louvard Y, Guerin Y, Fajadet J, Benveniste E, Cribier A, Bunouf P. 1995b
Coronary stenting without comadin. Phase II, III, IV, V. Predictors of major complications. Eur Heart J 1995;16(abstract suppl):249

Moriuchi M, Tobis JM, Mahon D, Gessert J, Griffith J, McRae M, Moussabeck O, Henry WL. 1990
The reproducibility of intravascular ultrasound imaging in vitro. J Am Soc Echocardiogr 1990;3:444-50

Moriuchi M, Gofdon IL, Begman A, Griffith J, Tobis JM. 1992
Anatomic and functional assessment of stenosis severity with intravascular ultrasound imaging in vitro. Am J Card Imag 1992;6:109-116

Mudra H, Klauss V, Blasini R, Rieber J, Kroetz M, Rieber J, Regar E, Theisen K. 1994
Utrasound guidance of Palmaz-Shatz intracoronary stenting with a combined intravascular ultrasound balloon catheter. Circulation 1994;90:1252-1261

Nakamura S, Colombo A, Gaglione A, Almagor Y, Goldberg SL, Maiello L, Finci L, Tobis JM. 1994
Intracoronary ultrasound observations during stent implantation. Circulation 1994;89:2026-34

Ng KH, Evans JL, Vonesh MJ, Meyers SN, Mills TA, Kane BJ, Aldrich WN, Jang YT, Yock PG, Rold MD, Roth SI, McPherson DD. 1994
Arterial imaging with a new forward-viewing intravascular ultrasound catheter, II. Three-dimensional reconstruction and display of data. Circulation 1994;89:718-23

Nishimura RA, Edwards WD, Warnes CA, Reeder GS, Holmes DR Jr, Tajik AJ, Yock PG. 1990
Intravascular ultrasound imaging: in vitro validation and pathologic correlation. J Am Coll Cardiol 1990;16:145-54

Nissen S, Grines C, Sublett K, Haynie D, Diaz C, Booth D, DeMaria A. 1990
Application of a new phased-array ultrasound imaging catheter in the assessment of vascular dimensions: In vivo comparison to cineangiography. Circulation 1990;81:660-666

Nissen SE, Gurley JC, Grines CL, Booth DC, McClure R, Berk M, Fischer C, DeMaria AN. 1991
Intravascular ultrasound assessment of lumen size and wall morphology in normal subjects and patients with coronary artery disease. Circulation 1991;84:1087-99

Palmaz JC, Garcia O, Kopp DT, Tio FO, Ciarvino V, Schatz RA, Rees C, Alvarado R, Lancaster JC, Bochert RD. 1989
Balloon expandable intra-arterial stents. Effects of antithrombotic medication on thrombus formation. In: Zeitler E (Ed): Pros and cons in PTCA and auxiliary methods. Berlin, Germany: Springer and Verlag; 1989:170-178

Pandian N, Kreis A, Brockway B. 1990
Detection of intra-arterial thrombus by intravascular high frequency two-dimensional ultrasound in vitro and in vivo studies. Am J Cardiol 1990; 65:1280-1283

Peters RJ, Kok WEM, van der Wal AC, Visser CA. 1994a
Determinants of echodensity at the intima-media interface with intracoronary ultrasound imaging. J Am Soc Echo 1995; in press

Peters RJ, Kok WEM, Rijsterborgh H, van Dijk M, Li W, The SHK, Visser CA. 1994b
Reproducibility and beat-to-beat variation of quantitative measurements on intracoronary ultrasound images. Doctoral thesis 1994, chapter 3:55-72

Peters RJ, Kok WE, Havenith MG, Rijsterborgh H, van der Wal A, Visser CA. 1994c
Histopathologic validation of intracoronary ultrasound imaging. J Am Soc Echocardiogr 1994;7:230-41

Peters RJ, Ge J, Linker DT, Visser CA, Yock PG. 1994d
Observer agreement on qualitative analysis of intracoronary ultrasound images. Circulation 1994;90:I-551

Peters RJ, Kok WE, Bot H, Visser CA. 1994e
Characterisation of plaque components with intracoronary ultrsound imaging: an in vitro quantitative study with videodensitometry. J Am Soc Echocardiogr 1994;7:616-23

Pflugfelder PW, Boughner DR, Rudas L, Kostuk WJ. 1993
Enhanced detection of cardiac allograft arterial disease with intracoronary ultrasonographic imaging. Am Heart J 1993;125:1583-91

Pignoli P, Tremoli E, Poli A, Oreste P, Paoletti R. 1986
Intimal plus medial thickness of the arterial wall; a direct measurement with ultrasound imaging. Circulation 1986;74:1399-406

Pinto FJ, St. Goar FG, Fischell TA, Stadius ML, Valantine HA, Alderman EL, Popp RL. 1992
Nitroglycerin-induced coronary vasldilatation in cardiac transplant recipients: evaluation with in vivo intracoronary ultrasound. Circulation 1992;85:69-77

Pinto FJ, St. Goar FG, Gao SZ, Chenzbraun A, Fischell TA, Alderman EL, Schroeder JS, Popp RL. 1993
Immediate and one-year safety of intracoronary ultrasonic imaging. Evaluation with serial quantitative angiography. Circulation 1993;88:1709-14

Popma JJ, Colombo A, Almagor Y, Wong SC, Mintz GS, Pichard AD, Kent KM, Satler LF, Ditrano CJ, Lewis LT, Leon MT. 1994
Quantitative angiographic analysis of a new ultrasound-guided stent implantation technique. J Am Coll Cardiol 1994;Abstract supplement:135A

Porter TR, Sears T, Xie F, Michels A, Mata J, Welsh D, Shurmur S. 1993
Intravascular ultrasound study of angiographically mildly diseased coronary arteries. J Am Coll Cardiol 1993;22:1858-65

Porter TR, Radio SJ, Anderson JA, Michels A, Xie F. 1994
Composition of coronary atherosclerotic plaque in the intima and media affects intravascular ultrasound measurements of intimal thickness. J Am Coll Cardiol 1994;23:1079-84

Post MJ, Borst C, Kuntz RE. 1994
The relative importance of arterial remodeling compared with intimal hyperplasia in lumen renarrowing after balloon angiplasty: a study in the normal rabbit and the hypercholesterolemic Yucatan micropig. Circulation 1994; 89:2816-2821

Potkin BN, Bartorelli AL, Gessert JM, Neville RF, Almagor Y, Roberts WC, Leon MB. 1990
Coronary artery imaging with intravascular high-frequency ultrasound. Circulation 1990;81:1575-85

Potkin BN, Keren G, Mintz GS, Douek PC, Pichard AD, Satler LF, Kent KM, Leon MB. 1992
Arterial responses to balloon coronary angioplasty: an intravascular ultrasound study. J Am Coll Cardiol 1992 Oct;20:942-51

Reddy KG, Suneja R, Nair RN, Dhawale P, Hodgson JM. 1993
Measurement by intracoronary ultrasound of in vivo arterial distensibility within atherosclerotic lesions. Am J Cardiol 1993;72:1232-7

Reiber JHC, Serruys PW, Kooijman CJ, Wijns W, Slager CJ, Gerbrands JJ, Schuurbriers JCH, Den Boer A, Hugenholtz PG. 1985
Assessment of short-, medium-, and long-term variations in arterial dimensions from computer-assisted quantitation of coronary cineangiograms. Circulation 1985;71:280-88

Rensing B, Hermans W, Deckers J, de Feyter P, Tijssen J, Serruys P. 1992
Lumen narrowing after percutaneous transluminal coronary balloon angioplasty follows a near Gaussian distribution: A quantitative angiographic study in 1,445 successfully dilated lesions. J Am Coll Cardiol 1992;19:939-45

Robert S, Miller AJ, Fagan SC. Ticlopidine: a new antiplatelet agent for cerbrovascular disease. Pharmacology 1991;11:317-322

Rosenfield K, Losordo DW, Ramaswamy K, Pastore JO, Langevin RE, Razvi S, Kosowsky BD, Isner JM. 1991
Three-dimensional reconstruction of human coronary and peripheral arteries from images recorded during two-dimensional intravascular ultrasound examination. Circulation 1991;84:1938-56

Rosenfield K, Kaufman J, Pieczek A, Langevin RE Jr, Razvi S, Isner JM. 1992
Real-time three-dimensional reconstruction of intravascular ultrasound images of iliac arteries. Am J Cardiol 1992;70:412-5

Sanborn T, Faxon D, Haudenschild C, Gottsman S, Ryan T. 1983
The mechanism of transluminal angioplasty: evidence for formation of aneurysms in experimental atherosclerosis. Circulation 1983;68:1136-40

Schatz R, Baim D, Leon M, Ellis S, Goldberg S, Hirshfeld J, Cleman M, Cabin H, Walker C, Stagg J, Buchbinder M, Teirstein P, Topol E, Savage M, Perez J, Curry R, Whithworth H, Sousa J, Tio F, Almagor Y, Pinder R, Penn I, Leondard B, Levine S, Fish S, Palmaz J. 1991
Clinical experience with the Palmaz-Schatz coronary stent: initial results of a multicentre study. Circulation 1991;83:148-161

Schwartz RS, Murphy JG, Edwards WD, Camrud AR, Vliestra RE, Holmes DR. 1991
Restenosis after balloon angioplasty. A practical proliferative model in porcine coronary arteries. Circulation 1991;82:2190-2200

Serruys P, Strauss BH, Beatt KJ, Bertrand ME, Puel J, Rickards AF, Meier B, Goy J-H, Vogt P, Kappenberger L, Sigwart U. 1991
Angiographic follow-up after placemment of a self-expanding coronary -artery stent. N Eng J Med 1991;324:13-17

Serruys P, Keane D. 1993
The Bailout Stent. Is a friend in need always a friend indeed? Circulation 1993;88:2455-2457

Serruys P, De Jaegere P, Kiemeneij F, Macaya C, Rutsch W, Heyndrickz G, Emanuelsson H, Marco J, Legrand V, Materne P, Belardi J, Sigwart U, Colombo A, Goy J-J, Van Den Heuvel P, Delcan J, Morel M-A for the BENESTENT study group. 1994
A comparison of balloon-expandable-stent implantation with balloon angioplasty in patients with coronary artery disease. N Engl J Med 1994;331:489-95

Siegel RJ, Ariani M, Fishbein M, Chae J, Park J, Maurer G, Forrester J. 1991
Histopathologic validation of angioscopy and intravascular ultrasound. Circulation 1991;84:109-117

Siegel RJ, Chae JS, Maurer G, Berlin M, Fishbein MC. 1993
Histopathologic correlation of the there-layered intravascular ultrasound appearance of normal adult human muscular arteries. Am Heart J 1993;126:872-8

Sigwart U, Puel J, Mirkovitch V, Joffre F, Kappenberger L. 1987
Intravascular stents to prevent occlusion and restenosis after transluminal angioplasty. N Engl J Med 1987;316:701-6

Spencer T, Ramo MP, Anderson T, Kearney P, Sutherland GR, Fox KAA, McDicken WN. Characterisation of atherosclerotic plaque by spectral analysis of intravascular ultrasound: An in vitro study with histological validation. To be presented at the British Medical Ultrasound Society, Torquay 1996 and for subsequent publication in the International Journal of Ultrasound.

St. Goar F, Pinto F, Alderman E, Fitzgerald P, Stadius M, Popp R. 1991
Intravascular ultrasound imaging of angiographically normal coronary arteries: An in vivo comparison with quantitative angiography. J Am Coll Cardiol 1991;18:952-958

St. Goar FG, Pinto FJ, Alderman EL, Fitzgerald PJ, Stinson EB, Billingham ME, Popp RL. 1992
Detection of coronary atherosclerosis in young adult hearts using intravascular ultrasound. Circulation 1992;86:756-63

Stary HC, Blankenhorn DH, Chandler AB, Glagov S, Insull W, Richardson M, Rosenfeld ME, Schaffer SA, Schwartz CJ, Wagner WD, Wissler RW. 1992
A definition of the intima of human arteries and of its atherosclerosis-prone regions. Circulation 1992;85:391-405

Stone GW, St. Goar F, Klette MA, Linnemeier TJ. 1993
Initial clinical experience with a novel low-profile integrated coronary ultrasound -angioplasty catheter: implications for routine use. J Am Coll Cardiol 1993;21:134A

Sudhir K, MacGregor JS, Barbant SD, Foster E, Fitzgerald PJ, Chatterjee K, Yock PG. 1993
Assessment of coronary conductance and resistance vessel reactivity in response to nitroglycerin, ergonovine and adenosine: in vivo studies with simultaneous intravascular two-dimensional and Doppler ultrasound. J Am Coll Cardiol 1993;21:1261-8

Tenaglia A, Buller C, Kisslo K, Phillips H, Stack R, Davidson C. 1992a
Intracoronary ultrasound predictors of adverse outcomes after coronary artery interventions. J Am Coll Cardiol 1992;20:1385-90

Tenaglia AN, Buller CE, Kisslo KB, Stack RS, Davidson CJ. 1992b
Mechanisms of balloon angioplasty and directional coronary atherectomy as assessed by intracoronary ultrasound. J Am Coll Cardiol 1992;20:685-91

Tenaglia AN, Kisslo K, Kelly S, Hamm MA, Crowley R, Davidson CJ. 1993
Ultrasound guide wire-directed stent deployment. Am Heart J 1993;125:1213-6

Tobis JM, Mallery J, Gessert J, Griffith J, Mahon D, Bessen M , Moriuchi M, McLeay L, McRae M, Henry W. 1989
Intravascular ultrasound cross-sectional arterial imaging before and after balloon angioplasty in vitro. Circulation 1989; 80:873-82

Tobis JM, Mallery J, Mahon D, Lehmann K, Zalesky P, Griffith J, Gessert J, Moriuchi M, McRae M, Dwyer M-L, Greep N, Henry W. 1991a
Intravascular ultrasound imaging of human coronary arteries in vivo. Analysis of tissue characterization in comparison with in vitro histological specimens. Circulation 1991;83:913-26

Tobis JM, Moriuchi M, Honye J, McRae M. 1991b
Intravascular ultrasound imaging following balloon angioplasty. Int J Card Imag 1991;6:191-205

Urbani MP, Picano E, Parenti G, Mazzarisi A, Fiori L, Paterni M, Pelosi G, Landini L. 1993
In vivo radiofrequency-based ultrasonic tissue charaterisation of the atherosclerotic plaque. Stroke 1993;24:1507-1512

Velican D, Velican C. 1981
Comparative study on age related changes and atherosclerosis involvement of the coronary arteries of male and female subjects up to 40 years of age. Atherosclerosis 1981, 38:39-50

Waller B. 1989
The eccentric coronary atherosclerotic plaque: morphologic observations and clinical relevance. Clin Cardiol 1989;12:14-20

Weissman NJ, Weyman AE. 1994
Images in Clinical Medicine: Directional Atherectomy. N Engl J Med 1994;330:539

Weyman AE. 1994
Physical principles, instrumentation, and routine examination. In: Weyman AE (Ed): Principles and practice of Echocardiography. Philadelphia, USA: Lea and Febiger; 1994:3-28

White CJ, Ramee SR, Collins TJ, Jain A, Mesa JE. 1992
Ambiguous coronary angiography: clinical utility of intravascular ultrasound. Cathet Cardiovasc Diagn 1992;26:200-3

Yamagishi M, Miyatake K, Tamai J, Nakatani S, Koyama J, Nissen SE. 1994
Intravascular ultrasound detection of atherosclerosis at the site of focal vasospasm in angiographically normal or minimally narrowed coronary segments. J Am Coll Cardiol 1994;23:352-7

Zamorano J, Erbel R, Ge J, Gorge G, Kearney P, Koch L, Scholte A, Meyer J. 1994
Spontaneous plaque rupture visualized by intravascular ultrasound. Eur Heart J 1994;15:131-3

Appendix 1

Abbreviations

DCA	Directional Coronary Atherectomy
ECG	Electrocardiograph
EEL	External elastic lamina
GTN	Glyceryl trinitrate
ICUS	Intracoronary ultrasound
IEL	Internal elastic lamina
IVUS	Intravacular ultrasound
LA	Lumen area
MLA	Minimum lumen area
MLD	Minimum lumen diameter
MxLD	Maximum lumen diameter
PA	Plaque area
PTCA	Percutaneous Transluminal Coronary Angioplasty
QCA	Quantitative coronary angiography
SD	Standard deviation
tPA	Tissue plasminogen activator
VA	Vessel area
%sten	Percent stenosis
2D	Two dimensional

Appendix 2

Relevant Publications and Abstracted Presentations

Published or accepted for publication

Kearney P, Erbel R, HJ Rupprecht, Ge J, Koch L, Voigtländer T, Stähr P, G. Görge, J. Meyer. Specific Lesion Morphology and Mechanisms of PTCA in Patients with Unstable Angina Observed with Intracoronary Ultrasound. Eur Heart J 1996 (May issue)

Kearney P. Intravascular ultrasound findings in the acute coronary syndromes. In: An atlas of intravascular ultrasound. Editor: Raimund Erbel , London, United Kingdom: Martin Dunitz (in press)

Kearney P. Coronary dissections. In: An atlas of intravascular ultrasound. Editor: Raimund Erbel , London, United Kingdom: Martin Dunitz (in press)

Ge J, Liu F, Kearney P, Görge G, Haude M, Baumgart D, Ashry M, Erbel R. Intravascular ultrasound approach to the diagnosis of coronary artery aneurysms. Am Heart J 1995;130:765-71

Kearney P, Starkey I, Sutherland G. Intravascular ultrasound. Current state of the art. Br Heart J 1995;73 (supplement 3): 16-25

Ge J, Erbel R, Zamorano J, Haude M, Kearney P, Görge G, Meyer J. Improvement of coronary morphology and flood flow after stenting. Int J Card Im 1995;11:81-87

Ge J, Liu F, Kearney P, Görge G, Haude M, Erbel R. Acute coronary artery closure following intracornoary ultrasound examination. Cathet Cardiovasc Diagn 1995;35:232-35

Ge J, Erbel R, Rupprecht H-J, Koch L, Kearney P, Görge G, Gerber T, Meyer J. Comparison of intravascular ultrasound and angiography in the assessment of myocardial bridging. Circulation 1994;89:1725-32

Kearney P, Erbel R, Ge J, Zamorano J, Koch L, Görge G, J.Meyer. Detection of spontaneous coronary artery dissection by intravascular ultrasound in a case of unstable angina. Cathet Cardiovasc Diagn 1994;32:58-61

Zamorano J, Erbel R, Ge J, Görge G, Kearney P, Scholte A, Meyer J. Vessel wall changes in the proximal nono-treated segment after PTCA. An in vivo intracoronary ultrasou nd study. Eur Heart J 1994;15:1505-11

Zamorano J, Erbel R, Ge J, Görge G, Kearney P, Koch L, Scholte A, Meyer J. Spontaneous plaque rupture visualised by intravascular ultrasound. Eur Heart J 1994;15:131-33

Koch L, Kearney P, Erbel R, Roth Th, Ge J, Brennecke R, Meyer J. Three dimensional reconstruction of intracoronary ultrasound images: roadmapping with simultaneously digitised coronary angiograms. In: IEEE Computers in Cardiology. Durham NC, USA. 1993: 89-91

Ge J, Erbel R, Zamorano J, Koch L, Kearney P, Schicketanz KH, Görge G, Gerber T, Meyer J. Coronary artery remodelling in atherosclerotic disease: an intravascular ultrasonic study in vivo. Coronary Artery Disease 1993; 4:981-86

Abstracted presentations at national and international meetings

Kearney P, Ramo P, Shaw T, Starkey I, McMurray J, Sutherland G. The reproducibility of IVUS measurements in unselected video frames assessed in sequential catheter pullbacks and in separate analysis sessions. Circulation 1995;92:I-78

Kearney P, Ramo P, Shaw T, Starkey I, McMurray J, Sutherland G. Assessment of the Reproducibility of Reference Lumen Quantitation with Intravascular Utrasound in Patients Undergoing Coronary Stenting. Circulation 1995;92:I-601

Spencer T, Ramo MP, Kearney P, Sutherland GR, Fox KAA, McDicken WN. Identificiation of different thrombus types by analysis of 30 MHz radiofrequency data. British Medical Ultrasound Society, Torquay 1996 (for subsequent publication in the International Journal of Ultrasound).

Spencer T, Ramo MP, Anderson T, Kearney P, Sutherland GR, Fox KAA, McDicken WN. Characterisation of atherosclerotic plaque by spectral analysis of intravascular ultrasound: An in vitro study with histological validation. British Medical Ultrasound Society, Torquay 1996 (for subsequent publication in the International Journal of Ultrasound).

Roth T, Koch L, Erbel R, Kearney P, Ramo P, Spencer T, Sutherland G. Development of a system of intracoronary ultrasound based frequency dependant tissue characterisation. In: Proceedings of "Echocardiography 1995", Rotterdam, The Nethlands. June 1995

Kearney P, Ramo P, Spencer T, Shaw S, Starkey I, Sutherland G. How important are image distortion artefacts when using mechanical intravascular ultrasound transducers? Kearney P, Ramo P, Spencer T, Shaw T, Starkey I, Sutherland G. Br Heart J 1995;73:43

Voigtländer T, Rupprecht H-J, Stähr P, Sharhag J, Kearney P, Meyer J. Coronary intervention in acute myocardial infarction: preinterventional morphology and postinterventional outcome assessed by intracoronary ultrasound. Circulation 1994;90:I-60

Kearney P, Starkey I, Fort S, McMurray J, Shaw T, Sutherland G. Does optimal stent deployment require intracoronary ultrasound guidance? Ir J Med Sci 1994 (Abstracts from the annual meeting of the Irish Cardiac Society)

Stähr P, Rupprecht H-J, Voigtländer T, Otto M, Kearney P, Klein C, Kirkpatrick C, Rudiger K, Meyer J. Intravascular ultrasound characterisation of normal segmental pulmonary arteries - an in vitro study with matched histological segments. Eur Heart J 1994;15:409

Kearney P, Koch L, Ge J, Görge G, Erbel R. PTCA mechanisms in stable and unstable angina analysed with intracoronary ultrasound before and after intervention. Circulation 1993:88;I-579

Kearney P, Erbel R, Ge J, H. Rupprecht, Görge G, Meyer J. Structural and functional assessment of coronary balloon angioplasty using intracoronary ultrasound and Doppler. Eur Heart J 1993;14:327

Kearney P, Erbel R, Ge J, G. Gorge, Meyer J. Mechanisms of coronary angioplasty analysed by intracoronary ultrasound before and after intervention. Eur Heart J 1993;14:327

Kearney P, Erbel R, Koch L, Ge J, Zamorano J, Görge G, Meyer J. Intracoronary ultrasound detected lumen area variation in myocardial bridges compared to normal segments. Eur Heart J 1993;14:110

Görge G, Erbel R, Gerber T, Kearney P, Ge J, Rupprecht HJ, Meyer J. Dissection after PTCA: comparison of angiography-IVUS. Eur Heart J 1993;14:25

Ge J, Erbel R, Kearney P, Görge G, Rupprecht HJ, Meyer J. High incidence of atheroma proximal to myocardial bridging observed by intravascular ultrasound: an insight into atherogenesis? Circulation 1993:88;I-550